METAL COMPLEXES OF PENDANT-ARM MACROCYCLIC LIGANDS

Ian Andrew Fallis (B.Sc.)

A thesis submitted for the degree of Doctor of Philosophy

ACKNOWLEDGEMENTS

To Mum & Dad

ABBREVIATIONS

General

abs	absorption
CD	circular dichroism
d	doublet
DMF	dimethyl formamide
EDTA	ethylenediamine tetra-acetic acid
en	ethylene diamine
EPR	electron paramagnetic resonance
LFSE	ligand field stabilisation energy
m	multiplet
m.p.	melting point
NHE	neutral hydrogen electrode
NMR	nuclear magnetic resonance
PEM	photo-elastic modulator
ppm	parts per million
tosyl, Ts	p-tolyl sulphonyl
UV	ultra-violet
vis.	visible
μ_B	Bohr magneton

Ligands

cyclam	1,4,8,11-tetrazacyclotetradecane
TCTA	N,N',N''-trisacetato-1,4,7-triazacyclononane
10aneN$_3$	1,4,7-triazacyclodecane.
12aneN$_3$	1,4,7-triazacyclododecane.

1,5,9-12aneN$_3$	1,5,9-triazacyclododecane.
9-aneN$_3$	1,4,7-triazacyclononane.
1,4,7-13aneN$_3$	1,4,7-triazacyclotridecane.
1,5,9-13aneN$_3$	1,5,9-triazacyclotridecane.
1,4,7-11aneN$_3$	1,4,7-triazacycloundecane.
L^{1}H$_3$	(*R*) and (*S*) N,N',N"-tris(2-hydroxypropyl)-1,4,7-triazacyclononane.
L^{2}H$_3$	N,N',N"-(tris-(2*R*)-hydroxy-3-methyl-butyl)-1,4,7-triazacyclononane
L^{3}H$_3$	N,N',N"-tris(2*R*-hydroxypropyl)-1,4,7-triazacyclodecane.
L^{4}H$_3$	N,N',N"-tris(2*R*-hydroxypropyl)-1,4,7-triazacycloundecane.
L^{5}H$_3$	N,N',N"-tris(2*S*-hydroxypropyl)-1,4,7-triazacyclododecane.
L^{6}H$_3$	N,N',N"-tris(2*R*-hydroxypropyl)-1,4,7-triazacyclotridecane.
L^{7}H$_3$	N,N',N"-tris(2*R*-hydroxypropyl)-1,5,9-triazacyclododecane.
L^{8}H$_3$	N,N',N"-tris(2*R*-hydroxypropyl)-1,4,8-triazacycloundecane.
L^{9}H$_3$	N,N',N"-tris(2*R*-hydroxypropyl)-1,5,9-triazacyclotridecane.
L^{10}H$_3$	N,N',N"-tris(2-hydroxy-2-methyl-propyl)-1,4,7-triazacyclononane.

L^{1}H$_3$ L^{2}H$_3$

L³H₃

L⁴H₃

L⁵H₃

L⁶H₃

L⁷H₃

L⁸H₃

L⁹H₃

L¹⁰H₃

CONTENTS

ABSTRACT

A series of tris-alcohol substituted triazamacrocyclic ligands has been prepared, with the purpose of investigating the effect of increasing steric strain upon the physical and spectroscopic properties of the resulting first row transition metal complexes. The ligands all contain N_3O_3 donor sets and are potentially hexadentate. With pendant-arm hydroxyl groups, the ligands may behave as alcohol donors or alkoxide donors. At low pH values the ligands remain protonated and act as alcohol donors, at high pH values deprotonation occurs an the ligands behave as alkoxides, with a concomitant increase in π-basicity.

The smaller ring sizes have been found to stabilise higher oxidation states, namely Cr(III), Mn(III) and Mn(IV). This is attributed to metal radius-to-ligand cavity fit. The larger ring sizes tend to coordinate exclusively to the divalent ions, Mn(II), Co(II), Ni(II), Cu(II) and Zn(II).

With 9 and 10 membered ring ligands, the manganese complexes may be monomeric or dimeric. The reaction of $MnCl_2$ with N,N',N"-tris(2S-hydroxypropyl)-1,4,7-triazacyclononane (L^1H_3) under mildly basic conditions produces the mixed valence dimeric $[Mn(II)L^1H_3L^1Mn(IV)]^{3+}$. Each metal centre exhibits different coordination geometry; the Mn(IV) component is pseudo-octahedral in geometry, and the Mn(II) component, trigonal prismatic. In the case of N,N',N"-tris(2R-hydroxypropyl)-1,4,7-triazacyclodecane (L^3H_3) the mixed valence dimer $[Mn(II)L^3H_3L^3Mn(III)]^{2+}$ is produced. The difference in oxidation state between the complexes of L^1H_3 and L^3H_3 is due to the larger ring in L^3H_3 stabilising the larger Mn(III). In addition, since the ligand has an unsymmetrical cavity the Jahn-Teller distortion of the d^4 Mn(III) ion may be supported. The spherical cavity of L^1H_3 does not support a tetragonally distorted ion.

N,N',N"-(tris-(2R)-hydroxy-3-methyl-butyl)-1,4,7-triazacyclononane (L^2H_3) has been shown to form a pseudo-octahedral Mn(IV) complex under aerobic conditions at

neutral pH. This ligand is very sterically hindered about the O,O',O" face of the complex, which effectively prevents any dimerisation processes occurring. The oxidation state of $[Mn(IV)L^2]^-$ can be controlled by altering the pH. Acidification results in oxidation of water, yielding a $[Mn(II)L^2H_3]^{2+}$ species, and successive basification results in reoxidation to $[Mn(IV)L^2]^-$. The Cr(III) complex of L^2H_3 has been prepared and its acid-base properties studied using electronic and circular dichroism spectroscopy. At low pH values the complex is protonated ($[Cr(III)L^2H_3]^{3+}$), and displays a $10Dq$ typical of Cr(III) in an N_3O_3 chromophore. Basification results in a large increase in the $10Dq$ value and a significant decrease in the B value, indicating an increase in π-donation with the ligand behaving as an alkoxide.

The Co(II) complexes of L^3H_3, N,N',N"-tris(2R-hydroxypropyl)-1,4,7-triazacyclo-undecane (L^4H_3) and N,N',N"-tris(2S-hydroxypropyl)-1,4,7-triazacyclododecane (L^5H_3) have been crystallographically characterised. The complex with L^3H_3 is a dimeric structure with two nitrate ions binding two $[Co(II)L^3H_3]^{2+}$ subunits together via hydrogen-bonds, with the geometry at each cobalt centre being almost perfectly trigonal prismatic. The structure of the complex with L^4H_3 is monomeric, with highly distorted bicapped tetrahedral geometry about the metal centre. Again, strong hydrogen bonding to the nitrate counter ions is in evidence. With L^5H_3 the structure is also monomeric with hydrogen-bonding to nitrate counter ions. The coordination geometry is trigonal prismatic, which is most unusual, given the unsymmetrical nature of the ligand.

The spectroscopic properties of the Co(II), Ni(II) and Cu(II) complexes of a large range of ligand ring sizes have been studied. Larger ring sizes result in weaker ligand fields. Ligand symmetry also has an effect on ligand field strength, with more unsymmetrical ligands again giving rise to weaker fields. The Cu(II) spectra indicate the possibility of highly trigonally distorted structures in solution. Given the trigonal prismatic structures of the analogous Co(II) complexes, it is possible that the Cu(II) complexes of L^3H_3 and L^5H_3 also have trigonal prismatic geometry.

The Zn(II) complexes of a range of ligands have been studied by one and two dimensional NMR spectroscopy. Results indicate that even with very strained ligand systems, the complexes remain hexadentate in solution. An NMR titration of L^1H_3 with $Zn(NO_3)_2$ indicates that the mechanism of complex formation is not simple, with a $[Zn(II)(L^1H_3)_4]^{2+}$ complex as a possible intermediate.

CHAPTER 1

GENERAL INTRODUCTION

"I think of myself as tall and quite slim."

Robbie Coltraine.

CONTENTS

(1.1) PREAMBLE

The chemistry of macrocycles and their complexes with metal ions has been of interest for many years, although relative to other chemical pursuits, this area of study is still young. The presence of macrocyclic ligand complexes in many fundamental biological processes has stimulated the study of macrocyclic complexes in a search for useful model systems. Involvement of macrocyclic systems in the subjects of host-guest chemistry and molecular recognition have resulted in the subject area now becoming "supramolecular chemistry" with all it's connotations of molecular architecture and nano-engineering. Macrocyclic chemistry manifests itself as the study of intra-molecular interactions and unusual forms of co-ordination chemistry. From a chemist's point of view, macrocycles provide a vast area of potential study. Macrocyclic complexes have many different properties from their non-cyclic analogues, and the probing of these properties by the large number of physical and chemical techniques now available have prompted intense investigations into natural, and the ever increasing number of synthetic, macrocyclic systems.

The presence of macrocyclic ligand complexes in nature has been appreciated for many years now. These include the haem and chlorin ligands involved in many vital processes such as oxygen transport, oxidative phosphorylation and photosynthesis. Other natural macrocycles include a number of antibiotics such as valinomycin and monactin. Synthetic macrocycles are to a large extent new additions to the chemical scene. Before 1960, the only synthetic macrocycles were a number of derivatives of the phthalocyanine system. This macrocycle, given its facile large scale synthesis from o-dicyanobenzene, is the most important commercial macrocycle to date. It's remarkable thermal stability, resistance to oxidation and its light fastness make it an excellent dye-stuff.

The 1960's saw the beginnings of a large number of synthetic macrocycle systems. The pioneering work of Curtis (1) demonstrated a template synthesis of C-substituted 14 membered rings with 4 nitrogen donors. The remarkable stability of the nickel complexes of such ligands promoted further investigation and it became apparent

that the macrocylic nature of the ligand resulted in a complex of exceptional stability and unusual redox properties. A number of template syntheses followed including the preparation of the archetypal macrocycle, cyclam.

The 1960's also heralded the synthesis of a range of ether containing macrocycles and macrobicycles known as the crown ethers (2) and cryptands (3). These ligands have resulted in a huge number of studies into the co-ordination chemistry of ions normally regarded as hard acceptors. The chemistry of the crown ethers and related compounds is vast and will not be enlarged upon, since they typically form complexes with non-transition elements.

(1.2) MACROCYCLES

(1.2.1) Synthesis of Macrocyclic Ligands

Nitrogen-based macrocyclic ligands are the prime concern of this work and only their preparation will be discussed. There are two methodologies used in the preparation of aza-macrocycles; template synthesis and open chain cyclisation.

Template synthesis was first successfully applied (unwittingly) to the preparation of Fe(II) phthalocyanine. Here an iron atom directs the association of reacting o-dicyanobenzene subunits and also stabilises the final product. Another important template synthesis is the preparation of cyclam (4). This is an example of a large group of syntheses that proceed *via* Schiff base intermediates. The final product is the very robust [Ni(II)cyclam]$^{2+}$. As an indication of this complex's inherent stability, treatment with sodium cyanide is required to liberate the macrocycle as a free base. The important feature of a template based synthesis is an *in-situ* ring closing reaction directed by the metal ion holding the reactive ends of the molecule together. This promotes ring closure and disfavours polymerisation and other undesirable side reactions. The main disadvantages of template syntheses are that the macrocycle has to be large (normally at

least 13 ring members) and that demetallation of the final product is necessary to yield the macrocyclic ligand. The template synthesis of some small (9 membered rings) sulfur macrocycles has been reported (5), but it is unlikely this method could be adapted to their nitrogen analogues.

Macrocycle synthesis from the direct reaction of open chain precursors can be performed under a variety of reaction conditions. Whilst such preparations are not defined as template syntheses, in some cases counter ions present have important effects on yields of reaction, and it seems likely that some form of template effect is occurring. Dilution of the reaction medium often has a drastic effect on yields. Many syntheses have been performed under conditions of high dilution with the use of precision dropping funnels for the addition of reactants. Such restrictions result in expensive preparations which yield relatively small quantities of material.

In 1972 Koyama & Yoshino (6) presented a low dilution, moderate-yield preparation of some triazamacrocycles. Richman & Atkins (7) modified this synthesis to provide a simple route to 9 to 24 membered macrocycles containing 3 to 8 nitrogen atoms. This synthesis (scheme.1.1) proceeds *via* tosylated intermediates to yield the final product as a pertosyl macrocycle. Tosyl groups are then removed by treatment with H_2SO_4.

Scheme 1.1. *Richman-Atkins preparation of 1,4,7-triazacyclononane*. Reagents and conditions. (i) NaH, dmf. (ii) $TsO(CH_2)_2OTs$, 110°C.
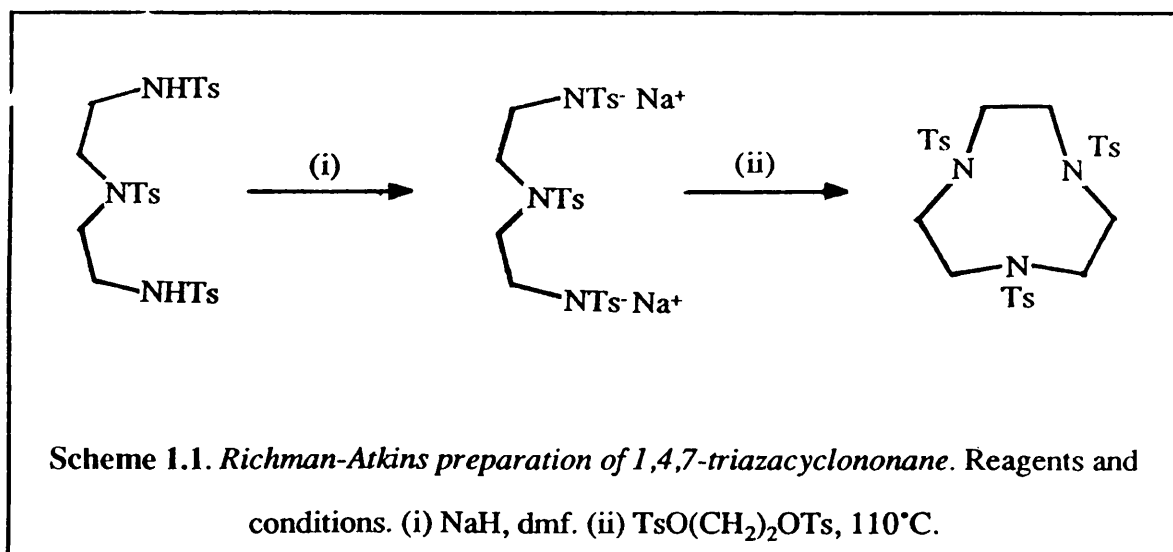
The tosyl groups in this preparation have three functions:

(1) Activation of primary amino function, by increasing the acidity of amino protons and stabilising the resulting anion.

(2) Protection of the secondary amine function.

(3) Conversion of the hydroxyl functions of diols to good leaving groups. Mesylates and halides have been shown to result in lower yields.

Richman & Atkins also demonstrated that this synthesis does not depend upon a template effect. When sodium counter ions are replaced with tetramethyl ammonium ions there is no significant change in yield, and it is now believed that steric interaction of the tosyl groups in the reactants causes the open chain intermediate to fold into a conformation that favours ring closure. Yields are reported at 50-80%. Briellmann *et al.* (8) have reported recently that these yields are erroneous and that considerable purification of the tosylated products is required.

An interesting cyclo-polymerisation of chiral aziridines has also been reported (9) yielding a mixture of tri- tetra- penta-and hexaaddition products. The starting materials however are prohibitively expensive to allow this preparation to be widely used. Aziridines also have a bad reputation for polymerising explosively.

A novel preparation of medium sized tri-azamacrocycles has recently been published (10), which uses a guanidinium based template (scheme 1.2).

Scheme 1.2. *Guanidinium based triaza-macrocycle synthesis.* Reagents and conditions. (i) NaH, Br(CH$_2$)$_3$Br, NaBF$_4$. (ii) LiAlH$_4$, thf.
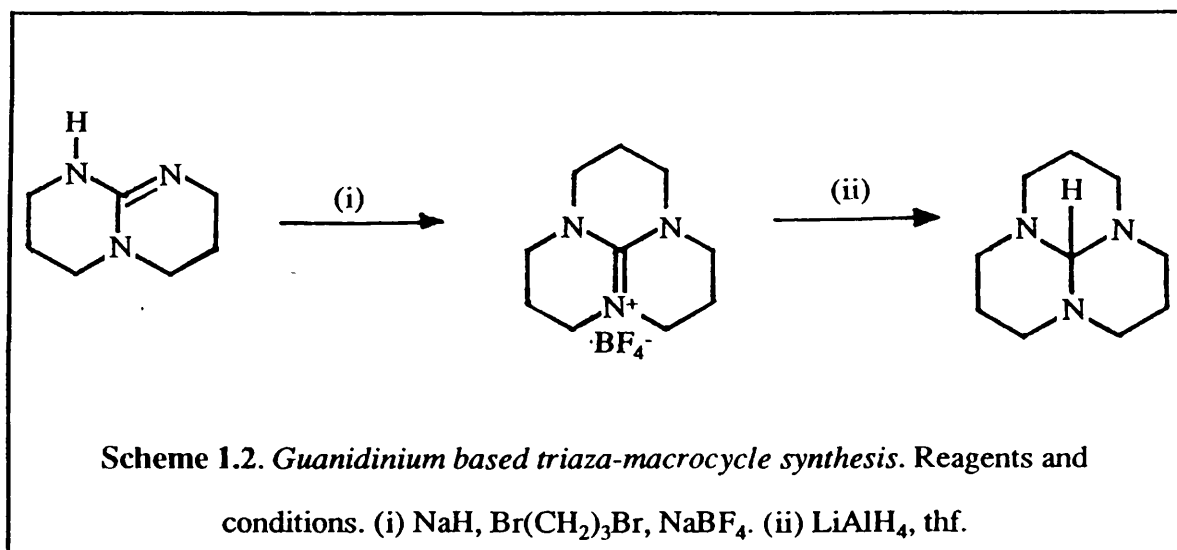
The final products may be treated with acid to yield the parent macrocycle; or with alkylating agents to afford selectively alkylated macrocycles. This synthesis proceeds in high yield with the main shortcoming, that due to excessive strain in the intermediate guanidinium ion, the preparation cannot be extended to 9 membered rings.

(1.2.2) Pendant Arm Macrocycles

The secondary amine functions of saturated aza-macrocycles provide a starting point for the preparation of many N-functionalised macrocyclic ligands. Simple alkyl derivatives have been examined, and their complexes show properties concomitant with a increase in steric hind rance and basicity (11). Many derivatives have been prepared that incorporate new donor atoms into the ligand, and it is these pendant arm-macrocycles that form the basis of the current work. Many pendant-arm derivatives have been prepared with the purpose of expanding the ligand's donor set to be potentially hexadentate. Fig.1.1 illustrates the pendant arm derivatives that have been characterised.
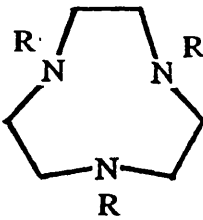
	R	Ref.
	CH_2CO_2H, $CH_2CO_2(C_2H_5)$	
	$CH_2CH_2SO_3H$, CH_2CH_2OH	(11)
	$CH_2PO_3H_2$, $CH_2P(O)(Ph)_2$	
	$CH_2CH_2NH_2$, $CH_2(2\text{-py})$	
	$CH_2(2\text{-}HOC_6H_5)$	(12)
	$CH_2P(O)PhOH$	(14)
	$CH_2(2\text{-bipy})$	(16),(17)
	$(2S$ or $2R)$ $CH_2CH(Me)OH$	this work, (18)
	$(2R)$ $CH_2CH(Me)OH$	this work
	$CH_2C(Me)_2OH$	this work

Fig. 1.1. *Pendant-arm derivatives of 1,4,7-triazacyclononane.*

The preparation of pendant arm macrocycles can follow one of several courses from the parent macrocycle:

(1) Nucleophilic attack by 2° nitrogen to displace halogen or tosylate leaving groups. This is the simplest form of derivatisation but may be complicated by quatern isation (e.g 9-aneN$_3$ with MeI) or elimination with the smaller, more basic macrocycles. For example Auerbach et al. (12) have prepared alkyl methyl phenoxy derivatives of 9-aneN$_3$.

(2) Nucleophilic attack at aldehyde carbonyl functions with reduction of the resulting imines.This method is the most useful way of introducing the 2-amino ethyl function into macrocycles by reaction with phthalamido acetaldehyde, reduction with Na(BH$_3$CN) and acid hydrolysis (13).

(3) Mannich type reaction. This is the common method for the methylation of macrocycles using formaldehyde/ formic acid. The method has also been used for the preparation of phosphinic acid derivatives (14) by the reaction of the parent macrocycle with formaldehyde and an alkyl phosphinic acid.

(4) Ring opening reactions. The ring opening of epoxides by amines is a well characterised reaction and provides a route to alkyl ethyl hydroxy substituted aza-macrocycles (15). The regiospecific attack at the least hindered carbon under basic or neutral conditions allows the introduction of chiral centres to the ligand. A number of optically active epoxides are commercially available or can be prepared from commercially available α-amino acids.

(1.2.3) Properties of Macrocycles

The acid-base behaviour of some simple macrocyclic systems is worthy of note. In general tri-azamacrocycles tend to be more basic than their linear analogues, as shown by higher first protonation constants. Also small tribasic macrocycles are more basic than larger ring sizes. For 9-aneN$_3$ the first protonation constant is approximately 10.5, which

makes it a strong organic base. The second and third protonation constants are lower than diethylene triamine, indicative of increasing repulsion between an incoming proton and the mono and/or di protonated macrocycle. The conformation of 9-aneN$_3$ results in the three nitrogen lone pairs pointing towards the centre of the macrocyclic cavity. Thus there is a co-operativity in the first protonation process. This is verified in the crystal structure of the mono perchlorate salt of N,N',N"-trimethyl-1,4,7-triazacyclononane (11), Me$_3$9-aneN$_3$ (fig. 1.2), which indicates a proton bound to one nitrogen atom, but also strongly hydrogen-bonded to the other nitrogen atoms. The bound proton lies out of the plane formed by the three nitrogen atoms, indicating that this ring size is too small for any form of equatorial co-ordination.
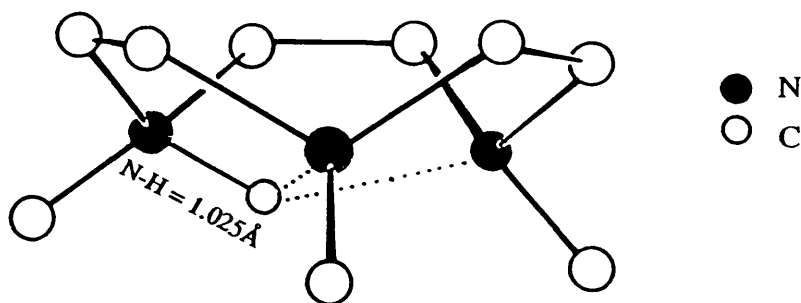
Fig.1.2 *The structure of the cation* [Me$_3$9-aneN$_3$H][ClO$_4$].

(1.3) TRANSITION METAL CHEMISTRY OF MACROCYCLIC LIGANDS

The transition metal chemistry of macrocyclic ligands is very extensive, and will only be touched upon here. The notion of size-match of metal radius to ligand cavity radius is an important concept in macrocyclic chemistry. Likewise in transition metal chemistry size-match has important effects upon structure and spectroscopic properties. Where the fit is good, formation constants will be large and stable complexes will result.

Where the fit is poor the system will distort in some manner. Occasionally if ligand-metal sizes (or shapes, in the case of very unsymmetrical ligands) differ by a large factor, it is possible that complex formation will not occur, and the metal will show a preference for the donor set present in the starting material over those of the macrocyclic ligand. It is also possible that where a metal is too large it may become more susceptible to oxidation, with metal radius being reduced on electron loss and hence a better metal-ligand fit is achieved. Also with large metal ions an increase in coordination number is possible.

It is now well established that larger ring sizes result in weaker ligand fields, due to lengthening of metal-ligand bonds. The converse is also true that smaller ligand cavities result in larger $10Dq$ values. As a consequence of this, smaller ring sizes stabilise smaller ions, and hence higher oxidation states. As an example, the ligand 1,4,7-triazacyclononae-N,N',N"-triacetate (TACNTA) forms a stable complex with Ni(II) (19). The nickel atom is bound very strongly and the complex is stable in dilute acid. If exposed to oxidising conditions, the blue colour of the Ni(II) complex is lost and a pink colouration develops. This is due to a neutral Ni(III)TACNTA complex. This complex is believed to be stabilised by the very efficient packing of TACNTA about Ni(III).

Koyama and Yoshino (6) prepared cobalt(III) complexes of a number of triazamacrocycles (9-aneN$_3$, 10-aneN$_3$, 1,4,8-11-aneN$_3$ and 1,5,9-12-aneN$_3$). It was found that with 9-aneN$_3$ and 10-aneN$_3$ bis-macrocyclic complexes were formed with a sandwich type structure Fig 1.3(a). With the larger ring sizes it is believed that piano-stool type structures are formed with one macrocycle and three halogens occupying the coordination sphere (Fig. 1.3(b)). The ligand field strength values with 9-aneN$_3$ and 10-aneN$_3$ can be incorporated into a brief spectrochemical series with [Co(en)$_3$]$^{3+}$ and Co(NH$_3$)$_6$]$^{3+}$ (field strength increasing left to right):

$$[Co(NH_3)_6]^{3+} < [Co(10\text{-aneN}_3)_2]^{3+} < [Co(en)_3]^{3+} < [Co(9\text{-aneN}_3)_2]^{3+}$$
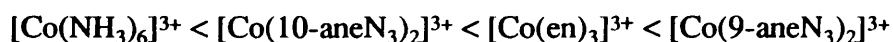
Thus it can be seen that smaller ring sizes produce larger ligand field strengths. Koppen *et al.* (20) prepared a bis(9-aneN$_3$) complex of Pt(II) in which both the macrocyclic ligands are bidentate. When this complex is heated in aqueous solution with excess perchlorate under aerobic conditions, a yellow precipitate of Pt(IV)(9-aneN$_3$)$_2$(ClO$_4$)$_4$ is produced

(fig.1.4). In the absence of macrocyclic donors Pt(IV) is normally only accessible under more rigorous conditions, indicating that the oxidation potential of Pt(II) is greatly reduced in the starting complex. Here Pt(II) is too large for the cavity formed by two 9-aneN₃ ligators. Upon oxidation the metal to cavity fit becomes good, and the resulting Pt(IV) species is six coordinate and very robust.
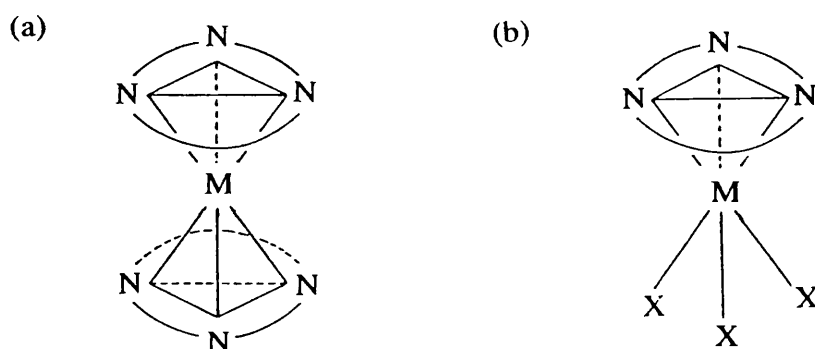
Fig. 1.3 (a) "Sandwich" type complexes of small triazamacrocycles.

(b) "Piano stool" type complexes of larger triazamacrocycles. X = halogen.
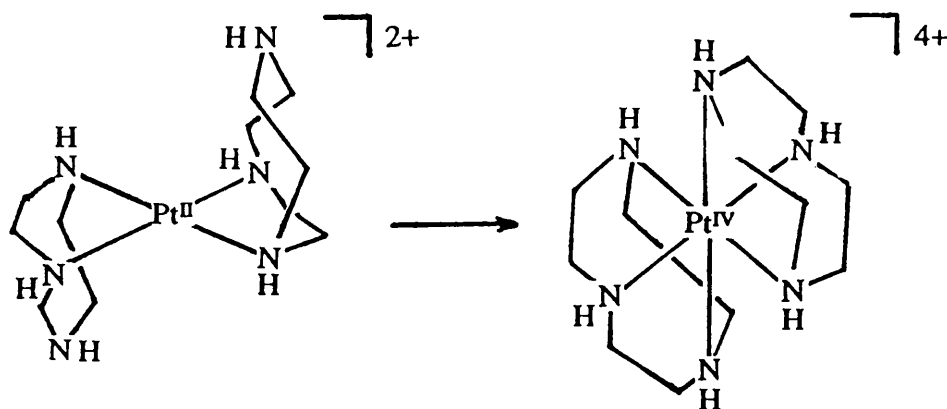
Fig.1.4 Reaction of Pt(II)-bis-1,4,7-triazacyclononane under oxidising conditions.

Reagents and conditions. 90°C, NaClO₄, O₂.

(1.4) STEREOCHEMISTRY OF TRANSITION METAL COMPLEXES. TRIGONAL PRISMATIC COORDINATION

Six coordinate transition metal complexes usually adopt octahedral geometry. The coordination chemistry of octahedral complexes requires no further comment. There are other possible coordination geometries, namely, the trigonal prism, the bicapped tetrahedron and the infinite number of possible intermediates between these extremes. An octahedron may also be regarded as a regular trigonal anti-prism. The various six coordinate geometries are illustrated in fig.1.5. The bicapped tetrahedron is a rare form of coordination geometry and is largely prevalent in low valence organometallic type compounds (21). The bicapped tetrahedron is mentioned as it has some relevance to the current work, but will be discussed no further.

octahedral
(trigonal anti-prism)

trigonal
prismatic

bicapped
tetrahedron

Fig. 1.5 *The possible geometries of 6 coordinate complexes.*
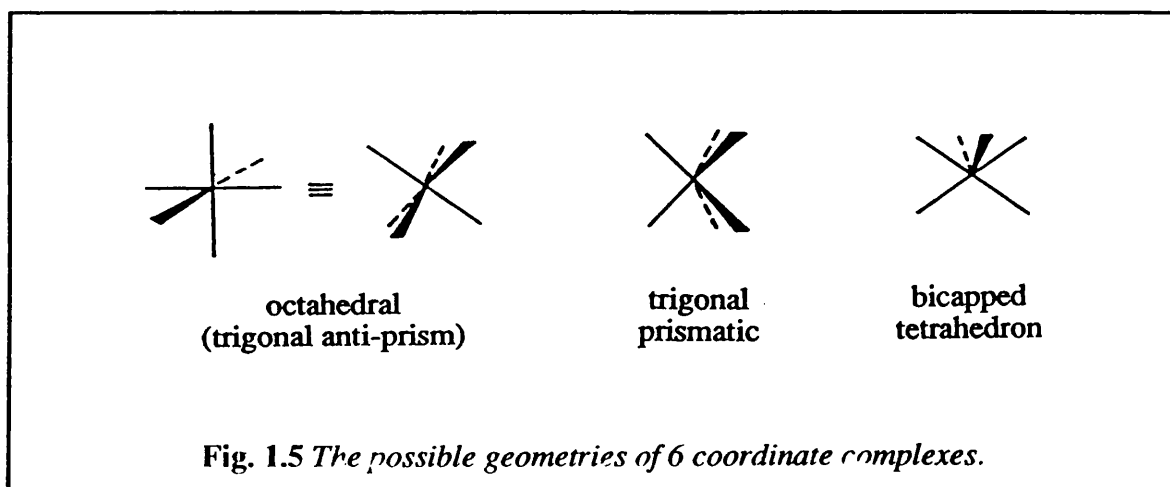
Trigonal prismatic co-ordination geometry is rare and for several decades the only known examples were MoS_2 and WS_2, which are ionic solids and have an infinite lattice structure. The presence of a trigonal prismatic (TP) intermediate in the racemisation mechanism of tris-chelate complexes was proposed by Bailar (22), but the first reported example of TP co-ordination in a discrete molecular compound was as late as 1965. Eisenberg and Ibers (23) prepared a dithiolato complex of rhenium, which displayed

almost perfect trigonal prismatic geometry. Several other dithiolato and diselenato trigonal prismatic complexes have since been prepared.

The stereochemical preference of a transition metal ion for one co-ordination geometry to another is determined by several factors. For six coordinate complexes (to which this argument is limited) inter-ligand repulsion usually results in octahedral co-ordination. An early study (24) demonstrated that with trigonal prismatic geometry metal-ligand bonding is increased. This study also confirmed that ligand-ligand repulsion is considerably greater in the trigonal prism compared with the octahedron. The destabilising effect of the increased ligand-ligand repulsion is usually larger than the increase in metal-ligand bonding. Thus for six unidentate ligands, octahedral co-ordination will result. This argument does not take into account π-bonding ligands. Deviation from this behaviour is only seen in cases where there are other (thermodynamic) reasons, examples being; first order Jahn-Teller tetragonal distortion in d^4 and d^9 ions and trigonal prismatic coordination in $W(Me)_6$ (25) and $[Zr(Me)_6]^{2-}$ (26), due to a second order Jahn-Teller distortion. This later effect has been shown by Wang and co-workers (27) to indicate that in 6 coordinate d^0 systems with non-bulky covalently bound ligands C_{3v} symmetry is in the prefered symmetry . With CrH_6 this results in the C_{3v} case being 17.5 kcal mol^{-1} more stable than D_{3h}, which is in turn 157 kcal mol^{-1} more stable than the O_h situation.

The Ti : twist angle (ϕ) of a six-coordinate complex with three fold symmetry is illustrated in fig.1.6. The angle is defined as 0° for a regular octahedron and 60° for a trigonal prism. It is important to note that polar angles (angles measured from the C_3 axis to donor atoms) remain constant during twisting processes.

The variation of d-orbital energies with twist angle have been calculated by three independent groups. Gillum et al. used an ionic model (28), Larsen et al. by angular overlap model treatment (29), and by Hoffmann et al. via an extended Huckel calculation (21). These studies will not be explicitly examined, but their general results will be used later in the interpretation of electronic spectra and crystal structure data.
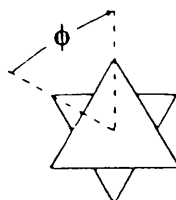
Fig.1.6 *Definition of twist angle (ϕ) in trigonal complexes.*

A qualitative one electron energy level diagram is displayed in fig 1.7. (21) . This shows how d-orbital energies are affected as the geometry of a six-coordinate complex is twisted from octahedral to trigonal prismatic. Most importantly it is seen that the lower t_{2g} level becomes split into a'_1 and e' levels; and that the overall d-orbital splitting ($e_g - t_{2g}$ $\{O_h\}$; $e'' - a'_1$ $\{D_{3h}\}$) is greater in the octahedral environment than in the trigonal prismatic. The reduction in d-orbital splitting will reduce the value of ligand field stabilisation energies in trigonally distorted complexes compared to their octahedral analogues.
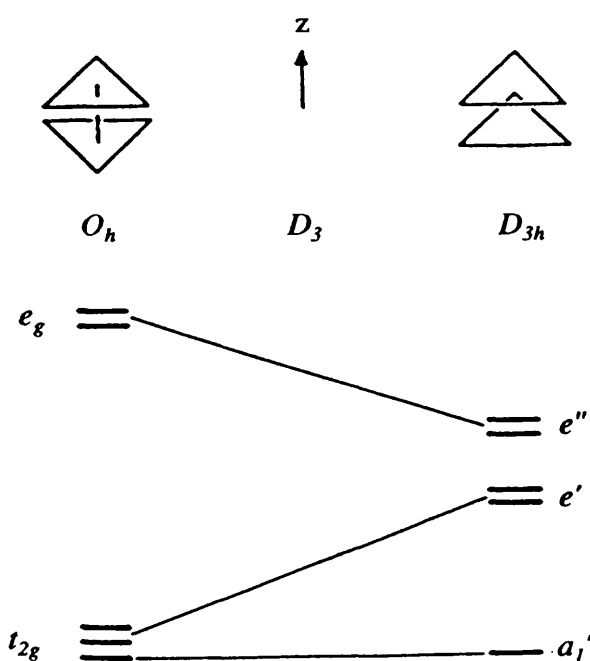
Fig. 1.7. *Ordering of energy levels in octahedral and trigonal prismatic ligand fields.*

This diagram represents the fate of pure d-orbitals and no account of metal-ligand orbital mixing is taken into account. The coordinate system is not that used in the normal consideration of octahedral complexes, since in D_{3h} symmetry d-orbitals no longer lie on the normal Cartesian axes. Thus e_g in the octahedral environment is now labelled as d_{xz} and d_{yz} instead of the normal $d_{x^2-y^2}$ and d_{z^2}. Hence, it can be seen that d_{z^2} is almost unaffected by the trigonal twist. This diagram immediately implies that low-spin d^6 will tend to be octahedral.

The variation of the d-orbital energies with increasing twist angle is shown in fig. 1.8 (28). This quantitatively verifies fig.1.7 and from the diagram final d-orbital energies (twist angle $= 60°$) can be obtained:

$$E(e'') = E(d_{xz,yz}) = 8/3 \ Dq$$

$$E(e') = E(d_{x^2-y^2}, d_{xy}) = -2/3 \ Dq$$

$$E(a_1') = E(d_{z^2}) = -4 \ Dq$$
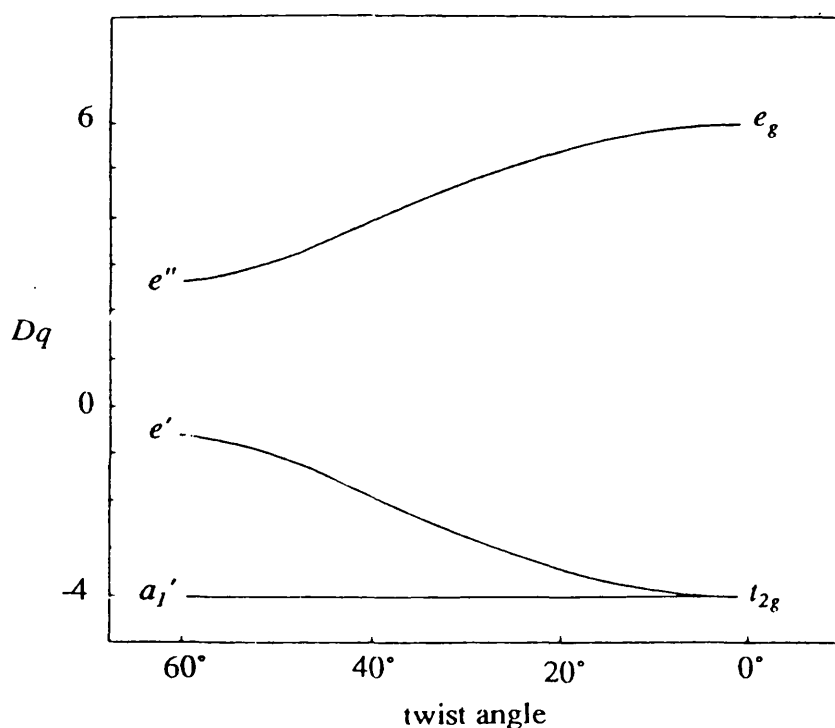
Fig.1.8. *Variation of d-orbital energy with changing twist angle.*

In certain cases an increase in twist angle of a complex will have no effect on the overall energy. These cases include those in which all the d-orbitals are equally occupied (d^0, high-spin d^5 and d^{10}). Also, since the energy of d_{z^2} is independent of twist angle, d^1 and low-spin d^2 ions will suffer no loss of LFSE on twisting from octahedral to trigonal prismatic geometry. Gillum *et al.* also calculated the variation of LFSE with twist angle. fig 1.9 displays the plot of ΔLFSE *versus* d-orbital configuration. ΔLFSE is defined as $LFSE_{octahedron} - LFSE_{trigonal prism}$, and it can be seen that the greatest loss of LFSE is in the d^6 case as expected from fig 1.7.

Fig.1.9. *Plot of ΔLFSE against d-orbital occupation.*
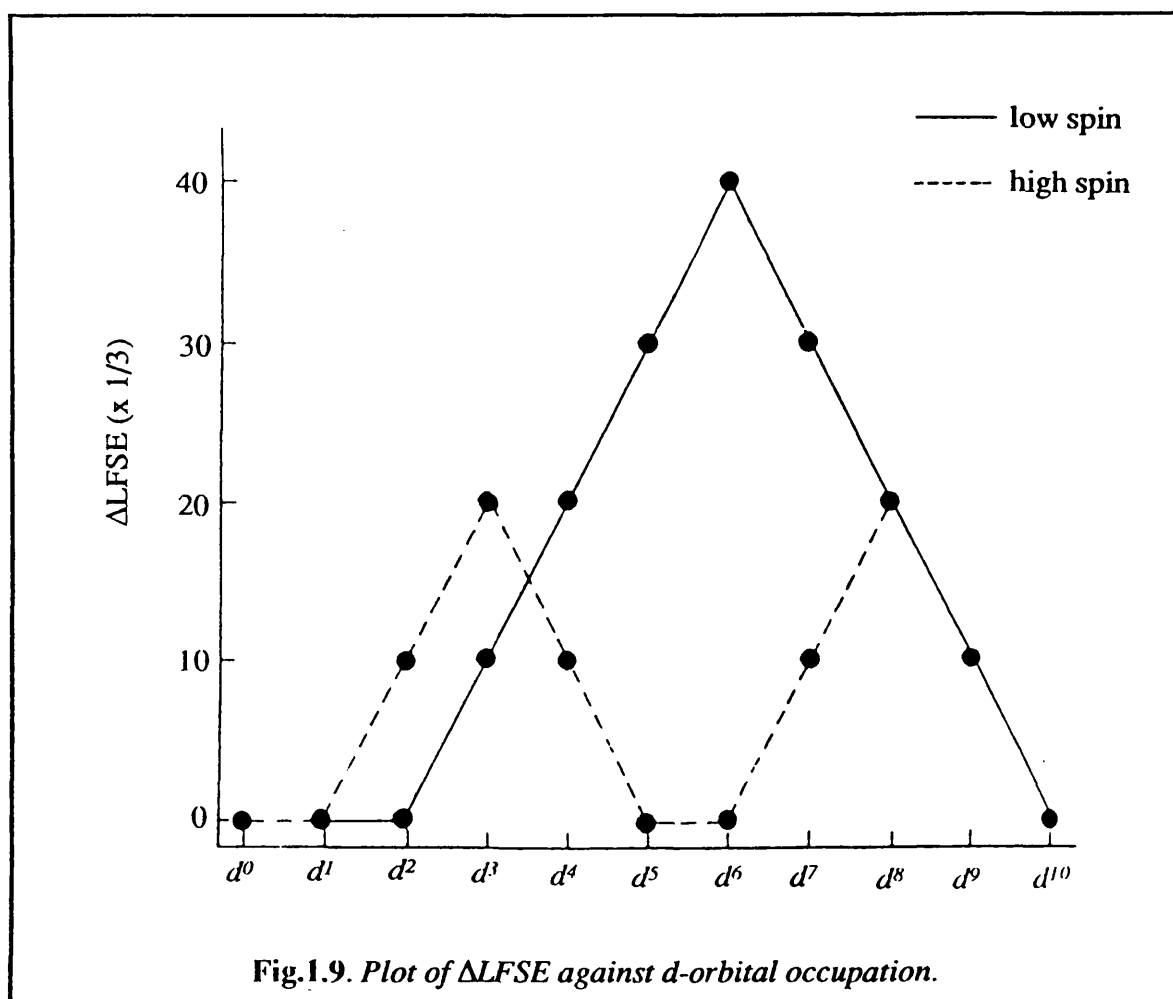
When discussing the energetics of stereochemical enviroments, the maxim of minimising non-bonding and maximising bonding interactions is the principal argument. Of course, bonding interactions include those between the ligand(s) and the metal centre,

but must also include those between the atoms of the ligand(s) themselves. This becomes of paramount importance when considering macrocyclic ligand systems, since by their very nature they contain many intramolecular bonding (and non-bonding repulsive) interactions. In a non-macrocyclic complex the bonding and non-bonding interactions, other than ligand field stabilisation energies, will remain approximately constant for the octahedral and trigonal prismatic co-ordination geometries. Hence the sterochemical preferences of the metal centre determine coordination geometry. For a macrocyclic system coordination geometry will be determined by the stereochemical preferences of the ligand(s) *versus* the stereochemical preferences of the metal ion namely bonding and steric factors *versus* the maximisation of LFSE.

Wentworth *et al.* prepared a Schiff base derivative of 1,3,5-triaminocyclohexane by reaction with pyridine-2-carboxaldehyde. The ligand (py)$_3$tach was unusual in that it contained three essentially planar chelating subunits. The structure of the Zn(II) complex of (py)$_3$tach was determined (30) and was shown to be a trigonal prism with the cyclohexane derived donor set slightly compressed (fig.1.10). The twist angle was very large at 56° (note the author has adopted a twist angle definition different to that of early workers). Mn(II), Fe(II), Co(II) and Ni(II) complexes were also prepared. The x-ray powder patterns of the [Mn(py)$_3$tach]$^{2+}$ and [Co(py)$_3$tach]$^{2+}$ were identical to that of [Zn(py)$_3$tach]$^{2+}$, implying that these complexes were isostructural and hence had almost TP geometry. The zinc and manganese complexes are TP because as d^5 and d^{10} ions respectively, the metal centre has no stereochemical preference for octahedral or TP geometry. Thus the rigid planar donor units of the ligand dictate the coordination geometry. The trigonal coordination of the Co(II) complex may seem surprising since fig. 1.8 would indicate a considerable loss of energy upon the twisting of a d^7 ion from octahedral to trigonal prismatic geometry. Another example of Co(II) in a trigonal prismatic enviroment is Bertrand's trimeric cobalt complex (31), [(Co(III)(OCH$_2$CH$_2$NH$_2$)$_3$)$_2$Co(II)]$^{2+}$. The anomalous behaviour of these cobalt complexes can be understood if interelectron repulsion parameters (Racah B) are included in ligand field energy calculations. Again refering to the analysis of Gillum *et al.* (28),

Fig.1.10. *Structure of [Zn(II)(py₃tach)]²⁺.*
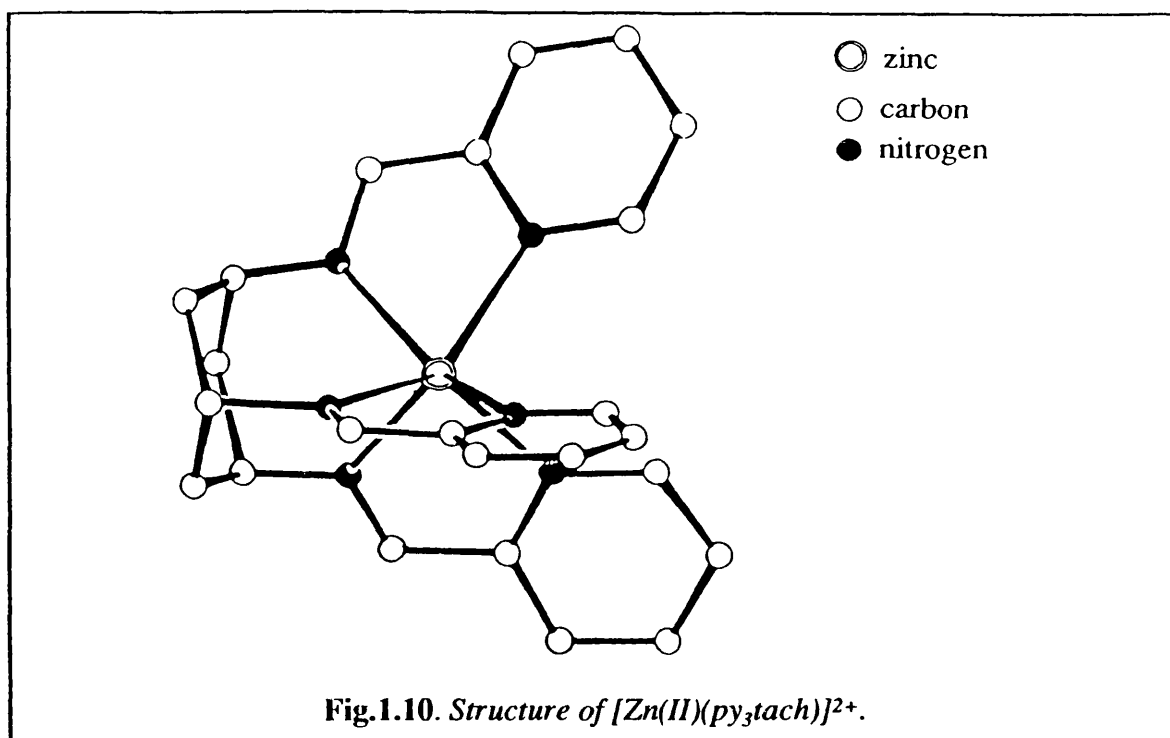
the difference between d-orbital energies in octahedral and trigonal prismatic fields for d^5 - d^{10} ions were calculated in terms of Dq and electron-electron repulsion parameters:

$$d^5 : E[(t_{2g})^3(e_g)^2] - E[(a'_1)^1(e')^2(e'')^2] = 0$$

$$d^6 : E[(t_{2g})^6] - E[(a'_1)^2(e')^4] = -40/3\ Dq - 10B$$

$$d^7 : E[(t_{2g})^5(e_g)^2] - E[(a'_1)^2(e')^3(e'')^2] = -10/3\ Dq + 3B$$

$$d^8 : E[(t_{2g})^6(e_g)^2] - E[(a'_1)^2(e')^4(e'')^2] = -20/3\ Dq - 3B$$

$$d^9 : E[(t_{2g})^6(e_g)^3] - E[(a'_1)^2(e')^4(e'')^3] = -10/3\ Dq$$

$$d^{10} : E[(t_{2g})^6(e_g)^4] \cdot E[(a'_1)^2(e')^4(e'')^4] = 0$$

It can be seen that for both low-spin d^6 and d^8 ions the inclusion of the Racah B parameter leads to an increased preference for octahedral geometry. In the case of the d^7 however, the interelectron repulsion is less in the TP field than in the octahedral field. Thus the loss of LFSE on twisting away from octahedral geometry is partially made up for by a reduction in interelectron repulsion. Churchill and Reis (32) demonstrated that the structure of Holm's (29) [Ni(II)(pccBF)][BF₄] (fig.1.11) was almost trigonal prismatic (twist angle = 58.5)°, with the chelating pyridyl-imino chelating units accurately planar. The structure of Fe(II)(pccBF)BF₄ was also determined (30), and this complex displayed

a twist angle of 39°. Low spin d^5 Fe(II) would be expected to be octahedral, but the ligand system cannot support octahedral coordination. The twist of the ligand away from TP coordination causes a loss of planarity in the pyidyl-imino side chain, and even a loss of planarity in the pyridine ring itself.
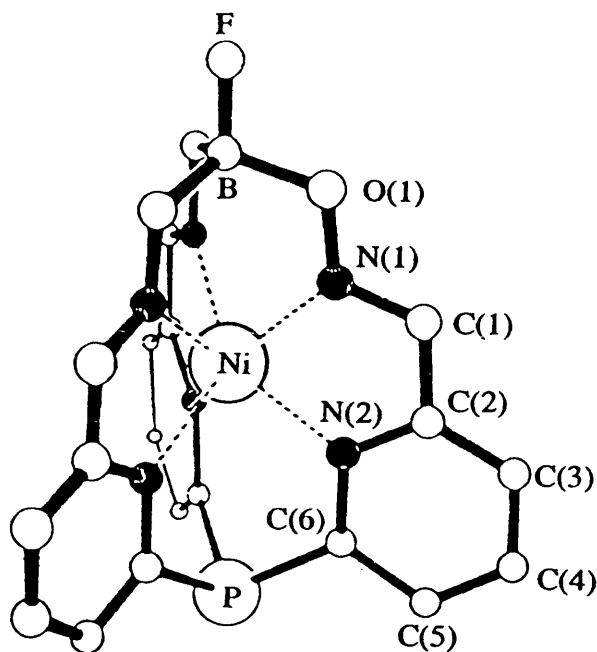
Fig.1.11. *Structure of* [Ni(pccBF)][BF$_4$].

Hoffmann (21) demonstrated that in the trigonal prism metal-to-ligand σ-bonding was sli̇ṭly greater than that of t'e octahedron, since in the TP case all five d-orbital participate in bonding. This effect depends upon the d-orbital energy, and is greatest for low lying d-orbitals. The energy of any orbital decreases as the atomic number increases (34). Hence trigonal prismatic coordination is slightly more favourable with elements to the right of the transition series. This partly explains the TP geometry of Ni(II)(pccBF)+, although the conformational rigidity of the ligand is the dominant factor. It must be remembered that d^0 and d^1 (and low-spin d^2) ions will also tend to be TP since d_{z^2} does not change in energy with increasing twist angle. In these cases ligand stereochemistry and metal ionic radius will determine geometry.

(1.5) OBJECTIVES

There is currently a great deal of interest in transition metal complexes of macrocyclic ligands. Much work has been done in varying the size and donor atom type in a number of macrocyclic systems. However, few results have been published which involve triazamacrocycles and less still with pendant-arm ligands. Also the coordination chemistry of alcohols is very limited, despite the potential biological relevance to metalloproteins and enzymes with serine and threonine residues at their reactive centres.

The project goal was to prepare a number of tris alcohol substituted triazamacrocycles, giving a series of ligands with an N_3O_3 donor set. With pendant-arm macrocycles it is possible to vary the steric properties in two ways. Firstly the ring size may be changed. This leads to the possibility of variable size-match selectivity and greatly affects the intramolecular properties of the complex. Secondly, the degree of substitution, and hence steric bulk of the pendant-arms may be varied. This will drastically alter the intermolecular interaction of the complexes with solvents and with other complexes. By altering the steric properties of transition metal complexes, the balance between the stereochemical requirements of the ligands and those of metals can be investigated. With alcohol donors there is also the possibility of deprotonation resulting in metal alkoxide complexes. There are many publications detailing complexes of phenoxide based complexes, but far fewer transition metal alkoxide complexes have been investigated.

The ligands prepared were optically pure. This has the advantages of producing non-racemic complexes which are more readily purified, and permits characterisation by circular dichroism spectroscopy.

The material is ordered by preference of a metal ion to tend towards octahedral coordination geometry. Namely metals which display strong preference for octahedral coordination (chromium and manganese) are discussed together, as are those showing a weak preference (cobalt, nickel and copper) and those with no electronic preference towards octahedral or trigonal geomteries (titanium and zinc).

References

1. Curtis, N.F. *J. Chem. Soc.*, **1960**, 4409.

2. Pedersen, C.J. *J. Am. Chem .Soc.*, **1967**, *89*, 7017.

3. Deiderich, B.; Lehn, J.M.; Sauvage, J.P. *Tetrahedron Letters.*, **1969**, *34*, 2885.

4. Barefield, E.K.; Wagner, F.; Herlinger, A.W.;Dahl, A.R. *Inorg. Synth.*, 16, 220.

5. Sellmann, D.; Zapf, L. *J. Organomet. Chem.*, **1985**, *289*, 57.

6. Koyama, H.; Yoshino, T. *Bull. Chem. Soc. Jpn.*, **1972**, *45*, 481.

7. Richman, J.E.; Atkins, T.J. *J. Am. Chem. Soc.*, **1974**, *96*, 2268.

8. Briellmann, M.; Kaderli, S.;Meyer, C.J.; Zuberbuhler, A.D., *Helv. Chim. Acta*, **1987**, *70*, 680

9. Tsuboyama, S., Sakurai, T., Tsuboyama, K. *J. Chem. Soc. Dalton Trans.*, **1987**, 721

10. Alder, R.W.; Mowiam, R.W.; Vachon, D.J.; Weisman, G.R., *J. Chem. Soc. Chem. Commun.*, **1991**, 507

11. Chaudhuri, P.; Wieghardt, K. *Progress in Inorganic Chemistry*; Lippard, S.J., Ed.; Wiley: New York, 1988; Vol. 35, p 329

12. Auerbach, U.; Eckert, U.; Weighardt, K.; Nuber, B.; Weiss, J. *Inorg. Chem.*, **1990**, 29, 938

13. Hammershoi, S.A.; Sargeson, A.M. *Inorg. Chem.*, **1983**, *22*, 3554

14. Cole, E.; Parker, D.; Ferguson, G.; Gallagher, J.F.; Kaitner, B., *J. Chem. Soc. Chem. Commun.* **1991**, 1473

15. Sayer, B.A.; Michael, J.P.; Hancock, R.D. *Inorg. Chim. Acta.*, **1983**, *77*, L63

16. Alcock, N.W.; McLaren, F.; Moore, P.; Pike, G.A; Roe, S.M., *J. Chem. Soc. Chem. Commun.* **1989**, 798.

17. Ziessel, R.; Lehn, J.-M. *Helv. Chim. Acta.*, **1990**, *73*, 1149.

18. Peacock, R.D.; Robb, J. *Inorg. Chim. Acta.*, **1986**, *121*, L15.

19. M.J. van der Merwe, J.C.A. Boeyens, R.D. Hancock, *Inorg. Chem.*, **1983**, *22*, 3490

20. Koppen, M.;Swiridorff, W.; Wieghardt, K.;Weiss, J. *J. Chem. Soc., Dalton Trans.*, **1983**, 1869

21. Hoffmann, H.R.; Howell, J.M.;Rossi, A.R. *J. Am. Chem. Soc.*, **1976**, *98*, 2484

22. Bailar, J.C. *J.Inorg. Nucl. Chem.*, **1958**, *8*, 165

23. Eisenberg, R.; Ibers, J.A. *J. Am. Chem. Soc.*, **1965**, *87*, 5798

24. Hultgren, R. *Phys. Rev.*, **1932**, *40*, 891

25. Haaland, A.; Hammel, A.; Rypded, K.; Volden, H.V. *J. Am. Chem. Soc.*, **1990**, *112*, 4547

26. Morse, P.M.; Girolami, G.S. *J. Am. Chem. Soc.*, **1989**, *111*, 4114

27. Wang, S.K.; Albright, T.A.; Eisenstein, O. *Inorg. Chem.*, **1989**, *28*, 1611

28. Gillum, W.O.; Wentworth, R.A.D.; Childers, R.F. *Inorg. Chem.*, **1970**, *9*, 1825

29. Larsen, E.; La Mar, G.N.; Wagner, B.E.; Holm, R.H. *Inorg. Chem.*, **1972**, *11*, 2052

30. Gillum, W.O.; Huffman, J.C.; Steib, W.E.; Wentworth, R.A.D. *J. Chem. Soc. Chem. Commun.*, **1969**, 843

31. Bertrand, J.A.; Kelly, J.A.; Vassien, E.G. *J. Am. Chem. Soc.*, **1969**, 2394

32. Churchill, M.R.; Reis, A.H. *J. Chem. Soc. Chem. Commun.*, **1970**, 879

33. Churchill, M.R.; Reis, A.H. *J. Chem. Soc. Chem. Commun.*, **1971**, 1307

34. Cotton, F.A.; Wilkinson, G. Advanced Inorganic Chemistry. 4th ed., Wiley, 622

CHAPTER 2

EXPERIMENTAL

"I like work. I could watch it all day."

Robert Nye, Faust.

"May all your doughnuts turn out like Fanny's"

Johnny Craddock

CONTENTS

(2.1) INSTRUMENTATION

(2.1.1) General

U.V.-visible spectra were obtained using a Perkin-Elmer Lambda 9 spectrophotometer. Reference and sample spectra were obtained in a TSL 1 cm semi-micro far-U.V. quartz cuvette. Corrected spectra were produced by sample-reference subtraction using the Perkin-Elmer PECSS suite of programs.

One-and two-dimensional NMR spectra were obtained on Perkin-Elmer RS 32 and Varian EM390 (90 MHz, continuous wave); and Bruker AM 200 and WP 200 spectrometers (200 Mhz, FT-NMR) using the Bruker Aspect 3000 suite of programs. All samples are referenced internally to solvent resonances. Deuterated solvents were purified by freeze-thaw degassing and stored under a nitrogen atmosphere, over 4Å molecular sieves.

FT-infra-red spectra were obtained on a Philips FTIR spectrometer. All samples were prepared as 8 mm diameter KBr discs using 300 mg of KBr and a press force of 8 tons.

(2.1.2) Magnetic Susceptibility Measurements

Magnetic susceptibilities were kindly determined by Dr. Phalguni Chaudhuri and Professsor Karl Weighardt (Ruhr-Universität, Bochum). Measurements were made in the temperature range 2.0-295 K using a SQUID magnetometer (MPMS, Quantum Design). The sample material was contained in a 4 mm quartz cell. Diamagnetic corrections for the sample holder and diamagnetic atoms were made using Pascal's constants and data was manipulated using standard instrument software.

(2.1.3) Circular Dichroism Spectrometer

Circular dichroism spectra were recorded using an instrument based upon a Jobin Yvon 0.6 m scanning monochromator. Light from a xenon arc lamp source is focused by a parabolic reflector and passes through the monochromator. The light is then polarised in the vertical plane by a Rochon quartz prism. Circularly polarized radiation is produced by passage through a photo-elastic modulator (PEM) which then passes through the sample in a quartz cuvette. The signal is detected at a photomultiplier tube, with phase sensitive detection achieved by a lock in amplifier referenced to the power supply of the PEM.

The PEM is central to the operation of the spectrometer. Plane polarised light can be viewed as a superposition of right and left cicularly polarised components, and is passed through a bar shaped crystal of calcium fluoride or silica. This crystal is periodically compressed and rarefied by the attachment of quartz piezoelectric elements which are excited by the modulator power supply at a frequency of approximately 50 kHz, (sinusoidal wave form), producing a periodically varying birefringence. This arises as a result of a periodic variation of the refractive indices of light in the x and y directions. The crystal is orientated such that the plane of the polarised light is at 45° to the fast and slow axes (x and y) of the crystal. This induced birefringence causes an accumulating phase difference between the x and y electric vector components of light passing through the crystal. The frequency of modulation is chosen such that the phase difference between the left and right components is 90° (i.e. quarter wave modulation). As the monochromator scans through light of decreasing wavelength the frequency of modulation is also adjusted to maintain quarter wave modulation.

(2.2) X-RAY CRYSTALLOGRAPHIC DATA COLLECTION

All crystallographic data was kindly obtained by Dr Louis J. Farrugia. Crystals were mounted in a general position on a glass fibre. Data were collected at ambient temperature on an Enraf-Nonius CAD4F automated diffractometer in the $\theta/2\theta$ scan mode, using graphite monochromated X-radiation (λ=0.71069 Å). Unit cell dimensions were determined using the SET4 routine by refinement of the setting angles ($11<\theta<13$), averaging angles from 4 diffracting positions. All calculations were performed on a MicroVAX 3600 computer using the Glasgow GX suite of programs.

(2.3) MATERIALS AND SOLVENTS

Chemicals, their suppliers and purity used in preparative work are listed in table 2.1. Solvents and purification methods are listed in table 2.2.

Table 2.1 Chemicals and suppliers.

(S)-Alanine (Lancaster)	99%
Butane-1,4-diol (Aldrich)	99%
Calcium hydride (Aldrich)	95+%
Chromium Chloride, sublimed, anhydrous (Aldrich)	99%
Cobalt Nitrate.6H$_2$O (Hopkin & Williams)	99%
Copper nitrate.3H$_2$O (Riedel de Haen)	99%
Diethylenetriamine (BDH)	99%
Ethane-1,2-diol (BDH)	99+%
Hexane-1,6-diol (Aldrich)	99%
3,3'Iminobispropylamine (Aldrich)	99%
Lithium aluminium hydride, powder (Aldrich)	95%

Manganese chloride.4H$_2$O (BDH)	99%
Nickel Nitrate.6H$_2$O (Aldrich)	99.999%
Pentane-1,5-diol (Aldrich)	97%
Propane-1,3-diol (BDH)	98%
(S)-Propylene oxide (Fluka)	99%
Sodium hydride[a]	60%
Sodium nitrite (BDH)	97+%
Triethylamine (Prolabo)	99%
p-Toluene sulphonyl chloride (Lancaster)	98%
(S)-Valine (Lancaster)	99%
Vanadium metal, powder (Goodfellow)	99.99%
Zinc nitrate.6H$_2$O (BDH)	99+%

a Dispersion in oil

All reagents were used without further purification, unless otherwise noted.

Table 2.2. Solvents and purification methods.

Absolute Ethanol	Twice distilled from magnesium turnings and iodine, under nitrogen, and stored over 4Å sieves.
Acetonitrile	Freshly distilled from calcium hydride under nitrogen.
Diethyl ether	Distilled under nitrogen from sodium benzophenone ketal.

Dimethyl formamide	Stored over calcined calcium oxide and then distilled in vacuo. Stored over 4Å sieves.
40-60°C Petroleum Ether	Distilled under nitrogen from sodium/potassium alloy.
Pyridine	Distilled from potassium hydroxide
Tetrahydrofuran	Distilled under nitrogen from sodium benzophenone ketal.

Dimethyl formamide supplied by Aldrich is sufficiently dry for macrocycle preparation if stored over activated 4Å sieves for several days prior to use. All other solvents were of technical grade, and unless otherwise noted used without further purification

(2.4) LIGAND SYNTHESIS

(2.4.1) Tri-aza Macrocycles

The syntheses presented are based upon the Richman and Atkins (1) modification of the method of Koyama and Yoshino (2).

(A) Bissulphonate Esters.

$$HO(CH_2)_xOH + TsCl \quad \text{-------->} \quad TsO(CH_2)_xOTs \qquad x = 2 - 6$$
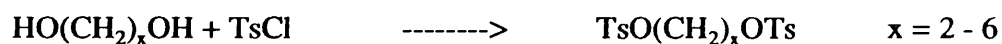
Method (1). The diol was dissolved in dry pyridine (10 ml/g of diol) followed by the addition of 5 equivalents of tosyl chloride at 0°C. The mixture was refrigerated overnight, poured into ice cold 1 M HCl, filtered, washed with copious volumes of water

and then recrystallised by dissolution in dichloromethane followed by the addition of 4 volumes of methanol.Yields 60-80%

Method(2). The diol was dissolved in dry triethylamine (5 ml/g of diol) and 2.2 equivalents of tosyl chloride was slowly added in small portions, with stirring, over a period of 2 hours. The mixture began to solidify and the solution was stirred for another 1 h. Methanol was then added and the product was broken up with a spatula, filtered and washed with a large volume of ethanol. The material was recrystallised as above. Yields 40-70%.

(i) 1,2-Bis[(p-tolylsulphonyl)oxy]ethane.

^{1}H NMR (CDCl$_3$) : δ=2.50 (s, 6H, Ar-C$\underline{H}_3$); δ=4.42 (s, 4H, -C$\underline{H}_2$-); δ=7.58 (dd, 8H, Ar-$\underline{H}$).

(ii) 1,3-Bis[(p-tolylsulphonyl)oxy]propane.

^{1}H NMR (CDCl$_3$) : δ=1.95 (q, 2H, -CH$_2$C$\underline{H}_2$CH$_2$-, J=6.1); δ=2.41 (s, 6H, Ar-C$\underline{H}_3$); δ=4.02 (t, 4H, TsOC$\underline{H}_2$, J=6.02); δ=7.51 (dd, 8H, Ar-$\underline{H}$, J=8.4)

(iii) 1,4-Bis[(p-tolylsulphonyl)oxy]butane.

^{1}H NMR (CDCl$_3$) : δ=1.53 (m, 4H, -C$\underline{H}_2$-); δ=2.47 (s, 6H, Ar-C$\underline{H}_3$); δ=4.01 (dd, 8H, TsO-C$\underline{H}_2$-); δ=7.54 (dd, 8H, Ar-$\underline{H}$).

(iv) 1,5-Bis[(p-tolylsulphonyl)oxy]pentane.

^{1}H NMR (CDCl$_3$) : δ=1.35 (m, 2H, C$\underline{H}_2$-); δ=1.49 (m, 4H, -C$\underline{H}_2$-); δ=2.44 (s, 6H, Ar-C$\underline{H}_3$); δ=4.00 (t, 4H, TsOC$\underline{H}_2$); δ=7.61 (dd, 8H, Ar-$\underline{H}$).

(v) 1,6-Bis[(p-tolylsulphonyl)oxy]hexane.

^{1}H NMR (CDCl$_3$) : δ=1.28 (m, 4H, -C$\underline{H}_2$-); δ=1.65 (m, 4H, -C$\underline{H}_2$-); δ=2.45 (s, 6H, Ar-C$\underline{H}_3$); δ=3.98 (t, 4H, TsOC$\underline{H}_2$); δ=7.60 (dd, 8H, Ar-$\underline{H}$).

N,N',N''-Tris(p-tolylsulphonyl)diethylenetriamine and N,N',N''-tris-(p-tolylsulphonyl)-3,3'iminobispropylamine.

H$_2$N(CH$_2$)$_y$NH(CH$_2$)$_z$NH$_2$ + TsCl   -------->

TsHN(CH$_2$)$_y$NTs(CH$_2$)$_z$NHTs   y = z = 2; y = z = 3

(i) N,N'N''-Tris(p-toluenesulphonyl)-diethylenetriamine. A 5 L beaker was equipped with a mechanical stirrer and a 2 L dropping funnel. The beaker was charged with 54.3 g (0.526 mol) diethylene triamine and 60 g (1.5 mol) of sodium hydroxide dissolved in 2 L of distilled water. The solution was vigorously stirred and 300 g (1.57 mol) of tosyl chloride dissolved in 2 L of diethyl ether was added dropwise over a period of 2 h. Stirring must be sufficiently vigorous to ensure adequate mixing of the two reaction phases. After a total reaction time of 3 h most of the ether had evaporated and the reaction mixture began to solidify. Stirring was continued for 1 h and 750 ml of methanol was then added. After stirring for a further 15 mins. the solid product was filtered off and washed with copious volumes of water. The material was then washed with methanol (1 L), ether (500 ml) and air-dried. Yield 201 g (67 %). m.p. 173-174°C.

^{1}H NMR (CDCl$_3$) : δ=2.41 (s, 3H, Ar-C$\underline{H}_3$); δ=2.58 (s, 6H, Ar-C$\underline{H}_3$); δ=2.95 (m, 4H, N-C$\underline{H}_2$); δ=3.10 (m, 4H, N-C$\underline{H}_2$); δ=7.45 (m, 12H, Ar-$\underline{H}$).

(ii) N,N,N''-Tris(p-toluenesulphonyl)-3,3'-iminobis-propylamine. The apparatus was similar to that used for N,N,N''-tris-(p-tolylsulphonyl)diethylenetriamine. 65.6 g (0.500 mol) of 3,3'-iminobispropylamine and 60 g (1.5 mol) sodium hydroxide were dissolved in 2 L of water. 286 g (1.5 mol). Tosyl chloride dissolved in 2 L of diethyl ether was added dropwise over a period of two hours. After addition was complete, a thick white oil began to separate out. Stirring was maintained for a further two hours and 1.5 L of methylene chloride was added to redissolve the white oil. The layers were separated and the aqueous layer was discarded. The organic layer was washed with sodium hydroxide (5M, 2x300 ml), hydrochloric acid (6M, 2 x500 ml) and water (3x500 ml). All aqueous layers were discarded. The organic layer was dried ($MgSO_4$) and solvent volume was reduced to 500 ml on a rotary evaporator. The solution was then allowed to slowly evaporate in a fume hood. After several days massive lustrous white crystalline deposits of the required product formed. Before evaporation was complete the material was broken up, filtered and quickly washed with small portions of cold methylene chloride. The material was then air-dried. Yield 211 g (71 %). m.p. 112-114°C.

^{1}H NMR ($CDCl_3$) : δ=1.75 (m, 4H, C$\underline{H}_2$); δ=2.22 (s, 3H, Ar-C$\underline{H}_3$); δ=2.46 (s, 6H, Ar-C$\underline{H}_3$); δ=2.97 (m, 4H, N-C$\underline{H}_2$); δ=3.13 (m, 4H, N-C$\underline{H}_2$); δ=7.75 (m, 12H, Ar-$\underline{H}$).

(C) N,N',N''-Tris(p-tolylsulphonyl)-triazacycloalkanes

(i) N,N',N''-Tris-(p-tolylsulphonyl)-1,4,7-triazacyclononane. A 5 L three necked round bottomed flask (flattened base) was fitted with a nitrogen inlet/outlet, a magnetic stirring bar, thermometer and an oil bath. The flask was purged with nitrogen and charged with 141.43 g (0.250 mol.) N,N',N''-tris(p-tolylsulphonyl)-diethylenetriamine dissolved in 2750 ml of dry DMF. The stirrer is started and 40 g (1.0 mol.) of sodium hydride (60% suspension in oil) was added in small portions over a period of 1 h., with a flow of nitrogen maintained throughout. Once the initial effervescence had ceased the

temperature was raised to 70°C and maintained for one hour (during this period a 5 L three necked round bottomed flask was equipped with a nitrogen inlet, a large filter funnel (with a pad of celite 535) and an adapter connected to a water aspirator). Once hydrogen evolution had ceased the warm solution was filtered with suction into the second flask under a strong flow of nitrogen. The initial reaction vessel was cleaned, dried and equipped with a large (5 cm) teflon coated stirring bar, a 1 L dropping funnel, a nitrogen inlet/outlet, an oil bath and a thermometer. The filtered solution was transferred rapidly under a strong flow of nitrogen to this flask and heated to 110°C. 92.61 g of 1,2-bis[(p-tolylsulphonyl)oxy]ethane dissolved in 1000 ml of dry DMF was then added dropwise over a period of 2 h. The solution was stirred for a further 4 h. maintaining heating throughout. The solution was allowed to cool and then reduced in volume to approximately 1 L (rotary evaporator; the recovered DMF was used again after storage over 4Å sieves). The solution was added slowly (dropping funnel) to 2 L of water in a large beaker whilst stirring with a glass rod to break up any lumps that have formed. The solid was then filtered off and washed with water (4x500 ml), methanol (3x250 ml) and ether (3x250 ml). Once dry the product was recrystallised by dissolution in the minimum volume of hot chloroform (the solution occasionally remained a little cloudy) followed by the addition of three volumes of cold ethanol. The solution was cooled to 0°C. Crystallisation commenced after 1 h. and was completed by refrigeration overnight. The product was collected by filtration and washed with ice-cold ethanol (2x200 ml) and ether (4x200ml). The product was recrystallised twice more, repeating the above procedure. Once dry the product was an off-white solid. Yield 84.21 g (56 %).

^{1}H NMR (CDCl$_3$) : δ=2.18 (s, 9H, Ar-C$\underline{H}_3$); δ=3.17 (s, 12H, N-C$\underline{H}_2$); δ=7.31 (dd, 12H, Ar-$\underline{H}$).

(ii) N,N',N"Tris(p-tolylsulphonyl)-1,4,7-triazacyclodecane. The procedure was analogous to that for N,N',N"-Tris-(p-tolylsulphonyl)-1,4,7-triazacyclononane except that the preparation was performed on a smaller scale. 70.72 g of N,N',N"-Tris-(p-

tolylsulphonyl)-diethylentriamine dissolved in 1400 ml of dry DMF was reacted with 20 g (0.5 mol.) of a 60% suspension of sodium hydride in oil. This was then reacted with 48.06 g of 1,3-bis[(p-tolylsulphonyl)oxy]-propane dissolved in 600 ml of dry DMF. Yield 38.62 g (51 %).

^{1}H NMR (CDCl$_3$) : δ=2.53 (m, 2H, -C$\underline{H}_2$-); δ=2.31 (s(b), 9H, Ar-C$\underline{H}_3$); δ=3.20 (m, 12H, N-C$\underline{H}_2$); δ=7.39 (m, 12H, Ar-$\underline{H}$).

(iii) N,N',N''-tris(p-tolylsulphonyl)-1,4,7-triazacycloundecane. The procedure was analogous to that for N,N',N''-tris(p-tolylsulphonyl)-triazacyclononane. 56.57 g N,N',N''-tris(p-tolylsulphonyl)-diethylenetriamine dissolved in 1100 ml of dry DMF was reacted with 16 g (0.4 mol.) of a 60 % suspension of sodium hydride. The resulting solution was then reacted with 39.85 g (0.1. mol.) of 1,4-bis[(p-tolylsulphonyl)oxy]butane dissolved in 500 ml of dry DMF. Yield 24.51 g (39 %).

^{1}H NMR (CDCl$_3$) : δ=2.14 (m, 4H, -C$\underline{H}_2$-); δ=2.40 (s(b), 9H, Ar-C$\underline{H}_3$); δ=3.25 (m, 12H, N-C$\underline{H}_2$); δ=7.45 (m, 12H, Ar-$\underline{H}$).

(iv) N,N',N''-tris(p-tolylsulphonyl)-1,4,7-triazacyclododecane. The procedure was analogous to that of N,N',N''-Tris-(p-tolylsulphonyl)-1,4,7-triazacyclononane. 84.86 g (0.15 mol.) of N,N',N''-tris-(p-tolylsulphonyl)-diethylenetriamine dissolved in 1600 ml of dry DMF was reacted with 24 g (0.6 mol.) of a 60 % suspension of sodium hydride in oil. The resulting solution was then reacted with 61.88 g (0.15 mol.) of 1,5-bis[(p-tolylsulphonyl)oxy]-pentane dissolved in 750 ml of dry DMF. Yield 33.21 g (34 %).

^{1}H NMR (CDCl$_3$) : δ=2.12 (m, 4H, -C$\underline{H}_2$-); δ=2.40 (s, 6H, Ar-C$\underline{H}_3$); δ=2.38 (s, 3H, Ar-C$\underline{H}_3$); δ=3.22 (m, 12H, N-C$\underline{H}_2$); δ=7.51 (m, 12H, Ar-$\underline{H}$).

(v) N,N',N''-tris(p-tolylsulphonyl)-1,4,7-triazacyclotridecane. The procedure was analogous to that of N,N',N''-Tris-(p-tolylsulphonyl)-1,4,7-triazacyclononane. 56.57 g (0.10 mol.) of N,N',N''-tris-(p-tolylsulphonyl)-diethylenetriamine dissolved in 1100 ml of dry DMF was reacted with 16 g (0.4 mol.) of a 60 % suspension of sodium hydride in oil. The resulting solution was then reacted with 41.25 g (0.10 mol.) of 1,6-bis[(p-tolylsulphonyl)oxy]-hexane dissolved in 500 ml of dry DMF. The crude product was dissolved in a minimum volume of cold methylene chloride. 3 volumes of cold methanol was added and the solution was refrigerated overnight. The resulting precipitate was then filtered off and discarded. An equivalent volume of ether was then added to the filtrate to precipitate the required product as a fine white powder. The product was filtered, washed with ether (5x50 ml) and air dried. Yield 18.91 g (29 %)

^{1}H NMR (CDCl$_3$) : δ=2.09 (m, 6H, -C$\underline{H}_2$-); δ=2.44 (s, 6H, Ar-C$\underline{H}_3$); δ=2.31 (s, 3H, Ar-C$\underline{H}_3$); δ=3.29 (m, 12H, N-C$\underline{H}_2$); δ=7.49 (m, 12H, Ar-$\underline{H}$).

(vi) N,N',N''-tris(p-tolylsulphonyl)-1,5,9-triazacyclododecane. The procedure was analogous to that of N,N',N''-Tris-(p-tolylsulphonyl)-1,4,7-triazacyclononane. 59.38 g (0.10 mol.) of N,N'N''-Tris(p-toluenesulphonyl)-3,3'-iminobis-propylamine dissolved in 1100 ml of dry DMF was reacted with 16 g (0.4 mol.) of a 60 % suspension of sodium hydride in oil. The resulting solution was then reacted with 38.45 g (0.10 mol.) of 1,3-bis[(p-tolylsulphonyl)oxy]-propane dissolved in 500 ml of dry DMF. Yield 28.67 g (45 %).

^{1}H NMR (CDCl$_3$) : δ=1.94 (m, 6H, -CH$_2$C$\underline{H}_2$CH$_2$-); δ=2.49 (s, 9H, Ar-C$\underline{H}_3$); δ=3.23 (m, 12H, N-C$\underline{H}_2$); δ=7.52 (dd, 12H, Ar-$\underline{H}$).

(vii) N,N',N''-tris(p-tolylsulphonyl)-1,5,8-triazacycloundecane. The procedure was analogous to that of N,N',N''-Tris-(p-tolylsulphonyl)-1,4,7-triazacyclononane. 29.69 g

(0.05 mol) of N,N'N"-Tris(p-tolyl-sulphonyl)-3,3'-iminobis-propylamine was dissolved in 600 ml of dry DMF and reacted with 8 g (0.2 mol.) of a 60 % suspension of sodium hydride in oil. The resulting solution was then reacted with 18.52 g (0.05 mol.) of 1,2-bis[(p-tolylsulphonyl)oxy]-propane dissolved in 300 ml of dry DMF. The reaction mixture was stirred overnight. Yield 18.34 g (59 %)

^{1}H NMR (CDCl$_3$) : δ=2.10 (m, 2H, -C$\underline{H}_2$-); δ=2.43 (s, 6H, Ar-C$\underline{H}_3$); δ=2.39 (s, 3H, Ar-C$\underline{H}_3$); δ=3.25 (m, 12H, N-C$\underline{H}_2$); δ=7.50 (m, 12H, Ar-$\underline{H}$).

(viii) N,N',N"-tris(p-tolylsulphonyl)-1,5,9-triazacyclotridecane. The procedure was analogous to that of N,N',N"-Tris-(p-tolylsulphonyl)-1,4,7-triazacyclononane. 29.69 g (0.05 mol) N,N'N"-Tris(p-tolyl-sulphonyl)-3,3'-iminobispropylamine was dissolved in 600 ml of dry DMF and reacted with 8 g (0.2 mol.) of a 60 % suspension of sodium hydride in oil. The resulting solution was then reacted with 19.92 g (0.05 mol.) of 1,4-bis[(p-tolylsulphonyl)oxy]-butane dissolved in 300 ml of dry DMF. The reaction mixture was stirred overnight. Yield 12.64 g (39%)

^{1}H NMR (CDCl$_3$) : δ=1.71 (m, 4H, -C$\underline{H}_2$-); δ=1.90 (m, 4H, -C$\underline{H}_2$-); δ=2.44 (s, 6H, Ar-C$\underline{H}_3$); δ=2.36 (s, 3H, Ar-C$\underline{H}_3$); δ=3.23 (m, 12H, N-C$\underline{H}_2$); δ=7.49 (m, 12H, Ar-$\underline{H}$).

(D) Triazacycloalkanes.

(i) [a] 1,4,7-Triazacyclononane. A 500 ml three necked round bottomed flask was equipped with a magnetic stirring bar, a nitrogen inlet/ outlet and an oil bath. The flask was then charged with 200 ml of conc. sulphuric acid and purged with nitrogen (20 mins.). 79.45 g (0.130 mmol.) of N,N',N"-tris-(p-tolylsulphonyl)-1,4,7-triazacyclononane was then added to the flask with stirring. The flask was heated to 115-120°C for 36-48 hours, whilst maintaining a nitrogen atmosphere. Caution was exercised in not allowing

the reaction temperature to rise above 120°C. The flask was allowed to cool and the reaction mixture was added dropwise with stirring to a *cooled* beaker containing 750 ml of ethanol. The 1,4,7-triazacyclononane polyhydrosulphate salt was precipitated as white floccules. 500 ml of ether was then added and the solution was refrigerated overnight. The precipitated grey/ brown solid was filtered off (glass microfibre paper) and washed with ether (3x100 ml). The solid was dissolved in a minimum amount of distilled water and the solution was basified to pH > 12 with 5 M aqueous sodium hydroxide. The solution was extracted with chloroform (3x250 ml) discarding the aqueous phase. The organic phase was dried ($MgSO_4$), filtered and the solvent removed (rotary evaporator) to give the required product as a viscous yellow oil. This was rapidly transferred (heating with an air gun was occasionally required) to a small Schlenk tube for storage. The oil rapidly solidified to form a crystalline mass. The material was best kept refrigerated. Yield 14.37 g (82 %)

^{1}H NMR ($CDCl_3$) : δ=2.28(s, C$\underline{H}_2$).

[b] 1,4,7-Triazacyclononane trihydrobromide. The procedure was similar to that for 1,4,7-Triazacyclononane except that once the polyhydrosulphate salt was dissolved in water, an equivalent volume of 48 % hydrobromic acid was added, and immediately a precipitate formed. The solution was refrigerated overnight to complete crystallisation. The solid was filtered and washed with small portions of cold 48 % hydrobromic acid, ethanol and ether. The product was air dried.

[c]   1,4,7-Triazacyclononane trihydrochloride. Once dry the 1,4,7-triazacyclononane trihydrobromide was dissolved in the minimum volume of boiling 36 % hydrochloric acid. The solution was allowed to cool and was refrigerated overnight. The product was filtered washed with cold 36 % hydrochloric acid, ethanol and ether and allowed to air dry. The product was usually recystallised twice more following the above procedure.

^{1}H NMR (D$_2$0) : δ=3.37 (s, C$\underline{H}_2$).

^{13}C NMR (D$_2$O) : δ=41.67 ($\underline{C}$H$_2$).

(ii) 1,4,7-Triazacyclodecane. The procedure was analogous to that for 1,4,7-triazacyclononane. 33.53 g (55 mmol.) of N,N',N"-tris-(p-tolylsulphonyl)-1,4,7-triazacyclodecane was reacted with 130 ml of concentrated sulphuric acid. The material crystallised as fine needles. Yield 4.66 g (58 %).

^{1}H NMR (CDCl$_3$) : δ=0.91 (m, 2H, -CH$_2$C$\underline{H}_2$CH$_2$-); δ=2.15 (m, 12H, N-C$\underline{H}_2$).

(iii) 1,4,7-Triazacycloundecane. The procedure was analogous to that for 1,4,7-triazacyclononane. 22.12 g (36 mmol.) of N,N',N"-tris-(p-tolylsulphonyl)-1,4,7-triazacycloundecane was reacted with 90 ml of concentrated sulphuric acid. Yield 2.25 g (40 %).

^{1}H NMR (CDCl$_3$) : δ=0.99 (m, 4H, -CH$_2$C$\underline{H}_2$C$\underline{H}_2$CH$_2$-); δ=2.12 (m, 12H, N-C$\underline{H}_2$).

(iv) 1,4,7-Triazacyclododecane. The procedure was analogous to that for 1,4,7-triazacyclononane. 31.29 g (49 mmol.) of N,N',N"-tr$^{...}$-(p-tolylsulphonyl)-1,4,7-triazacyclododecane was reacted with 120 ml of concentrated sulphuric acid. Yield 4.95 g (55 %).

^{1}H NMR (CDCl$_3$) : δ=2.17 (m, 12H, N-C$\underline{H}_2$); δ=1.17 (m, 4H,NCH$_2$-C$\underline{H}_2$-); δ=1.00 (m, 2H, -CH$_2$C$\underline{H}_2$CH$_2$-).
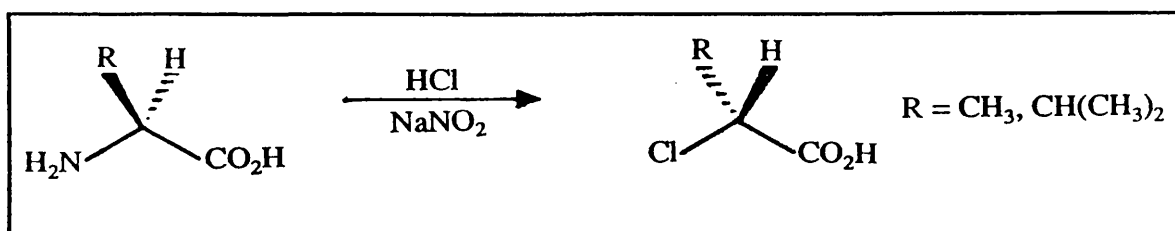
(v) 1,4,7-Triazacyclotridecane. The procedure was analogous to that for 1,4,7-triazacyclononane. 18.85 g (30 mmol.) of N,N',N"-tris-(p-tolylsulphonyl)-1,4,7-

triazacyclotridecane was reacted with 80 ml of concentrated sulphuric acid. Yield 1.34 g (25 %).

^{1}H NMR (CDCl$_3$) : δ=2.16 (m, 12H, N-CH$_2$); δ=1.20 (m, 4H,NCH$_2$-CH$_2$-); δ=0.95 (m, 4H, -CH$_2$CH$_2$CH$_2$CH$_2$-).

(vi) 1,5,9-Triazacyclododecane. The procedure was analogous to that for 1,4,7-triazacyclononane. 27.50 g (43 mmol.) of N,N',N"-tris-(p-tolylsulphonyl)-1,5,9-triazacyclodecane was reacted with 120 ml of concentrated sulphuric acid. Yield 3.12 g (41 %).

^{1}H NMR (CDCl$_3$) : δ=1.52 (m, 6H, -CH$_2$CH$_2$CH$_2$-); δ=2.63 (m, 12H, N-CH$_2$).

(vii) 1,5,8-Triazacycloundecane. The procedure was analogous to that for 1,4,7-triazacyclononane. 18.12 g (29 mmol.) of N,N',N"-tris-(p-tolylsulphonyl)-1,5,9-triazacyclodecane was reacted with 75 ml of concentrated sulphuric acid. Yield 2.74 g (59 %).

^{1}H NMR (CDCl$_3$) : δ=1.41 (m, 4H, -CH$_2$CH$_2$CH$_2$CH$_2$-); δ=2.33 (m, 12H, N-CH$_2$).

(viii) 1,5,9-Triazacyclotridecane. The procedure was analogous to that for 1,4,7-triazacyclononane. 12.30 g (19 mmol.) of N,N',N"-tris-(p-tolylsulphonyl)-1,5,9-triazacyclodecane was reacted with 120 ml of concentrated sulphuric acid. Yield 1.97 g (56 %).

^{1}H NMR (CDCl$_3$) : δ=1.63 (m, 8H, -CH$_2$-); δ=2.61 (m, 12H, N-CH$_2$).

(2.4.2) (R)-Methyl Oxirane and (R)-Isopropyl Oxirane

The syntheses of (R)-methyl oxirane and (R)-isopropyl oxirane were based upon the preparations of Koppenhoefer and Schurig (3,4). The preparation yields mono substituted oxiranes of high enantiomeric purity from commercially available α-amino acids bearing aliphatic side chains. The initial step is the preparation of (S)-2-chloroalkanoic acids by the diazotisation of alanine or valine in aqueous hydrochloric acid. Subsequent reduction with lithium aluminium hydride in ether affords (S)-2-chloroalkanols (chlorohydrins), which are cyclised to the appropriate oxirane using aqueous potassium hydroxide. The oxiranes are distilled as they are formed to prevent alkaline hydrolysis.

(A) (S)-2-Chloroalkanoic Acids.

$$R \quad H \qquad \xrightarrow[\text{NaNO}_2]{\text{HCl}} \qquad R \quad H \qquad R = CH_3, CH(CH_3)_2$$

$$H_2N \diagdown CO_2H \qquad\qquad Cl \diagdown CO_2H$$

(i) (S)-2-Chloropropionic acid. A 5 L, three necked, flattened base round bottomed flask was equipped with a 500 ml dropping funnel, a thermometer and a large (5cm) teflon coated stirring bar. The flask was charged with 89.1 g (1 mol.) of (S)-alanine dissolved in 1300 ml of 5 mol l^{-1} hydrochloric acid. The flask was cooled in an ice/salt bath (some alanine recrystallised from the solution, but redissolved as the reaction proceeded). Once the temperature had reached 5°C a pre-cooled solution of 110 g of sodium nitrite dissolved in 400 ml of water was added dropwise at a rate of 2 ml/ min (approximately 40 drops/ min.), maintaining cooling throughout. After a total reaction time of 5 h the ice bath was removed and the solution was allowed to stand overnight. The solution was transferred to a 5 L round bottomed flask which was then evacuated

with a water aspirator for 5 h to remove nitrogen oxides. During this period the solution changed from yellow to almost colourless. The solution was then stirred and 100 g of sodium carbonate was added in 4 portions. Once gas evolution had ceased, the reaction mixture was extracted with 4x400 ml portions of ether. The combined ethereal layers were reduced to 400 ml on a rotary evaporator at atmospheric pressure. The solution was then washed with 50 ml of brine, which was then extracted with 3 x 100 ml portions of ether. The combined organic layers were then dried over calcined calcium chloride for 24 h. The solution was filtered and the ether was removed on a rotary evaporator at atmospheric pressure (bath temperature 70°C), affording a yellow oily residue (67 g). The oil was distilled under reduced pressure (using a water aspirator) through a 5 cm vigreux column. A brown fraction was collected and discarded (b.p.< 85°C, 20 mm). The fraction distilling at 91-93°C (20 mm), was collected to give 64.5 g (59%) of the required product.

^{1}H NMR (CDCl$_3$) : δ=1.67 (d, 3H, -C$\underline{H}_3$,J=7.0); δ=4.41 (q, 1H, -C$\underline{H}$-CH$_3$); δ=11.97 (s, 1H, -CO$_2$H).

^{13}C NMR (CDCl$_3$) : δ=21.18 ($\underline{C}$H$_3$), δ=52.04 ($\underline{C}$H), δ=176.45 ($\underline{C}$O$_2$H).

(ii) (S)-2-Chloro-3-methylbutanoic acid. The procedure was analogous to that for (S)-2-chloropropionic acid except that 1900 ml of 5 mol l^{-1} hydrochloric acid was used to dissolve 93.73 g (0.8 mol) of (S)-valine, and 80 g of sodium carbonate was used in the neutralisation step. The product was distilled with no forerun (b.p. 143-145°C, 15 mm).Yield 66.4 g (60%).

^{1}H NMR (CDCl$_3$) : δ=1.04 (m, 6H, -CH(C$\underline{H}_3$)$_2$); δ=2.32 (m, 1H, -C$\underline{H}$(CH$_3$)$_2$); δ=4.16 (d, 1H, -C$\underline{H}$CL-CH(CH$_3$)$_2$, J=6.1); δ=11.31 (s(b), 1H, -CO$_2$$\underline{H}$)

^{13}C NMR (CDCl$_3$) : δ=17.71 (CH$_3$); δ=19.53 (CH$_3$), δ=32.41 (-CH(CH$_3$)$_2$); δ=63.66 (-CHCl-CO$_2$H), δ=175.65 (CO$_2$H)

(B) (S)-2-Chloroalkan-1-ols.
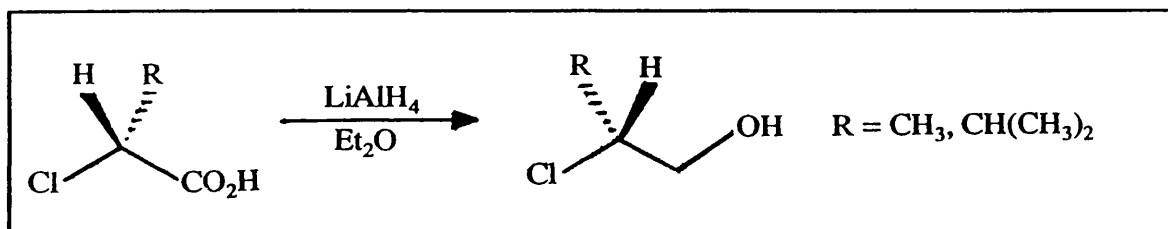
(i) (S)-2-Chloropropan-1-ol. A 2 L, three necked flattened base round bottomed flask was fitted with a 250 ml dropping funnel, stopper, large teflon coated stirring bar and an efficient double surface condenser. The dropping funnel was fitted with a nitrogen inlet and the condenser with a nitrogen outlet. The glassware was flame dried under a flow of nitrogen. Once cool, 11.5 g (0.3 mol) of lithium aluminium hydride was placed in the flask, followed by the slow addition (15 min) of 500 ml of dry diethyl ether. The suspension was then cooled to 0°C in an ice bath. A solution of 27.1 g of (S)-2-chloropropionic acid in 200 ml of dry diethyl ether was then added with vigorous stirring over 10 min. Caution was exercised to prevent the ether from refluxing too vigorously. After a total reaction time of 15 min (longer reaction times were to be avoided to prevent hydrogenolysis of the chlorine-carbon bond), 25 ml of water was cautiously added dropwise through the dropping funnel under a strong flow of nitrogen, with cooling and vigorous stirring. Once hydrogen evolution had ceased the reaction mixture was poured into a 3 L beaker containing 720ml of 1 mol l^{-1} sulphuric acid (72 g concentrated H$_2$SO$_4$ + 650 g of crushed ice) as rapidly as possible. Prolonged exposure of the chlorohydrin to basic conditions caused premature epoxide formation and reduction in yield. The ether layer was removed and retained. The aqueous layer was extracted with 2x250 ml portions of ether. The combined ether layers were washed with 50 ml of water, 50 ml of saturated
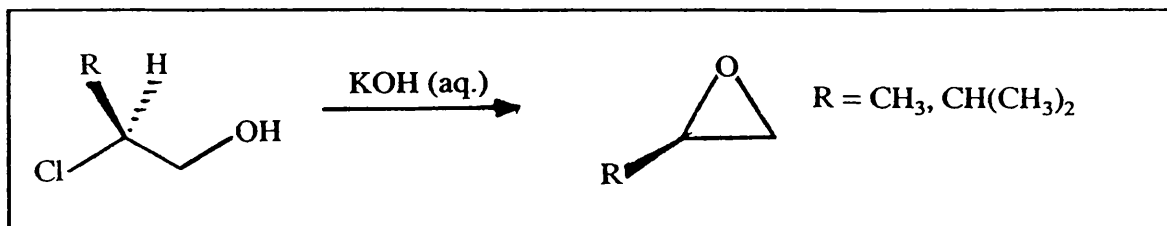
sodium carbonate solution and 50 ml of saturated sodium bicarbonate solution. Each of the aqueous layers were extracted with 2x50 ml portions of ether as quickly as possible to prevent epoxide formation. The combined ether layers were concentrated on a rotary evaporator at atmospheric pressure (bath temperature 50-60°C) to 400 ml, dried over sodium sulphate, filtered and concentrated at atmospheric pressure (rotary evaporator, bath temperature 60-70°C) to yield a pale yellow/green oil. It was important to remove all ether at this stage since it would have been difficult to remove ether from the low boiling epoxide final products. The oil was distilled at atmospheric pressure under nitrogen (15 cm vigreaux column) to give a colourless oil (b.p. 140-142°C).Yield 14.12 g (59%).

^{1}H NMR (CDCl$_3$) : δ=1.39 (d, 3H, -C$\underline{H}_3$, J=6.7); δ=3.48 (s, 1H, -O$\underline{H}$); δ=3.59 (m, 2H, -C$\underline{H}_2$-OH); δ=4.01 (m, 1H, -C$\underline{H}$Cl-)

(ii) (*S*)-2-Chloro-3-methylbutan-1-ol. The procedure was analogous to that for (*S*)-2-chloropropan-1-ol except that 27.3 g (0.2 mol) of (*S*)-2-chloro-3-methylbutanoic acid was reacted with 9.1 g (0.24 mol) of lithium aluminium hydride over a total reaction period of 30 min. The reaction was quenched with 20 ml of water and neutralised with 600 ml of 2 N sulphuric acid (60 g concentrated H$_2$SO$_4$ + 540 g of ice). Distillation at reduced pressure afforded a colourless oil (b.p 109-111°C, 95 mm). Yield 16.9 g (69%).

^{1}H NMR (CDCl$_3$) : δ=0.97 (m, 6H, -CH(C$\underline{H}_3$)$_2$); δ=2.03 (m, 1H, -C$\underline{H}$(CH$_3$)$_2$); δ=3.73 (m, 2H, -C$\underline{H}_2$-OH); δ=3.85 (m, 1H, -C$\underline{H}$Cl-)

^{13}C NMR (CDCl$_3$) : δ=17.80 (C$\underline{H}_3$); δ=19.91 (C$\underline{H}_3$); δ=31.20 (-C$\underline{H}$(CH$_3$)$_2$); δ=65.26 -C$\underline{H}_2$-OH); δ=71.50 (-C$\underline{H}$Cl-)

(C) (R)-2-Alkyloxiranes

(i) (R)-2-methyloxirane. (Note: Oxiranes are suspected carcinogens). The cyclisation of the previously prepared chlorohydrins was performed in specially adapted distillation apparatus (fig. 2.1). The oxirane was simultaneously distilled as it was formed to prevent alkaline hydrolysis of the product.

Fig.2.1. *Epoxide distillation apparatus.*
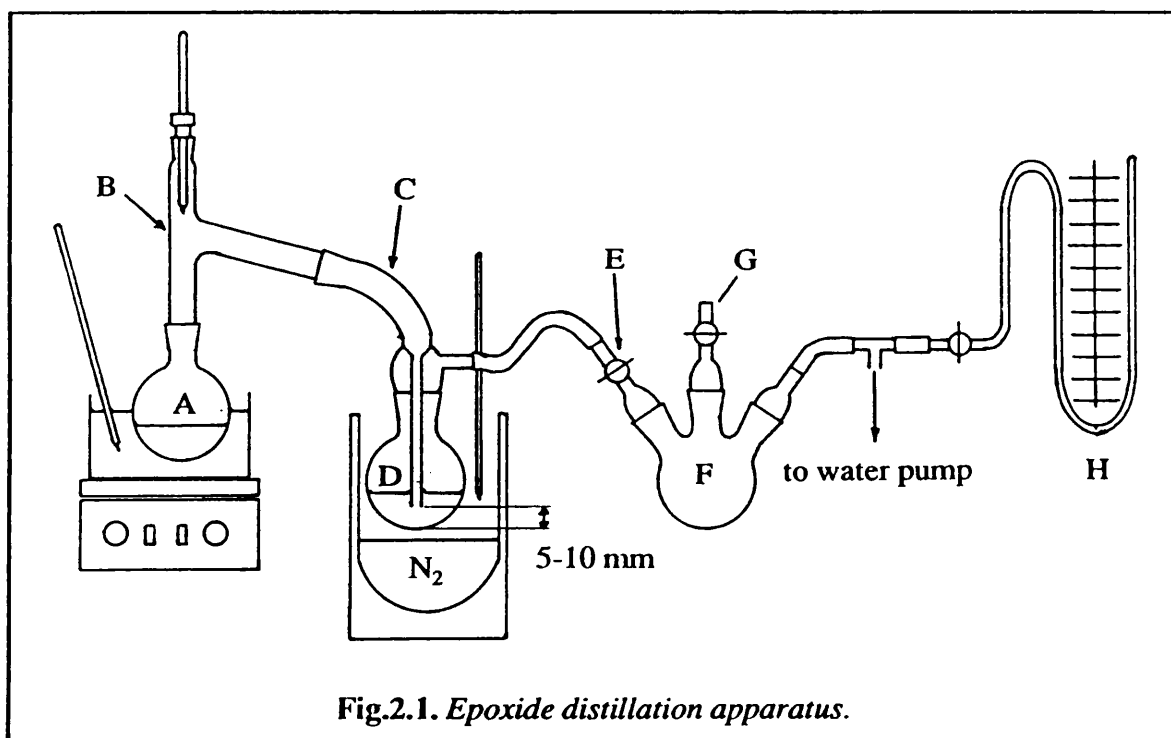
A narrow necked (B 14) 100 ml round bottomed flask (A) was fitted with a teflon coated stirring bar, a Claisen stillhead (B) fitted with a thermometer and connected to a modified receiver adapter (C). A 50 ml round bottomed flask (D) served as a trap for the oxirane. The receiver adaptor was constructed so that the end of the extended receiver pipe was 10 mm from the bottom of the receiver flask. This was to prevent clogging of the receiver

pipe and ensure efficient trapping of the product. The vacuum outlet of the receiver adaptor was connected via a stopcock (E) to a three necked round bottomed flask (F), fitted with a flexible pipe carrying a flat pipe clamp (G). The third neck of the flask was equipped with a T-piece, which was connected to a manometer (H) and a water aspirator. Flask (A) was charged with 14.1 g (0.149 mol) of (S)-2-chloropropan-1-ol and immersed in an ice bath equipped with a stirrer/hotplate and a lab jack. A low temperature thermometer was placed at the same height as flask D. Once the apparatus was assembled stopcock E was closed and flask D air-cooled to -80°C by placing it in a Dewar flask partially filled with liquid nitrogen, with the top of the flask insulated with glass wool. The temperature of D was controlled by adjusting the height of the Dewar flask with a lab jack. Pipe clamp G was tightened to give a pressure of 100 mmHg. The thermometer was briefly removed from the stillhead and a pre-cooled solution of 14.7 g (0.262 mol) of potassium hydroxide dissolved in 14 ml of water was rapidly introduced to flask A. The thermometer was quickly replaced maintaining efficient cooling of A throughout. The solution was then <u>vigorously</u> stirred (Note: Chlorohydrins are immiscible with water). Stopcock E was then gently opened for short periods of time until the pressure in the system was constant at 100 mmHg, whilst A was maintained at 0°C. The ice bath was then replaced with a water bath at 15-20°C. As the flask warmed up, the cyclisation commenced and a white precipitate of potassium chloride was seen forming. Approximately once/min. stopcock E was gently opened for 3-5 seconds to maintain gentle distillation of the oxirane. After 10 min. the temperature of the water bath was gradually raised to 30°C (Note: Attention was paid to the manometer throughout the course of the reaction. If water pressure varied at the aspirator, pressure in flask F might rise above 100 mmHg. If stopcock G was then opened, oxirane in D would be blown back into the reaction vessel. In the event of a pressure increase clamp G was tightened to reduce the pressure in F to 100 mmHg). After a total reaction time of 40 mins. stopcock E was closed and pipe clamp G was fully opened. The stillhead thermometer was then removed, admitting air to the system. Flask D was then allowed to warm to 0°C. Occasionally a two phase system was formed, the lower phase being co-distilled water.

This lower phase was removed and saturated with sodium chloride to yield a small volume of oxirane, which was combined with the main fraction. The apparatus was dismantled, cleaned and reassembled for redistillation of the oxirane.

With stopcock E closed and flask D at room temperature the wet oxirane was then placed at position A (50 ml flask) and cooled in ice to 0°C. With the stillhead thermometer removed, powdered calcium hydride was added in small potion over 2-4 hrs, until hydrogen evolution had ceased. The pressure in F was then reduced to 100 mmHg and the stillhead thermometer was replaced. Flask D was then cooled to -80°C. The oxirane was distilled as previously described. Great caution was exercised to prevent the oxirane from boiling too vigorously. Trap D was then allowed to warm to 10°C. The final anhydrous oxirane was obtained as a clear mobile liquid. It was stored in the refrigerator in an air tight bottle. Yield 6.15 g (7.4 ml, 71%).

^{1}H NMR (CDCl$_3$) : δ=1.21 (d, 3H, -C$\underline{H}_3$, J=5.2); δ=2.33 (m, 1H, -$\underline{H}$-CH-CH(CH$_3$)O-); δ=2.65 (m, 1H, -$\underline{H}$-CH-CH(CH$_3$)O-); δ=2.88 (m, 1H, -CH$_2$-C$\underline{H}$(CH$_3$)O-)

(ii) (R)-2-isopropyloxirane.(Note: the author found (R)-2-isopropyl oxirane to cause drowsiness and severe headaches) The procedure was analogous to that for (R)-2-methyloxirane. 16.8 g (0.137 mol) of (S)-2-chloro-3-methylbutan-1-ol was reacted with 15.6 g (0.24 mol) potassium hydroxide dissolved in 13.5 ml of water. During the reaction the bath temperature was raised to 50°C. After 40 mins. the pressure was reduced to 50 mmHg for an additional 5 mins. The oxirane was then redistilled from calcium hydride by repeating this procedure. Yield 10.0 g (85%).

^{1}H NMR (CDCl$_3$) : δ=0.93 (d, 3H, $\underline{H}_3$C-CH-CH$_3$, J=6.7); δ=0.86 (d, 3H H$_3$C-CH-C$\underline{H}_3$, J=6.8); δ=1.37 (m, 1H, -C$\underline{H}$(CH$_3$)$_2$); δ=2.41 (m, 1H, pr^i-C$\underline{H}$-CH$_2$O-); δ=2.60 (m, 2H, pr^i-CH-C$\underline{H}_2$-O-)

^{13}C NMR (CDCl$_3$) : δ=17.93 (-$\underline{C}$H$_3$); δ=18.82 (-$\underline{C}$H$_3$); δ=30.64 (-$\underline{C}$H(CH$_3$)$_2$); δ=45.82 (-CH-$\underline{C}$H$_2$O); δ=57.37 (-$\underline{C}$H-CH$_2$-O-)

(iii) 1,1-Dimethyloxirane, was prepared by repeating the epoxide preparation and distillation process with 1-chloro-2-methyl-2-propanol.

^{1}H NMR (CDCl$_3$) : δ=1.32 (s, 6H, -C$\underline{H}_3$); δ=2.59 (s, 2H, -C$\underline{H}_2$-).

(2.4.3) Optically Pure N,N',N''-Tris[(2-alkyl-2-hydroxy)ethyl]-triazamacrocycles

The syntheses of N substituted macrocycles by reaction with epoxides was based upon the method of Sayer *et al.* (5). Dry absolute ethanol was essential to all the following preparations. Alkyl oxiranes were conveniently dispensed using graduated volumetric pipettes. The ligand products were conveniently used as ethanol solutions made up in volumetric flasks.

$R = CH_3, CH(CH_3)_2$
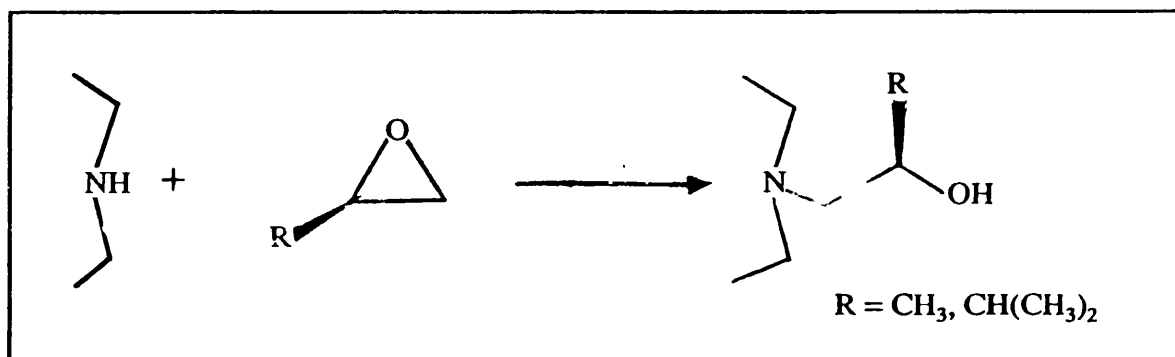
(a)(i) N,N',N''-Tris-(2S)-2-hydroxypropyl-1,4,7,triazacyclononane (L^{1}H$_3$.HCl).In a 100 ml round bottomed flask 1,4,7-triazacyclononane trihydrochloride 5.05 g (21.2 mmol.) was dissolved in a minimum amount of water (about 10 ml). 2.6 g (65 mmol.) of sodium hydroxide was then added slowly with cooling. 40 ml of ethanol was added and the solution was refrigerated overnight. The precipitated sodium chloride was filtered off

and washed with a little ice cold ethanol. The solvents were removed to yield 1,4,7-triazacyclononane as a cloudy oil (the cloudiness was found to be residual NaCl). This was taken up in dry absolute ethanol and cooled. 5 ml (4.15 g, 71.4 mmol.) of (S)-2-methyloxirane (Fluka) was added in one portion. The reaction vessel was stoppered and placed in the refrigerator overnight. The solution was then allowed to stand at room temperature for a further 6 days. Solvents were removed (avoiding excessive heating) to afford a tacky mass of N,N',N"-Tris-(2S)-2-hydroxypropyl-1,4,7-triazacyclononane hydrochloride, which was recrystallised from a small volume of isopropyl alcohol to yield the required product as the monohydrochloride salt. Yield 4.39 g (61 %).

(ii) N,N',N"-Tris-(2R)-2-hydroxypropyl-1,4,7,triazacyclononane (L^{1}H$_3$). In a 25 ml round bottomed flask 2.32 g (17.9 mmol.) of 1,4,7-triazacyclononane was dissolved in 10 ml of dry absolute ethanol. The solution was cooled and 5.5 ml (5.39 g, 78.5 mmol.) of (R)-2-Methyloxirane was added in one portion and the flask was then securely stoppered. The flask was allowed to stand at room temperature for 7 days. Solvents were removed to afford the required product as a viscous yellow oil, which upon refrigeration crystallised to a solid with no sharp melting point. The material was sufficiently pure to be used without further purification. Yield 5.33 g (97 %)

^{1}H NMR (CDCl$_3$) : δ=1.03 (d, 9H, CH$_3$, J = 6.2); δ=2.24-2.79 (m, 18H, -CH$_2$-N); δ=3.80 (m, 3H, -CH(CH$_3$)).

^{13}C NMR (CDCl$_3$): δ=19.99 (CH$_3$); δ=52.98 (b)(-CH$_2$-, ring); δ=63.50 (-CH-CH$_3$); δ=66.65 (-CH$_2$-, arm).

(b) N,N',N"-tris-[(2R)-2-hydroxy-3-methyl-butyl]-1,4,7-triazacyclononane (L^{2}H$_3$). The procedure was analogous to that for (L^{1}H$_3$), reacting 1.05 g (8.13 mmol) 1,4,7-triazacyclononane with 2.45 g (28 mmol) of 2-(R)-isopropyl oxirane. The reaction

mixture was allowed to stand for 10 days. The product crystallised as fine needles with no sharp melting point, Yield 3.15 g (quantitative).

^{1}H NMR (CDCl$_3$): δ= 0.83 (m. 18H, -CH(C$\underline{H}_3$)$_2$); δ=1.53 (m, 3H, -C$\underline{H}$(CH$_3$)$_2$); δ=2.33-2.82 (m, 18H, N-C$\underline{H}_2$); δ=3.33 (m, 3H, -C$\underline{H}$-OH); δ=5.47 (s(b), 3H, -O$\underline{H}$).

^{13}C NMR (CDCl$_3$): δ=18.08 ($\underline{C}$H$_3$); δ=18.40 ($\underline{C}$H$_3$); δ=31.96 (-$\underline{C}$H(CH$_3$)$_2$); δ=53.11 (b)(N-$\underline{C}$H$_2$); δ=62.53 (b)(N-$\underline{C}$H$_2$); δ=71.87 (-$\underline{C}$H-OH)

(c) N,N',N''-tris-(2R)-2-hydroxypropyl-1,4,7,triazacyclodecane (L^{3}H$_3$). The procedure was analogous to that for (L^{1}H$_3$), reacting 850 mg (5.9 mmol) 1,4,7-triazacyclodecane with 1.16 g (20 mmol, 1.4 ml) of (R)-propylene oxide. Yield 1.87 g (quantitative).

^{1}H NMR (CDCl$_3$): δ=0.97 (m, 9H, C$\underline{H}_3$); δ=1.73 (m, 2H, CH$_2$C$\underline{H}_2$CH$_2$); δ=2.3-3.1 (m, br, 18H, C$\underline{H}_2$); δ=3.75 (m, 3H, C$\underline{H}$-CH$_3$).

(d) N,N',N''-tris-(2R)-2-hydroxypropyl-1,4,7,tri-azacycloundecane (L^{4}H$_3$). The procedure was analogous to that for (L^{1}H$_3$), reacting 730 mg (_4 _ mmol) 1,4,7-triazacycloundecane with 0.95 g (16 mmol, 1.15 ml) of (R)-propylene oxide. Yield 1.53 g (quantitative).

^{1}H NMR (CDCl$_3$): δ=1.01 (m, 9H, -C$\underline{H}_3$); δ=1.62 (m, 4H, -C$\underline{H}_2$-); δ=2.1-2.9 (m, 18H, N-C$\underline{H}_2$-); δ=3.73 (m, 3H, -C$\underline{H}$-CH$_3$).

(e) N,N',N''-tris-(2S)-2-hydroxypropyl-1,4,7,tri-azacyclododecane (L^{5}H$_3$). 3.34 g (19.5 mmol) of 1,4,7-triaza-cyclododecane was dissolved in 5 ml of absolute ethanol. To this was added 5 ml of (S)-propylene oxide (4.14 g, 71 mmol). The solution was allowed

to stand at room temperature for 24 h. 5 ml of water was then added to precipitate the product as lustrous white plates. The material was recrystallised by dissolution in ethanol followed by the slow addition of an equal volume of water. Yield 4.10 g (61 %).

^{1}H NMR (CDCl$_3$): δ=1.03 (m, 9H, -C$\underline{H}_3$); δ=1.14 (m, 2H,-CH$_2$C$\underline{H}_2$CH$_2$-); δ=1.56 (m, 4H, -C$\underline{H}_2$-); δ=1.81-2.47 (m, 18H, N-C$\underline{H}_2$-); δ=3.76 (m, 3H, -C$\underline{H}$-CH$_3$).

^{13}C NMR (CDCl$_3$): δ=19.83 (-$\underline{C}$H$_3$); δ=20.18 (-$\underline{C}$H$_2$-);δ=24.33 (-$\underline{C}$H$_2$-); δ=50.55 (-$\underline{C}$H$_2$-); δ=62.14 (-$\underline{C}$H-CH$_3$); δ=63.20 (-$\underline{C}$H-CH$_3$); δ=63.67 (-$\underline{C}$H$_2$-).

Calc. for C$_{18}$H$_{39}$N$_3$O$_3$ C: 62.55, H: 11.38, N: 12.17. Found C: 63.20, H:10.87, N: 11.28.

(f) N,N',N''-tris-(2R)-2-hydroxypropyl-1,4,7-triazacyclotridecane (L^{6}H$_3$). The procedure was analogous to that for (L^{1}H$_3$), reacting 550 mg (2.97 mmol) 1,4,7-triazacyclotridecane with 0.60 g (10 mmol, 0.73 ml) of (R)-propylene oxide. Yield 1.06 g (quantitative).

^{1}H NMR (CDCl$_3$): δ=1.03 (m, 9H, -C$\underline{H}_3$); δ=1.14 (m, 2H,-CH$_2$C$\underline{H}_2$CH$_2$-); δ=1.56 (m, 4H, -C$\underline{H}_2$-); δ=1.81-2.47 (m, 18H, N-C$\underline{H}_2$-); δ=3.76 (m, 3H, -C$\underline{H}$-CH$_3$).

(g) N,N',N''-tris-(2R)-2-hydroxypropyl-1,5,9-triazacyclododecane (L^{7}H$_3$). The procedure was analogous to that for (L^{1}H$_3$), reacting 900 mg (5.25 mmol) 1,5,9-triazacyclododecane with 1.07 g (18 mmol, 1.29 ml) of (R)-propylene oxide. Yield 1.81 g (quantitative).

^{1}H NMR (CDCl$_3$): δ=1.07 (d, 9H, -C$\underline{H}_3$, J=6.1); δ=1.63 (m, 6H, -CH$_2$C$\underline{H}_2$CH$_2$-); δ=2.05-2.67 (m (b), 18H, N-C$\underline{H}_2$); δ=3.81 (m, 3H, -C$\underline{H}$(CH$_3$)$_2$).

^{13}C NMR (CDCl$_3$): δ=19.91 (C̲H$_3$); δ=23.29 (C̲H$_2$); δ=50.90 (b, C̲H$_2$ (ring)); δ=62.78 (C̲H$_2$ (arm)); δ=63.37 (C̲H).

(h) N,N',N"-tris-(2R)-2-hydroxypropyl-1,4,8-triazacycloundecane (L^{8}H$_3$). The procedure was analogous to that for (L^{1}H$_3$), reacting 300 mg (1.91 mmol) of 1,4,8-triazacyclododecane with 0.39 g (6.7 mmol, 0.46 ml) of (R)-propylene oxide. Yield 0.63 g (quantitative).

^{1}H NMR (CDCl$_3$): δ=1.05 (m, 9H, -C̲H$_3$); δ=1.69 (m, 4H, -C̲H$_2$-); δ=2.1-2.8 (m, 18H, N-C̲H$_2$-); δ=3.77 (m, 3H, -C̲H-CH$_3$).

(i) N,N',N"-tris-(2R)-2-hydroxypropyl-1,5,9-triazacyclotridecane (L^{9}H$_3$). The procedure was analogous to that for (L^{1}H$_3$), reacting 300 mg (1.62 mmol) of 1,5,9-triazacyclotridecane with 0.33 g (5.7 mmol, 0.40 ml) of (R)-propylene oxide. Yield 0.58 g (quantitative).

^{1}H NMR (CDCl$_3$): δ=1.02 (m, 9H, -C̲H$_3$); δ=1.44 (m, 8H,-C̲H$_2$-); δ=1.8-2.6 (m, 18H, N-C̲H$_2$-); δ=3.70 (m, 3H, -C̲H-CH$_3$).

(j) N,N',N"-tris-2-methyl-2-hydroxy-propyl-1.4.7-triazacyclononane (L^{10}H$_3$). The procedure was analogous to that for (L^{1}H$_3$), reacting 545 mg (4.22 mmol) of 1,4,7-triazacyclononane with 0.95 g (13.2 mmol) of 1,1-dimethyloxirane. The reaction time was extended to 14 days. Yield 1.46 g (quantitative).

^{1}H NMR (CDCl$_3$): δ=1.17 (s, 6H, -C̲H$_3$); δ=2.53 (s, 6H, -C̲H$_2$-(arm)); δ=2.92 (s, 6H, -C̲H$_2$-(ring)).

(2.4.4) Note on the Preparation of Ligands.

The reaction mixture of the macrocycles and epoxides was first allowed to stand in the refrigerator overnight. Yields were low and the NMR spectra of the products indicated a mixture of mono; bis-and tris-functionalised macrocycles, and also unreacted starting material. The reaction was found to proceed more satisfactorily with longer reaction times of at least 5 days, and allowing the reaction mixture to stand at room temperature. The NMR spectra of the products indicated only one tris functionalised macrocycle was present. Analysis of the ligands was not possible due to their highly hygroscopic nature. These reactions may be slow due an internal hydrogen-bonding interaction which would reduce the reactivity of unsubstituted ring nitrogen atoms.

The preparation of $L^{10}H_3$ is presented for reference purposes only. The transition metal chemistry of this ligand has not been thoroughly investigated.

(2.5) PREPARATION OF TRANSITION METAL COMPLEXES OF N,N',N''-TRIS-[(2-ALKYL-2-HYDROXY)-ETHYL]-TRIAZAMACROCYCLES

The syntheses presented are arranged by ligand type. In some cases full characterisation is presented in results and discussion sections. Where required preparations used distilled water or freshly distilled absolute ethanol.

(A) Complexes of N,N',N''-tris-(2S)-2-hydroxypropyl-1,4,7-triazacyclononane (L^1H_3).

(i) $[Mn(II)L^1H_3L^1Mn(IV)](PF_6)_3$. In a 50 ml beaker 0.34 g (1.00 mmol) of L^1.HCl dissolved in 10 ml of water was added to 0.23 g (1.16 mmol) of $MnCl_2.6H_2O$ dissolved in 10 ml of water. The pH of the colourless solution was adjusted to 8 with 4 M NaOH at which time a deep red colour began to form. The solution was allowed to stand overnight, an excess of $[NH_4][PF_6]$ was added and the resulting red-brown precipitate was filtered

off. The material was recrystallised from a minimum volume of boiling acetonitrile to give small, well formed, dark red prisms. Yield 350 mg (65 %).

Calc. for $C_{30}H_{63}F_{18}Mn_2N_6O_6P_3$ C: 31.34, H: 5.61, N: 7.31, P: 8.08. Found. C: 31.26, H: 5.53, N: 7.23, P: 7.98.

Crystal data: $[Mn(II)L^1H_3L^1Mn(IV)](PF_6)_3$.

M = 1149.6; space group $R3$; a = 10.472(1)Å, b = 10.472(1)Å, c = 36.637(7)Å; V = 3479(4)Å^3, Z = 3, D_c = 1.65 g cm^{-1}, μ(Mo-K$_a$) = 7.4 cm^{-1}; R(F$_o$) = 0.038; R$_w$(F$_o$) = 0.049.

(ii) $[Co(II)L^1H_3][NO_3]_2$. This preparation was performed under a nitrogen atmosphere, using standard Schlenk line techniques and degassed solvents throughout. 70 mg (mmol) of $Co(II)(NO_3)_2.6H_2O$ was dissolved in 20 ml of absolute alcohol. 70 mg (mmol) of L^1H_3 dissolved 5 ml of absolute alcohol was added in one portion. The solution became orange initially and within a few minutes pale pink in colour. The solvent was reduced to 5 ml and refrigerated. Small pink crystals were formed after a few days. The mother liqour was removed by syringe. The product washed with acetone. The material was then pumped dry. Yield 89 mg (79%)

(iii) Reference samples of $[Ni(II)L^1H_3]^{2+}$ and $[Cu(II)L^1H_3]^{2+}$ were prepared as previously described (6).

(B) Complexes of N,N',N"-tris-[(2R)-2-hydroxy-3-methyl-butyl]-1,4,7-triazacyclo-nonane (L^2H_3). 3.15 g of N,N',N"-tris-[(2R)-2-hydroxy-3-methyl-butyl]-1,4,7-triaza-cyclononane was taken up in 50 ml of absolute ethanol in a volumetric flask to give a 0.162 mol l^{-1} (63 mg/ml) solution. It is worth noting that this ligand is rather insoluble in water.

(i) Cr(III)(L²)(PF₆)₃.

(a) Cr(III)Cl₃(thf)₃. 3.22 g (20.3 mmol) of anhydrous chromium chloride was placed in a Schlenk tube under nitrogen. A granule of acid cleaned zinc metal followed by 30 ml of dry air-free tetrahydrofuran were then placed in the Schlenk tube. The Schlenk tube was sealed with a reflux condenser fitted with a nitrogen inlet/outlet. The mixture was refluxed for 6 h during which time an intense purple colour was produced. The hot solution was filtered under nitrogen through a sintered glass frit into a Schlenk tube. The solvent was reduced to one-half its volume and the solution was refrigerated overnight. The purple microcrystalline material was filtered under nitrogen washed with 2x2 ml of ice cold tetrahydrofuran and dried in vacuo. Yield 5.03 g (66 %).

Calc. for $C_{12}H_{24}Cl_3Cr$ C: 38.47, H: 6.46. Found C: 38.28, H: 6.51.

(b) Cr(III)(L²H₃)(PF₆)₃. 3 ml (189 mg, 0.488 mmol) of the ligand solution were placed in a dry Schlenk tube and the solvent was removed in vacuo. The ligand was then dissolved in 15 ml of dry tetrahydrofuran. In a second Schlenk tube 175 mg (4.37 mmol) of sodium hydride (60% suspension in oil) was washed with 3x20 ml portions of dry 40-60°C petroleum ether and then dried *in vacuo*. The ligand solution was then added to the sodium hydride (with caution) under nitrogen. After effervescence had subsided (approx. 1 h.) the solution was filtered under nitrogen through a small pad of celite. 184 mg (0.491 mmol) of Cr(III)Cl₃(thf)₃ was dissolved in 15 ml of dry tetrahydrofuran in a Schlenk tube under nitrogen. The ligand solution was then added and an intense green colour was produced. The solution was refrigerated for 24 hours and solvents were then removed in vacuo. 10 ml of water was then added and a pale purple solution was produced. 10 ml of conc hydrochloric acid was then added to give an intense pink solution. An excess of [NH₄][PF₆] was then added and the solution was allowed to stand overnight in a 50 ml beaker at room temperature. The required product was formed as intense pink needles

which were filtered on a glass sinter and washed with small portions of cold 12.5 mol l^{-1} hydrochloric acid. Yield 121 mg (28 %).

Calc. for $C_{21}H_{45}CrF_{18}N_3O_3$ C: 28.83, H: 5.19, N: 4.81. Found C: 30.01, H: 6.38, N: 4.69.

I.R. (KBr): ν = 841 (P-F).

(ii) Mn(IV)(L^2)(PF$_6$).H$_2$O. In a 25 ml beaker 64.1 mg (0.324 mmol) of MnCl$_2$.4H$_2$O was dissolved in 2 ml of water. 2 ml of the ligand solution (126 mg, 0.325 mmol) was then added and immediately a dark brown colour was produced. The mixture was allowed to evaporate to dryness and was redissolved in 5 ml of water. An excess of [NH$_4$][PF$_6$] dissolved in 1 ml of water was added. A brown precipitate formed and the solution was refrigerated overnight. The solid was filtered off, washed with water and air-dried. The material was recrystallised by the slow evaporation of a covered acetone solution to give the required product as massive black crystals. Yield 101 mg (51 %).

Calc. for $C_{21}H_{42}MnN_3O_3.H_2O$; C: 41.86, H: 7.36, N: 6.97, F: 18.92. Found: C: 42.28, H: 7.46, N: 6.99, F: 18.77.

I.R. (KBr): ν = 3433, 1630 cm^{-1} (H$_2$O); ν = 839 cm^{-1} (P-F).

Crystal data: [Mn(IV)L^2][PF$_6$].H$_2$O.

M = 602.5; monoclinic, space group; $P2_1$ (No. 4, C^2_2); a = 8.4160(7)Å, b = 11.992(1)Å, c = 14.222(1)Å, b = 103.934(7)°; V = 1393.1(2)Å^3; Z = 2; D_c = 1.44 g cm^{-1}; F(000) = 634; (Mo-K$_a$) = 5.80 cm^{-1}; R(R$_w$) = 0.040

(iii) Ni(L²H₃)(PF₆)(NO₃).H₂O. In a 5 ml beaker 94.0 mg (0.323 mmol) of Ni(NO₃)₂.6H₂O was dissolved in 2 ml of absolute ethanol. 2 ml of ligand solution (126 mg, 0.325 mmol) was added and there was a colour change from intense green to blue (a small amount of nickel hydroxide was produced but this redissolved as the reaction proceeded). The solution was allowed to evaporate to dryness producing a lilac coloured glass. This was redissolved in 2 ml of water and an excess of [NH₄][PF₆] dissolved in 1 ml of water was added. Immediately a purple precipitate was formed. The solution was refrigerated overnight, filtered, washed with water and recrystallised by the slow evaporation of an acetonitrile solution. The product was collected by filtration and washed with acetone to give purple triangular pyramidal crystals. Yield 212 mg (89 %).

Calc. for $C_{21}H_{47}F_6N_4NiPO_7$ C: 37.57, H:7.06, N: 8.35. Found : C: 37.06, H: 6.83, N: 8.35

I.R. (KBr): ν =3381, 1630 cm⁻¹ (H₂O); ν =1346 cm⁻¹ (N-O); ν = 841 cm⁻¹ (P-F)

(iv) Cu(L²H₃)(PF₆)₂. The method was analogous to that for Ni(L²H₃)(PF₆)(NO₃).H₂O. 78 mg (0.323 mmol) of Cu(NO₃)₂.3H₂O was reacted with 2 ml of ligand solution. The hexafluorophosphate salt was recystallised by the slow evaporation of a water/acetonitrile (1:1) solution to give the product as lustrous plates. Attempts : grow crystallographic qv dity crystals failed. Yield 91 mg (38 %)

Calc. for $C_{21}H_{45}CuF_{12}P_2$ C: 34.04, H: 6.12, N: 5.67. Found : C: 39.77, H: 5.84, N: 5.48.

I.R. (KBr) ν = 841 cm⁻¹ (P-F).

(v) Zn(L²H₃)(PF₆)₂.3H₂O. The method was analogous to that for Ni(L²H₃)(PF₆)(NO₃).H₂O. 95 mg (0.319 mmol) of Zn(NO₃)₂.6H₂O was reacted with 2 ml of ligand solution. The product was recrystallised by the slow evapoation of a methanol solution to yield the product as white needles. Yield 112 mg (43 %)

Calc. for $C_{21}H_{51}N_3O_6F_{12}P_2Zn$ C: 31.65, H: 6.45, N: 5.27. Found C: 31.74, H: 6.38, N: 5.18.

I.R. (KBr): ν = 841 cm^{-1} (P-F), ν = 3893, 1634 cm^{-1} (H_2O).

(C) Complexes of N,N',N''-tris-(2R)-2-hydroxypropyl-1,4,7-triazacyclodecane (L^3H_3). A solution of 1.87 g of N,N',N''-tris-(2R)-2-hydroxypropyl-1,4,7-triazacyclodecane in ethanol was prepared in a 25 ml volumetric flask to give a 0.236 mol l^{-1} (74.8 mg/ml) solution.

(i) $[Mn(II)L^3H_3L^3Mn(III)][PF_6]_2.H_2O$. In a 10 ml beaker was placed 140 mg (0.707 mmol) of $MnCl_2.4H_2O$ dissolved in 2 ml of water. 3 ml (224 mg, 0.707 mmol) of the ligand solution was added. Immediately a brown colour was produced. Oxidation was completed by the addition of a few drops of 4 M sodium hydroxide. The solution was allowed to evaporate to dryness and was redissolved in 3 ml of water. An excess of $[NH_4][PF_6]$ dissolved in 0.5 ml of water was then added. The solution was cooled to 0°C for 3 h and the resulting precipitate was collected upon a sintered glass funnel. The dark brown microcrystalline material was recrystallised by dissolution and slow evaporation of an acetonitrile solution. The material was then washed with small portions of cold acetone, to afford large black lustrous crystals. Yield 185 mg (49 %).

Calc. for $C_{32}H_{68}F_{12}Mn_2N_6O_8P_2$ C: 36.08, H: 6.44, N: 7.89. Found; C: 36.11, H: 6.40, N: 8.34.

I.R. (KBr): ν = 840 cm^{-1} (P-F).

(ii) (a) Co(L³H₃)(PF₆)₂. In a 10 ml beaker 137 mg (0.471 mmol) of Co(NO₃)₂.6H₂O was dissolved in 2 ml of absolute ethanol. To this was added 2 ml (150 mg, 0.472 mmol) of the ligand solution. There was a colour change from pink to a brown-red hue. The solution was covered and allowed to evaporate slowly to afford massive crystals of Co(L³H₃)(NO₃)₂. The nitrate salt was converted to the hexafluorophosphate salt by dissolution in a small volume of water (5 ml) followed by the addition of excess [NH₄][PF₆] dissolved in water (2 ml). After a few hours a microcrystalline precipitate of the title compound appeared. The solution was allowed to stand overnight and was then filtered (retaining the mother liquor) to afford the product as small hygroscopic crystals. Attempts to grow crystallographic quality crystals failed. Yield 113.2 mg (36 %)

Calc. for C₁₆H₃₅CoF₁₂N₃O₃P₂ C: 38.39, H: 7.05, N: 14.00. Found C: 38.49, H: 6.60, N: 13.99.

I.R. (KBr): ν = 839 cm⁻¹ (P-F).

(b) [(Co(II)L³H₃)₂(NO₃)₂][PF₆]₂. The mother liquor from the above prepartion was allowed to evaporate down to 4 ml in volume. The solution was filtered, covered with a watch glass and allowed to evaporate very slowly (approx. 2 weeks) down to 1 ml, to afford the title complex as a large dark red-brown crystal. Yield 61.2 mg (22 %). A small piece of this crystal was broken off for crystallographic analysis.

Calc. for C₃₂H₇₀Co₂F₁₂N₈O₁₂P₂ C: 32.94, H: 6.05, N: 9.60. Found C: 32.97, H: 6.01, N: 9.65.

I.R. (KBr): ν = 1385 cm⁻¹ (N-O); n = 837 cm⁻¹ (P-F).

Crystal data for [Co(II)L³H₃(NO₃)₂H₃L³Co(II)][PF₆]₂.

M = ; triclinic, space group p_1 (No.1 C^1_1); a = 8.5064(9)Å, b = 9.764(3)Å, c = 15.3110(20)Å, α = 83.710(20), β = 89.531(8), γ = 74.624(20); V = 1218.49(49)Å^3; Z = 2; Dc = 1.59 g cm^{-1}; F(000) = 606; m(Mo-K$_\alpha$) = 8.48 cm^{-1}.

(iii) Ni(L^{3}H$_3$)(PF$_6$)$_2$. In a 5 ml beaker 137 mg (0.471 mmol) of Ni(NO$_3$)$_2$6H$_2$O was dissolved in 2 ml of absolute ethanol. 2 ml (150 mg, 0.473 mmol) of ligand solution was then added and a green precipitate of nickel hydroxide was formed. The solution was filtered through glass microfibre filter paper and allowed to evaporate to dryness to give a green-blue glassy solid. This was dissolved in 2 ml of water and excess [NH$_4$][PF$_6$] dissolved in 1 ml of water was added. The solution was refrigerated overnight and the resulting blue solid was filtered off and washed with water. The material was recrystallised twice by the slow evaporation of an acetonitrile solution to give large pale blue crystals. Yield 14 mg (4 %)

Calc. for C$_{16}$H$_{35}$F$_{12}$N$_3$NiO$_3$P$_2$ C: 38.05, H: 6.99, N: 13.87. Found C: 38.65, H: 7.23, N: 13.23

(iv) Cu(L^{3}H$_3$)(PF$_6$)$_2$. In a 10 ml beaker 113 mg (0.468 mmol) of Cu(NO$_3$)$_2$.6H$_2$O was dissolved in 3 ml of absolute ethanol. To this was added 2 ml (150 mg, 0.473 mmol) of the ligand solution with a deep green colour being produced immediately. The solution was allowed to evaporate to dryness to produce a pale blue microcrystalline solid. This was dissolved in 3 ml of water and an excess [NH$_4$][PF$_6$] dissolved in 1 ml of water was added and the solution was refrigerated overnight. The resulting solid was filtered and recrystallised from acetonitrile by the addition of an equal volume of water followed by refrigeration. Yield 125 mg (39 %)

Calc. for C$_{16}$H$_{35}$CuF$_{12}$P$_2$ C: 28.65, H: 5.26, N: 6.27. Found C: 29.96, H: 5.63, N: 6.39

I.R. (KBr): ν = 837 cm^{-1} (P-F).

(v) $Zn(L^3H_3)(PF_6)_2$. In a 5 ml beaker 140 mg (0.471 mmol) of $Zn(NO_3)_2.6H_2O$ was dissolved in 3 ml of absolute ethanol. 2 ml (150, 0.473mmol) of ligand solution was then added and the solvents were allowed to evaporate to give a colourless glass. This was dissolved in 2 ml of water, an excess $[NH_4][PF_6]$ dissolved in 1 ml water was added and the solution was refrigerated overnight. The product appeared as white needles which upon filtration lost solvent to yield an amorphous white powder. Attempts at recrystallisation were unsuccessful. Yield 58 mg (18 %)

Calc. for $C_{16}H_{35}F_{12}N_3O_3P_2Zn$ C: 31.64, H: 5.81, N: 6.92. Found C: 31.31, H: 6.01, N: 6.69

I.R. (KBr): $v = 839$ cm^{-1} (P-F).

(D) Complexes of N,N',N''-tris-(2R)-2-hydroxypropyl-1,4,7-triazacycloundecane (L^4H_3). A solution of 1.53 g of N,N',N''-tris-(2R)-2-hydroxypropyl-1,4,7-triazacycloundecane in ethanol was prepared in a 25 ml volumetric flask to give a 0.185 mol l^{-1} (61.2 mg/ml) solution.

(i) $Co(L^4H_3)(NO_3)_2.H_2O$. In a 50 ml beaker 106 mg (0.364 mmol) of $Co(NO_3)_2.6H_2O$ was dissolved in 10 ml of absolute ethanol. 2 ml (122 mg, 0,369 mmol) of ligand solution was added. The solution became pale purple in hue and was allowed to evaporate very slowly to give the product as a tacky mass of small purple crystals. This was dissolved in ethanol and ether was added to precipitate a fine lilac powder, which was filtered and recrystallised by the slow evaporation of an ethanol solution. Yield 44 mg (25%).

Calc. for $C_{17}H_{37}CoN_5O_9.H_2O$ C: 38.35. H: 7.38, N: 13.15. Found C: 38.54, H: 7.44, N: 13.19.

Crystal data: $[Co(II)L^4H_3][NO_3]_2.H_2O$.

$M = 532.46$; orthorhombic, space group $P2_12_12_1$ (No. 19, D^4_2); $a = 9.9105(9)$Å, $b = 14.914(1)$Å, $c = 16.460(1)$Å; $V = 2430.7(4)$Å^3; $Z = 4$; $D_c = 1.455$ g cm^{-1}; F(000) = 1132; (Mo-K_a) = 7.60 cm^{-1}; R(R$_w$) = 0.039

(ii) $Ni(L^4H_3)(NO_3)_2.2H_2O$. In a 5 ml beaker 106 mg (0.364 mmol) of $Ni(NO_3)_2.6H_2O$ was dissolved in 2 ml of absolute ethanol and 2 ml (122 mg, 0.369 mmol) of the ligand solution was added. The solution immediately became a deep bottle green colour. The solution was allowed to evaporate to 1 ml and the resulting large green prisms were filtered and washed with cold methylene chloride/ethanol (4:1 v/v). Yield 91 mg (54 %).

Calc. for $C_{17}H_{37}NiN_5O_9.2H_2O$ C: 37.11, H: 7.51, N: 12.73. Found: C: 37.56, H: 7.29, N: 12.86.

I.R. (KBr): $v = 1385$ cm^{-1} (N-O)

(iii) $Cu(L^4H_3)(PF_6)_2$. The method was analogous to that for $Ni(L^4H_3)(NO_3)_2$. The resulting blue nitrate was produced as a powder and dissolved in 10 ml of water. An excess of $[NH_4][PF_6]$ was added and the resulting blue precipitate was recrystallised by the slow evaporation of an acetonitrile/water (1:1) solution to give clusters of deep blue rod shaped crystals. Yield. 25 mg (10 %)

Calc. for $C_{17}H_{37}CuF_{12}P_2$ C: 29.81, H: 5.44, N: 6.13. Found: C: 29.54, H: 5.26, N: 6.45.

I.R. (KBr): ν = 843 cm⁻¹ (P-F)

(iv) Zn(L⁴H₃)(NO₃)₂.H₂O The procedure was analogous to that for Ni(L⁴H₃)(NO₃)₂. 109 mg (0.366 mmol) of Zn(NO₃)₂.6H₂O was reacted with 2 ml (122 mg, 0,369 mmol) of ligand solution. The product was obtained as large colourless crystals. Yield 67 mg (34 %)

Calc. for $C_{17}H_{37}N_5O_9Zn.H_2O$. C: 37.97, H: 7.32, N: 13.49. Found C: 38.18, H: 6.87, N: 13.07

I.R. (KBr): ν = 1385 cm⁻¹ (N-O)

(E) Complexes of N,N',N''-tris-(2R)-2-hydroxypropyl-1,4,7-triazacyclododecane (L⁵H₃).

(i) Co(L⁵H₃)(NO₃)₂. 185 mg (0.636 mmol) of Co(NO₃)₂.6H₂O was dissolved in 10 ml of absolute ethanol. 223 mg (0.645 mmol) of L⁵ dissolved in 5 ml of absolute ethanol was then added. The colour changed from pale pink to deep red-brown. The solution was allowed to evaporate slowly. After a few hours well formed crystals of the required product formed. The material was filtered off and washed with cold ether. (Note: if the solution was allowed to evaporate completely the material redissolved in the water of hydration contained in the staring material, yielding an amorphous pink solid). Yield.107 mg (35 %)

Calc. for $C_{18}H_{39}CoN_5O_9$ C: 40.89, H: 7.44, N: 13.26. Found C: 40.99, H: 7.52, N: 13.35.

(ii) Ni(L⁵H₃)(NO₃)₂.H₂O. 155 mg (0.533 mmol) of Ni(NO₃)₂.6H₂0. was dissolved in 5 ml of absolute ethanol. 185 mg (0.535 mmol) of L⁵ dissolved in 5 ml of absolute ethanol was added in one portion. The colour changed from pale to deep green. Slow

evaporation of the solvent yielded lustrous prisms which lost solvent upon filtration to give green semi-crystalline material. Yield 89 mg (34 %)

Calc. for $C_{18}H_{39}NiN_5O_9.H_2O$. C: 39.62, H: 7.58, N: 12.84. Found C: 39.62, H: 7.76, N: 12.84

(iii) (a) $Cu(L^5H_3)(NO_3)_2.H_2O$. In a 25 ml beaker 140 mg (0.579 mmol) of $Cu(NO_3)_2.3H_2O$ was dissolved in 10 ml of absolute ethanol. 201 mg (0.582 mmol) of L^5 dissolved in 5 ml of absolute ethanol was then added. The solution changed from a pale blue to a deep green colour. Evaporation of the solvent yielded the product as an amorphous blue-green solid. Yield 119 mg (37 %)

Calc. for $C_{18}H_{39}CuN_5O_9.H_2O$. C: 39.26, H: 7.51, N: 12.73. Found C: 39.11, H: 7.79, N: 12.76

(b) $Cu(L^5H_3)(PF_6)_2.H_2O$ 43 mg of $Cu(L^5H_3)(NO_3)_2.H_2O$ was dissolved in 15 ml of water. An excess of $[NH_4][PF_6]$ was added. The solution was refrigerated for 5 days to give the required product as attractive deep green hexagonal prisms. Yield 53 mg (95 %).

Calc. for $C_{18}H_{39}CuF_{12}N_3O_3P_2.H_2O$. C: 30.16, H: 5.77. N: 5.71. Found C: 29.67, H: 5.60, N: 5.71.

I.R. (KBr): $\nu = 841$ cm^{-1} (P-F)

(iv) $Zn(L^5H_3)(NO_3)_2$. In a 10 ml beaker 130 mg (0.437 mmol) $Zn(NO_3)_2.6H_2O$ was dissolved in 5 ml of absolute ethanol, and 152 mg (0.440 mmol) of L^5 dissolved in 2 ml of absolute ethanol was added. The solution was allowed to evaporate down to 2 ml and the resulting crystalline solid was filtered off and washed with dichloromethane. Yield 88 mg (42 %).

Calc. for $C_{18}H_{39}N_5O_9Zn$ C: 40.42, H: 7.35, N: 13.09. Found C: 40.44, H: 6.64, N: 13.04

(F) Complexes of N,N',N"-tris-(2R)-2-hydroxypropyl-1,4,7-triazacyclotridecane (L^6H_3).

All attempts at preparing complexes of this ligand proved unsuccessful. Materials of variable analysis were formed on all occasions.

(G) Complexes of N,N',N"-tris-(2R)-2-hydroxypropyl-1,5,9-triazacyclododecane (L^7H_3). A solution of 1.81 g of N,N',N"-tris-(2R)-2-hydroxypropyl-1,4,7-triazacyclodecane in ethanol was prepared in a 25 ml volumetric flask to give a 0.210 mol l^{-1} (72.4 mg/ml) solution.

(i) Co(L^7H_3)(NO$_3$)$_2$.H$_2$O In a 25 ml beaker 121 mg (0.416 mmol) of Co(NO$_3$)$_2$.6H$_2$O was dissolved in 10 ml of absolute ethanol. 2 ml of ligand solution (145 mg, 0.419 mmol) was added and the colour changed to deep red-purple. The solution was allowed to evaporate to 5 ml and large purple lozenge shaped crystals of the product were formed. The material was filtered and washed with a little cold ethanol. Yield 134 mg (57 %)

Calc. for $C_{18}H_{39}CoN_5O_9$.H$_2$O. C: 39.56, H: 7.56, N: 12.82. Found C: 39.88, N: 7.24, H: 12.87.

I.R. (KBr): ν = 1385 cm^{-1} (N-O).

(ii) Ni(L^7H_3)(PF$_6$)$_2$.H$_2$O. In a 10 ml beaker 120 mg (0.413 mmol) of Ni(NO$_3$)$_2$.6H$_2$O was dissolved in 5 ml of absolute ethanol. 2 ml of ligand solution (145 mg, 0.419 mmol) was added in one portion. The solution darkened and a small amount of nickel hydroxide was precipitated. The solution was filtered and allowed to evaporate to

dryness. The resulting amorphous green solid was dissolved in water (3 ml), and excess [NH$_4$][PF$_6$] dissolved in water was added. The resulting clear green solution was allowed to evaporate slowly to afford the title complex as massive green hexagonal crystals. Yield 70 mg (23 %).

Calc. for C$_{18}$H$_{39}$F$_{12}$N$_3$NiO$_3$P$_2$.H$_2$O. C: 30.36, H: 5.80, N: 5.90. Found C: 30.29, H: 5.09, N: 5.78.

I.R. (KBr): v = 839 cm^{-1} (P-F).

(iii) (a) Cu(L^{7}H$_3$)(PF$_6$)$_2$.H$_2$O (Blue product) In a 25 ml beaker 2 ml (145 mg, 0.419 mmol) of ligand solution was added to 97 mg (0.405 mmol) of Cu(NO$_3$)$_2$.H$_2$O dissolved in 10 ml of absolute ethanol. The solution initially became deep green in hue. The solution was covered and on standing overnight became pale blue in colour. Evaporation of the solvent afforded a blue form of the nitrate salt as microcrystalline material. This was taken up in a minimum volume of water and an excess of [NH$_4$][PF$_6$] dissolved in water was added. The solution was refrigerated for several days to produce the title complex as well formed pale blue crystals. Yield 89 mg (30 %).

Calc. for C$_{18}$H$_{39}$CuF$_{12}$N$_3$O$_3$P$_2$.H$_2$O. C: 30.15, H: 5.76, N: 5.86. Found C: 29.85, H: 5.68, N: 5.84

I.R. (KBr): v = 841 cm^{-1} (P-F).

(b) Cu(L^{7}H$_3$)(NO$_3$)$_2$.H$_2$O (Green product). In a 5 ml beaker 2 ml (145 mg, 0.419 mmol) of ligand solution was added to 97 mg (0.405 mmol) of Cu(NO$_3$)$_2$.H$_2$O dissolved in 2 ml of absolute ethanol. The solution became very intense green and was allowed to stand uncovered overnight to produce the title complex as a large green single crystal. Yield (based on Cu(L^{7}H$_3$)(NO$_3$)$_2$.H$_2$O) 19.7 mg (8 %).

The mother liquors were then allowed to evaporate, dissolved in water and treated with aqueous $[NH_4][PF_6]$, to give material of identical physical propeties to $Cu(L^7)(PF_6)_2$.

Calc. for $C_{18}H_{39}CuN_5O_9.H_2O$ C: 40.59, H: 7.39, N: 13.16. Found C: 39.15, H: 7.20, N: 12.66

(iv) $Zn(L^7H_3)(PF_6)_2$. In a 5ml beaker 2 ml of ligand solution (145 mg, 0.419 mmol) was added to 121 mg (0.407 mmol) of $Zn(NO_3)_2.6H_2O$ dissolved in 2 ml of absolute ethanol. The solution was allowed to evapoate to dryness to give a colourless amorphous solid. This was dissolved in 3 ml of water and excess $[NH_4][PF_6]$ dissolved in 1 ml of water was added. The solution was allowed to evaporate very slowly (several weeks) to afford the title complex as large colourless crystals. Yield 139 mg (48 %).

Calc. for $C_{18}H_{39}F_{12}N_3O_3P_2Zn$ C: 30.89, H: 5.62, N: 5.62. Found C:31.07, H: 5.55, N: 6.28

I.R. (KBr): $\nu = 835$ cm^{-1} (P-F).

(H) Complexes of N,N',N''-tris-(2R)-2-hydroxypropyl-1,4,8-triazacycloundecane (L^8H_3). 0.63 g of (L^8H_3) was dissolved in absolute ethanol in a 25 ml volumetric flask to give a 7.60×10^{-2} mol l^{-1} (25.2 mg/ml.) solution.

(i) $Co(L^8H_3)(NO_3)_2$. In a 5 ml beaker 66 mg (0.227 mmol) of $Co(NO_3)_2.6H_2O$ was dissolved in 1 ml of absolute ethanol. 2 ml (75.6 mg, 0.227 mmol) of ligand solution was added with the solution becoming a deep rose-pink colour. The solution was allowed to evaporate until almost dry, with the product formed as large purple crystals. The material was filtered off, washed with very cold ethanol and then with ether. Yield 51 mg (49 %).

Calc. for $C_{17}H_{39}CoN_5O_{10}$ C: 38.35, H: 7.38, N: 13.15. Found C: 37.57, H: 7.14, N: 12.83

(ii) Ni(L^{8}H$_3$)(PF$_6$)$_2$. The method was analogous to that for Co(L^{8}H$_3$)(NO$_3$)$_2$. The reaction mixture immediately produced a green precipitate of nickel hydroxide, which redissolved on the addition of 2 ml of water. After 5 days excess [NH$_4$][PF$_6$] was added and precipitated green microcystalline material. The solution was filtered and the product was redissolved in water to give a blue solution. The material was crystallised by the slow evaporation of an acetonitrile/water (1:1) solution. The material lost solvent to afford pale blue plates. Crystals (of presumably Ni(L^{8}H$_3$)(PF$_6$)$_2$.xH$_2$O) could be stored indefinitely in a sealed vial with one drop of the mother liquors. Yield 45 mg (43%).

Calc. for C$_{17}$H$_{37}$F$_{12}$N$_3$NiO$_3$P$_2$. C: 30.04, H: 5.49, N: 6.19. Found C: 30.04, H: 5.39, N: 6.34

I.R. (KBr): v = 837 cm^{-1} (P-F).

(iii) Cu(L^{8}H$_3$)(PF$_6$)$_2$. The method was analogous to that for Co(L^{8}H$_3$)(PF$_6$)$_2$. The nitrate salt was produced as an amorphous pale blue solid. This was dissolved in 1 ml of water, an excess of [NH$_4$][PF$_6$] was added and on cooling a blue precipitate was produced. This was filtered and recrystallised by the slow evaportion of a water solution, to afford deep blue needles which lost solvent upon drying. Yield 39 mg (37%).

Calc. for C$_{17}$H$_{37}$CuF$_{12}$N$_3$O$_3$P$_2$ C: 28.81, H:5.44, N:6.13. Found C: 29.62, H: 5.45, N: 6.38.

I.R. (KBr): v = 835 cm^{-1} (P-F).

(iv) Zn(L^{8}H$_3$)(PF$_6$)$_2$. The method was analogous to that for Co(L^{8}H$_3$)(NO$_3$)$_2$. The nitrate salt was produced as a colourless amorphous solid. This was dissolved in 2 ml of water and the solution was filtered. An excess of [NH$_4$][PF$_6$] dissolved in 1 ml of water was added and the solution was refrigerated overnight. The hexafluorophosphate salt was

precipitated as white plates. The mother liquor was evaporated down to 1 ml and refrigerated to afford a second crop of material. Yield 44 mg (28 %)

Calc. for $C_{17}H_{37}F_{12}N_3O_3P_2Zn$ C: 29.77, H: 5.44, N: 6.13. Found C: 29.55, H: 5.41, N: 6.05

I.R. (KBr): $\nu = 836$ cm^{-1} (P-F).

(I) Complex of N,N',N''-tris-(2R)-2-hydroxypropyl-1,5,9-triazacyclotridecane (L^{9}H$_3$). 0.58 g of L^9 was dissoved in ethanol in a 25 ml volumetric flask to give a 6.45×10^{-2} mol l^{-1} (23.2 mg/ml) solution.

Ni(L^{9}H$_3$)(NO$_3$)$_2$. In a 5 ml beaker 55 mg (0.189 mmol) of Ni(NO$_3$)$_2$.6H$_2$O was dissolved in 2 ml of absolute ethanol. 3 ml of ligand solution was then added. The solution became a deeper hue of green. The solution was evaporated to dryness to afford a tacky green mass. Washing with ether yielded the material as a green powder which was recrystallised by the slow evapoarion of an ethanol solution. Yield 34 mg (32%).

Calc. for $C_{19}H_{41}NiN_5O_9$. C: 32.23, H: 5.84, N: 5.93. Found C: 32.44, H:5.83, N: 5.99.

References

1. Richman, J.E.; Atkins, T.J. *J. Am. Chem. Soc.*, 1974, *96*, 2268

2. Koyama, H.; Yoshino, T. *Bull. Chem. Soc. Jpn.* 1972, *45*, 481

3. Koppenhoefer, B; Schurig, V. *Org. Synth.* 1984, 151.

4. Koppenhoefer, B; Schurig, V. *ibid.* 1984, 160.

5. Sayer, B.A.; Michael, J.P.; Hancock, R.D. *Inorg. Chim. Acta.* 1983, *77*, L63

6. Robb, J. Ph.D. Thesis. University of Glasgow.

CHAPTER 3

CHROMIUM AND MANGANESE COMPLEXES OF N,N',N"-TRIS-(2-ALKYL-2-HYDROXYETHYL)-1,4,7-TRIAZACYCLOALKANES

"In the dark there dwells a light; and the darkness cannot comprehend it."

St. John (1: 5)

CONTENTS

3.1 INTRODUCTION

(3.1.1) Chromium

The macrocyclic chemistry of chromium is not extensive although several complexes of triazamacrocycles have been reported (1). Cr(III) complexes are in general difficult to prepare and those of macrocyclic ligands are no exception. This is due to the kinetic inertness associated with the d^3 configuration. There are a number of macrocyclic chromium complexes relevant to the current work. Of note is [Cr(III)TCTA] (TCTA = N,N',N"-trisacetato-1,4,7-triazacyclononane)(2). The ligand favours small hard metal centres and strongly disfavours larger ions. This is reflected in the Cr(III)/ Cr(II) couple which has a value of -1.17 V. L^1H_3 has been shown elsewhere (3) to form a dimeric

hydrogen bridged complex of Cr(III). This complex, $[Cr(III)L^1H_3L^1Cr(III)]^{3+}$, has unusual acid-base properties. Upon acidification both components of the dimer become protonated and the dimer dissociates into two monomeric $[Cr(III)L^1H_3]^{3+}$ subunits. With basification complete deprotonation occurs with concomitant hydrogen-bond rupture and dimer dissociation. These changes can be followed spectroscopically. With L^2H_3 it was hoped that the acid base behaviour could be followed with the steric bulk of the ligand preventing dimerisation. Partially protonated forms of $[Cr(III)L^2]$ could then be studied.

(3.1.2) Manganese

The coordination chemistry of manganese is well established, though not as extensive as certain other members of the first row transition series. The most stable oxidation state is +2, but this rapidly oxidises under alkaline conditions. The +3 state is also well characterised but often disproportionates, as exemplified by the solution state instability of the $[Mn(H_2O)_6]^{3+}$ ion. The ground state configuration of Mn(III) is $3d^4$ and as such, subject to Jahn-Teller distortion. Mn(IV) chemistry in the absence of suitable ligands, is often dominated by the highly stable and insoluble MnO_2. Once formed however, complexes of the +4 state display octahedral geometry and considerable stability due to a large LFSE ($-6/5$ Δ_0).

Mn(II) under normal conditions has a high-spin d^5 configuration, and as such is devoid of LFSE. Octahedral co-ordination is most common, but as indicated earlier trigonal prismatic geometry is also a possibility. Tetrahedral (e.g. $[MnCl_4]^{2-}$) and square-planar geometries are less common. Oxygen and nitrogen donors predominate and for magnetically isolated species magnetic moments of approximately 5.9 μ_B are found and agree well with the predicted spin-only value.

A great deal of work has been done upon carboxylate and amino acid donors, but relatively little has been reported on the macrocyclic chemistry of Mn(II). Fig. 3.1 illustrates a recently reported (4) Mn(II) complex of L^1H_3. This complex is formed under

neutral conditions and the structure shows that the alcohol pendant-arm groups of the ligand remain protonated. These groups are hydrogen bonded to the $[MnCl_4]^{2-}$ counter-ion. This hydrogen bonding interaction and the steric requirements of the ligand, in the absence of LFSE, dominate the geometry of the complex, causing a twist of 37.4° away from octahedral co-ordination.

Fig. 3.1. *The structure of the cation in* $[Mn(II)L^1H_3][MnCl_4]$.
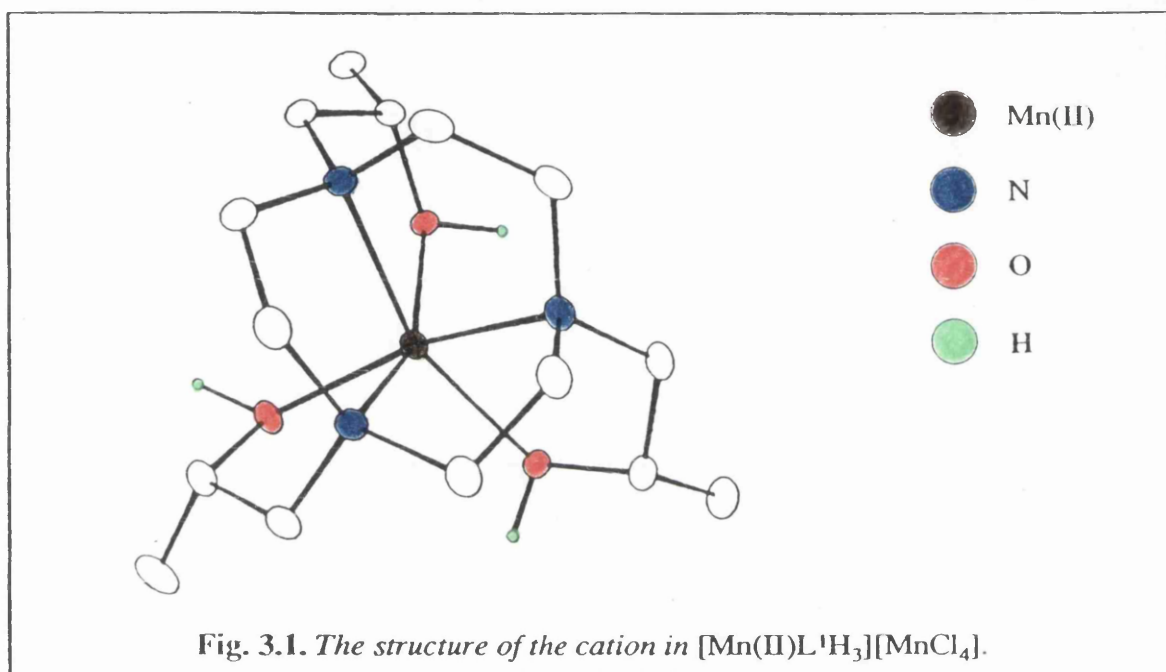
When $[Mn(II)L^1H_3]^{2+}$ is exposed to alkaline conditions it slowly oxidises to give a deprotonated Mn(IV) species. No intermediate Mn(III) species is isolated in this case. It is likely that a ligand with an "ellipsoidal cavity" and a threefold axis such as L^1H will be unable support an ion which tends to tetragonally distort in a Jahn-Teller fashion. It must be noted that a trigonal distortion does not remove the degeneracy of an E ground state, although second order Jahn-Teller distortion can manifest itself in this manner. Cole *et al.* (5) have reported a rare example of a Cu(II) system which shows no appreciable tetragonal distortion at 298 K or 129K. No explanation for this phenomenon has been advanced, although the presence of a dynamic Jahn-Teller effect is possible. Thus oxidation to Mn(IV) is made possible by the destabilisation of a postulated Mn(III) intermediate and the stabilising effect of a deprotonated ligand's alkoxide donors. In this

case the tendency of Mn(III) to disproportionate to Mn(II) and Mn(IV) may explain the difficulty in detecting Mn(III) intermediates. In simple systems this disproportionation is driven by the formation of insoluble MnO_2; however a strongly bound ligand such as $(L^1)^{3-}$ (a tris-alkoxide) stabilises Mn(IV). Mn(III) complexes of macrocyclic ligands have been prepared (1) but all these complexes exhibit sizeable Jahn-Teller distortions. Auerbeck and co-workers (6) have reported a manganese(III) complex with the pendant-arm macrocyclic ligand 1,4,7-tris(3-tert-butyl-2-hydroxybenzyl)-1,4,7-triazacyclononane. The magnetic and electrochemical properties of this compound confirm it as a genuine Mn(III) complex, but no structural details are presented and a Jahn-Teller distortion may or may not be present.

Mn(IV) complexes are in general rare and part of aim of the work was to prepare some Mn(IV) macrocyclic complexes. The $3d^3$ configuration results in a tendency towards octahedral co-ordination. Of the known examples Schiff bases, bipy (bipy = 2,2'-bipyridyl) and alkoxides (including phenoxides) present the largest group of ligands that stabilise Mn(IV). Many of these compounds are stable in water at neutral pH, but are often reduced by water in acidic media. Mn(IV) also displays a tendency to form binuclear and higher nuclearity complexes with bridging ligands; oxo and carboxylate ligators being particularly common. A small number of macrocyclic complexes of Mn(IV) have been reported: $[Mn(IV)TPP(OMe)_2]$ (TPP=tetra-phenylporphyrin) (7) and a tetranuclear oxo-bridged adamantane type cluster reported by Weighardt et al. (8). The former complex is of note since it is formed upon the addition of methanol to $[Mn(TPP)Cl][SbCl_6]$, which is believed to be a Mn(III) species with a radical cation TPP ligand. This indicates the stabilising effect of alkoxides on the Mn(IV) state.

(3.1.3) Bioinorganic Chemistry of Manganese. Photosystem II (9)

A great deal of interest is being currently shown in the poorly understood bioinorganic chemistry of manganese, which has in turn prompted a drive to develop simple models to mimic natural systems. Manganese plays a role in a number of

important biochemical processes. In some systems only redox inactive Mn(II) (non basic environments) is present, and often other divalent ions may be substituted (e.g Mg^{2+}). There are however other systems where redox active manganese centres play vital roles, such as superoxide dismutase, pseudo-catalase, a ribonucleotide reductase and most importantly the oxygen generating centres in photosystem II (PS II), a vital component of the photosynthetic process in higher plants.

Photosynthesis occurs within the chloroplasts of higher plants and also in some algae. A number of photosynthetic bacteria have been extensively studied (e.g. *Rhodopseudomonas*), and much is now understood of their photosynthetic metabolism. These species, however do not have a PS II equivalent and hence are devoid of manganese centres.

The chloroplast is a complex organelle consisting of an outer membrane, an inner membrane and thylakoid vesicles. It is at the thylakoid membrane that PS II is located. PS II has several key functions,

(1) Oxidation of water to produce oxygen.

(2) Reduction of plastoquinone (electron transport to photosystem I)

(3) To increase the pH of the thylakoid space, creating a pH gradient across

the thylakoid membrane, which drives ATP synthesis.

It is important to note that oxygen evolution occurs with a concomitant [points (1) and (3)] increase in pH.

The smallest unit of purified PS II capable of supporting oxygen evolution consists of a least 7 polypeptides with some units present in multiple copies. Two of these peptides, D1 and D2, probably co-ordinate most of the redox and photochemical activity of PS II. D1 and D2, and bear a strong resemblance to the manganese free reactive centres of photosynthetic bacteria. This structure however, sheds no light on the location or role of the manganese centres of PS II.

The overall reaction of photosystems I and II may be written,

$$2H_2O + 2NADP^+ \longrightarrow O_2 + 2NADPH + 2H^+$$
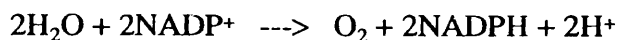
and it can be seen that water is used as a reductant for NAPH$^+$ and also as a Bronsted acid source. PS II supplies electrons to PS I via a series of bound and mobile plastoquinones and two cytochromes (b_{559} and c_{552}), with plastocyanin acting as a final electron acceptor. Plastocyanin contains a Cu^{2+} ion in an N_2S_2 ligand array, near the surface of a small polypeptide. The reduced form of plastocyanin then reduces the oxidised form of P700, the reaction centre of PS I. PS I is now reactivated for NADPH production.

It has been shown that in each complete reaction (10) PS II undergoes 4 separate photon induced events (i.e. 2 water molecules are converted to one of oxygen). When PS II is allowed to equilibrate in the dark and is then exposed to flashes of light, it is found that maximum oxygen evolution is achieved on the 3rd flash and every 4th flash thereafter. The dark state is now commonly labelled as S_1 and the next three states S_2, S_3 and S_4 respectively. Oxygen evolution occurs rapidly from the S_4 state to generate an S_0 state. In the dark S_2 and S_3 are quickly reduced to S_1 (half-lifes approx. 1 min.); and S_0 is oxidised to S_1 (half-life approx.10 min).

The role of manganese in PS II is poorly understood. EXAFS studies have shown that 4 manganese atoms are present in each photosynthetic unit, probably as a pair of dimeric subunits, with individual centres within a dimeric unit separated by a distance of 2.7 Å. This implies a μ-oxo bridged species. The possibility of a trimeric unit with a satellite monomeric unit cannot be ruled out. Electron spin echo nuclear spin envelope modulation (e.s.e.e.m.) investigations (11) indicate that the primary co-ordination sphere is dominated by oxygen donors, but there is a strong possibility that nitrogen donors may be present. The co-ordination number at the manganese centre is probably six. For oxygen donors in a polypeptide environment the possible amino-acid residues are: glutamic acid and aspartic acid (carboxylate donors); tyrosine (phenoxide donors); threonine and serine (alcohol or alkoxide donors). The ligands prepared in this work are amino-alcohols and as such may provide useful reference compounds for current photosynthesis research.

RESULTS AND DISCUSSION

(3.2) [Cr(III)L^{2}H$_3$][PF$_6$]$_3$

(3.2.1) Synthesis of [Cr(III)L^{2}H$_3$][PF$_6$]$_3$.

In preparing any chromium complex the choice of metal based starting material is important. The most common starting material is hydrated chromium chloride ([CrCl$_2$(H$_2$O)$_4$]Cl.2H$_2$O). This complex is kinetically inert and as such must be first modified to allow facile ligand replacement. Commonly [CrCl$_2$(H$_2$O)$_4$]Cl.2H$_2$O is boiled in a donor solvent such as dimethyl formamide or dimethyl sulphoxide. At high temperatures ligand replacement occurs more rapidly and the equilibrium position is constantly shifted with water being driven off from the hot reaction mixture. The resulting complexes are species such as CrCl$_3$(dmf)$_3$ or CrCl$_3$(dmso)$_3$, and a ligand added to solutions of these complexes will displace the more labile dmf and dmso ligands. However with L^{1}H$_3$ and L^{2}H$_3$ this method of preparation proved to give very low yields and also required tedious column chromatography on Sephadex to isolate the desired products.

It was found that tris sodium alkoxides of L^1 and L^2 were moderately soluble in tetrahydrofuran. CrCl$_3$(thf)$_3$ is a well established starting material in organometallic chemistry, but is not often used in other forms of chromium coordination chemistry. Upon addition of the tris-sodium salt of L^{2}H$_3$ (i.e. (L^2)$^{3-}$) to a thf solution of CrCl$_3$(thf)$_3$ a fine precipitate of NaCl was produced. The initial green complex produced is assumed to be the fully deprotonated complex [Cr(III)L^2] but this material proved particularly moisture sensitive and no analysis could be obtained. Upon treatment with water the solution took on a purple hue which was attributed to a mixture of partially protonated complexes, [Cr(III)L^{2}H$_x$][HO$^-$]$_{3-x}$ (x = 1-3). Again, these intermediates could not be isolated in a workable form. Upon treatment with a strong acid a deep red-pink colour resulted and this was attributed to [Cr(III)L^{2}H$_3$]$^{3+}$. This was verified by the addition of

excess $[NH_4][PF_6]$, which promoted the growth of crystalline $[Cr(III)L^2H_3][PF_6]_3$. This material gave an acceptable analysis. The yield was not high, but attempts to prepare this material by other methods failed.

(3.2.2) Acid-Base Behaviour. Electronic and Circular Dichroism Spectroscopy.

As indicated above the spectroscopic properties of $[Cr(III)L^2H_3]^{3+}$ are strongly dependent upon pH. The absorption and circular dichroism spectra of a sample of $[Cr(III)L^2H_3][PF_6]_3$ in acetonitrile solution is displayed in figure 3.2(a). Upon dissolution the material changes from an intense pink to a pale purple hue. This is probably a complex to solvent proton transfer. The structure of $[Cr(III)L^2H_3]^{3+}$ is presumably analogous to a protonated subunit of the dimeric Cr-L^1 complex (vide supra), with the bulky isopropyl groups preventing dimer formation.

The absorption and circular dichroism spectra of $[Cr(III)L^2H_3][PF_6]_3$ dissolved in a 4:1 mixture of acetonitrile and 12 mol l^{-1} hydrochloric acid is displayed in fig 3.2(b). This solution has the characteristic intense pink colouration of the solid complex, indicating that it remains protonated at low pH values. The complex is stable in 12 mol l^{-1} hydrochloric acid for several months. When the material was originally prepared it was not d that low polarity solvents such as ether caused the complex to slowly dissolve and take on a purple cast. This indicates that the complex is very acidic, since it seems likely that protonation of weak bases such as ether is occurring.

Finally the absorption and circular dichroism spectra of $[Cr(III)L^2H_3][PF_6]_3$ in a 4:1 acetonitrile-triethylamine solution is displayed in fig.3.2(c). This solution is deep green in colour, but slow acidification results in a purple and eventually an intense pink hue. This represents slow protonation of the complex, and is completely reversible, with basification resulting in a green solution again.

The complex can have no higher than C_3 symmetry. However microsymmetry at the metal centre will be approximately octahedral, and octahedral labels will therefore be used in assigning absorption bands (table 3.1). In all cases the third expected transition is obscured by charge transfer bands.

The low energy transition for $[Cr(III)L^1H_3L^1Cr(III)]^{3+}$ is at 540 nm, which is intermediate between the acidic and basic values for $[Cr(III)L^2H_3]^{3+}$ noted above. This is explained by assuming that the protonation level at each chromium centre in $[Cr(III)L^1H_3L^1Cr(III)]^{3+}$ is one half of that of $[Cr(III)L^2H_3]^{3+}$ and $[Cr(III)L^2]$. The "neutral" form of $[Cr(III)L^2]$ has the low energy band occurring at 558 nm which is almost exactly halfway between the value of the acidic and basic forms. Hence the protonation level at each chromium centre is approximately 1.5. This of course is only an average situation. With L^1 dimerisation occurs at this stage of protonation. This cannot occur in the case of L^2 and it is concluded that the "neutral" form of the complex is a mixture of $[Cr(III)L^2H]^+$ and $[Cr(III)L^2H_2]^{2+}$ in equilibrium. This is confirmed by an examination of the lineshapes of the CD spectra. In the "neutral" form the higher energy band is split into components with identical positions to the bands in the acidic and basic forms of the complex. Noting that the $\Delta\varepsilon$ values of the acid form are greater than those of the basic form, it is probable that in MeCN solution $[Cr(III)L^2H_3]^{3+}$ is predominantly in one of the basic forms; $[Cr(III)L^2H_2]^{2+}$, $[Cr(III)L^2H]^+$ or $[Cr(III)L^2]$.

The ligand field splitting value for Cr(III) is given simply by the energy of the lowest transition. This gives values of 19150 cm^{-1} (Racah $B = \,98$ cm^{-1} for the acidic form and 17000 cm^{-1} (Racah $B = 740$ cm^{-1}) for the basic form. These figures are rationalised by considering the alcohol donors in the acidic form of the complex are poorer π-donors than the alkoxide donors of the basic form. π-donation to the t_{2g}^3 set is a repulsive interaction and thus greater π-donation in the basic form weakens metal-ligand bonding and increases d-d electronic repulsion. This is reflected in lower ligand field splitting and higher interelectron repulsion values. Conversely with the acidic form protonation of the oxygen donor atoms reduces π-bonding which in turn reduces electron density at the metal centre. This reduces interelectron repulsion and permits closer ligand-

metal approach causing a stronger ligand field. As expected the $10Dq$ value for the acid form is typical for that of an N_3O_3 ligand field, being intermediate between the values for $[Cr(III)(H_2O)_6]^{3+}$ (17,400 cm^{-1}) and that of $[Cr(III)(NH_3)_6]^{3+}$ (21,550)(13). The $10Dq$ of the basic form is particularly low.

The circular dichroism spectra are typical of d^3 ions in a trigonally distorted octahedral field. The g factors are of a magnitude that confirms the two visible bands as d-d transitions. The lower energy band in both cases is split into $^4A_2 \rightarrow {}^4E(T_{2g})$ and $^4A_2 \rightarrow {}^4A_2(T_{2g})$ components of opposite sign. The higher energy transition is unambiguously assigned as the magnetic dipole allowed $^4A_2 \rightarrow {}^4E(T_{1g})$ transition. These spectra bear considerable resemblance to the spectra of Cr(TCTA) (12), with two absorption bands giving rise to three bands in the CD spectrum. The CD spectra are somewhat unsymmetrical due to the absorption bands overlapping to some extent, although the degree of overlap is less than for [Cr(III)TCTA]. It is interesting to note that the $\Delta\varepsilon$ values for the acidic form are very much greater than for the basic. This is possibly due to a greater degree of twist in the acidic form giving rise to greater optical activity. It can be speculated that this occurs due to repulsion between bound protons at the O_3 face of the complex in a similar fashion to the steric interaction of axial protons in cyclohexane rings. There would also be a large electrostatic component to this repulsive interaction.

Noting the fact that the acetate ligands in [Cr(III)TCTA] are good π-donors, the $10Dq$ values of [Cr(III)L^{2}H$_3$]$^{3+}$ and [Cr(III)TCTA] (19500 cm^{-1}) are surprisingly similar. Hancock (14) has explained the high ligand field strengths of TCTA complexes by postulating that acetate donors are sterically very efficient, which allows short metal-ligand bond lengths and larger $10Dq$ values. Ligands with methylene residues adjacent to the donor atoms are not sterically efficient and the presence of the bulky isopropyl group in L^2 will cause even less efficient packing of the ligand about the metal centre. Thus the poor π-donor ability of the acid form of [Cr(III)L^{2}H$_3$]^3 is counteracted by the steric inefficiency of L^2.
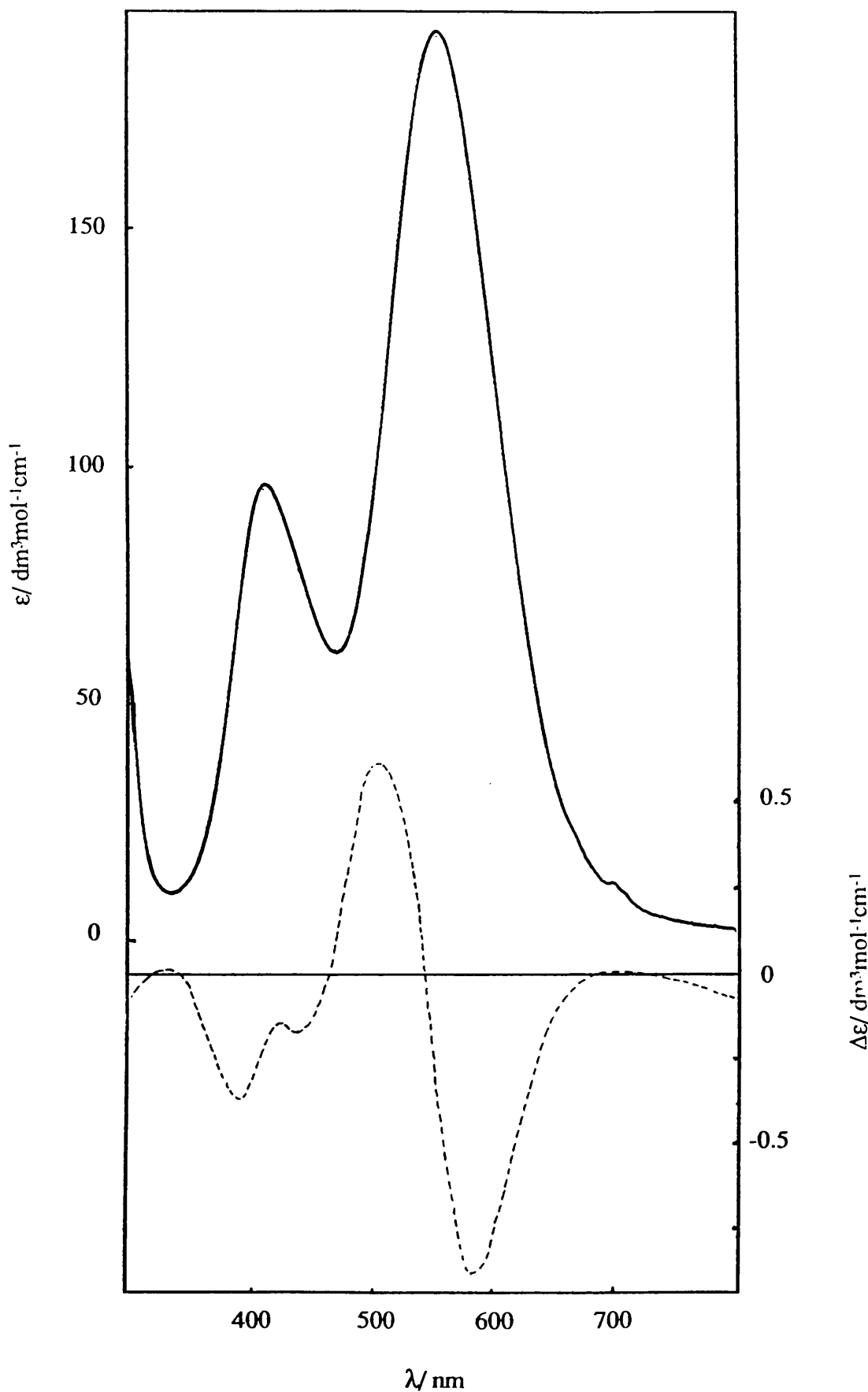
Fig. 3.2(a). *Absorption and circular dichroism spectra of* [Cr(III)L²H₃][PF₆]₃

in acetonitrile solution. "Neutral" form.
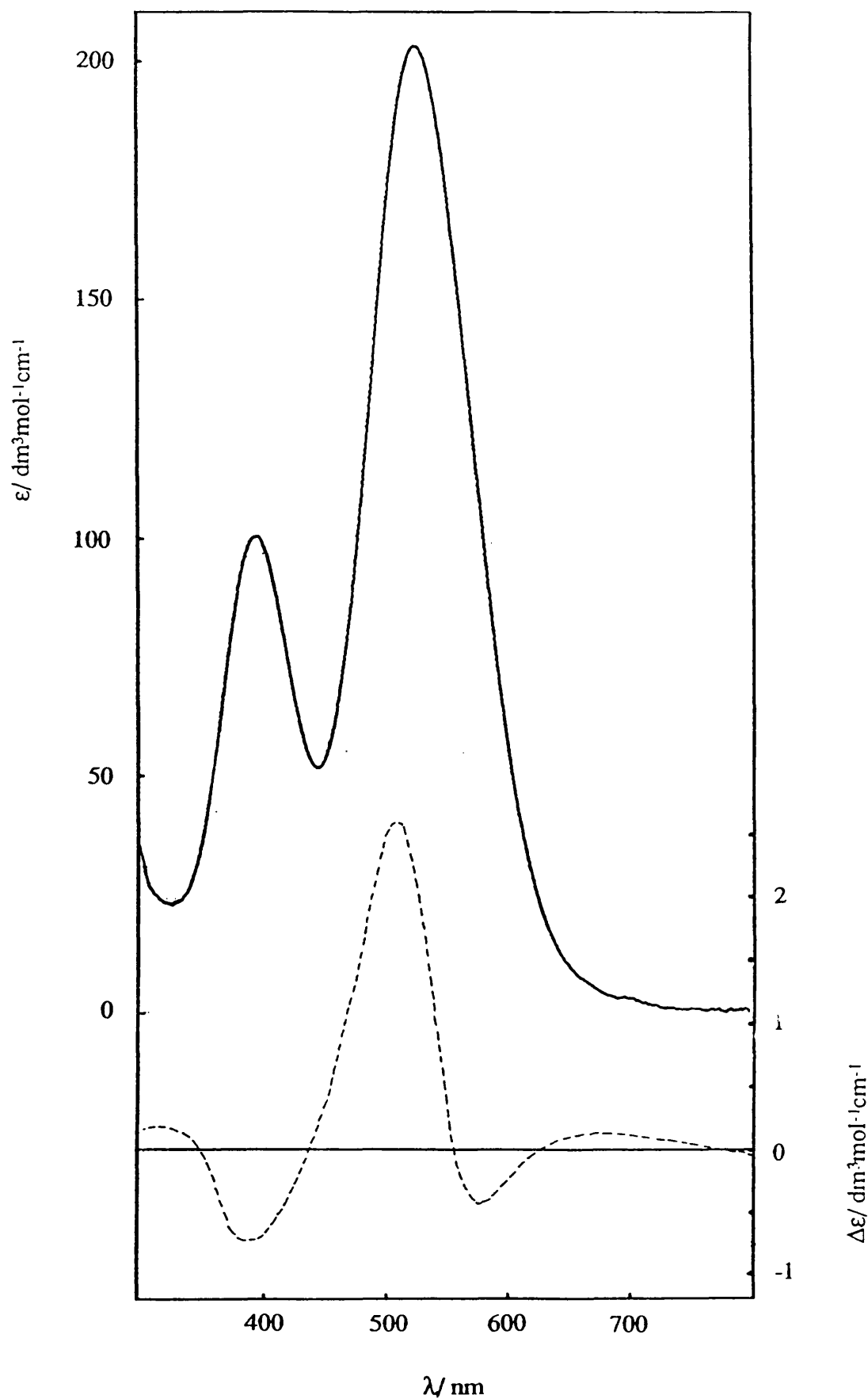
Fig. 3.2(b). *Absorption and circular dichroism spectra of* $[Cr(III)L^2H_3][PF_6]_3$

in acetonitrile-hydrochloric acid (12 mol l^{-1}) solution. Acidic form.
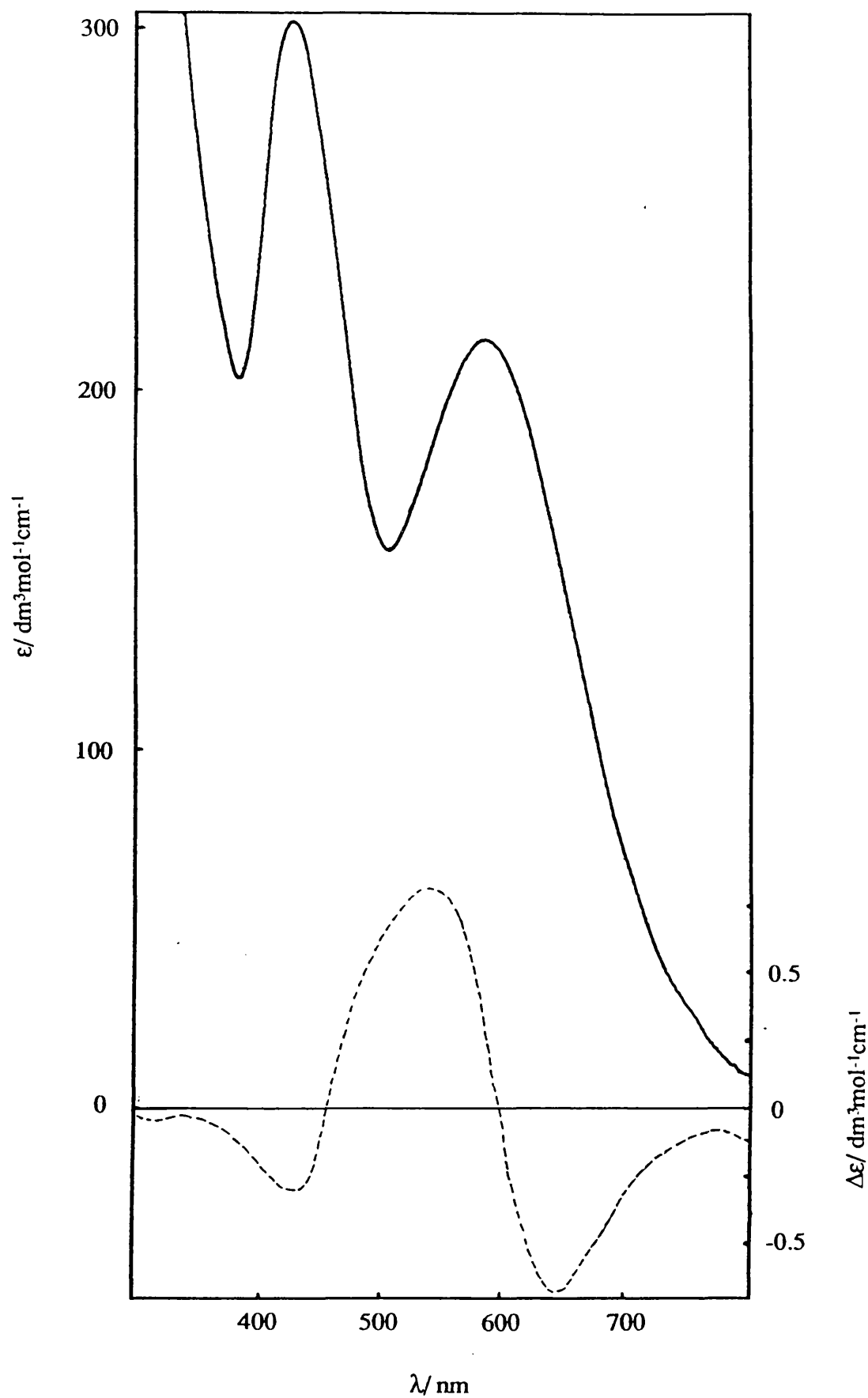
Fig. 3.2(c). *Absorption and circular dichroism spectra of* [Cr(III)L²H₃][PF₆]₃

in acetonitrile-triethylamine solution. Basic form.

Table 3.1. Absorption and Circular Dichroism Characteristics of $[\text{Cr(III)L}^2\text{H}_3]^{2+}$ in various media. ($10Dq$ [cm^{-1}], B [cm^{-1}], λ [nm], ε [mol^{-1}l cm^{-1}], $\Delta\varepsilon$ [mol^{-1}l cm^{-1}], $g = \Delta\varepsilon/\varepsilon$.

		Conditions	
	Neutral	Acidic	Basic
$10Dq$	-	17000	19150
B	-	740	598
$^4A_{2g} \rightarrow {}^4T_{2g}$			
λ_{abs}	558	522	587
ε	190	205	215
λ_{cd} (-ve max)	-	580	651
$\Delta\varepsilon$ (-ve max)	-	-0.44	-1.37
$10^3.g$ (-ve max)	-	2.15	6.37
λ_{cd} (+ve max)	-	505	538
$\Delta\varepsilon$ (+ve max)	-	2.64	1.64
$10^3.g$ (+ve max)	-	12.9	7.63
$^4A_{2g} \rightarrow {}^4T_{1g}$			
λ_{abs}	413	391	422
ε	95	100	300
λ_{cd}	-	388	424
$\Delta\varepsilon$	-	-0.76	-0.66
$10^3.g$	-	7.60	2.20

(3.3) MANGANESE COMPLEXES OF L^1H_3, L^2H_3 AND L^3H_3.

(3.3.1) Preparation of Manganese Complexes of L^1H_3, L^2H_3 and L^3H_3.

The preparation of the manganese complexes of L^1H_3, L^2H_3 and L^3H_3, as expected, were all found to be pH sensitive. With increasing pH the reaction mixtures of ligand solution and $MnCl_2$ were found to darken more rapidly, indicating oxidation to Mn(IV). In the case of L^1H_3 use of excessive base was found to result in solutions from which no material could be crystallised, but basification to pH 8 resulted in the formation of the dimeric cation $[Mn(II)L^1H_3L^1Mn(IV)]^{3+}$. The addition of $[NH_4][PF_6]$ resulted in the precipitation of $[Mn(II)L^1H_3L^1Mn(IV)][PF_6]_3$ as a brown-red powder. Some of the material was used for variable temperature magnetic moment measurement, and the remainder was recrystallised for crystallographic purposes.

The reaction of L^2H_3 and $MnCl_2$ was unusual in that it was noticed that the solution darkened appreciably without the addition of base. This oxidation at neutral pH is surprising since most Mn(II) complexes are stable to aerobic oxidation at pH 7. A small quantity (approximately 1 mg) of a colourless white material was also isolated from the reaction mixture and the infra-red spectrum of this material indicated the presence of C-H, O-H and P-F stretching. This white material is therefore tentatively formulated as $[Mn(II)L^2H_3][PF_6]_2$ by analogy with the colourless $[MnL^1H_3][MnCl_4]$. Attempts to prepare more significant quantities of $[Mn(II)L^2H_3][PF_6]_2$ by the acidification of MeCN solutions of $[Mn(IV)^2][PF_6].H_2O$ resulted in colourless solutions from which no crystalline material could be isolated. These solutions presumably contained $[Mn(II)L^2H_3]^{2+}$ since on basification these solutions darkened, which upon evaporation precipitated $[Mn(IV)L^2][PF_6].H_2O$.

$[Mn(III)L^3H_3L^3Mn(II)][PF_6]_2.2H_2O$ was prepared in a similar manner to $[Mn(II)L^1H_3L^1Mn(IV)][PF_6]_3$, except that slightly more basification was required to complete the reaction. In contrast to L^1H_3, an examination of the elemental analysis of

[Mn(III)L³H₃L³Mn(II)][PF₆]₂.2H₂O indicated that the cation had a 2+ charge and hence could not be a [Mn(II), Mn(IV)] species.

Attempts at the preparation of Mn complexes of larger ring size ligands were unsuccessful. In all cases addition of ligand to aqueous solutions of MnCl₂ resulted in the precipitation of MnO₂. Neutralisation of solutions resulted in the isolation of protonated ligands only.

(3.3.2) STRUCTURE AND SPECTROSCOPIC PROPERTIES OF [Mn(II)L¹H₃L¹Mn(IV)][PF₆]₃

(3.3.2.1) Oxidation State Assignment and Crystal Structure

In describing the structure of [Mn(II)L¹H₃L¹Mn(IV)][PF₆]₃ difficulty was encountered in assigning oxidation states to the metal centres present. It is clear from the elemental analysis that a dimeric cation is present with a 3+ charge, which is required to balance three [PF₆]⁻ counter ions. The crystal structure and atom labelling scheme of [Mn(II)L¹H₃L¹Mn(IV)]³⁺ is presented in fig. 3.4.

The dimeric nature of the complex is confirmed with the cation consisting of two metal centres and two ligands linked *via* hydrogen-bonds. It can also be seen that the hydrogen-bonding interaction between the two "halves" is not symmetric, and that the structure consists of a protonated ligand (L¹H₃) and a deprotonated ligand (L¹)³⁻. The ligand-set therefore has a total charge of 3-, leaving a total charge of 6+ on the metal centres. To complicate matters, a little residual electron density was found in the difference map which could have been a further non-bridging proton, disordered about three possible sites on either component of the dimer. This would indicate a ligand-set charge of 2- and a total metal centre charge of 5+. Hence there a number of possible total oxidation states: [Mn(II), Mn(III)], [Mn(III), Mn(III)], [Mn(II), Mn(IV)]. Mn(I)

possibilities have not been included since it is very unlikely that a hard donor such as L^1H_3 would form stable complexes with a soft centre such as Mn(I).

Fig. 3.4. *Structure of the cation in* $[Mn(II)L^1H_3L^1Mn(IV)][PF_6]_3$

Fig. 3.5 shows each half of the dimer as viewed along the C_3 axis. It is obvious that there are different geometries at each metal centre. The protonated component has almost perfect trigonal prismatic geometry (twist angle $\phi = 60.0°$). Mn(III) (d^3) and Mn(IV) (d^4) would tend to be octahedral since they both require significant LFSE. Thus this half is designated as a Mn(II) centre. An examination of the metal-ligand bond lengths (table 3.2) shows that the metal-ligand distances in this component of the dimer are almost identical to the bond lengths in $[Mn(II)L^1H_3]^{2+}$, confirming this as a Mn(II) centre. This is also supported by the fact that this component remains protonated, since Mn(II) has a tendency to be acid stable. Alcohol donors will tend to deprotonate in

Mn(III) and Mn(IV) complexes, since the presence of the more highly charged ion (*i.e.* a stronger Lewis acid) results in the co-ordinated alcohol group becoming more acidic.
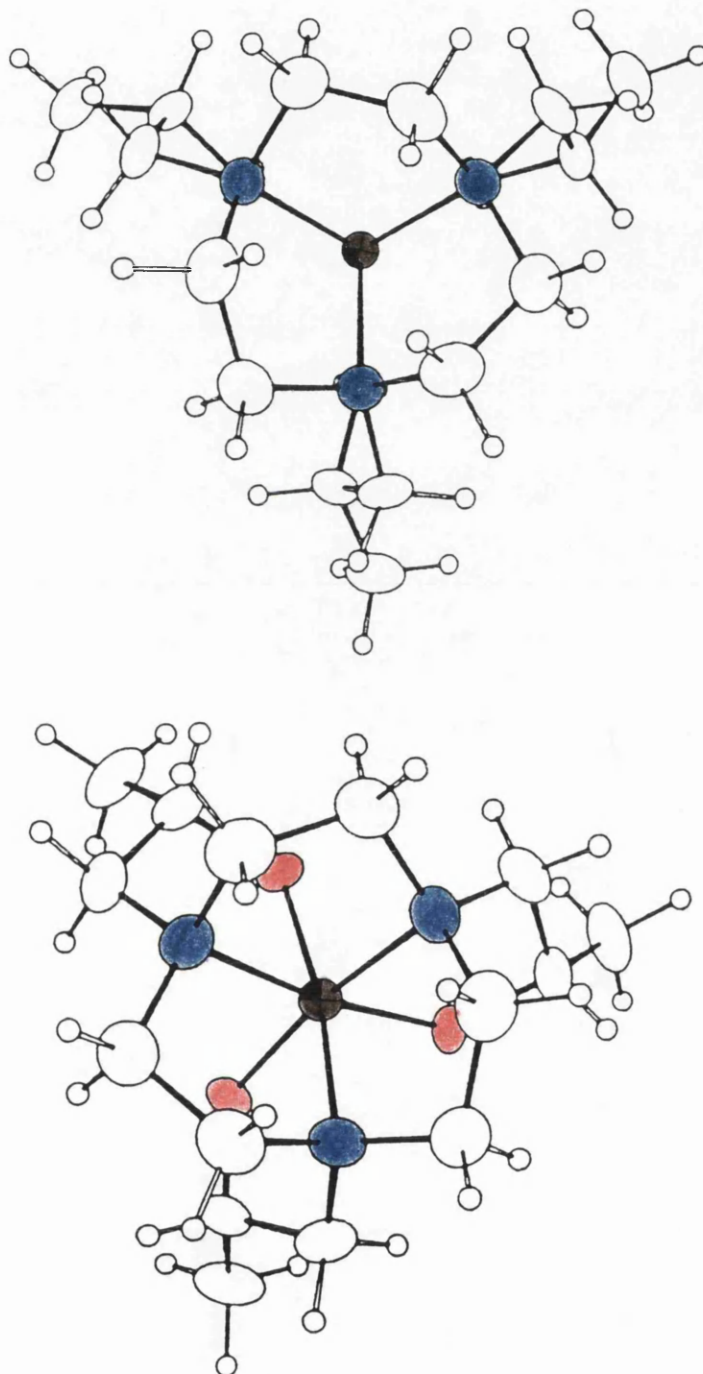
Fig. 3.5. *Views of each half of* [Mn(II)L^{1}H$_3$L^{1}Mn(IV)]$^{3+}$ *looking down the C$_3$ axis.*

The deprotonated component displays a twist angle of 10.9°, and hence is almost octahedral. It should be appreciated that the pendant-arms of L^1 are too "short" to allow perfect octahedral geometry as is indicated in $[Co(III)L^1H_3L^1Co(III)]^{3+}$ (15) which has an average twist angle of 10.7°, despite low-spin Co(III) (d^6) having maximum LFSE (-12/5 Δ_0) for perfect octahedral geometry (see chapter 4). Mn(III) and Mn(IV) would both be expected to adopt octahedral co-ordination. However, Mn(III) is a d^4 ion, and as such would be expected to exhibit a significant Jahn-Teller distortion. The metal atoms of the dimer lie on a three fold axis and all Mn-O and Mn-N bonds lengths are identical, indicating the absence of a Jahn-Teller distortion. The complex is therefore a [Mn(II), Mn(IV)] dimer. The Mn-Mn distance is 4.653 Å.

Both units of the dimer have a δ conformation for the exocyclic chelate rings. Surprisingly the endocyclic rings have opposite conformation; λ for the Mn(IV) half (as in $[Co(III)L^1H_3L^1Co(III)]^{3+}$) and δ for the Mn(II). The conformation inversion of the Mn(II) half is a result of the trigonal prismatic co-ordination. The chirality of the Mn(IV) half as defined by the pendant arms is Δ, and hence the overall chirality is $\Delta(\lambda\delta)$.

Table 3.2. Selected Bond Lengths (Å) and Bond Angles (deg) for
$[Mn(II)L^1H_3L^1Mn(IV)]^{3+}$

Mn(1)-N(1)	2.251 (5)	Mn(2)-N(2)	2.051 (5)
Mn(1)-O(1)	2.142 (4)	Mn(2)-O(2)	1.857 (4)
O(1)-H(1)	0.906 (4)	O(2)-H(1)	1.841 (3)
N(1)-Mn(1)-N(1)'	78.6 (2)	N(2)-Mn(2)-N(2)'	84.5 (2)
O(1)-Mn(1)-O(1)'	91.8 (2)	O(2)-Mn(2)-O(2)'	96.2 (2)
N(1)-Mn(1)-O(1)	77.0 (2)	N(2)-Mn(2)-O(2)	96.0 (2)

It is interesting to note the ratio of the Mn-O bond lengths to the Mn-N bond lengths in the two components of the dimer. In the Mn(II) portion (and also in $[Mn(II)L^1H_3]^{2+}$) the Mn-O distances are 0.11Å shorter than the Mn-N distances. Whereas in the Mn(IV) component the Mn-O distances are shorter than the Mn-N distances by 0.19Å. The absolute values of the bond lengths will naturally be smaller for the Mn(IV) (ionic radius 53 pm) than for the Mn(II) component (ionic radius 67 pm), but it is not obvious why the Mn-O distance should be shorter than the Mn-N in the Mn(IV) case. The Mn(IV) centre has a t_{2g}^3 configuration and as such the e_g set is empty and allows closer approach of the pendant-arm donor atom, due to reduced electronic repulsion. Thus depopulation of the anti-bonding e_g set results in increased bonding. The Mn(IV) component is also an alkoxide, and a superior π-donor to the alcohol donors of the Mn(II) component. This will lead to a greater degree of p-donation to t_{2g}^3 for the Mn(IV) component. Such donation would result in partial double bond character and shortening of the Mn-O bond lengths. The nitrogen donors have no non-bonding electron pairs available and hence cannot participate in π-bonding. This is a nice example of π-bonding in transition metal chemistry, for which direct evidence, is rare.

Wieghardt and co-workers have also reported in association with Belal *et al.* (4) the preparation of $[Mn(IV)L'][ClO_4]$, where L'=N,N',N''-tris-(2-hydroxyethyl)-1,4,7-triazacyclononane. This complex is monomeric and shows bond leng 's, bond-angles and twist angle similar to the Mn(IV) component of $[Mn(II)^1H_3L^1Mn(IV)]^{3+}$. This complex was prepared by using 35 % H_2O_2 as an oxidant and hence it is possible that dimer formation was circumvented by the use of a strong oxidant. However it is also possible that the use of the optically pure L^1H_3, which "locks" 5 membered chelate rings into a common configuration allows the formation of a stable dimeric intermediate, which resists further (aerobic) oxidation. It is also possible that the combination of octahedral and trigonal prismatic geometries is an efficient packing of ligands and metal centres in $[Mn(II)L^1H_3L^1Mn(IV)]^{3+}$. Weighardt has noted (16) that it was only with difficulty that crystalline material was obtained with the non-dissymmetric $[Mn(IV)L']^+$.

(3.3.2.3) Magnetic Moment Measurement

The temperature dependant magnetic moment and magnetic susceptibility of [Mn(II)L^{1}H$_3$L^{1}Mn(IV)][PF$_6$]$_3$ are displayed in fig. 3.6. The magnetic moment, μ varies from 7.1 μ_B at 295 K to 4.4 μ_B at 2 K. For two magnetically independent metal centres the total (spin only) magnetic moment, for a [Mn(II), Mn(IV)] system, would be given by $((\mu_1^2 + \mu_2^2)^{1/2}) = (5.92^2 + 3.87^2)^{1/2} = 7.07$ μ_B. On this basis an oxidation state assignment of [Mn(II), Mn(IV)] seems reasonable. The Mn(II) component has a ^6S ground state and as such will display almost exactly spin-only behaviour (5.93 μ_B). The spin-only value of the Mn(IV) component is then 3.90 μ_B, which is good agreement for a high-spin d^4 species. With complete anti-parallel coupling ($S=1$ ground state) a moment of 2.83 μ_B would be expected, which is not achieved at 2 K.

The temperature dependence of the magnetic susceptibility is interpreted using the Heisenberg-Dirac-van Vleck (HDVV) model for magnetic superexchange (17). The spin exchange Hamiltonian, $H_{HDVV} = -2JS_1.S_2$ was used to fit the data, where J is the spin superexchange coupling constant, S_1 and S_2 are the total spin values of the metal centres (5/2 - [Mn(II)], 3/2 - [Mn(IV)]). In the final analysis of the data, terms for temperature-independent (field induced) paramagnetism or for paramagnetic contaminants were found to be unnecessary to achieve an acceptable fit with the data, and gave $J = -0.66$ cm^{-1} with $g = 2.06$. The negative value of the coupling constant implies antiferromagnetic superexchange. This is to be expected from a coupling *via* an [O-H-O] bridge devoid of complete orthogonalities. The value of the coupling constant falls within the range of values found for a number of dinuclear Cr(III) complexes (18). It should be appreciated that the value of this coupling constant is very small. The energy difference between the parallel and anti-parallel states is given by $2J$, and with 83.59 cm^{-1}/KJ, this has a value of 15.79 J mol^{-1}. Use of the Boltzmann distribution shows that at room temperature both states are almost equally populated (N$_{parallel}$ / N$_{antiparallel}$ = N$_p$ / N$_a$ = 0.9939). Even at 17 K N$_p$ / N$_a$ = 0.90. Only at the last few data points does the upper state become significantly depopulated [N$_p$ / N$_a$ = 0.40 (2 K), 0.74 (6 K), 0.83 (10 K), 0.89 (15 K), 0.91 (20 K)].
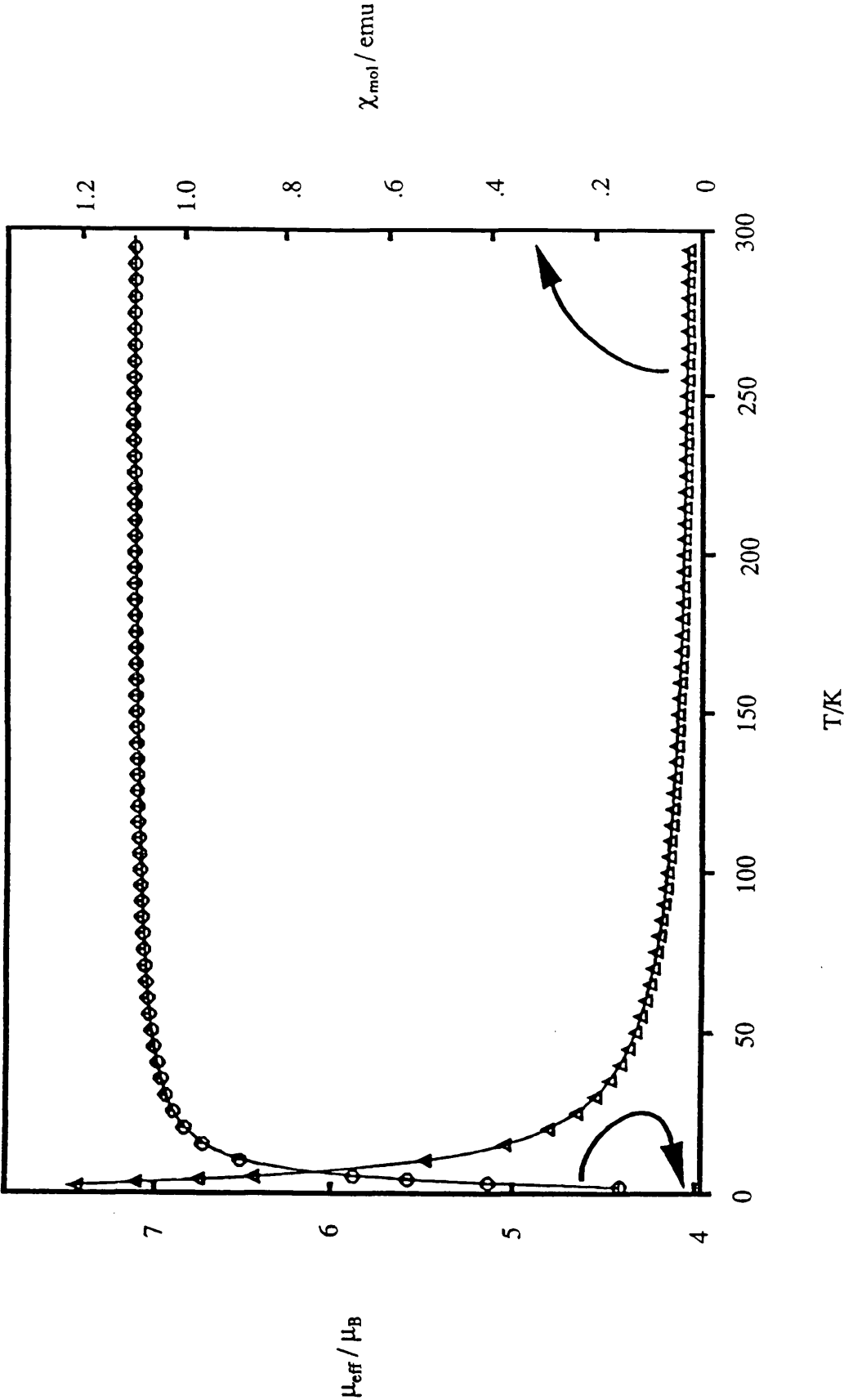
Fig..3.6. Variable temperature measurements of magnetic moment, μ_B, and magnetic susceptibility, χ_{mol}/ emu, for $[Mn(II)L^IH_3L^IMn(IV)][PF_6]_3$.

(3.3.2.4) Electronic and Circular Dichroism Spectroscopy

The electronic and circular dichroism spectra of $[Mn(II)L^1H_3L^1Mn(IV)][PF_6]_3$ are presented in fig.3.7. The spectra obtained are essentially that of the Mn(IV) portion of the dimer, since the Mn(II) portion is in a ^6S ground state and only spin-forbidden transitions would be possible. The two high energy bands and a shoulder are assigned as charge transfer bands due to their high extinction coefficients ($\varepsilon = 9000$ $mol^{-1}l$ cm^{-1}). The lower two bands have extinction coefficients of 1000 $mol^{-1}l$ cm^{-1} and it seems likely that these too are charge transfer bands, although the possibility of d-d transitions cannot be ruled out.

The lowest spin-allowed transition for a d^3 ion is $^4A_{2g} \rightarrow {}^4T_{2g}$ and in isoelectronic Cr(III) complexes has $\varepsilon = 200$ $mol^{-1}l$ cm^{-1} (vide supra)(19). Were the lowest band in the visible region due to a d-d transition, it would be expected to have a similar ε value. The circular dichroism spectrum provides more conclusive evidence as to the origins of the observed transitions. The $^4A_{2g} \rightarrow {}^4T_{2g}$ band is magnetic-dipole allowed, and should have a dissymmetry factor ($g=\Delta\varepsilon/\varepsilon$) of the order of 10^{-2}. The dissymmetry factors of the lower three bands are 5.0×10^{-4}, 2.5×10^{-3} and 1.0×10^{-3}. The Cr(III) species has a g factor of 1×10^{-2}. Thus the lower energy bands are assigned as charge transfer transitions.

In an experiment to confirm the oxidation state assignment the electronic spectrum of $[Mn(II)L^1H_3L^1Mn(IV)][PF_6]_3$ dissolved in acetonitrile was recorded. The solvent was then slowly evaporated and the resulting purple material was redissolved in triethylamine/acetontrile (1:4). The electronic spectrum was again obtained using 1:4 triethylamine/acetontrile as the reference. It was observed that the basified material now had *exactly double* the extinction coefficient of the neutral material. This is rationalised by assuming the dimer is deprotonated upon basification and the colourless Mn(II) portion of the dimer now oxidises to Mn(IV). $[Mn(II)L^1H_3L^1Mn(IV)][PF_6]_3$ has a similar extinction coefficient to that of $[Mn(IV)L^2][PF_6].H_2O$ (*vide infra*).
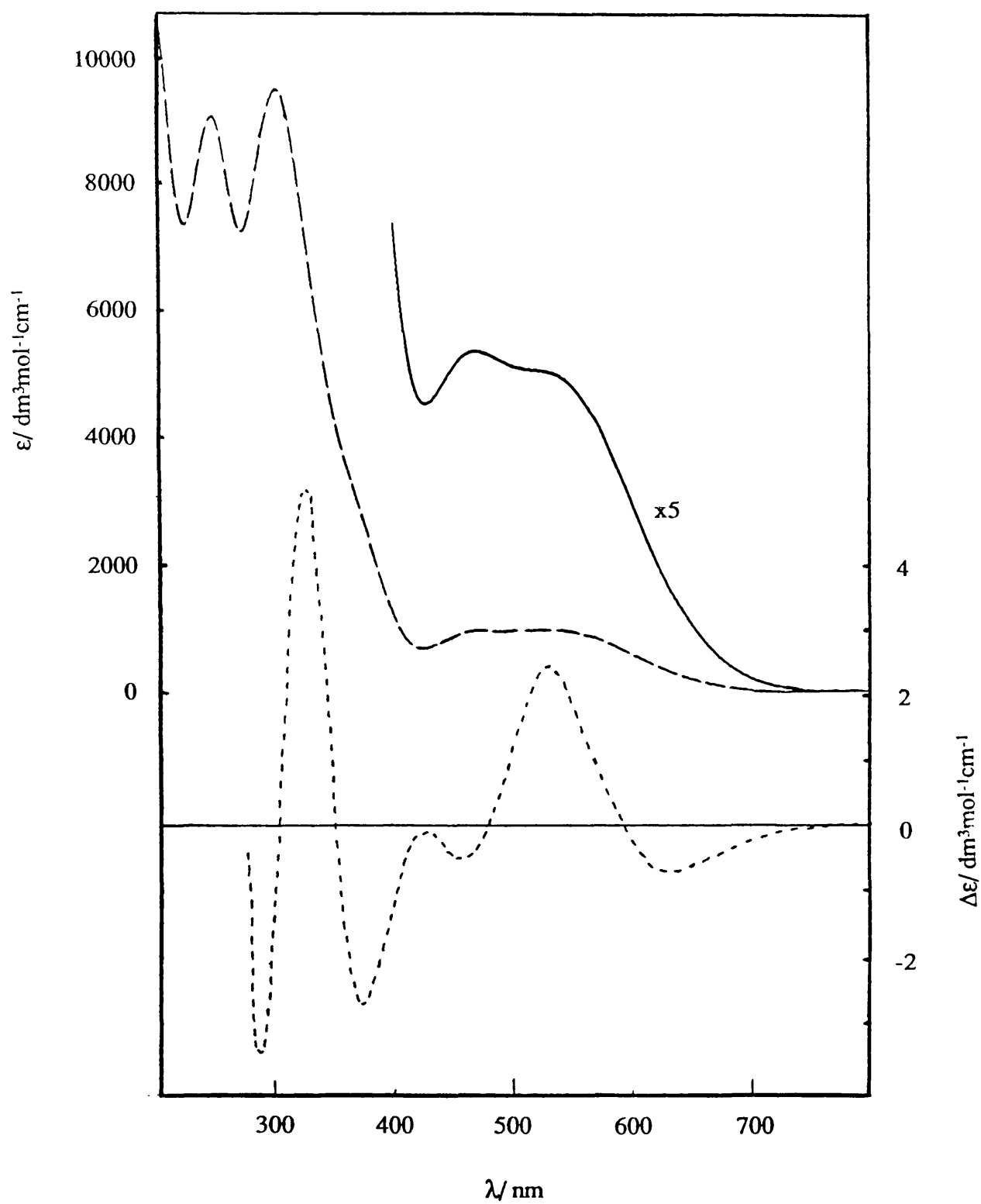
Fig.3.7. *Absorption and circular dichroism spectra of* [Mn(II)L¹H₃L¹Mn(IV)][PF₆]₃ *in acetonitrile solution.*

(3.3.2.5) Cyclic Voltammetry

The electrochemistry of $[Mn(II)L^1H_3L^1Mn(IV)][PF_6]_3$ was investigated by cyclic voltammetry and is presented in fig. 3.8. There is one fully-reversible reduction at -0.06 V (0.54 V *vs* NHE); one quasi-reversible reduction at -0.64 V (-0.06 V *vs* NHE); and one irreversible oxidation at +1.07 V (+1.65 V *vs* NHE). The fully reversible process is assigned to a [Mn(II), Mn(IV)] -> [Mn(II), Mn(III)]. This is not unreasonable since a [Mn(II), Mn(III)] species would be expected to maintain a dimeric structure in solution, as indicated by the [Mn(II), Mn(III)] nature of $[Mn(III)L^3H_3L^3Mn(II)]^{2+}$ (*vide infra*). The quasi-reversible process is assigned as [Mn(II), Mn(III)] -> [Mn(II), Mn(II)]. This reduced species could be formally viewed as Mn(II) tris alkoxide-Mn(II) tris-alcohol species. The alkoxide portion would be expected to be somewhat unstable since alkoxide ligators are typically good π donors. Mn(II) has a $t_{2g}^3 e_g^2$ configuration, and is a poor π-acceptor. Mn(II) is also destabilised by basic conditions, which also helps explain the inherent instability of the alkoxide component of the reduced dimer. This formalism is probably an extreme point of view and the real situation would be an intermediate structure in which both halfs of the dimer become chemically equivalent as partial alcohol/ alkoxide subunits. This has a precedent in the case of $[Co(III)L^1H_3L^1Co(III)]^{3+}$, which contains two crystallographically inequivalent subunits which have been shown to be equivalent in solution on the NMR timescale (15). The irreversible oxidation is assigned as a [Mn(II), Mn(IV)] -> 2[Mn(IV)]. This is justified in assuming that any oxidation of the Mn(II) centre will lead to a significant increase in the acidity of the dimer, with deprotonation resulting in dissociation. The potential of this process is appropriate to a Mn(II) -> Mn(IV) oxidation by molecular oxygen (+1.23 V *vs* NHE). This oxidation results in a dissociation of the dimer due to a loss of hydrogen-bonding and is probably chemically, and therefore electrochemically irreversible. It is impossible from a simple electrochemical study to state what the fate of the bridging protons may be, but it is worth noting that acetonitrile may be trimerised to 2,4,6-trimethyl-1,3,5-

triazane.HCl in the presence of hydrochloric acid (20). Thus it is likely that the solvent will act as Bronsted base.

Fig.3.8. *Cyclic voltammogram of* $[Mn(II)L^1H_3L^1Mn(IV)][PF_6]_3$ *in acetonitrile solution. Reference is* Ag/Ag^+ (0.1 mol l^{-1} $AgNO_3$ in MeCN)
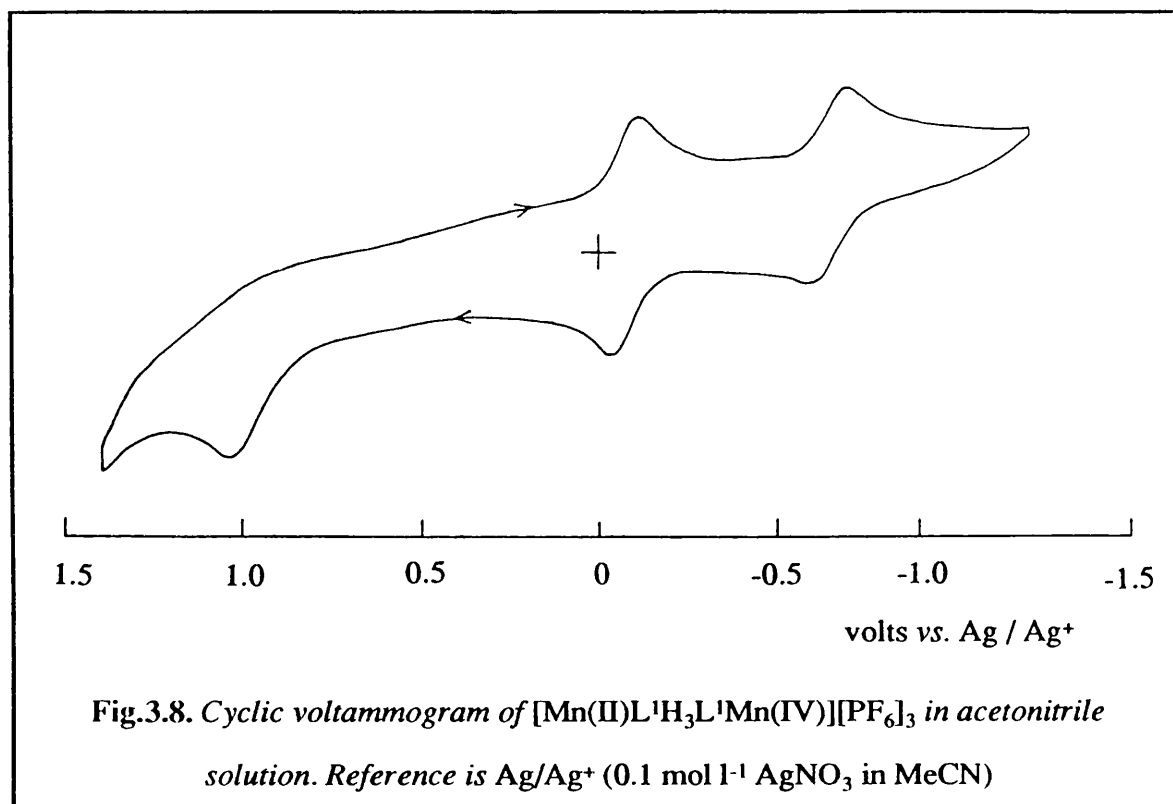
(3.3.3) STRUCTURE AND SPECTROSCOPIC PROPERTIES OF $[Mn(IV)L^2][PF_6].H_2O$

(3.3.3.1) General Remarks

L^2H_3 was prepared to investigate the effect of increasing steric hindrance at the O_3 hydrogen-bond acceptor face of a $[Mn(IV)(N,N',N''\text{-tris}$ alkoxy-1,4,7-triazacyclononane)]$^-$ moiety. Model building studies (Chemmod routine) indicated that an increase in size of the alkyl group at the chiral centre of L^1 would partially or completely block dimer formation. The epoxide syntheses of Koppenhoefer *et al.* (see chapter 2)

provided a simple route to replace the methyl group of L^1 with the isopropyl group of L^2. The possibility of the preparation of a *tert*-butyl derivative was considered, but the preparation of *tert*-butyl oxirane from *tert*-leucine would have proven prohibitively expensive.

(3.3.3.2) Crystal Structure of $[Mn(IV)L^2][PF_6].H_2O$

The crystal structure and space-filling views of $[Mn(IV)L^2][PF_6].H_2O$ are presented in fig. 3.9 and fig. 3.10 respectively. The structure is monomeric, and from the space-filling view it can be seen that the bulk of the isopropyl groups will prevent dimerisation. Also the steric restriction at the O,O',O" face is such that the water molecule of crystallisation is not within hydrogen bonding distance of the oxygen donor atoms. The chirality of the complex as determined by the pendant-arms is Λ. The endocyclic chelate rings are of δ configuration, and the exocyclic rings are of λ. Thus the overall chirality is $\Lambda(\delta\lambda)$. This is the opposite chirality as the $Mn(IV)$ component of $[Mn(II)L^1H_3L^1Mn(IV)]^{3+}$, but it is noted that L^1H_3 is of S configuration and L^2H_3 is of R configuration. The cation has pseudo-trigonal symmetry.

The complex has almost octahedral geometry, with a twist angle of $10.8°$. A selec on of bond lengths and ond angles is presented in table 3.3. The bond length s about the central metal atom are essentially the same as that of the $Mn(IV)$ omponent of the $[Mn(II)L^1H_3L^1Mn(IV)]^{3+}$ cation. Thus the oxidation state is assigned as $Mn(IV)$. This is confirmed by the absence of any long N-Mn-O axis which would imply a Jahn-Teller distortion and hence a d^3 ion. Again it can be seen that the Mn-O bond lengths are significantly shorter than the Mn-N bond lengths, implying a p^π-t_{2g}^3 bonding interaction.

Comparison of $[Mn(IV)L^2]^+$ to $[Mn(IV)L']^+$ $(L'=N,N',N"$-tris-2-hydroxy-ethyl-1,4,7-triazacyclononane) (4) indicates considerable structural similarity within the cations. However, the intramolecular properties of the two complexes are considerably different. With $[Mn(IV)L^2]^+$ the crystal array consists of entirely independent units,

whereas with [Mn(IV)L']+ there is a weak hydrogen bonding interaction between the O,O',O" face of the cation and the methylene residues of the macrocycle of another cation in the unit cell. The steric bulk of L² effectively prevents this interaction.

Table 3.3. Selected Bond Lengths (Å) and Bond Angles (deg.) for [Mn(IV)L²]+

Mn-N(1)	2.052 (3)	Mn-N(4)	2.049 (3)
Mn-N(7)	2.044 (3)	Mn-O(1)	1.819 (3)
Mn-O(4)	1.826 (3)	Mn-O(7)	1.831 (3)
N(1)-Mn-N(4)	93.9 (2)	N(1)-Mn-N(7)	84.8 (2)
N(4)-Mn-N(7)	83.9 (2)	N(1)-Mn-O(1)	84.2 (2)
N(4)-Mn-O(4)	84.1 (2)	N(7)-Mn-O(7)	84.2 (2)
O(1)-Mn-O(4)	97.7 (1)	O(1)-Mn-O(7)	96.3 (1)
O(4)-Mn-O(7)	97.0 (1)		
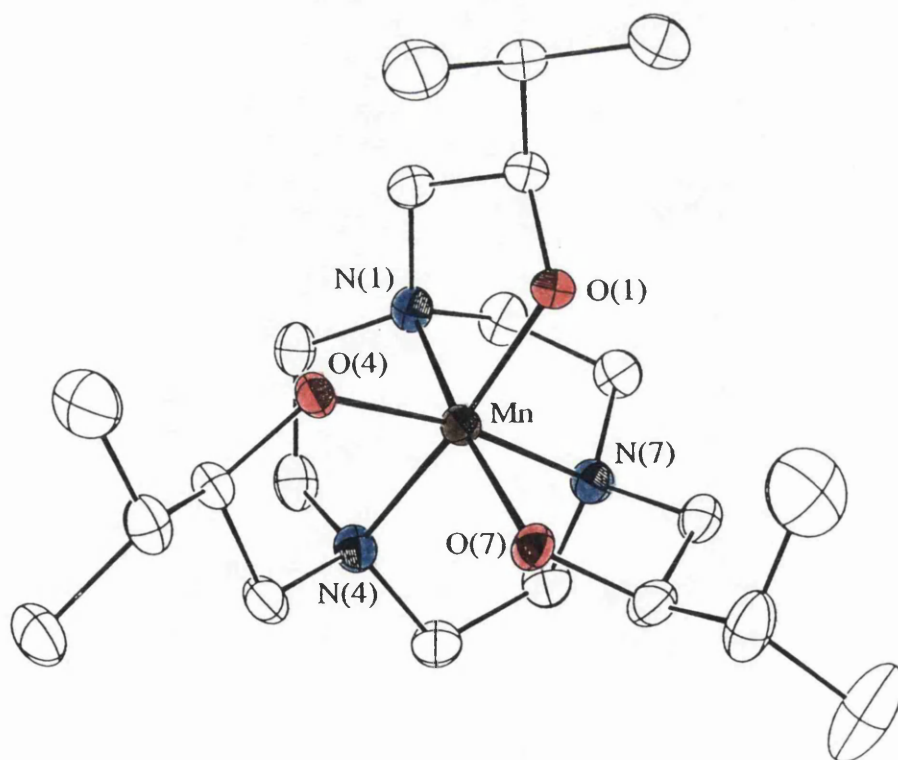
Fig. 3.9. *Structure of the cation in* [Mn(IV)L²][PF₆].H₂O.
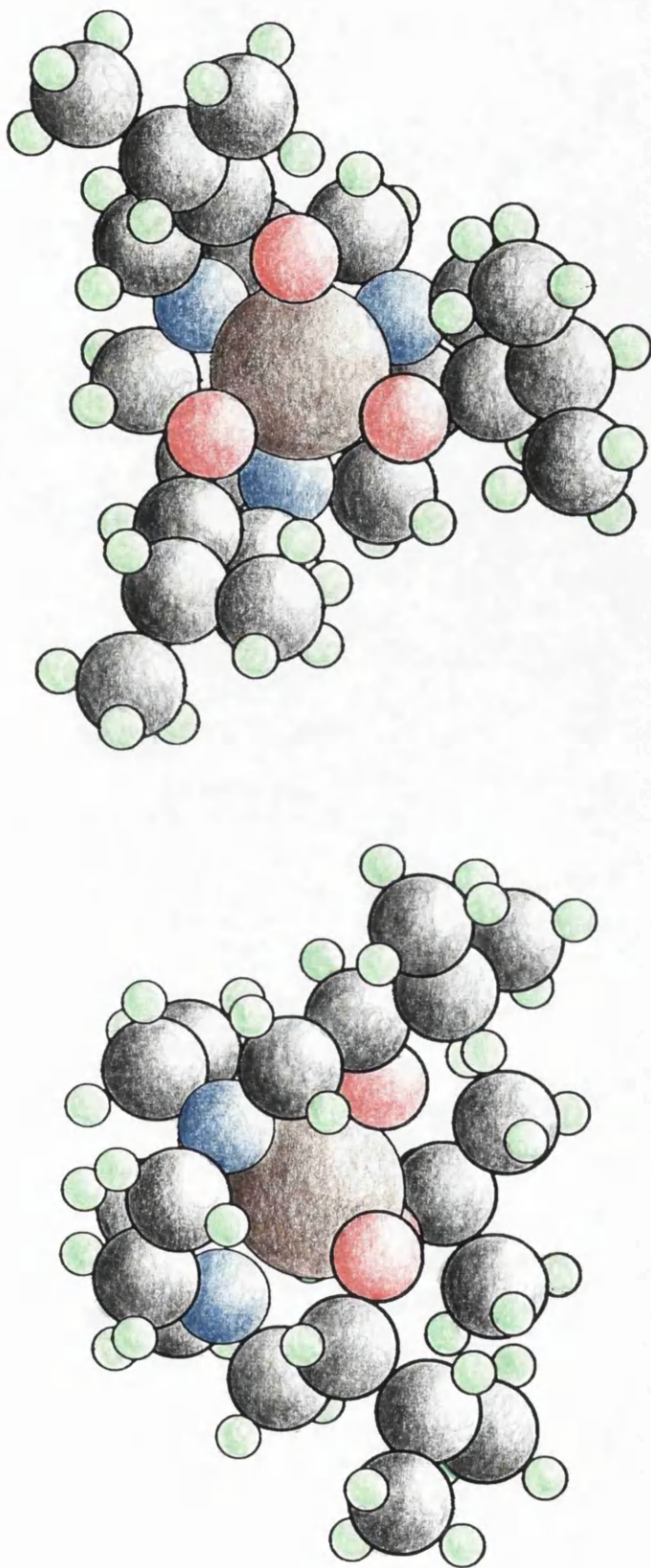
Fig. 3.10. *Spacefill views of* [Mn(IV)L²]⁺.

(3.3.3.3) Electronic and Circular Dichroism Spectroscopy. Comparison with $[Mn(II)L^1H_3L^1Mn(IV)]^{3+}$.

The electronic and circular dichroism spectra of $[Mn(IV)L^2][PF_6].H_2O$ are presented in fig. 3.11. The absorption spectrum bears some resemblance to that of $[Mn(II)L^1H_3L^1Mn(IV)]^{3+}$ with the additional feature of a weak shoulder at 350 nm. The bands are more prominent with $[Mn(IV)L^2]^+$. From the extinction coefficients ($\varepsilon = 1000$ $mol^{-1}l$ cm^{-1} or greater) all bands are assigned as charge transfer processes. However the CD spectrum is considerably different. Noting that L^2 if of opposite configuration to L^1, the lowest energy bands in the visible region of $[Mn(II)L^1H_3L^1Mn(IV)]^{3+}$ and $[Mn(IV)L^2]^+$ are both split into two components of opposite sign. In $[Mn(IV)L^2]^+$ the next band (shoulder at 480 nm) is also split into two bands of opposite sign , whereas with $[Mn(II)L^1H_3L^1Mn(IV)]^{3+}$ the band is not split. Again there is a band with one component before the intense u.v. charge transfer bands.

The differences between the positions of the bands in the absorption spectra between $[Mn(II)L^1H_3L^1Mn(IV)]^{3+}$ and $[Mn(IV)L^2]^+$ are possibly due to a difference in the π-donor properties of the alkoxide ligators in each complex. In $[Mn(II)L^1H_3L^1Mn(IV)]^{3+}$ the alkoxide donors are hydrogen-bonded to the $[Mn(II)L^2H_3]^{2+}$ subunit, and will hence be poorer π-donors than those in $[Mn(IV)L^2]^+$. The two highest transitions occur at slightly higher energy for $[Mn(IV)L^2]^+$ If these transitions were ligand–p^π to metal e_g or t_{2g} transitions a decrease in π-donor ability would cause these transitions to occur at a higher energy. This is not the case, and hence these bands are assigned as ligand-σ to metal e_g and t_{2g} transitions, with donation to t_{2g}^3 occurring at higher energy. This implies that the remaining lower energy transitions are ligand-π to metal transitions in origin.
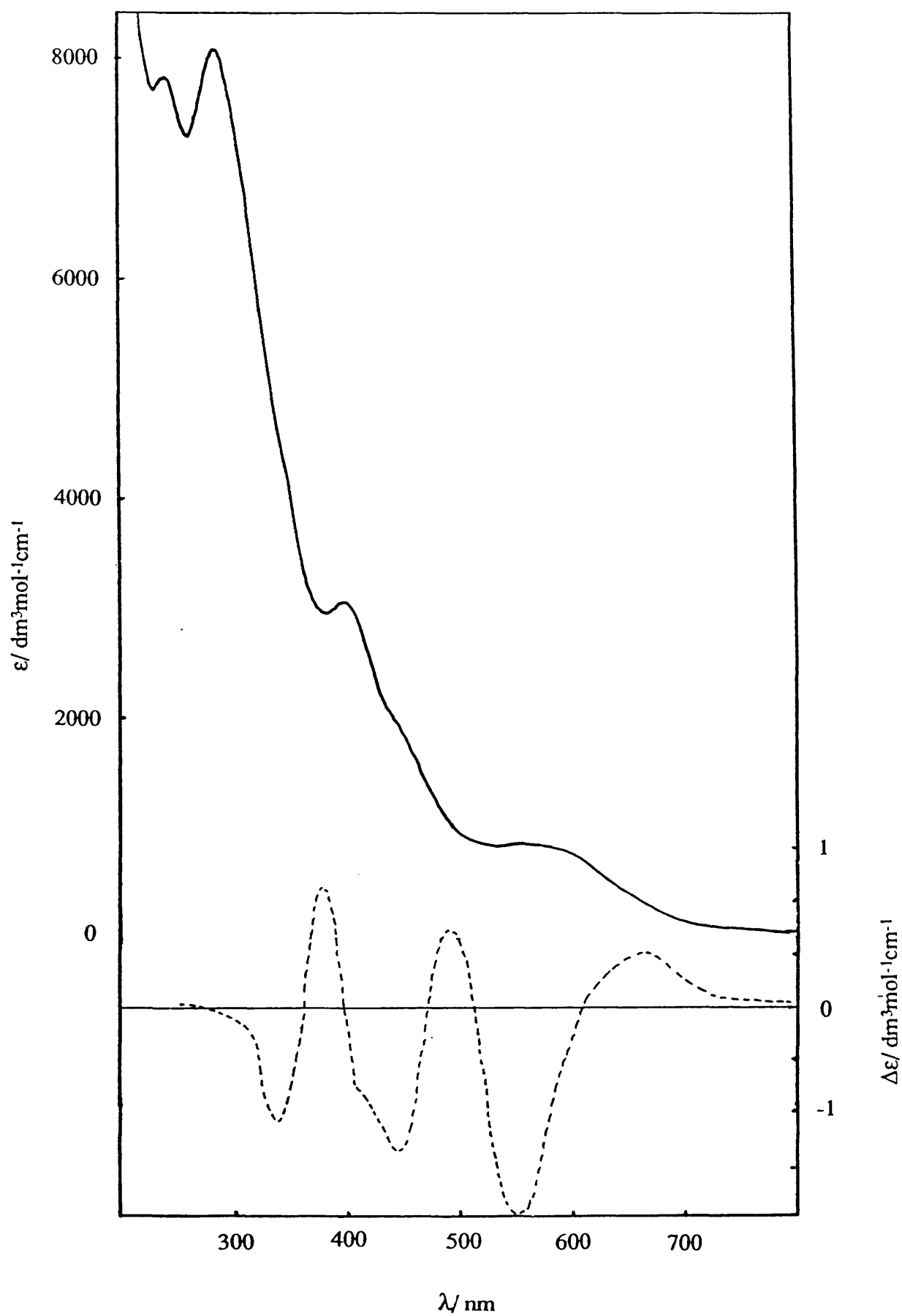
Fig 3.11. *Absorption and circular dichroism spectra of* [Mn(IV)L²][PF₆].H₂O

(3.3.3.4) Electron Paramagnetic Resonance Spectroscopy.

The EPR spectrum of $[Mn(IV)L^2][PF_6].H_2O$ presented in fig 3.10., was kindly supplied by Dr. Lesley Yellowlees (Edinburgh). The data was obtained from a sample as a frozen (77 K) acetonitrile solution. There are two components observed in the spectrum with g values of 3.674 and 1.922. These values are typical for a d^3 ion with axial symmetry in a strong ligand field: for a recent example see reference (22). Thus the assignment of a Mn(IV) species is confirmed. The room temperature spectrum, as to be expected, was very broad and no hyperfine coupling to ^{55}Mn was seen.

$g = 1.922$

$g = 3.674$

Fig.3.11. *EPR spectrum of* $[Mn(IV)L^2][PF_6].H_2O$ *in frozen (77K) acetonitrile solution.*
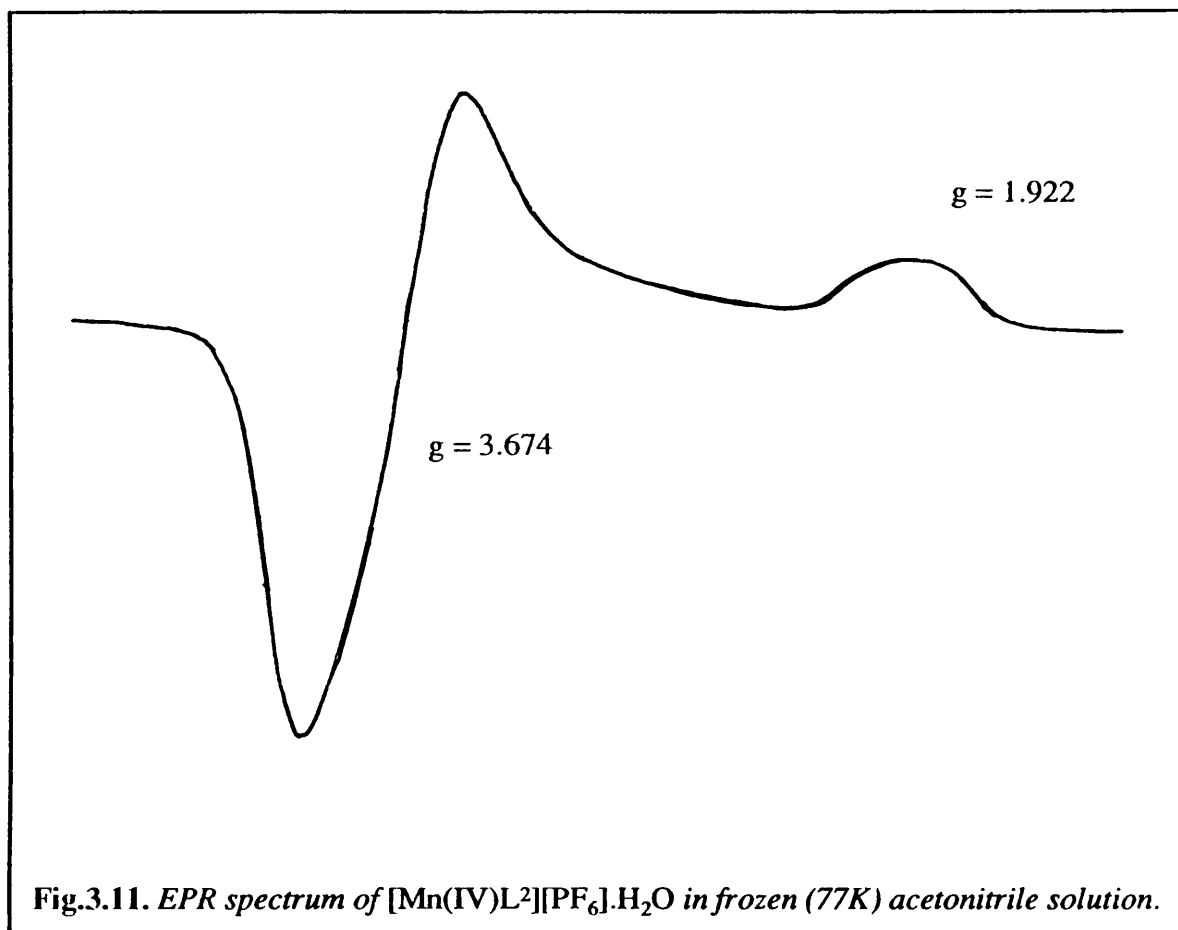
(3.3.3.5) Cyclic Voltammetry.

The cyclic voltammogram of [Mn(IV)L^2][PF$_6$].H$_2$O is presented in fig 3.11. 4Å molecular sieves were used during this experiment to absorb the water molecule of crystallisation present in the complex. There are two irreversible reductions, at -0.58 V (vs Ag/Ag$^+$) and at -0.79 V (vs Ag/Ag$^+$). As expected, the complex shows no oxidation activity. The first reduction is assigned as a Mn(IV) -> Mn(III) process, and the second is assigned as a Mn(III) -> Mn(II) process. The potentials at which these reductions occur are high, especially compared to the reduction processes of the isoelectronic Mn(IV) component of [Mn(II)L^{1}H$_3$L^{1}Mn(IV)]$^{3+}$. It can be postulated that the steric bulk of L^2 prevents efficient complex-electrode interaction, with [Mn(IV)L^2]$^+$ behaving as a micro-micelle. This is only a suggested explanation of these potentials since it is known that many complexes contain fully encapsulated metal ions (e.g. sepulchrates), but display redox activity at lower potentials.

Fig.3.12. *Cyclic voltammogram of* [Mn(IV)L^2][PF$_6$].H$_2$O *in MeCN solution.*

Reference is Ag / Ag$^+$ (0.1 mol l^{-1} Ag(NO$_3$)$_2$

(3.3.4) STRUCTURE AND SPECTROSCOPIC PROPERTIES OF [Mn(II)L³H₃L³Mn(III)][PF₆]₂.2H₂O.
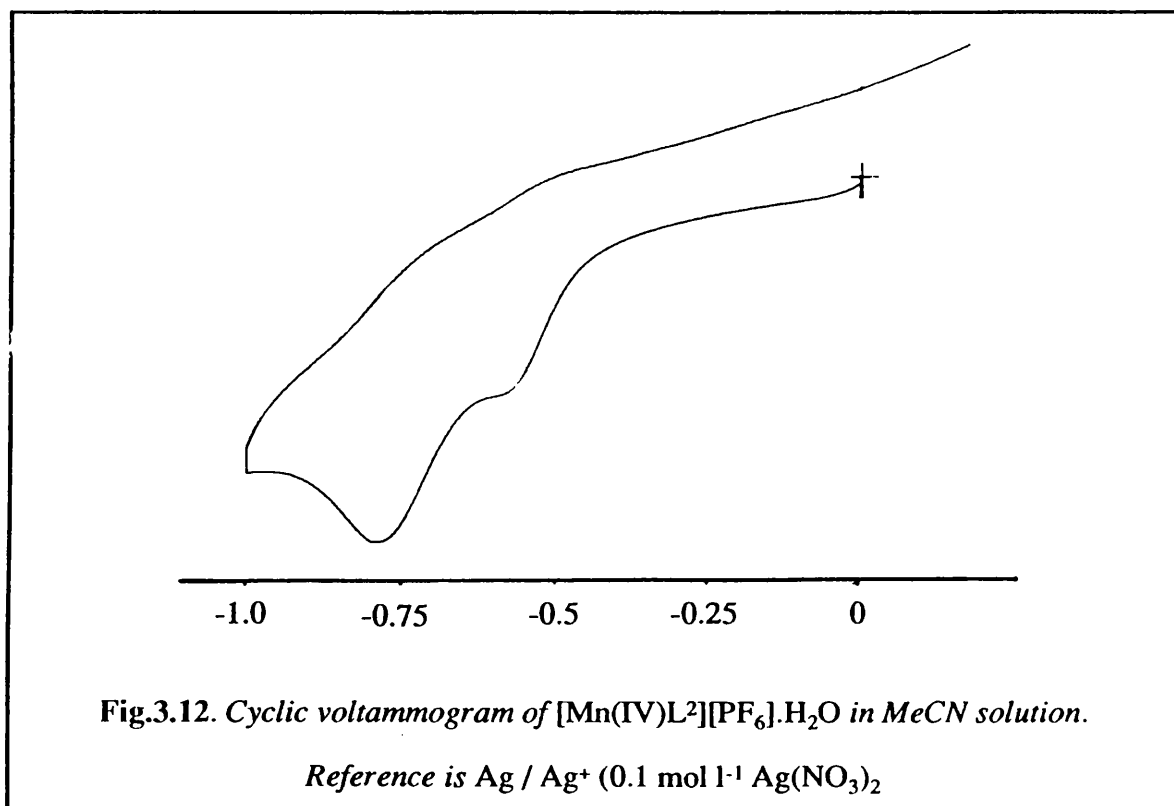
(3.3.4.1) General Remarks

With L^3H_3 any complex prepared will be inherently unsymmetrical, and hence spectroscopic properties will be complex. Also with the larger ring sizes it is likely that the lower 2+ oxidation state will be more stable by a more favourable metal to cavity radius fit.

(3.3.4.2) [Mn(II)L³H₃L³Mn(III)][PF₆]₂.2H₂O. Crystallographic Study

Several attempts were made at solving the x-ray diffraction data obtained for $[Mn(II)L^3H_3L^3Mn(III)][PF_6]_2.2H_2O$. The Patterson calculation revealed that there was a Mn-Mn distance of approximately 4.6 Å which is the same value obtained for $[Mn(II)L^1H_3L^1Mn(IV)][PF_6]_3$, thus the structure is a dimer. The space group obtained implied the presence of three-fold axes which when the cation can only have C_s symmetry must mean the structure is highly disordered, with the $-C_3H_6-$ portion of the ligand disordered about three possible positions in each component of the dimeric structure. This would give pseudo-trigonal symmetry. A [Mn(II), Mn(III)] oxidation state assignment is reasonable since the Mn(III) component of a dimer would be deprotonated and hence neutral, leaving a $[Mn(II)L^3H_3]^{2+}$ component to balance the two $[PF_6]^-$ counter ions. A [Mn(II), Mn(IV)] assignment is ruled out since such a dimeric cation would have a 3+ charge and would require three anionic counter ions. This would require the presence of a very rare bihydroxide ($[HOHOH]^-$). Such counter ion is very unlikely since they are only stable in highly hydrated systems (21). With an Mn(IV) an non-octahedral structure is very unlikely. It will be shown later that L^3H_3 (chapter 5) does not support octahedral coordination geometry with Co(II). Also L^3H_3 Co(II) complexes do not

oxidise to give Co(III) complexes. Co(III) and Mn(IV) have very similar ionic radii, and as such it seems unlikely that a Mn(IV) complex is possible with L^3H_3. A Mn(III) (d^4) complex is possible with L^3H_3 since the ligand is unsymmetrical and can accommodate a Jahn-Teller distortion.

(3.3.4.3) $[Mn(II)L^3H_3L^3Mn(III)][PF_6]_2.2H_2O$. Absorption and Circular Dichroism Spectroscopy.

The absorption and circular dichroism spectra of $[Mn(II)L^3H_3L^3Mn(III)][PF_6]_2.2H_2O$ are presented in fig.3.13. The absorption spectrum resembles those of $[Mn(II)L^1H_3L^1Mn(IV)][PF_6]_3$ and $[Mn(IV)L^2][PF_6].H_2O$ consisting of strong charge transfer bands in the near-U.V., and weaker charge transfer bands in the visible region. Unfortunately Mn(III) spectra tend to be obscured by strong charge transfer bands and definitive assignment of the oxidation state is difficult. Repeating the basification experiment noted in section (3.3.2.4) the extinction coefficient doubled upon addition of triethylamine, confirming the presence of a Mn(II) component.

(3.3.4.4) $[Mn(II)L^3H_3L^3Mn(III)][PF_6]_2.2H_2O$. Electron Paramagnetic Resonance Spectroscopy.

The EPR spectrum of $[Mn(II)L^3H_3L^3Mn(III)][PF_6]_2.2H_2O$ as a frozen solution in acetontrile/tetrahydrofuran is presented in fig.3.14(a). The spectrum is extremely complex and definite assignment is not possible. However, there are a number of conclusions that can be drawn from the spectrum. Most apparent is the difference with the spectrum of $[Mn(IV)L^2][PF_6].H_2O$, indicating that a simple Mn(IV) complex is not present. The sextet at $g=1.971$ is assigned as an uncoupled, high-spin d^5 ion. An expansion of this region is presented in fig.3.14(b). (note this expanded spectrum was obtained from a frozen
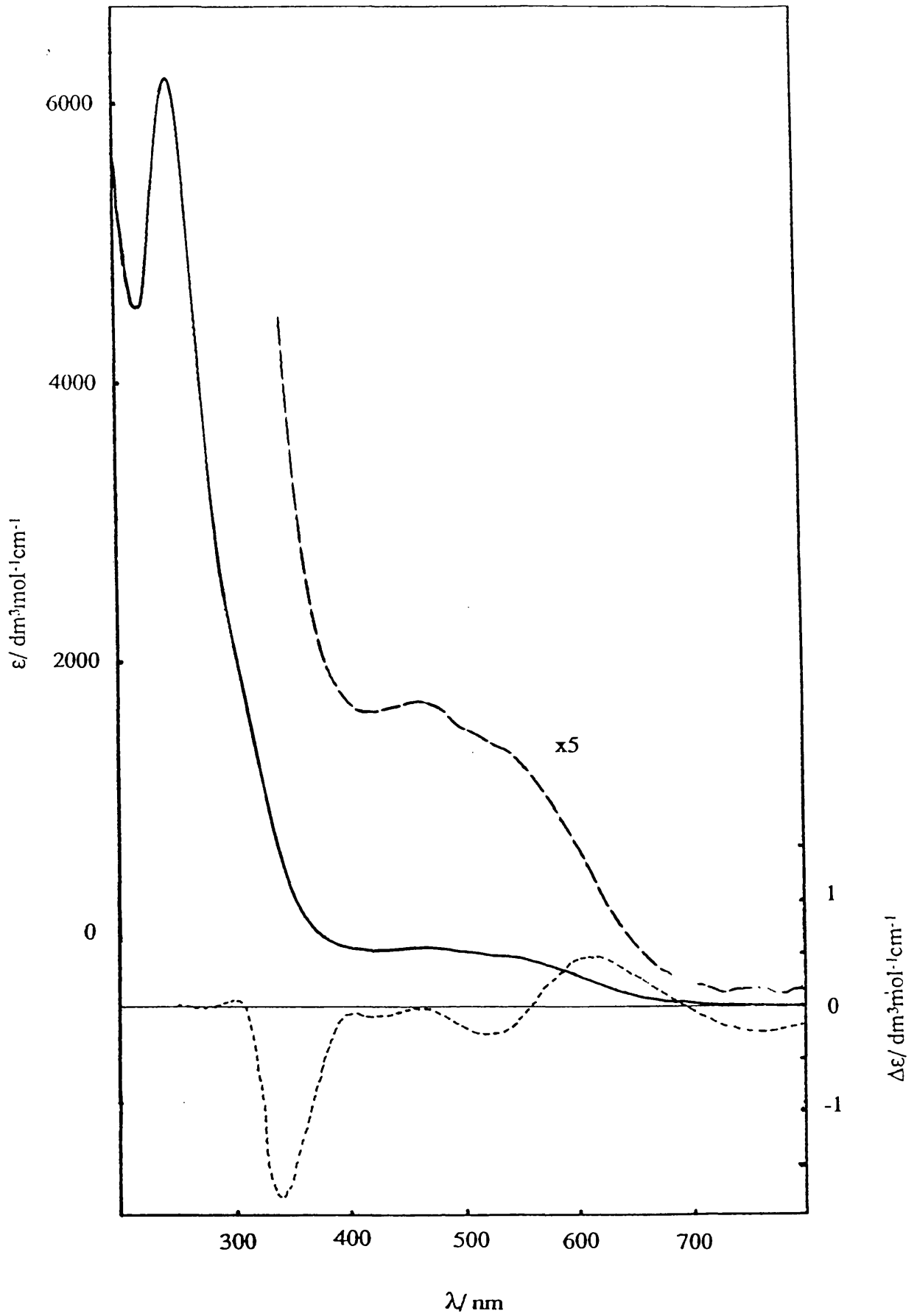
Fig.3.13. *Absorption and Circular Dichroism Spectra of*

$[Mn(II)L^3H_3L^3Mn(III)][PF_6]_2.2H_2O$ *in acetonitrile solution.*

Fig. 3.14(a). *EPR spectrum of* [Mn(II)L³H₃L³Mn(III)][PF₆]₂.2H₂O *in frozen*

MeCN/thf solution (77 K).

(b). *Expansion of the g=2 region (frozen dmf/thf solution).*
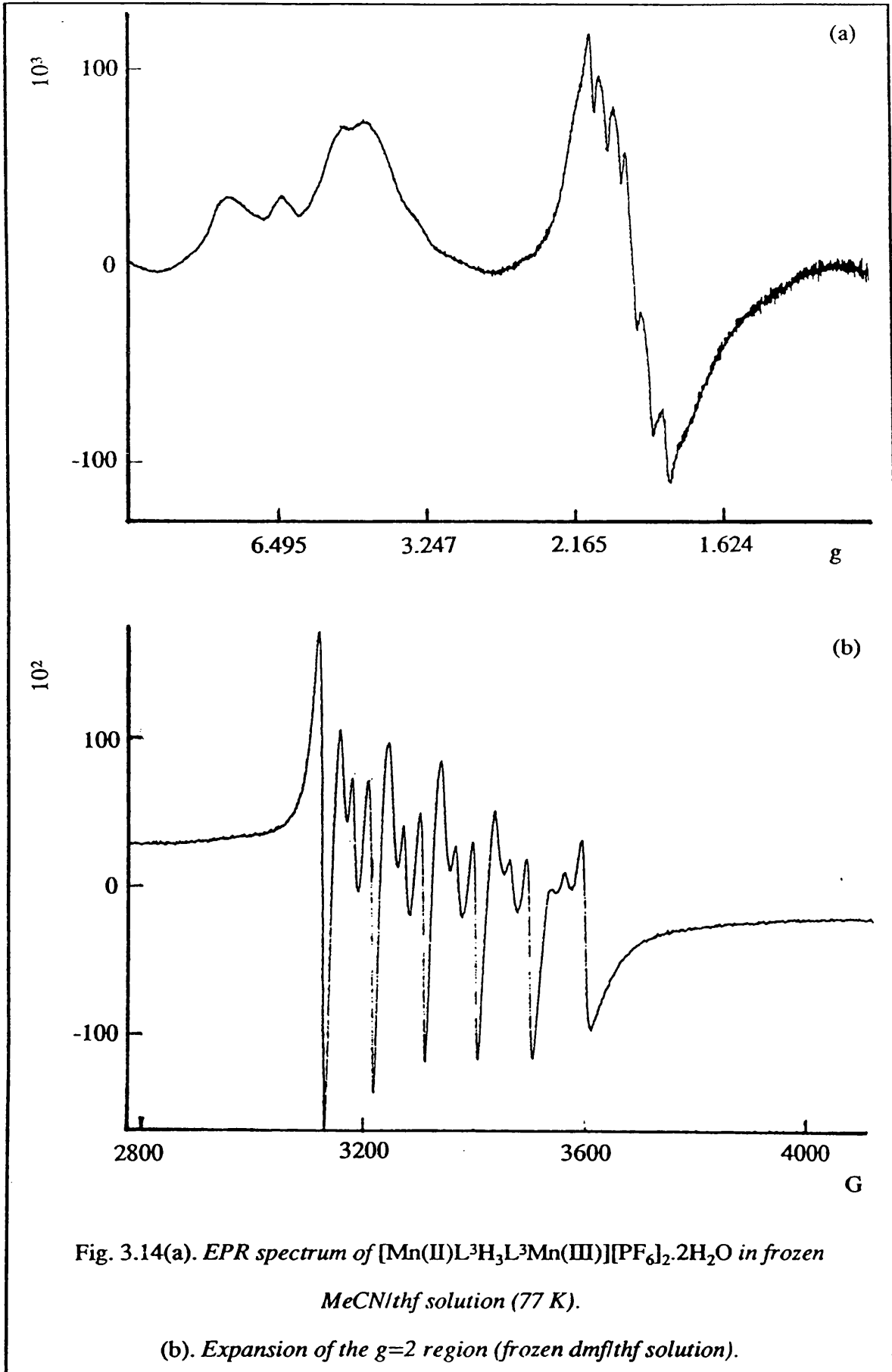
acetonitrile/dimethylformamide solution). This signal shows much hyperfine structure, due to coupling to ^{55}Mn ($I=5/2$). This again is indicative of a magnetically isolated Mn(II) centre. The remaining signals of the spectrum cannot be simply attributed to a Mn(III) centre, although there is a report of Mn(III) signals occurring at $g=6-8$ (23).

(3.3.4.5) $[Mn(II)L^3H_3L^3Mn(III)][PF_6]_2.2H_2O$. Cyclic Voltammetry.

In an attempt to obtain a definitive assignment of the oxidation states of $[Mn(II)L^3H_3L^3Mn(III)][PF_6]_2.2H_2O$ the cyclic voltammogram in acetonitrile solution was obtained (fig.3.15, scan rate $+ 5$ mVs^{-1}). The quasi-reversible oxidation at -0.04 V (vs.Fc/Fc$^+$) is assigned as a [Mn(II), Mn(III)] -> [Mn(III), Mn(III)] process. The reversible reduction at -0.65 V (vs. Fc/Fc$^+$) is assigned as a [Mn(II), Mn(III)] -> [Mn(II), Mn(II)] process. These assignments are based upon a comparison to voltammogram of $[Mn(II)L^1H_3L^1Mn(IV)][PF_6]_3$. Voltages as high as 1.85 (vs. Fc/Fc$^+$) did not reveal any further oxidation activity analogous to the [Mn(II), Mn(IV)] -> 2[Mn(IV)] process observed in $[Mn(II)L^1H_3L^1Mn(IV)][PF_6]_3$.

The difference in redox behaviour between $[Mn(II)L^1H_3L^1Mn(IV)][PF_6]_3$ and $[Mn(II)L^3H_3L^3Mn(III)][PF_6]_2.2H_2O$ is attributed to the difference in ring size of the parent macrocycle. With L^3H_3 it is unlikely that an octahedral complex can be formed, and thus a Mn(IV) complex is strongly disfavoured. This is verified by the lack of a high potential oxidation in $[Mn(II)L^1H_3L^1Mn(IV)][PF_6]_3$. Also L^3H_3, with it's unsymmetrical cavity, permits a Mn(III) centre to tetragonally distort. In the case of L^1H_3 the ligand may adopt trigonal and octahedral configurations, thus both Mn(II) and Mn(IV) ions are supported. The intermediate can be detected electrochemically, but attempts to prepare bulk quantities of an Mn(III) intermediate failed.
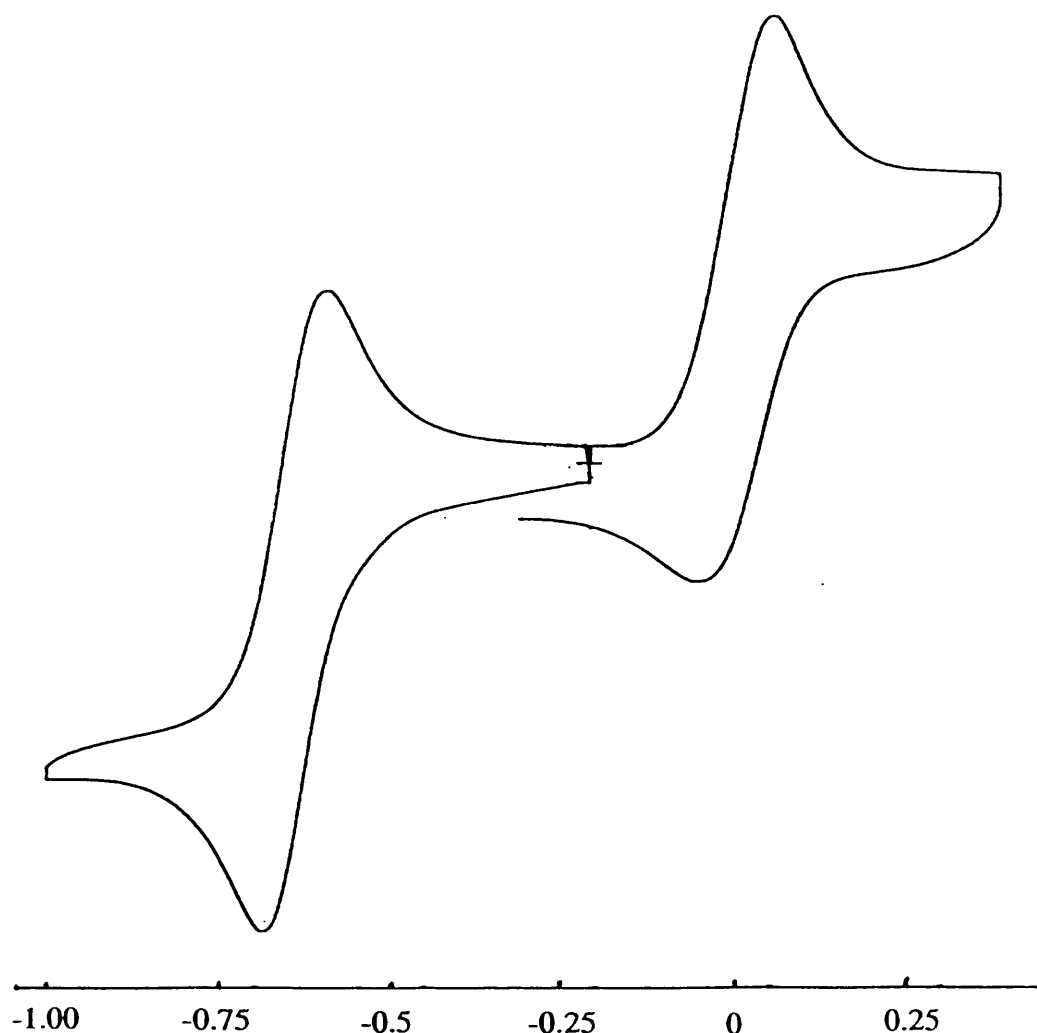
Fig. 3.15. *Cyclic voltammogram of* [Mn(II)L³H₃L³Mn(III)][PF₆]₂.2H₂O *in MeCN*

solution. Reference is Fc /Fc⁺.

The oxidation wave shows some irreversibilty in the [Mn(III), Mn(III)] ->

[Mn(II), Mn(III)] portion of the cycle. This implies that some form of structural change

occurs upon oxidation. Presumably a twisting motion coupled (to attain LFSE) with a

tetragonal distortion of the d^4 ion (to accommodate Jahn-Teller distortion. This

rearrangement appears to be slow, given the low scan rate at which the voltammogram

was obtained

3.3 CONCLUSIONS

The chromium and manganese coordination chemistry of oxidation of L^1H_3, L^2H_3 and L^3H_3 is dependent on two main factors: pH and ligand steric properties.

The pH of the particular system involved will determine whether the pendant arm donors behave as alcohols or alkoxides, and hence affect their π-donor properties. With $[Cr(III)L^2H_3][PF_6]_3$ this can be followed spectroscopically, and in the manganese complexes by an examination of bond lengths about the metal centre. Spectroscopically the d-d activity of the manganese complexes are obscured by charge transfer bands, but since the acidified Mn(II) species are essentially colourless oxidation state assignment is simply a matter of examining extinction coefficients. With L^1H_3 and L^3H_3 the pH value also determines whether the complexes will be monomeric or dimeric. Highly acidic or basic conditions will result in complete protonation and deprotonation respectively, resulting in hydrogen-bond rupture. At intermediate pH values, the protonation level at each complex becomes less than three, and dimeric species form. In the case of L^1H_3 it is probable that slightly basic conditions result in very rapid oxidation to a Mn(III) species which will be unstable given the spherical coordination sphere. The increase in charge will result in an increase of the acidity of the remaining pendant-arm alcohol groups, resulting in further deprotonation and oxidation to Mn(IV). For L^3H_3, the cavity is too large for the hypersmall Mn(IV) ion, and cannot support an octahedral mode of coordination. Hence oxidation stops at the Mn(III) state in both dimeric and monomeric structures.

The steric demands of the ligands affects both the oxidation states and the intramolecular properties of their complexes. With L^2H_3 the steric bulk of the pendant-arms effectively stops dimer formation. In this case oxidation state is determined solely by the pH value. The symmetrical nature of the ligand cavities with L^1H_3 and L^3H_3 precludes the isolation of Mn(III) complexes. With the larger ring sizes there is no reason why Mn(II) complexes should not be stable in solution. However, the large carbonaceous backbone does not permit coordination to the smaller Mn(III) and Mn(IV) ions.

References

1. Chaudhuri, P.; Wieghardt, K. *Progress in Inorganic Chemistry*; Lippard, S.J., Ed.; Wiley: New York, 1988; Vol. 35, p 329.

2. Weighardt, K.; Bossek, U.; Chaudhuri, P.; Herrmann, W.; Menke, B.C.;Weiss, J. *Inorg. Chem.* **1982**, *21*, 4308.

3. Farrugia, L.J.; Macdonald, N.M.; Peacock, R.D. To be published.

4. Belal, A.; Chaudhuri, P.; Fallis, I.; Farrugia, L.J.; Hartung, R.; Macdonald, N.M.; Nuber, B.; Peacock, R.D.; Weiss, J.; Weighardt, K. *Inorg. Chem.* **1991**, *30*, 4397.

5. Cole, E.; Parker, D.; Ferguson, G.;Gallagher, J.F.; Kaitner, B. *J. Chem. Soc. Chem. Commun.* **1991**, 1473

6. Auerbeck,U.; Eckert, U.; Weighardt, K.; Nuber, B.; Weiss, J. *Inorg. Chem.* **1990**, *29*, 938.

7. Spreer, L.O.; Maliyackel, A.C.; Otvos, J.W.; Calvin, M. *J. Am. Chem. Soc.* **1986**, *108*, 1949.

8. Weieghardt, K.; Bossek, U.; Gebert, W. *Angew. Chem. , Int. Ed., Eng.* **1983**, *22*, 328

9. Brudwig, G.W.; Crabtree, R.H. Progress in Inorganic Chemistry; Lippard, S.J., Ed.; Wiley, New York, 1989; Vol. 37, p 99.

10. Forbush, B.; Kok, B.; McGloin, M. *Photochem. Photobiol.* **1971**, *14*, 307.

11. Britt, R.D.; Sauer, K.; Klein, M.P. Progress in Photosynthesis Research; Biggins, J., Ed.; Vol. 1, Nijhoff, Dordrecht, 1987, p. 573.

12. Robb, J. Ph.D Thesis. University of Glasgow. 1987

13. Lever, A.B.P. Inorganic Electronic Spectroscopy. Studies in Physical and Theoretical Chemistry; Elsevier, Amsterdam, 1984; Vol. 33, p.419.

14. Hancock, R.D. *Progress in Inorganic Chemistry*; Lippard, S.J., Ed.; Wiley: New York, 1989; Vol. 37, p 187.

15. A.A. Belal, A.A.; L.J. Farrugia, L.J.; R.D. Peacock, R.D.; Robb, J. *J. Chem. Soc., Dalton Trans.* **1989**, 931.

16. Weighardt, K. Private communication.

17. Gerloch, M. Progress in Inorganic Chemistry; Lippard, S.J., Ed.; Wiley, New York, 1989; Vol. 26, p 1.

18. Weieghardt, K.; Bossek, U.; Gebert, W. *Angew. Chem., Int. Ed., Eng.* **1983**, *22*, 328

19. Macdonald, N.M.; Peacock, R.D. Manuscript in preparation.

20. March, J.; Advanced Organic Chemistry; Wiley; New York, 1985; p. 864.

21. N. N. Greenwood and A. Earnshaw; Chemistry of the Elements; Pergammon; Oxford, 1984.

22. Dutta, S.; Basu, P.; Chakravorty, A. *Inorg. Chem.* **1991**, *30*, 4031.

23. Dexheimer, S.L.; Gohdes, J.W.; Chan, M.K.; Hagan, K.S.; Armstrong, W.H.; Klein, M.P. *J. Am. Chem. Soc.* **1989**, *111*, 8923.

CHAPTER 4

COBALT, NICKEL AND COPPER COMPLEXES OF N,N',N''-TRIS-(2-ALKYL-2-HYDROXYETHYL)-TRIAZAMACROCYCLES

.

"Speak Spirit!, from thine inorganic voice"

Percy Bysshe Shelly, Prometheus Unbound

CONTENTS

(4.1) INTRODUCTION

(4.1.1) Structural Aspects

As part of a programme to investigate the effects of increasing steric strain in first row transition metal macrocyclic complexes, model building studies were undertaken. Most commercial micro-computer based modelling programmes do not permit "inorganic" modelling, since they do not contain the appropriate force constants applicable to transition metals. In addition, these programmes do not adequately deal with the stereochemical demands of d-block ions (namely ligand field stabilisation energy) nor variable co-ordination numbers and geometries. With these restrictions in mind simple "ball and stick" type models were used for a series of N,N',N''-tris-(2-hydroxy-isopropyl)-triazamacrocycles.

High-spin Co(II) has a significant LFSE of -4/5 Δ_o and under normal circumstances would be expected to adopt octahedral (or tetrahedral) co-ordination geometry, but as discussed earlier, trigonal prismatic coordination may also result, due to a reduction of interelectron repulsion. Co(III) is normally low-spin, except in the very weak ligand fields (e.g. [CoF$_6$]$^{3-}$), and as such has a maximum LFSE of -12/5 Δ_o. Thus Co(III) always (except for a few non relevant exceptions) adopts close to octahedral configurations. The Co(III) complex of L^{1}H$_3$ has been reported by Belal et al. (1) and is illustrated in fig. 4.1.

The structure is dimeric with one subunit formally a tris-alkoxide and the other a tris-alcohol. Thus the proton lability of co-ordinated alcohols is evident in this complex as already seen with Cr(III) and Mn(IV). The dimer subunits are not crystallographically identical, but this is believed to be a packing effect. The two halves of the dimer have an average twist angle of 10.2° which is very close to the Mn(IV) component of [Mn(II)L^{1}H$_3$L^{1}Mn(VI)]$^{3+}$. [Co(III)L^{1}H$_3$L^{1}Co(III)]$^{3+}$ has a Δ_o value of 16,230 cm^{-1} in

Fig. 4.1. *Structure of* [Co(III)L¹H₃L¹Co(III)]³⁺.
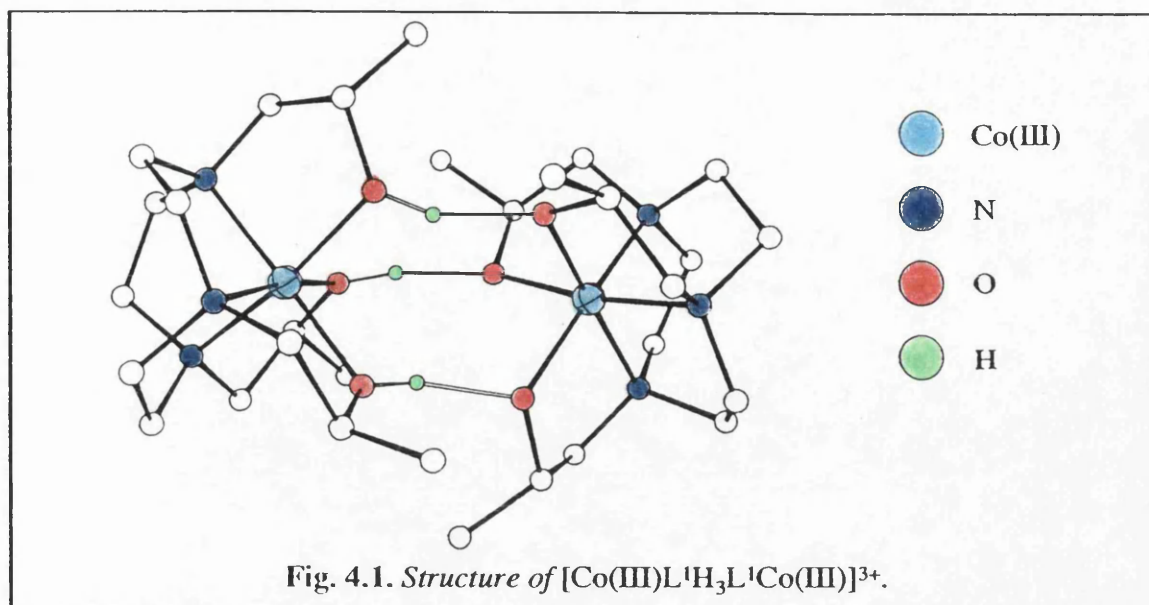
neutral MeCN solution. This is a little smaller than might be expected, due to the slight twist away from octahedral co-ordination. Larsen *et al.* (2) have demonstrated that in trigonal complexes the ideal geometry can be slightly trigonally distorted, with a twist angle of 5-10°, depending upon the bite size (in this case N-Co-O) of the ligands in question.

When $Co(II)Cl_2.6H_2O$ dissolved in water is reacted with L^1H_3 the solution immediately becomes dark brown, which is probably an intermediate peroxo species. Hence $Co(II)L^1H_3$ is rather air-sensitive. The large LFSE of Co(III) is the driving force behind this rapid aerobic oxidation, although the oxidation is much slower in alcoholic solution (several weeks in air tight vessels). Hancock (3) has defined Co(III) as a "hypersmall" ion and therefore it is deduced that the cavity formed by L^1H_3 upon coordination is likewise very small. This is borne out by a comparison of the ionic radii (values in pm) of species which form air-stable complexes with L^1H_3; V(IV) (58); Cr(III) (61.5); Mn(IV) (53): Co(III) (54.5) (4). On the basis of this data it was not certain whether L^3H_3 would form a Co(II) or a Co(III) complex, since the inclusion of one more methylene residue did not seem to increase the cavity size significantly. L^3H_3 has been shown to stabilise Mn(III), which has an ionic radius of 64.5 pm, and under normal

conditions this complex did not oxidise to a Mn(IV) species. Mn(IV) and Co(III) have almost identical ionic radii and both show a preference for octahedral environments. These facts implied that L^1H_3 would stabilise Co(II) and not Co(III).

L^1H_3 also forms stable complexes with Mn(II), Ni(II), Cu(II) and Zn(II), all of which are larger than the ions noted above. However these ions do tend to have smaller LFSE values (due to lower charge which will result in smaller ligand field splitting values), and as stated earlier, more susceptible to trigonal distortions. This implies that L^1H_3 is a flexible ligand, and it would be reasonable to expect L^3H_3 and larger ring ligands to be even more flexible. In the case of $[Ni(II)L^1H_3]^{2+}$ no oxidation to Ni(III) is observed. This is possibly due to the fact that Ni(III) is strongly oxidising and may degrade L^1H_3 before deprotonation and/or dimerisation takes place. The analogous acetate ligand TCTA (see introduction) does stabilise a Ni(III) complex. This complex was prepared under acidic conditions and it is now apparent (chapter 4) that with alcoholate/alkoxide donors acidic conditions stabilise low oxidation states by the protonation of alkoxide donors and reducing their π-basicity. These studies were also hampered by the difficulty of preparing salts of $[Ni(II)L^1H_3]^{2+}$ which are soluble in oxidation inert media. The structure of $[Ni(II)L^1H_3]^{2+}$ (5) is presented in fig.4.2.

Fig. 4.2. *Structure of* $[Ni(II)L^1H_3]^{2+}$
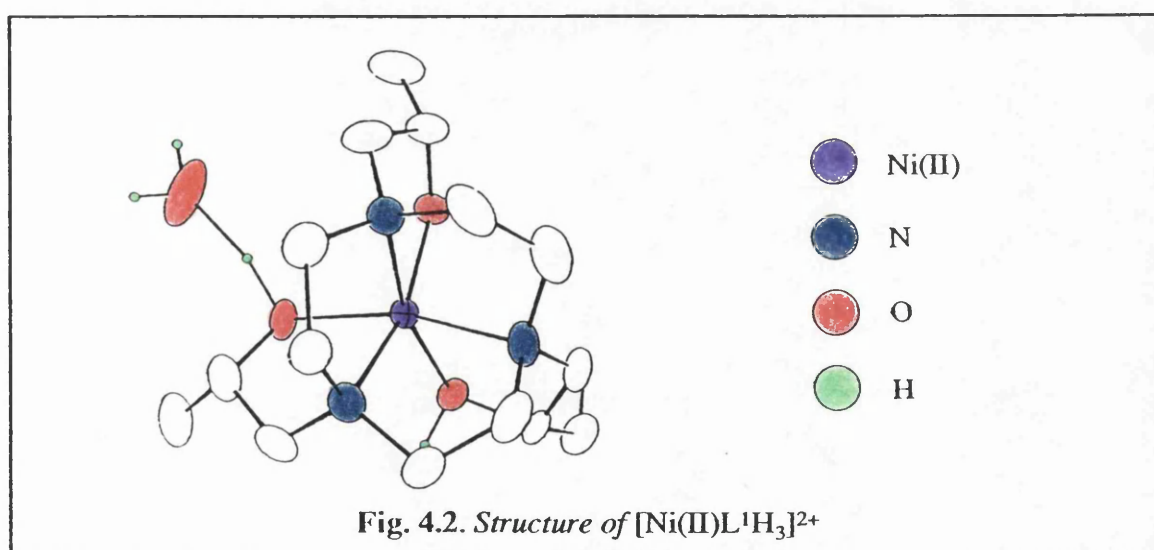
Ni(II)
N
O
H

The structure is trigonally distorted with a twist angle of 17.5°. This twist angle is somewhat larger than that observed in $[Mn(II)L^1H_3L^1Mn(IV)]^{3+}$ and $[Co(III)L^1H_3L^1Co(III)]^{3+}$, which given the smaller LFSE value of Ni(II) indicates a tendency for a trigonal arrangement of donor atoms in L^1H_3.

With the larger ring size ligands prepared it was suspected that only divalent cations would form stable complexes, based upon the metal-to-cavity fit concept. Of interest here was the coordination geometry resulting in these strained ligands. Much work has been done on varying the size of tetra-aza macrocycles and their pendant-arm derivatives, but few studies have been made upon triaza-macrocycles. Tri-aza macrocycles differ from their tetra-aza analogues in that they form predominantly *fac*-type complexes. In L^4H_3, L^5H_3, L^6H_3, L^7H_3, L^8H_3 and L^9H_3 there is a series of ligands in which some members can (in theory) bridge *trans* position of a metal ion and some which cannot. Also with the larger members of the series, tetra-aza macrocycles have been shown to form stable complexes but it remained to be seen whether triaza derivatives would also do so.

It was believed that because of ring strain L^5H_3 (but not L^4H_3) would form five coordinate Co(II) complexes, since it was impossible for this ligand to adopt an octahedral co-ordination mode. Nonoyama and Nonoyama (6) prepared a series of mono-[1,4,7-triazamacrocycle] palladium(II) complexes with ring sizes of 9, 12, 13, 14, 15 and 17. With ring sizes 9 and 12 the ligand is bidentate and two 1,4-nitrogen atoms span *cis* positions, as illustrated in fig.4.3(b). With ring sizes of 13 or greater the ligand is tridentate and the structure is that illustrated in fig. 4.3(a).

Thus with Pd(II) a hexamethylene unit is the minimum required to span *trans* positions. Palladium(II) and cobalt(II) have ionic radii of 86 pm and 74.5 pm (4) respectively. Accounting for the smaller ionic radius of Co(II) there seemed a possibility of 5 coordinate complexes with L^5H_3 and L^6H_3. This also ruled out the possibility of a

Co(III) species since non-octahedral Co(III) is very unlikely. It was believed that in the Co(II) case the pentamethylene and hexamethylene bridges would block the sixth coordination site. Surprisingly attempts to prepare complexes of L^6H_3 failed. It is likely that with this   ligand steric strain becomes too severe upon complex formation and metal to ligand orbital overlap is too weak. Also with L^9H_3 a cobalt(II) complex could not be isolated. Models indicate that the cavity of L^9H_3 is too large to coordinate without excessive compression of bond angles in the macrocyclic chelate rings.
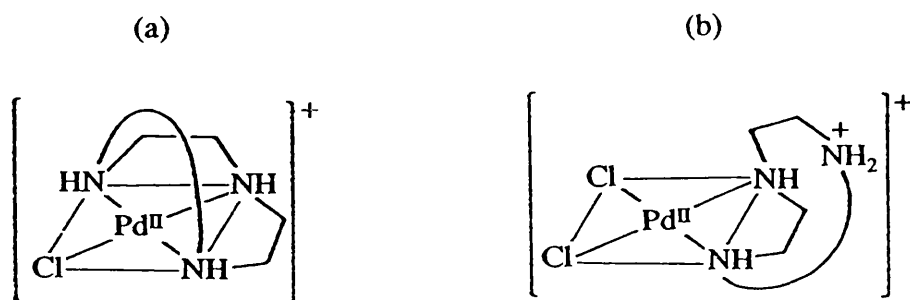
Fig. 4.3. (a) *Tridentate-[triazamacrocycle] complexes of* Pd(II).

(b) *Bidentate-[triazamacrocycle] complexes of* Pd(II).

(4.1.2) Spectroscopy

Complexes in which the chromophore has D_3 symmetry, exemplified by tris-chelates, require no comment, as there are thousands of examples cited in the literature. For general references see Lever (7). Gillum *et al.* (8) and Larsen *et al.* (2), both examined the spectra of a number of ions in TP environments. The results they obtained for d^7 ions in trigonal prismatic environments are worth considering, though more detailed accounts are to be found in the original papers. A rigorous treatment will be not

strictly relevant for the purposes of the current work, since many of the complexes prepared were of lower symmetry than D_{3h} or even C_{3v}.

The Tanabe-Sugano diagram for d^7 ions in trigonal prismatic ligand fields was calculated by Gillum *et al.*. The diagram is presented with the absorption spectrum of [Co(II)py$_3$tach] in fig. 4.4 (see chapter one for details of this ligand). [Co(II)py$_3$tach] is believed to have almost perfect trigonal prismatic geometry. The most obvious feature of this spectrum is the splitting of the high energy band into $^4E''$ and $^4A_2'$ components.

It is evident that all ^4T terms present in the "parent" octahedral environment are now split into terms of lower degeneracy, and this results in more observable bands in absorption spectra. An increase in the number of bands would be expected, but spectra of Co(II) complexes often lack resolution to observe the effect of the reduction in symmetry. This trend may be extended to environments of lower symmetry. As the symmetry of the chromophore is reduced from D_{3h} to C_1 all states would be reduced to A terms. This helps explain the complexity of some the spectra obtained in the current work, despite that in
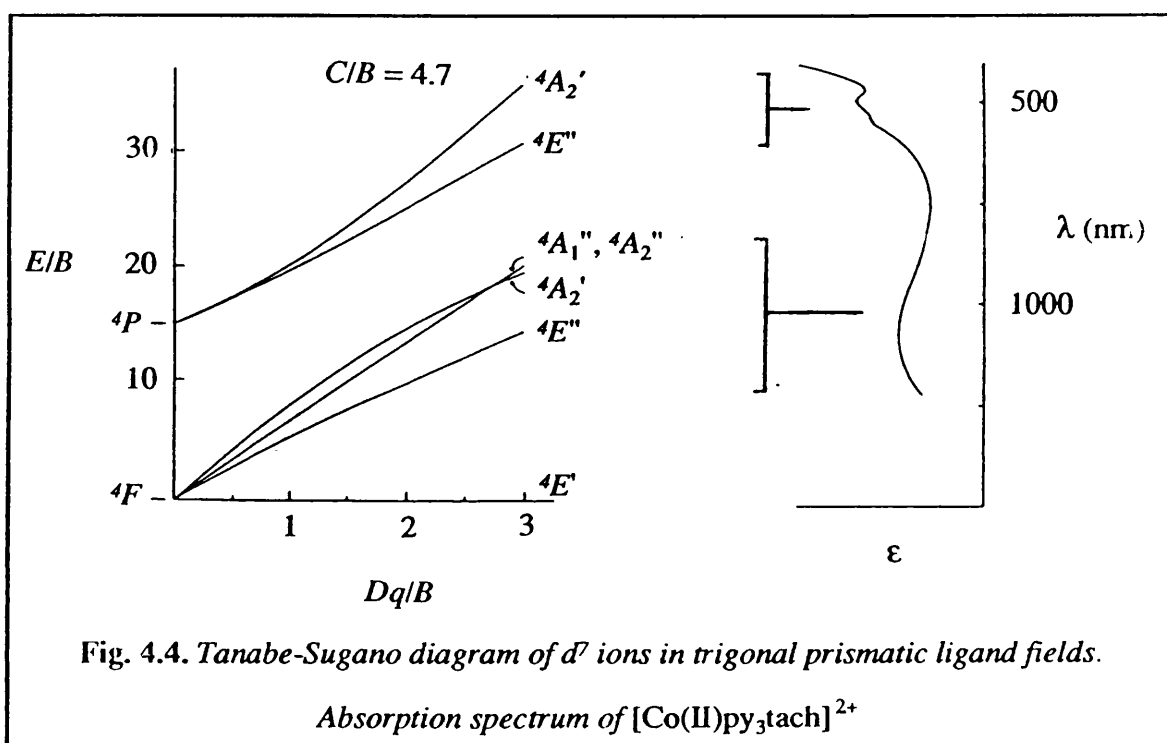
Fig. 4.4. *Tanabe-Sugano diagram of d^7 ions in trigonal prismatic ligand fields. Absorption spectrum of* [Co(II)py$_3$tach]$^{2+}$

some cases crystallographic data indicates trigonal prismatic microsymmetry. The ligands used in the work of Gillum *et al.*, and that of Larsen *et al.*, were based upon pyridine type donors, and as such are potential π-acids, whereas the ligands used in the current work are π-donating, alcohols and alkoxides, which reduce 10 Dq values. Holm also experienced difficulty in assigning Co(II) spectra due to intense charge transfer bands of Co(I) impurities. It must be remembered that with Co(II) spectra the band shapes are often complex since transitions to excited doublet states (spin forbidden) are observed by borrowed intensity from the allowed quartet transitions.

Larsen *et al.* and Gillum *et al.* also calculated the Tanabe-Sugano diagram for Ni(II) in a trigonal prismatic field (fig. 4.5). This diagram also includes singlet states derived from the ^1D term, since by spin orbit coupling there is a possible mixing of singlet and triplet states. It is unlikely that the nickel complexes prepared in the current work will be of trigonal prismatic geometry, since the ligands involved are too flexible and hence will tend adopt octahedral coordination geometries. The diagram is presented as a qualitative guide to the analysis of spectra.
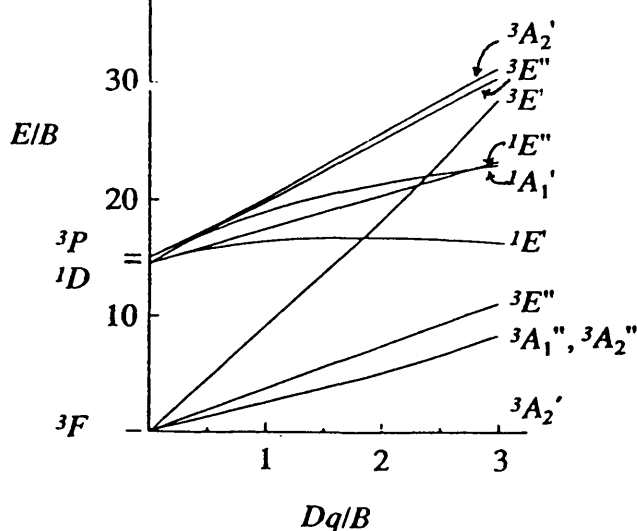
Fig.4.5. *Tanabe-Sugano diagram of d^8 ions in trigonal prismatic ligand fields.*

Copper(II) is a d^9 ion, and in the absence of distortions should display simple electronic spectra. The ground configuration of $t_{2g}^6 e_g^3$ is however highly susceptible to Jahn-Teller distortion, which normally results in a tetragonal distortion, and the absorption spectrum consists of a single broad unsymmetrical absorption. The ligands in the current work tend to promote trigonal distortions, but these distortions do not break the degeneracy of the E_g ground state. It can be argued that an optically pure ligand with an N_3O_3 donor set has C_1 (or C_3 in the case of L^1H_3 and L^2H_3) point symmetry and all complexes thereof will have similar symmetry. Since all states under C_1 symmetry reduce to A terms any ground state degeneracy is removed. Such distortions however may not be sufficient to "override" the Jahn-Teller effect, and so further (J-T) asymmetry must be introduced into the system.

The ground state in trigonal fields is (d_{xz}^1, d_{yz}^2) or (d_{xz}^2, d_{yz}^1) as indicted in the one electron energy level diagram presented in chapter one. Normally trigonally distorted Cu(II) complexes display 2 bands in the absorption spectrum, but further distortions of the chromophore will result in each of these bands becoming unsymmetrical. It is also important to remember that L^1H_3 and similarly disposed ligands do not appear to support Jahn-Teller distortions, due to cyclic constraints.

(4.2) RESULTS AND DISCUSSION

(4.2.1) Preparation of Materials

Ethanol was used as a solvent in all complex preparations due to the insolubility (or low miscibility) of the ligands in water. Cobaltous nitrate was used because of its better solubility in ethanol and it was noted that with L^5H_3 crystallographic quality crystals could be obtained directly from the reaction mixture. All materials prepared were isolated as 1:1 ligand to metal complexes.

The complex with L^1H_3 was kept at all times under vacuum or a nitrogen atmosphere, to prevent oxidation to a peroxo-Co(II) species or a Co(III) species. Such oxidation products would be expected to have considerably more intense absorption bands than the required Co(II) complex and would obscure the weaker Co(II) d-d transitions. $[Co(II)L^1H_3][NO_3]_2$ slowly decomposed (oxidised) in sealed glassware over a period of days. Oxidation to a Co(III) species could not be completely avoided.

With L^3H_3 crystalline material was obtained from the reaction mixture but microanalysis indicated a mixture of products. Conversion to the hexafluorophosphate salt afforded two products, $[Co(II)L^3H_3][PF_6]_2$ and $[(Co(II)L^3H_3)_2(NO_3)_2][PF_6]_2$. The later was obtained as a large single crystal of dimensions 9mm x 5 mm x 4mm. $[Co(II)L^3H_3][PF_6]_2$ was a pink hygroscopic microcrystalline solid, and could not be satisfactorily recrystallised. The preparation of complexes of L^4H_3, L^5H_3, L^7H_3, L^8H_3 and L^9H_3 was as presented in chapter 2 and require no further comment.

(4.2.2) Crystal Structures of [(Co(II)L³H₃)₂(NO₃)₂][PF₆]₂, [Co(II)L⁴H₃][NO₃]₂.H₂O and [Co(II)L⁵H₃][NO₃]₂.

(4.2.3.1) Crystal Structure of [(Co(II)L³H₃)₂(NO₃)₂][PF₆]₂.

From an examination of the empirical formula of the title complex it was assumed that the structure would be that of a molecular cation, $[Co(II)L^3H_3]^{2+}$, and associated counter ions. The only unusual feature was that the complex crystallised as a double salt. The structures of $[Co(II)L^4H_3][NO_3]_2.H_2O$ and $[Co(II)L^5H_3][NO_3]_2$ were determined prior to that of $[(Co(II)L^3H_3)_2(NO_3)_2][PF_6]_2$ and it was believed that some hydrogen bonding to the nitrate counter ions (*vide infra*) was likely. The structure and atom labelling scheme of $[(Co(II)L^3H_3)(NO_3)_2]^{2+}$ is presented in fig. 4.6. The structure is dimeric with 2 nitrate ions binding two $[Co(II)L^3H_3]^{2+}$ subunits together. The complex crystallised in space group P_1, and so every atom in the unit cell is unique (i.e. no point symmetry). The structure of the cation however, is pseudo-centrosymmetric. The nature of the nitrate bridging units is most unusual, and is a very rare mode of hydrogen bonding for nitrate ions. A space-filling view of the structure is presented in fig. 4.7. This indicates how little free space exists is the central cavity between the two $[Co(II)L^3H_3]^{2+}$ subunits. This tight packing arrangement may explain why this complex is only sparingly soluble in water, bearing in mind that nitrates are generally very soluble in aqueous media.

Views of the subunits down the metal-metal axis are presented in fig. 4.8. It is apparent that both subunits are very close to trigonal prismatic co-ordination geometry. The N_3 and O_3 planes are not parallel, and hence true trigonal prismatic geometry cannot be achieved. The six-membered chelate ring is very distorted, and adopts a pseudo-twist-boat conformation. The exocyclic and endocyclic chelate rings are both of λ conformation. This is in contrast to $[Co(III)L^1H_3L^1Co(III)]^{3+}$, where the endocyclic and exocyclic chelate rings are of opposite conformation. This is a consequence of trigonal prismatic coordination, as seen in the Mn(II) component of $[Mn(II)L^1H_3L^1Mn(IV)]^{3+}$ (chapter 3). $[(Co(II)L^3H_3)_2(NO_3)_2][PF_6]_2$, with WMe_6 and $[ZrMe_6]^{2+}$ represent the only

reported cases of trigonal prismatic geometry in a saturated, and therefore flexible, ligand systems. All other cases of trigonal prismatic geometry involve rigid planar ligands with ex*t*ensively delocalsied functionalities. A selection of bond lengths and bond angles are presented in table 4.1.

Table 4.1. Selected bond lengths (Å) and bond angles (deg.) in $[(Co(II)L^3H_3)_2(NO_3)_2][PF_6]_2$

Co(1)-N(11)	2.147(7)	Co(1)-N(14)	2.160(8)
Co(1)-N(18)	2.204(7)	Co(1)-O(11)	2.145(7)
Co(1)-O(14)	2.101(7)	Co(1)-O(18)	2.089(6)
Co(2)-N(21)	2.156(8)	Co(2)-N(24)	2.145(9)
Co(2)-N(28)	2.159(9)	Co(2)-O(21)	2.116(8)
Co(2)-O(24)	2.162(7)	Co(2)-O(28)	2.074(8)
N(11)-Co(1)-N(14)	82.4(3)	N(11)-Co(1)-O(18)	81.0(3)
N(14)-Co(1)-N(18)	94.9(3)	N(11)-Co(1)-O(11)	76.2(3)
N(14)-Co(1)-O(14)	78.2(3)	N(18)-Co(1)-O(18)	79.4(3)
N(21)-Co(2)-N(24)	87.2(4)	N(21)-Co(2)-N(28)	82.1(4)
N(24)-Co(2)-N(28)	91.5(3)	N(21)-Co(2)-O(21)	78.2(3)
N(24)-Co(2)-O(24)	78.8(3)	N(28)-Co(2)-O(28)	78.5(3)
Co(1)-N(14)-C(15)	112.5(6)	Co(2)-N(24)-C(25)	113.1(8)
N(14)-C(15)-C(16)	113.3(8)	N(24)-C(25)-C(26)	113.6(15)
C(15)-C(16)-C(17)	114.1(12)	C(25)-C(26)-C(27)	121.0(17)
C(16)-C(17)-N(18)	114.3(8)	C(26)-C(27)-N(28)	118.5(17)
C(17)-N(18)-Co(1)	113.6(6)	C(27)-N(28)-Co(2)	115.4(9)

In an experiment to determine if $[(Co(II)L^1H_3)_2(NO_3)_2]^{2+}$ maintained a dimeric structure in solution, absorption spectra of $[(Co(II)L^3H_3)_2(NO_3)_2][PF_6]_2$ and $[Co(II)L^3H_3][PF_6]_2$ were obtained as an aqueous solutions and dispersion in KCl disks. The main band in the visible region of $[Co(II)L^3H_3][PF_6]_2$ occurs at 494 nm (*vide infra*) in the solution state spectrum. $[Co(II)L^3H_3][PF_6]_2$ is presumed to be in monomeric in solution. The same value is obtained for $[(Co(II)L^3H_3)_2(NO_3)_2][PF_6]_2$ in solution and solid

state. This experiment is therefore ~~inconclusive~~ but does imply that upon dissolution the chromophore does not significantly change in constitution or geometry. The dimeric nature of $[(Co(II)L^3H_3)_2(NO_3)_2][PF_6]_2$ is believed to be a function of crystallisation in the presence of nitrate.
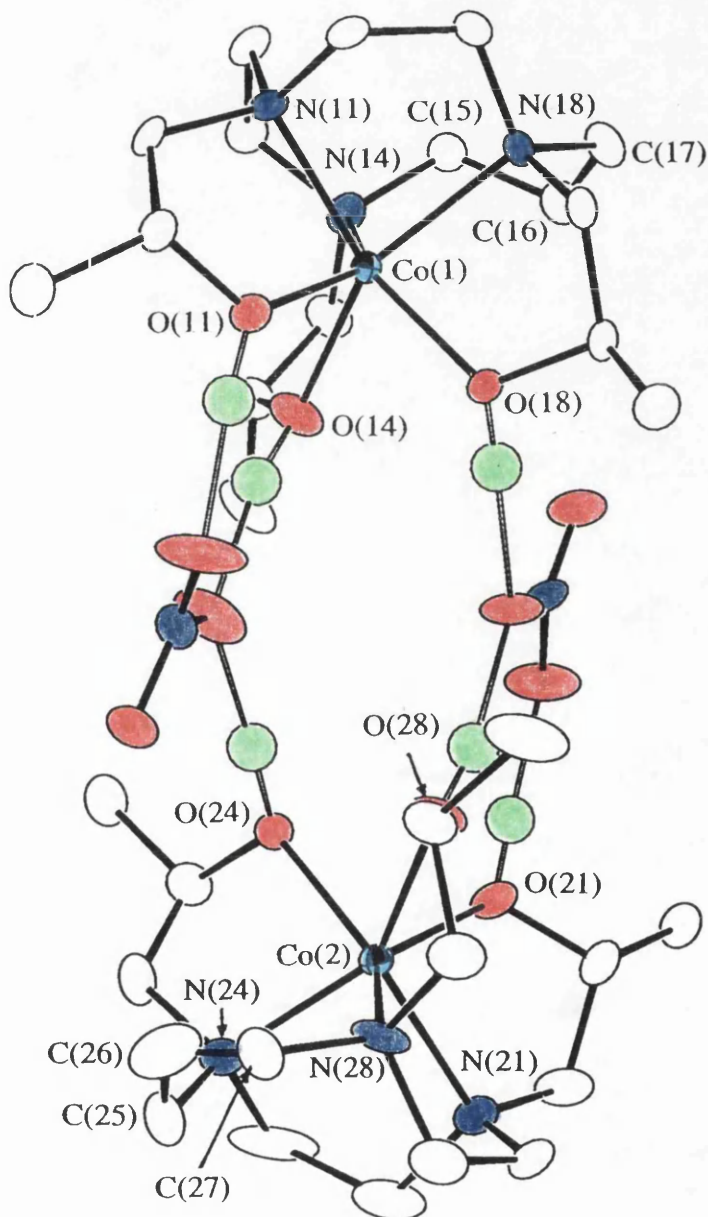
Fig.4.6. *Structure and atom labelling scheme of* $[(Co(II)L^3H_3)_2(NO_3)_2]^{2+}$.
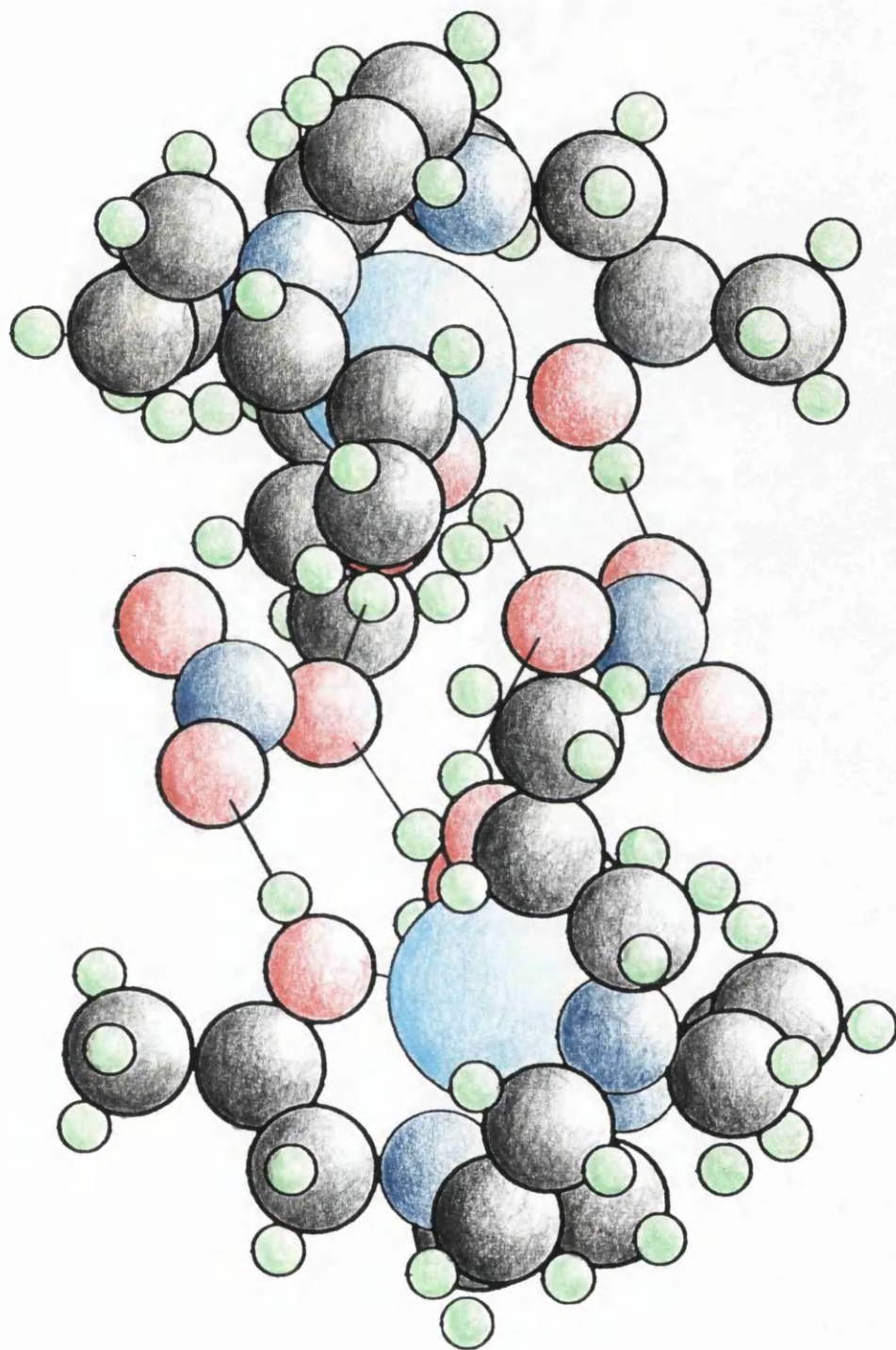
Fig.4.7. *Spacefill view of* $[(Co(II)L^3H_3)_2(NO_3)_2]^{2+}$.
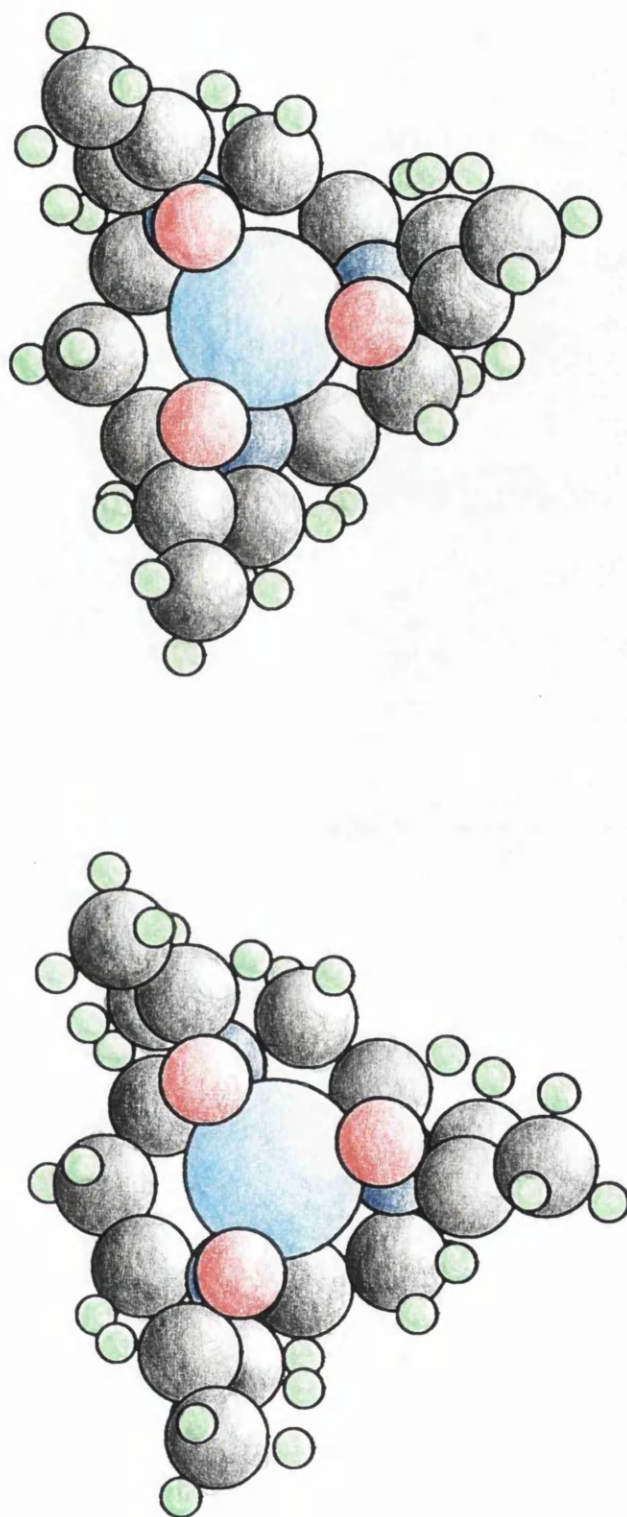
Fig. 4.8. *Views of the* [Co(II)L³H₃]²⁺ *components of* [(Co(II)L³H₃)₂(NO₃)₂]²⁺, *looking down the Co-Co axis.*

(4.2.2.2) Crystal Structure of [Co(II)L^{4}H$_3$][NO$_3$]$_2$.H$_2$O

The crystal structure and atom labelling scheme of [Co(II)L^{4}H$_3$]$^{2+}$ is presented in fig. 4.9. The geometry about the central atom is very distorted. The complex has a distorted bicapped tetrahedral structure. The severe distortion is most apparent upon examination of a selection of bond angles and bond lengths (table 4.2). The effect of the "bulk" of the C$_4$ bridge can be appreciated from the spacefill view presented in fig.4.10. Upon cursory examination this out of the L^3-L^4-L^5 series approximates octahedral geometry most closely. This complex also, by a small margin, has the shortest metal to ligand bond lengths

The exocyclic chelate rings are of λ conformation. The 5-membered endocyclic chelate rings are of opposite conformation, one of λ and one δ. This is a very unusual feature of cyclic systems, in which usually all 5-membered chelate rings are of the same conformation. This feature is also unique in the present work.

The hydrogen bonding *motif* of [(Co(II)L^{3}H$_3$)$_2$(NO$_3$)$_2$][PF$_6$]$_2$ is maintained in [Co(II)L^{4}H$_3$][NO$_3$]$_2$.H$_2$O (fig. 4.11). The two nitrate counter ions are linked to two of the hydroxyl functions via single hydrogen bridges. The remaining hydroxyl group is bonded to the water molecule of crystallisation. In an experiment conducted to determine whether a mixed nitrate hexafluorophosphate analogous to [(Co(II)L^{3}H$_3$)$_2$(NO$_3$)$_2$][PF$_6$]$_2$ could be prepared, an aqueous solution of [Co(II)L^{4}H$_3$][NO$_3$]$_2$.H$_2$O was treated with a slight excess of [NH$_4$][PF$_6$]. Upon slow evaporation of the solution large rose-pink crystals were formed. The vibrational spectrum indicated the presence of both [PF$_6$]$^-$ and [NO$_3$]$^-$ ions. A comparison of the vibrational spectra of [Co(II)L^{4}H$_3$][NO$_3$][PF$_6$] and [(Co(II)L^{3}H$_3$)$_2$(NO$_3$)$_2$][PF$_6$]$_2$ could not provide any firm evidence as to any structural similarities between the complexes.

Table 4.2. Selected bond lengths (Å) and bond angles (deg.) in [Co(II)L⁴H₃][NO₃].H₂O

Co-N(1)	2.180(4)	Co-N(4)	2.140(4)
Co-N(9)	2.125(4)	Co-O(1)	2.094(3)
Co-O(4)	2.068(3)	Co-O(9)	2.191(3)

O(1)-Co-O(4)	92.7(2)	O(1)-Co-O(9)	80.4
O(4)-Co-O(9)	84.5(2)	N(1)-Co-N(4)	82.3(2)
N(1)-Co-N(9)	82.7(2)	N(4)-Co-N(9)	108.9(2)
O(1)-Co-N(1)	77.8(2)	O(4)-Co-N(4)	81.4(2)
O(9)-Co-N(9)	76.7(2)	Co-N(4)-C(5)	119.8(3)
N(4)-C(5)-C(6)	117.5(4)	C(5)-C(6)-C(7)	118.1(4)
C(6)-C(7)-C(8)	114.6(4)	C(7)-C(8)-N(9)	111.1(4)
C(8)-N(9)-Co	114.3(3)		
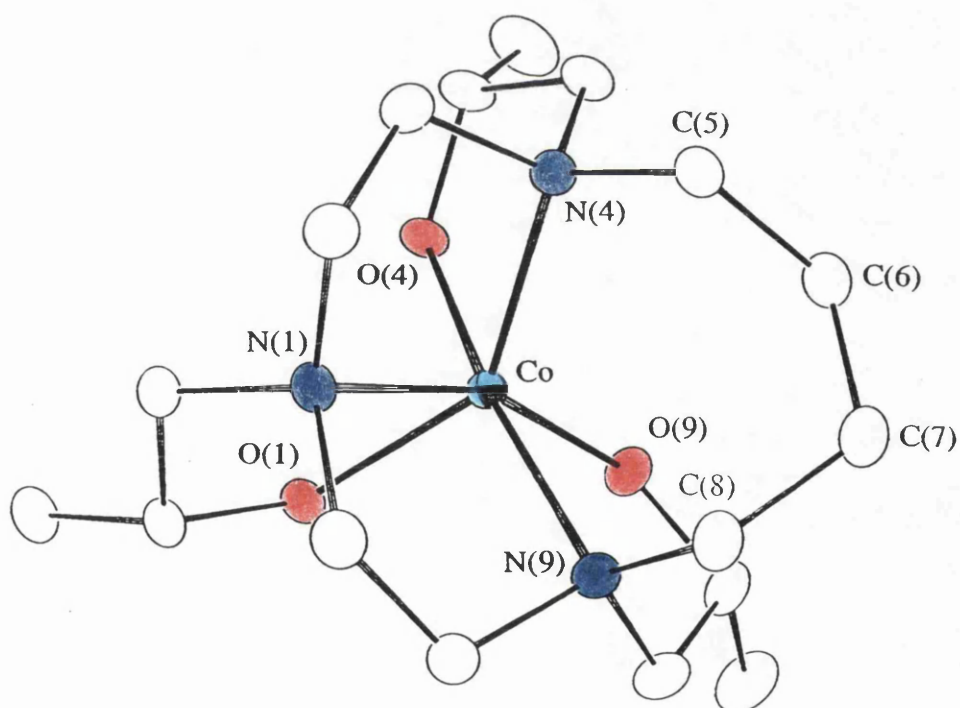
Fig.4.9. *Structure and atom labelling scheme of the cation in* [Co(II)L⁴H₃][NO₃]₂.H₂O.
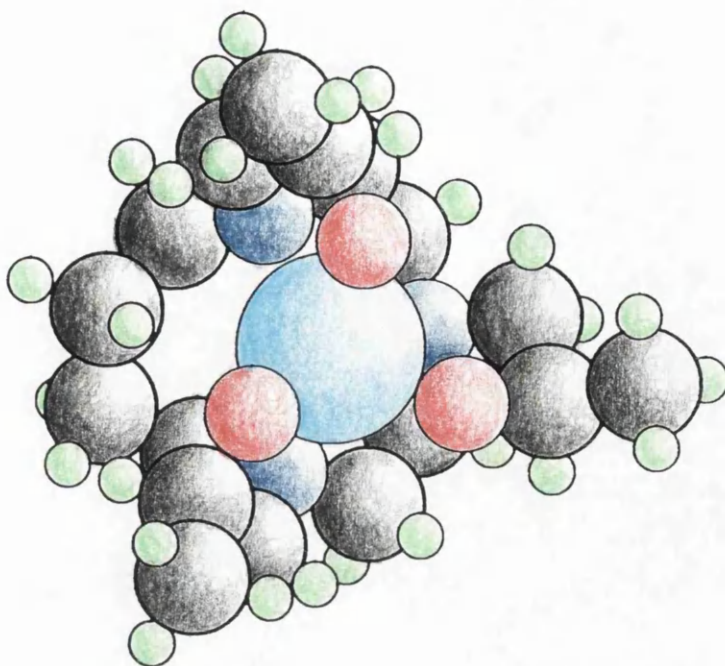
Fig.4.10. *Spacefill view of the cation in* [Co(II)L^{4}H$_3$][NO$_3$]$_2$.H$_2$O.
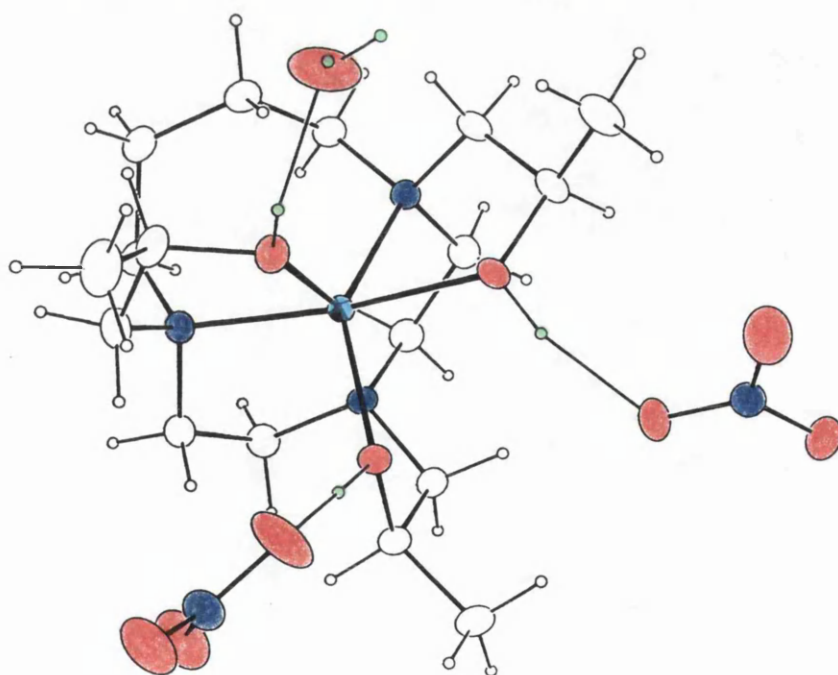
Fig.4.11. *Structure and hydrogen bonding to nitrate counter ions in*

[Co(II)L^{4}H$_3$][NO$_3$]$_2$.H$_2$O.

(4.2.2.3) Crystal Structure of [Co(II)L⁵H₃][NO₃]₂

Firstly it must be noted that L⁵H₃, is of (S)-configuration, and hence chelate rings will be of opposite conformation to those of L³H₃ and L⁴H₃. The structure of [Co(II)L⁵H₃]²⁺ is displayed in fig.4.12. with a space filling diagram displayed in fig.4.13. The geometry of the complex is a truncated trigonal prism. Some relevant bond-lengths and bond-angles are presented in table 4.3. The exocyclic and endocyclic chelate rings are of the δ configuration, characteristic of trigonal prismatic co-ordination.

Fig. 4.14 displays [Co(II)L⁵H₃]²⁺ and the hydrogen-bonding to the nitrate counter ions. One of the nitrate ions is unidentate and the other is bidentate. A mixed nitrate-hexafluorophosphate salt was prepared and crystallised as fine needles. The crystals were not of crystallographic quality and could not be recrystallised due to the material being insoluble in all common solvents. The vibrational spectrum indicated the presence of [NO₃]⁻ and [PF₆]⁻ counter ions.

As with L³H₃ this presents a rare case of trigonal prismatic geometry with a non-rigid ligand system. The structure of [Co(II)L⁵H₃][NO₃]₂ is very unusual since it was believed that such an unsymmetrical ligand would not result in a six coordinate complex.

Table 4.3. Selected bond lengths (Å) and bond angles (deg.) in [Co(II)L⁵H₃][NO₃]₂.

Co-O(1)	2.108(4)	Co-O(4)	2.135(4)
Co-O(10)	2.177(4)	Co-N(1)	2.224(4)
Co-N(4)	2.282(4)	Co-N(10)	2.167(4)
O(1)-Co-O(4)	80.7(2)	O(1)-Co-O(10)	114.2(2)
O(4)-Co-O(10)	78.5(2)	N(1)-Co-N(4)	80.4(2)
N(1)-Co-N(10)	80.8(2)	N(4)-Co-N(10)	116.5(2)
Co-N(4)-C(5)	118.9(3)	N(4)-C(5)-C(6)	114.9(4)
C(5)-C(6)-C(7)	114.3(5)	C(6)-C(7)C-(8)	114.0(5)
C(7)-C(8)-C(9)	113.3(5)	C(8)-C(9)-N(10)	112.5(5)
C(9)-N(10)-Co	118.9(3)		
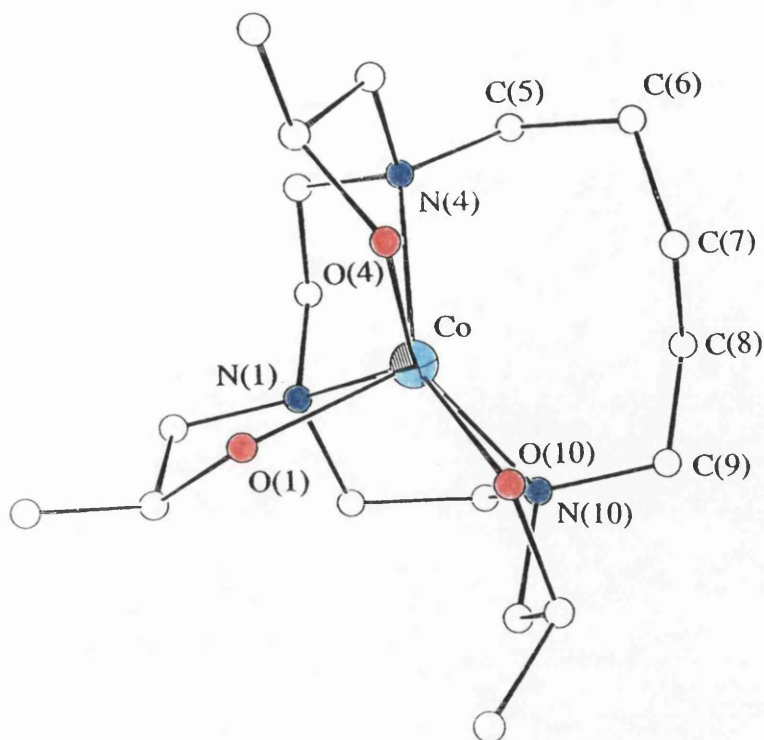
Fig.4.12. *Structure and atom labelling scheme of the cation in* [Co(II)L⁵H₃][NO₃]₂.
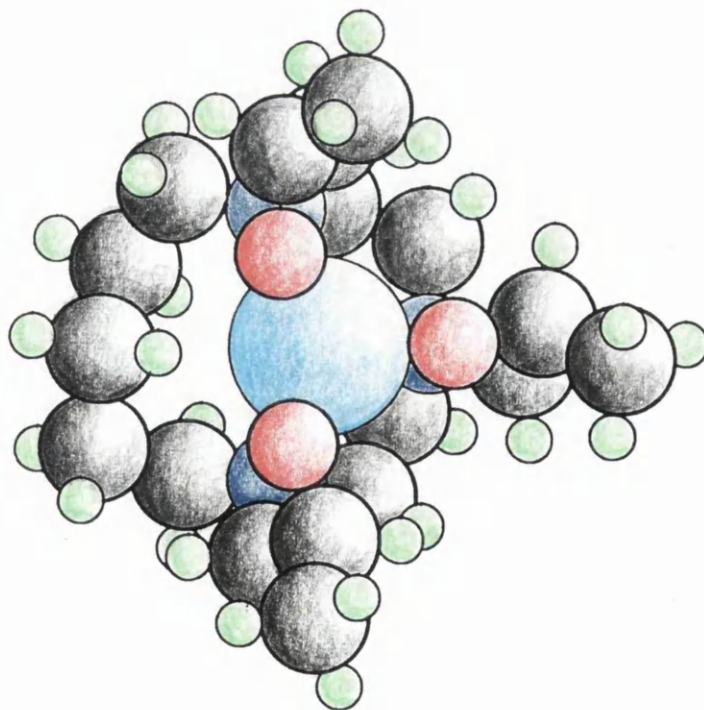
Fig.4.13. *Spacefill view of the cation in* [Co(II)L⁵H₃][NO₃]₂.
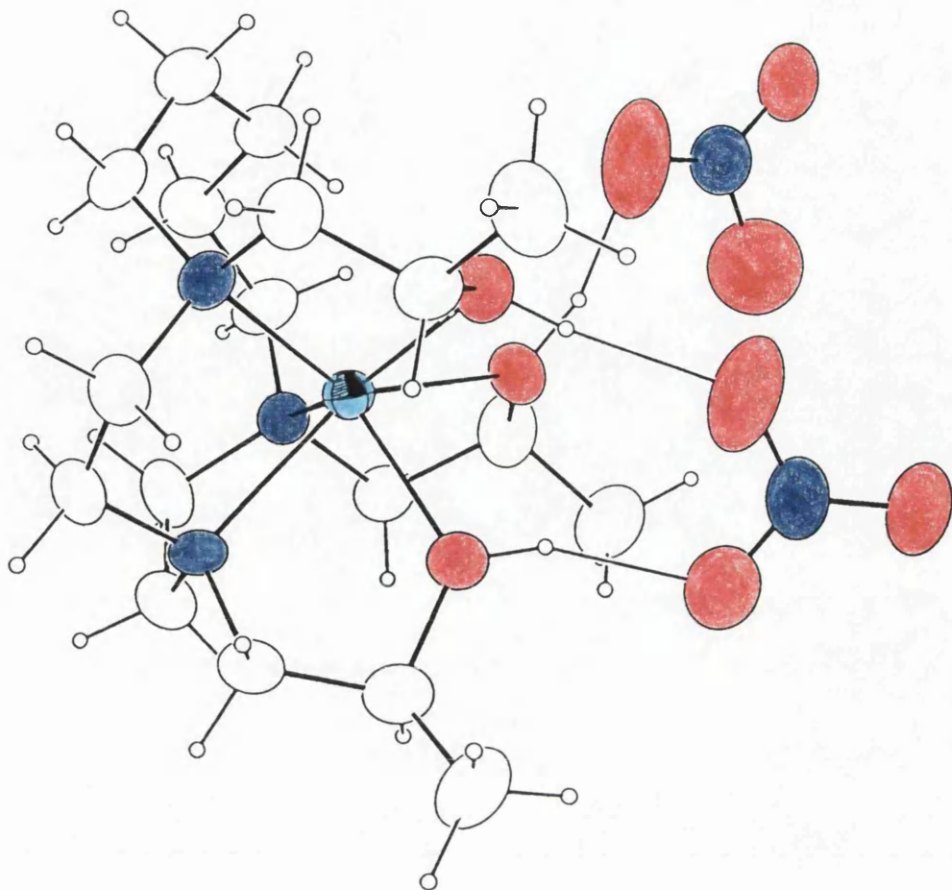
Fig.4.14. *Structure and hydrogen bonding to nitrate counter ions in*

$[Co(II)L^5H_3][NO_3]_2$.

An examination of the bond angles in the larger chelate rings of $[(Co(II)L^3H_3)_2(NO_3)_2]^{2+}$, $[Co(II)L^4H_3]^{2+}$ and $[Co(II)L^5H_3]^{2+}$ reveals considerable distortion of the ligand backbones. Molecular mechanics studies (3) indicate that distortions of bond angles are of relatively low energy compared to distortions of bond lengths. However, considering the *number* of bonds in these chelate systems which are significantly distorted the total strain energy must be large. This explains the resistance of these species to oxidation to Co(III), since with contraction of the metal radius, bond angle distortion would become even more severe.

(4.2.3) Electronic and Circular Dichroism Spectroscopy

(4.2.3.1) General Notes

With Co(II) complexes the assignment of electronic spectra can be difficult, and with the unsymmetrical ligands prepared in this work definite assignment of transitions is not possible. The complexes of L^3H_3, L^4H_3 and L^5H_3 have been shown to have non-octahedral geometries. Despite this octahedral labels derived from the parent ^4F and ^4P states will be used in assigning absorption bands. The bands which occur in the visible region have extremely complex envelopes, due to excited doublet states gaining borrowed intensity from the quartet states.

For purposes of observing trends the data for the cobalt complexes prepared are presented in table 4.4. The $^4T_{1g} \rightarrow \ ^4T_{2g}$ (F) (a two electron process) absorption is very weak and it is not possible assign in most cases. Several of the spectra display shoulders to the low energy side of the $^4T_{1g} \rightarrow \ ^4T_{1g}$ (P) band which may be due to the $^4T_{1g} \rightarrow \ ^4T_{2g}$ (F) transition. The spectra are displayed in the figures listed in the table. The complexity of the spectra results in very intricate CD bandshapes. No attempt is made at assigning transitions in the CD spectra, since without more data this would be mere speculation. Due to the complex nature of the CD spectra, peak maxima, minima and $\Delta\varepsilon$ are not detailed, with it being sufficient to state that all complexes display optical activity and their g factors are of the order of 10^{-2}. This verifies all bands in the region 300-800 nm are d-d in origin.

Some complexes are of approximate trigonal prismatic geometry. Under D_{3h} the transition $E' \rightarrow A_2'$ is electric dipole forbidden. The presence of a large number of bands in the absorption spectra is indicative of lower than D_{3h} symmetry (C_{3v} or C_1), since in crystal fields of lower symmetry this transition becomes allowed.

Table 4.4. Absorption spectra characteristics of $[Co(II)L^nH_3]^{2+}$ (n = 1, 3, 4, 5, 7 and 8). λ [nm] (ε [dm^3 mol^{-1} cm^{-1}]). All spectra were obtained as water solutions, except $[Co(II)L^3H_3][PF_6]_2$ (acetonitrile).

Complex	Fig.	$^4T_{2g}$ (F)	$^4T_{1g}$ (P)
$[Co(II)L^1H_3][NO_3]_2$	4.15	1076 (5.0)	491 (7.1)
$[Co(II)L^3H_3][PF_6]_2$	4.16(a),(b)	1082 (5.4)	494 (9.1)
$[Co(II)L^4H_3][NO_3]_2$	4.17(a),(b)	1183 (4.9)	516 (11)
$[Co(II)L^5H_3][NO_3]_2$	4.18(a),(b)	1132 (4.5)	531 (13)
$[Co(II)L^7H_3][NO_3]_2$	4.19(a),(b)	1220 (5.5)	517 (21)
$[Co(II)L^8H_3][NO_3]_2$	4.20(a),(b)	1174 (8.5)	507 (18)

The spectrum of $[Co(II)L^1H_3]^{2+}$ bears some resemblance to that of $[Co(II)py_3tach]$ but it is believed that $[Co(II)L^1H_3]^{2+}$ is not trigonal prismatic. The band at 372nm is too high in energy to be due to a Co(II) complex, and is therefore assigned to a Co(III) impurity (possibly $[Co(III)L^1H_3L^1Co(III)]^{2+}$) which would have an extinction coefficient of approximately 10 times that of a Co(II) species. This also implies a component of the band at 491 nm is also due to a Co(III) impurity.

An examination of the positions of the $^4T_{1g}$ (P) -> $^4T_{1g}$ (F) transition reflects the ligand field strength and hence the ring size. Comparison of $[Co(II)L^1H_3]^{2+}$ to $[Co(II)L^7H_3]^{2+}$ (trigonally symmetric complexes) supports the notion of larger rings result in smaller ligand field splitting values. Model building suggests that $[Co(II)L^7H_3]^{2+}$ cannot adopt a strain free octahedral geometry, and it is believed that $[Co(II)L^7H_3]^{2+}$ will be trigonally compressed. This is reflected in $[Co(II)L^7H_3]^{2+}$ having a significantly higher

extinction coefficient than $[Co(II)L^1H_3]^{2+}$, due to a relaxation of the electric dipole selection rule.

In the series L^1H_3, L^3H_3, L^4H_3 and L^5H_3 there is a progression of ring size and increasing asymmetry which is reflected in the rapidly increasing wavelength of the $^4T_{1g}$ (F) -> $^4T_{1g}$ (P) absorption. A comparison of the isomeric pairs of complexes; $[Co(II)L^4H_3]^{2+}$ and $[Co(II)L^8H_3]^{2+}$, $[Co(II)L^5H_3]^{2+}$ and $[Co(II)L^7H_3]^{2+}$; indicates that the more unsymmetrical rings result in weaker ligand fields, due to increased steric strain. The bond lengths of the complexes for which crystallographic data is available confirms this, with longer bond lengths, and hence smaller metal-ligand overlap, occurring in the larger ring sizes.

For $[Co(II)L^1H_3]^{2+}$ and $[Co(II)L^3H_3]^{2+}$ the positions of both the $^4T_{1g}$ -> $^4T_{1g}$ (F) and the $^4T_{1g}$ -> $^4T_{1g}$ (P) transitions are very similar. This suggests that the ligand field splitting in these complexes has approximately the same value. This raises the question of why does $[Co(II)L^1H_3]^{2+}$ oxidise very rapidly in air and $[Co(II)L^3H_3]^{2+}$ does not. Attempts at the chemical oxidation of $[Co(II)L^3H_3]^{2+}$ with O_2 and alkaline H_2O_2 failed, resulting in optically inactive solutions. Thus it seems likely that where L^1H_3 is flexible and can coordinate both in a trigonal prismatic and octahedral conformations, L^3H_3 cannot, showing a preference for trigonal prismatic geometry.

(4.2.4) Nickel Complexes

With the nickel complexes prepared in this work no crystal data is currently available, except that of $[Ni(II)L^1H_3][Cl]_2.H_2O$ discussed above. Hence all assignments of absorption bands and structural possibilities must be speculative. Materials were prepared as outlined in chapter 2. Material used for spectroscopic purposes was recrystallised twice.

A summary of the absorption data with a list of figures is presented in table 4.5. The $10Dq$ and B values listed are only approximate, being calculated from Tanabe-

Sugano data for octahedral complexes. The spin forbidden $^3A_{2g} \rightarrow {}^1E_g$ transition can be seen in a number of the spectra but is not assigned. For the calculation of $10Dq$ and B the highest and lowest energy transitions were used to avoid problems of wrong assignment of the middle transition due to mixing of the ^1E_g and $^3T_{1g}$ states. Due to lack of symmetry in most of the complexes the CD spectra in the 300-800 nm region are extremely complex.

A cursory examination of the $10Dq$ values indicates, as expected, the smaller ring sizes result in larger ligand field splitting values. A notable exception is the large $10Dq$ value obtained for $[Ni(II)L^9H_3]^{2+}$, which also has a B value significantly different from the complexes prepared. This indicates a different chromophore in $[Ni(II)L^9H_3]^{2+}$ from the other members of the series. Given the very large ring size of L^9H_3 it is not likely that the ligand is hexadentate, and the remaining coordination sites of Ni(II) are occupied by water. The $10Dq$ value is similar to that of $[Ni(II)L^1H_3]^{2+}$, and it is likely that the structure consists of L^9H_3 bonded via nitrogen atoms and three oxygen donors. The complex is significantly optically active and hence it is probable that one or two pendant-arm donors remain bound. The remaining coordination site(s) are presumably occupied by water molecules.

In comparing $[Ni(II)L^1H_3]^{2+}$, $[Ni(II)L^2H_3]^{2+}$ and $[Ni(II)L^7H_3]^{2+}$ (*i.e.* potentially trigon̄al complexes) a large difference in the ligand field strength is observed with the larger ring size. Also of note is the large B value obtained for $[Ni(II)L^2H_3]^{2+}$ which is due to the inductive effect of the pendant-arm isopropyl groups. Ni(II) has a $t_{2g}^6 \, e_g^2$ configuration, and as such, an increase in electron density at the pendant arm oxygen will lead to an increase in both the σ and π donor properties of the ligand. This will result in greater interelectron repulsion and hence the higher observed B value. The marginally weaker ligand field in $[Ni(II)L^2H_3]^{2+}$ compared to that of $[Ni(II)L^1H_3]^{2+}$ is attributed to intramolecular steric crowding preventing close metal to ligand contact. The $10Dq$ value

of $[Ni(II)L^7H_3]^{2+}$ is exceptionally low. Assuming that the ligand is hexadentate, metal to ligand bond distances will be very long.

$[Ni(II)L^4H_3]^{2+}$, $[Ni(II)L^8H_3]^{2+}$; and $[Ni(II)L^5H_3]^{2+}$, $[Ni(II)L^7H_3]^{2+}$, represent isomeric pairs of complex cations. With L^4H_3 and L^8H_3 the $10Dq$ values are very similar, with L^8H_3 producing the marginally stronger ligand field. The structure of $[Co(II)L^4H_3]^{2+}$ was shown above to be very distorted, but of the materials that have been crystallographically characterised, most closely approaches octahedral geometry. Is is probable that $[Ni(II)L^4H_3]^{2+}$ has a similar structure. With the more symmetrical L^8H_3 octahedral geometry is most likely, and hence the ligand field parameters are understandably similar. With $[Ni(II)L^5H_3]^{2+}$ and $[Ni(II)L^7H_3]^{2+}$ the $10Dq$ value for the more symmetrical L^7H_3 is surprisingly smaller. This is difficult to explain given that for the analogous Co(II) complexes L^7H_3 produces the stronger ligand field. The smaller ionic radius of Ni(II) may result in very long N-Ni bond lengths and it is possible that the three C_3 bridges in L^7H_3 is a more significant sterically crowding factor that the C_5 bridge of L^5H_3. As seen with Co(II), Ni(II) fails to complex with L^6H_3. Given the trends of ligand field strengths noted in the Ni(II) complexes prepared, the $10Dq$ value of $[Ni(II)L^6H_3]^{2+}$ would be very low. Given that for $[Ni(II)(H_2O)_6]^{2+}$ $10Dq = 8500$ cm^{-1} complex formation is unlikely on thermodynamic grounds.

Complexes of $L^{10}H_3$ have not yet been fully characterised, but treatment of $[Ni(II)L^{10}H_3][NO_3][PF_6]$ with $[NO][PF_6]$ in acetonitrile solution indicates a significant colour change. The oxidation product is believed to be $[Ni(III)L^{10}H_3]^{3+}$. With L^1H_3 no Ni(III) complex could be prepared. This is attributed to the strongly oxidising nature of Ni(III), which may result in the oxidation of the pendant-arm alcohol groups. $L^{10}H_3$ is a tertiary alcohol, and hence lacks α hydrogen atoms, rendering the ligand more stable to strongly oxidising conditions. A $[Ni(III)L^{10}H_3]^{3+}$ moiety would be expected to dimerise by analogy with $[Cr(III)L^1H_3L^1Cr(III)]^{3+}$ and $[Co(III)L^1H_3L^1Co(III)]^{3+}$. However, molecular modelling studies indicate that at the O,O',O" hydrogen-bond acceptor-donor face $L^{10}H_3$ is too sterically hindered to permit dimer formation.

Table 4.5. Absorption spectra charecteristics of $[Ni(II)L^nH_3]^{2+}$ (n =1, 2, 3, 4, 5, 7, 8 and 9). $10Dq$, B (cm^{-1}); λ [nm] (ε [dm^3 mol^{-1} cm^{-1}]). All spectra were obtained as water solutions, except $[Ni(II)L^3H_3][PF_6]_2$ (acetonitrile). Ground state is $^3A_{2g}$.

Complex	Fig.	$10Dq$	B	$^3T_{2g}$	$^3T_{1g}(F)$	$^3T_{1g}(P)$
$[Ni(II)L^1H_3][Cl]_2.H_2O$	21	10770	862	930 (24)	557 (7.4)	357 (10)
$[Ni(II)L^2H_3][NO_3][PF_6].H_2O$	22(a),(b)	10670	933	931 (40)	557 (13)	348 (29)
$[Ni(II)L^3H_3][PF_6]_2$	23(a),(b	10380	895	964 (12)	575 (9.6)	361 (13)
$[Ni(II)L^4H_3][NO_3]_2$	24(a),(b)	9435	925	1064 (15)	597 (8.7)	357 (16)
$[Ni(II)L^5H_3][NO_3]_2$	25(a),(b)	9105	915	1148 (16)	715 (8.4), 627 (8.0)	393 (25)
$[Ni(II)L^7H_3][NO_3]_2$	26(a),(b)	8940	890	1117 (11)	653 (16)	393 (26)
$[Ni(II)L^8H_3][NO_3]_2$	27(a),(b)	9480	892	1053 (17)	615 (15)	380 (22)
$[Ni(II)L^9H_3][NO_3]_2$	28(a),(b)	10760	692	1061 (2.2)	639 (3.5)	384 (7.3)

(4.2.5) Copper Complexes

As with the nickel complexes noted above no definitive crystallographic data was available. Data sets were collected for $[Cu(II)L^5H_3][PF_6]_2$ and $[Cu(II)L^7H_3][PF_6]_2$, but at the current time these structures have not been solved. Materials were prepared as indicated in chapter 2. It is worth noting that different products could be obtained when different concentrations of metal salt and ligand solution were used. With highly concentrated reaction mixtures intense green solutions were produced from which green nitrate salts could be isolated. Dissolution of these salts in water followed by treatment with $[NH_4][PF_6]$ resulted in the precipitation of pale blue materials. With L^5H_3 however, the intense green colour persisted. With dilute reaction conditions deep blue solutions were initially produced which became lighter in hue. These solutions precipitated pale blue hexafluorophosphate salts upon treatment with excess $[NH_4][PF_6]$. It is possible that with different reaction conditions different structural isomers are formed, but without more data further comment would be highly speculative.

The absorption spectral characteristics of the Cu(II) complexes prepared are presented in table 4.6. with a listing of figures. The bands are assigned assuming approximate six coordinate trigonal symmetry. There is the possibility of five coordinate Cu(II). Such systems can have trigonal symmetry and their spectra may resemble those of :x coordinate Cu(II) (9). Auerbeck et al. (10) have prepared the Cu(II) complex of 1,4,7-tris-(2-hydroxybenzyl)-1,4,7-triazacyclononane. The complex is five coordinate with all three ring nitrogens and two pendant-arm oxygen atoms coordinated. Coordination geometry is intermediate between trigonal bipyramidal and square-based pyramidal. This complex displays absorption bands mainly in the visible region. With 5-coordinate species absorption is mainly in the visible region whilst with the complexes prepared in the current work, absorption spectra characteristic of highly trigonally distorted 6 coordinate species are obtained. The assignments presented in table 4.6 are based upon 6 coordinate trigonally distorted species (see chapter 1 for energy level diagram).

Table 4.6. Absorption spectra characteristics of $[Cu(II)L^nH_3]^{2+}$ (n =1, 3, 4, 5, 7 and 8), λ [nm] (ε [dm^3 mol^{-1} cm^{-1}]). All spectra were obtained as acetonitrile solutions. Ground state is (d_{xz}^1, d_{yz}^2) or (d_{xz}^2, d_{yz}^1).

Complex	Fig.	d_{xy}, $d_{x^2-y^2}$	d_{z^2}
$[Cu(II)L^1H_3][PF_6]_2$	29	-	714 (44)
$[Cu(II)L^2H_3][PF_6]_2$	30(a),(b)	-	722 (50)
$[Cu(II)L^3H_3][PF_6]_2$	31(a),(b)	1304 (29)	692 (49)
$[Cu(II)L^4H_3][PF_6]_2$	32(a),(b)	1253 (59)	731 (61)
$[Cu(II)L^5H_3][PF_6]_2$	33(a),(b)	1080 (25)	745 (29)
$[Cu(II)L^7H_3][PF_6]_2$	34(a),(b)	1470 (41)	797 (61)
$[Cu(II)L^8H_3][PF_6]_2$	35(a),(b)	1357 (77)	771 (79)

As expected, the spectra of $[Cu(II)L^1H_3][PF_6]_2$ and $[Cu(II)L^2H_3][PF_6]_2$ are very similar. The approximate d-orbital splitting value is 14000 cm^{-1}. The presence of only one main absorption is indicative of approximate octahedral geometry.

Of particular note is $[Cu(II)L^3H_3][PF_6]_2$, which has the d_{z^2} -> d_{xy}, $d_{x^2-y^2}$ absorption at a slightly higher energy than both $[Cu(II)L^1H_3][PF_6]_2$ and $[Cu(II)L^2H_3][PF_6]_2$. This implies that the overall d-orbital splitting value in $[Cu(II)L^3H_3][PF_6]_2$ is greater. It is possible that with $[Cu(II)L^3H_3][PF_6]_2$ almost perfect trigonal prismatic geometry is achieved, as is seen with $[(Co(II)L^3H_3)_2(NO_3)_2][PF_6]_2$. This is very unusual as trigonal distortion tends to result in weaker ligand fields. Theoretically Cu(II) displays only a slightly smaller tendency towards trigonal prismatic geometry than Co(II) (chapter 1). It has been shown that L^3H_3 Can support a Jahn-Teller distortion in $[Mn(II)L^3H_3L^3Mn(III)][PF_6]_2.H_2O$, and it is probable that $[Cu(II)L^3H_3][PF_6]_2$ has trigonal

prismatic geometry with a superimposed tetragonal distortion. The susceptibility of Cu(II) to trigonal distortion and the tendency of L^3H_3 to coordinate in trigonal prismatic geometry explains the relatively large ligand field strength of $[Cu(II)L^3H_3][PF_6]_2$. Cu(II) is a relatively large ion, and it is also possible that the ligand cavity to metal size match is good. Again this would result in stronger ligand fields.

$[Cu(II)L^7H_3][PF_6]_2$ potentially has pseudo-octahedral geometry. However, the presence of two main absorption bands indicates a strongly trigonally distorted 6-coordinate structure. Relative to $[Cu(II)L^1H_3][PF_6]_2$ these bands are considerably red shifted, which indicates a rather weak ligand field. Thus it is likely that $[Cu(II)L^7H_3][PF_6]_2$ in solution is a highly compressed trigonal prism. In the solid state, preliminary crystallographic studies indicate a highly distorted structure. Elements of (pseudo)-trigonal symmetry are present but crystal disorder was found to be high. It is therefore possible that a long axis due to Jahn-Teller distortion is present disordered about three possible positions. As found with Co(II) and Ni(II), L^7H_3, despite its symmetrical nature, produces the smallest ligand field splitting value. Again, without more data, this is attributed to three C_3 bridges causing more severe steric strain than the two C_2 and one C_n bridge of the other ligands. It is worth noting that with the isomeric pair of complexes $[Cu(II)L^4H_3][PF_6]_2$ and $[Cu(II)L^8H_3][PF_6]_2$, the later has the smaller overall d-orbital splitting value. Again this suggest the presence of 6-membered chelate is very seve re factor in the steric strain of this type of complex.

Of the spectra characteristic of trigonal complexes, that of $[Cu(II)L^5H_3][PF_6]_2$ displays the highest energy absorption bands. This is surprising when it is considered that L^5H_3 is the most unsymmetrical free ligand, and contains a twelve membered ring. This may imply a good cavity to metal fit and also a tendency for L^5H_3 to adopt trigonal prismatic coordination geometry. This has some precedent in that the Co(II) complex of L^5H_3 is trigonal prismatic. Therefore it is not unreasonable to state that $[Co(II)L^5H_3]^{2+}$ and $[Cu(II)L^5H_3]^{2+}$ are isostructural. This of course, does not include any further (Jahn-Teller) distortion in the Cu(II) complex.

(4.2.6) Spectra.
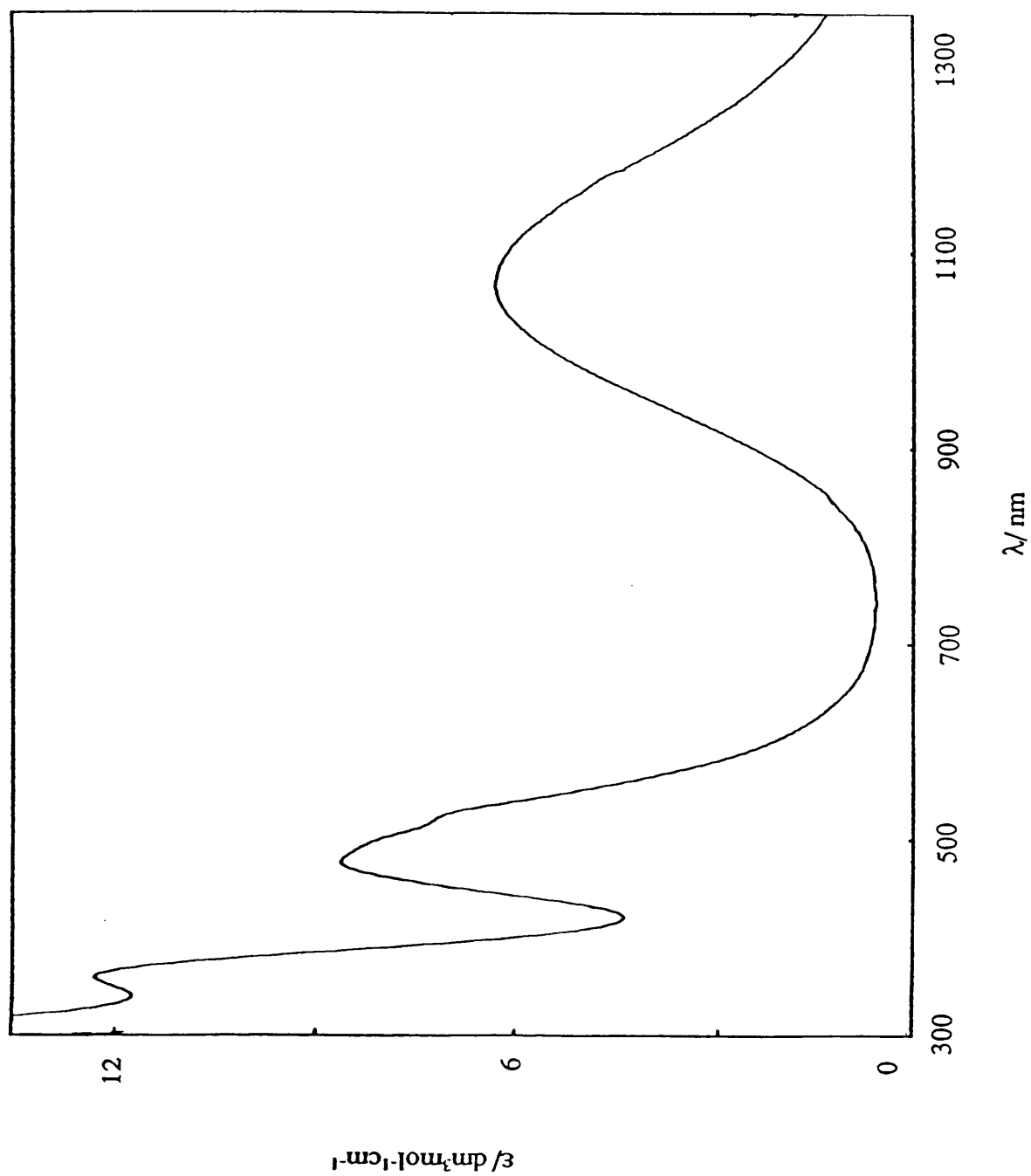
Fig.4.15. *Absorption Spectrum of* [Co(II)L^{1}H$_3$][NO$_3$]$_2$ *in ethanol solution.*
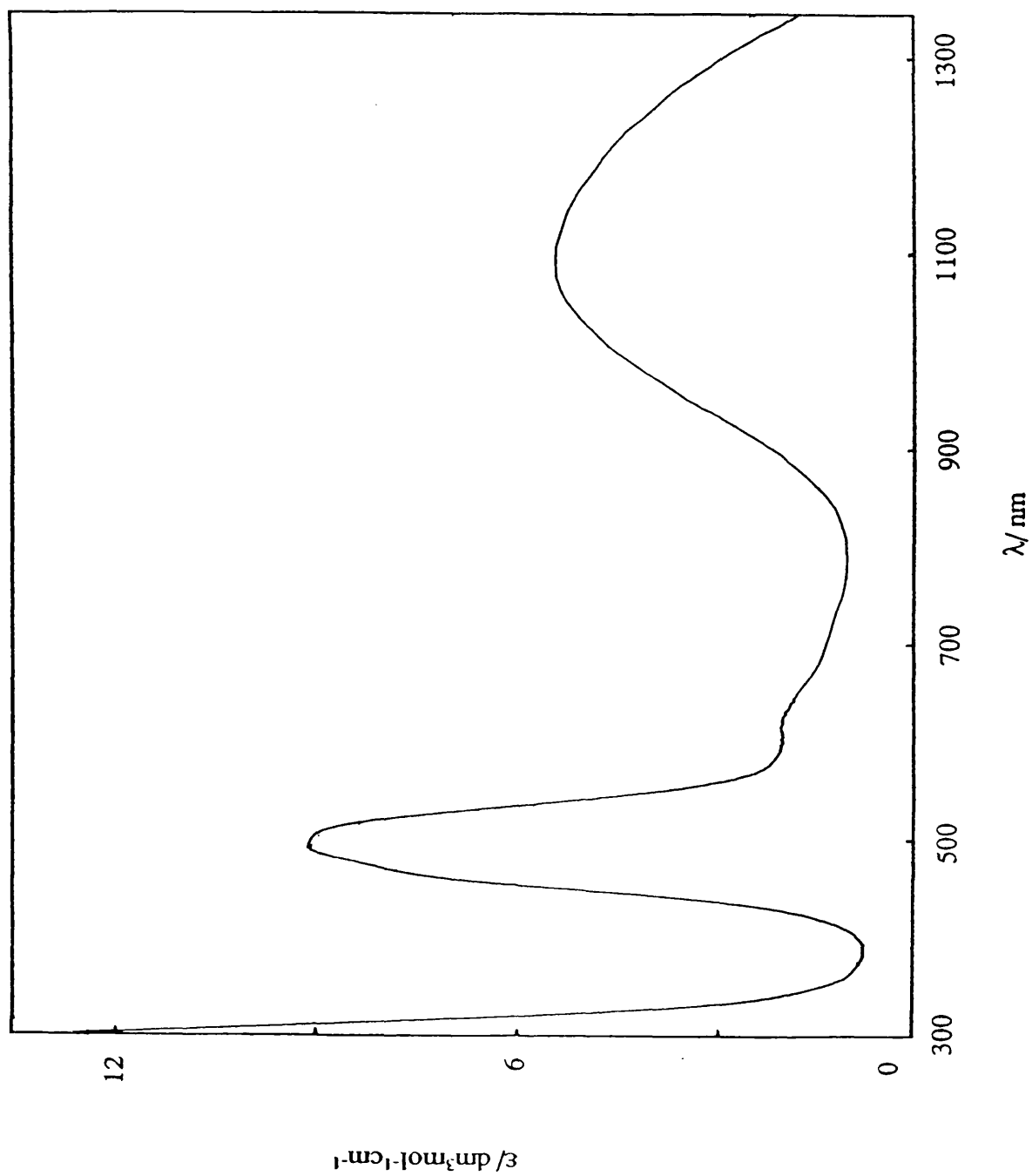
Fig.4.16(a). *Absorption Spectrum of* [Co(II)L³H₃][PF₆]₂ *in acetonitrile solution.*
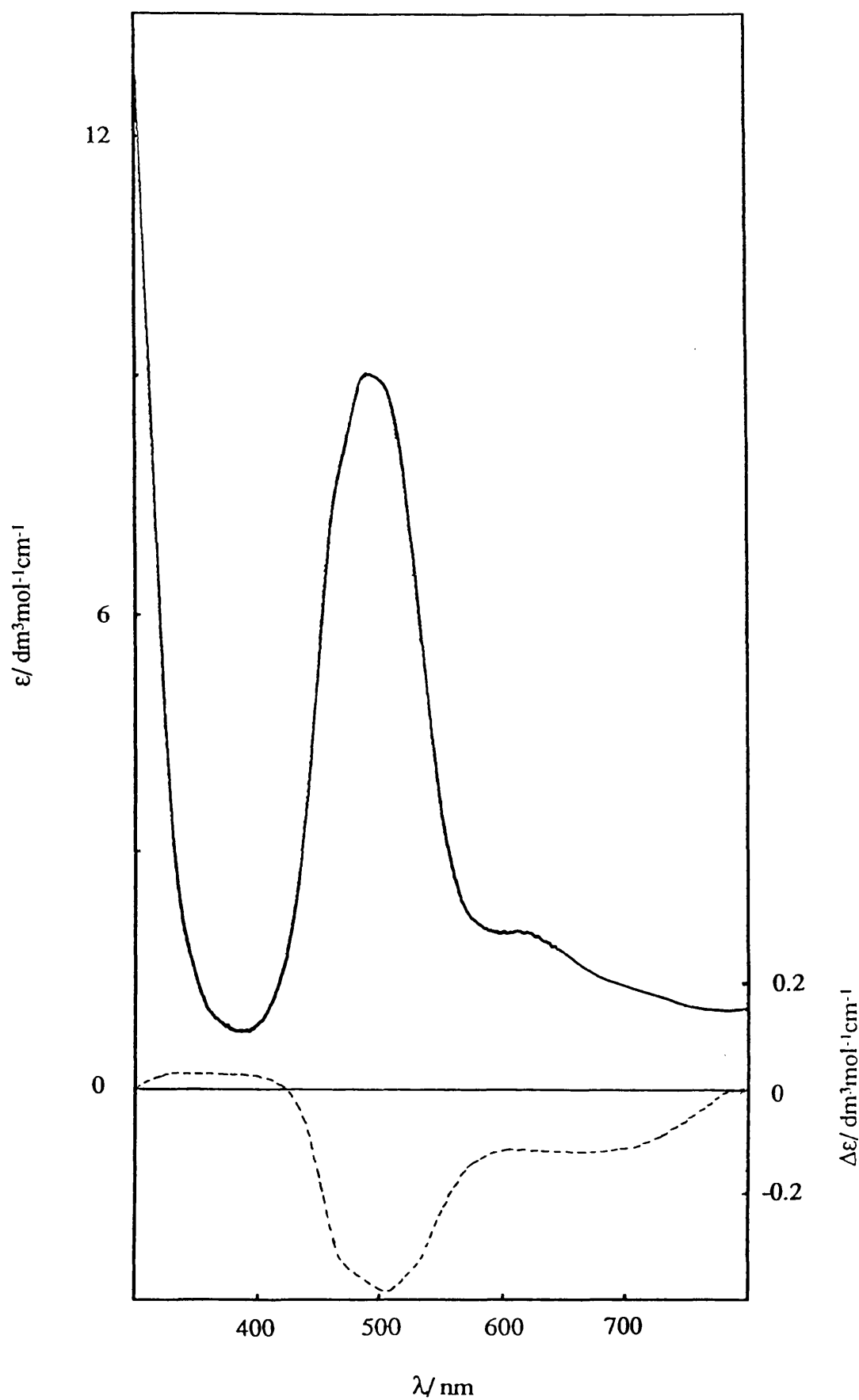
Fig.4.16(b). *Absorption and Circular Dichroism Spectra of* [Co(II)L³H₃][PF₆]₂ *in*

acetonitrile solution.
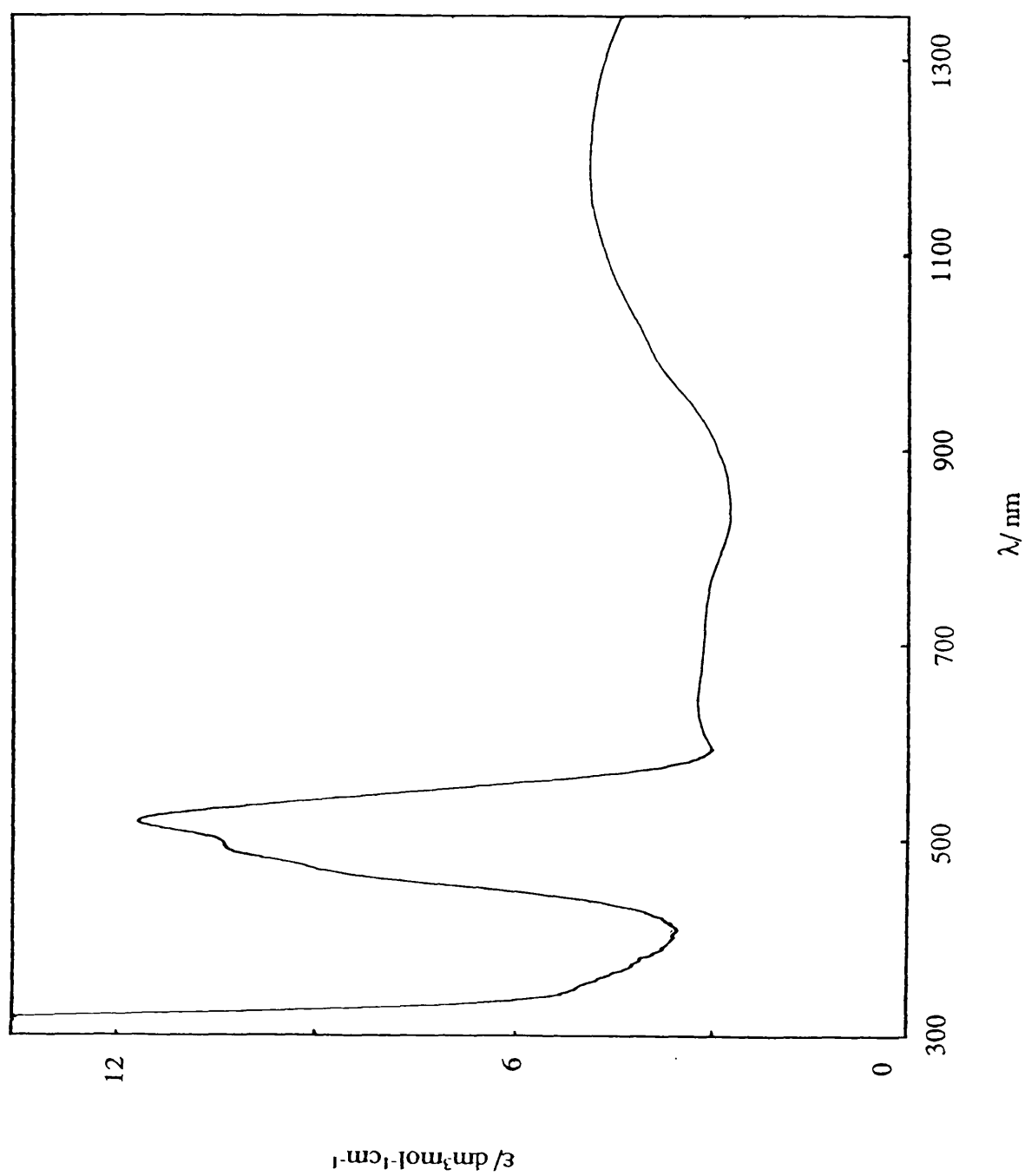
Fig.4.17(a). *Absorption Spectrum of* [Co(II)L⁴H₃][NO₃]₂ *in water solution.*
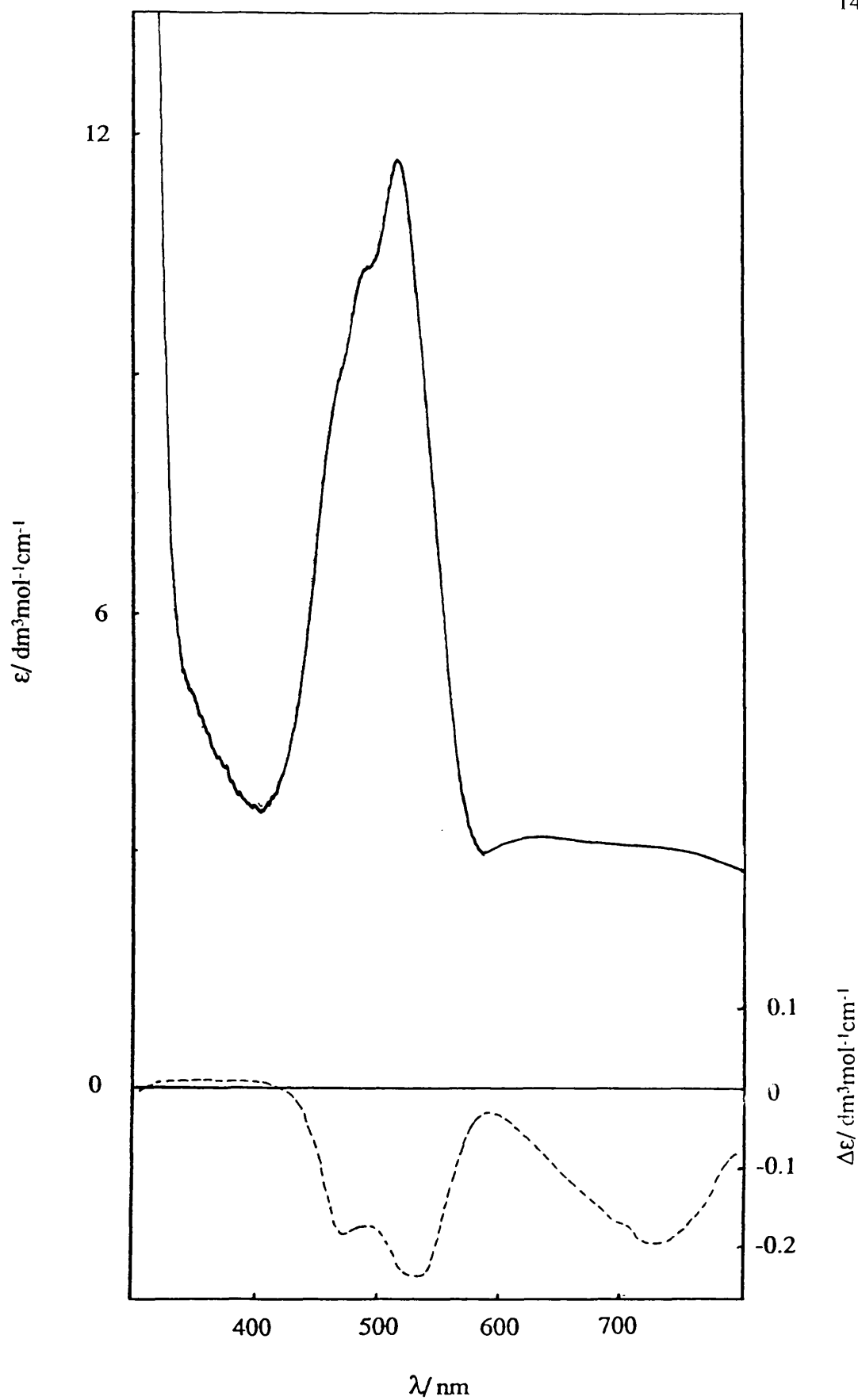
Fig.4.17(b). *Absorption and Circular Dichroism Spectra of* [Co(II)L⁴H₃][NO₃]₂ *in water solution.*

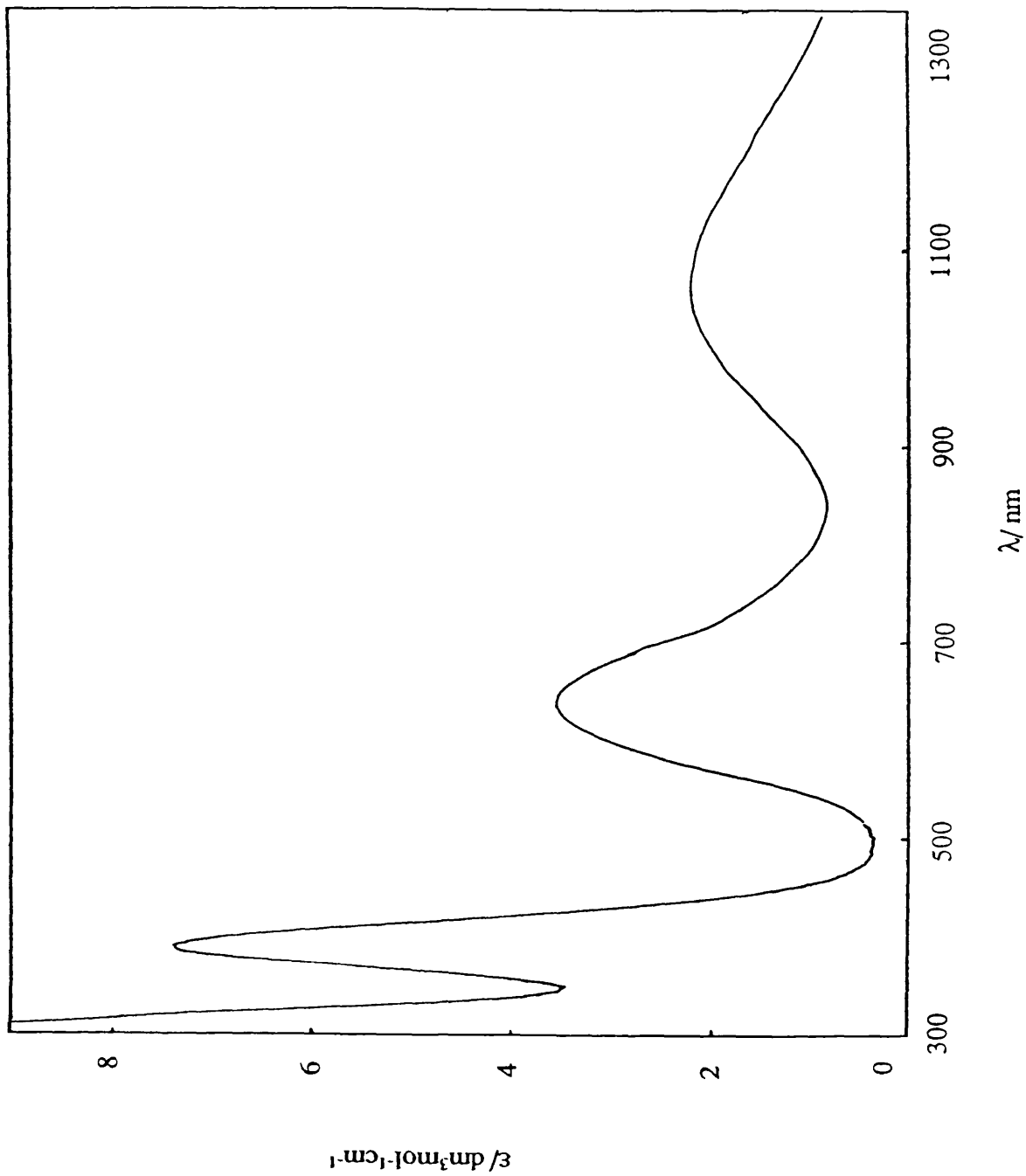Fig.4.18(a). *Absorption Spectrum of* [Co(II)L⁵H₃][NO₃]₂ *in water solution.*
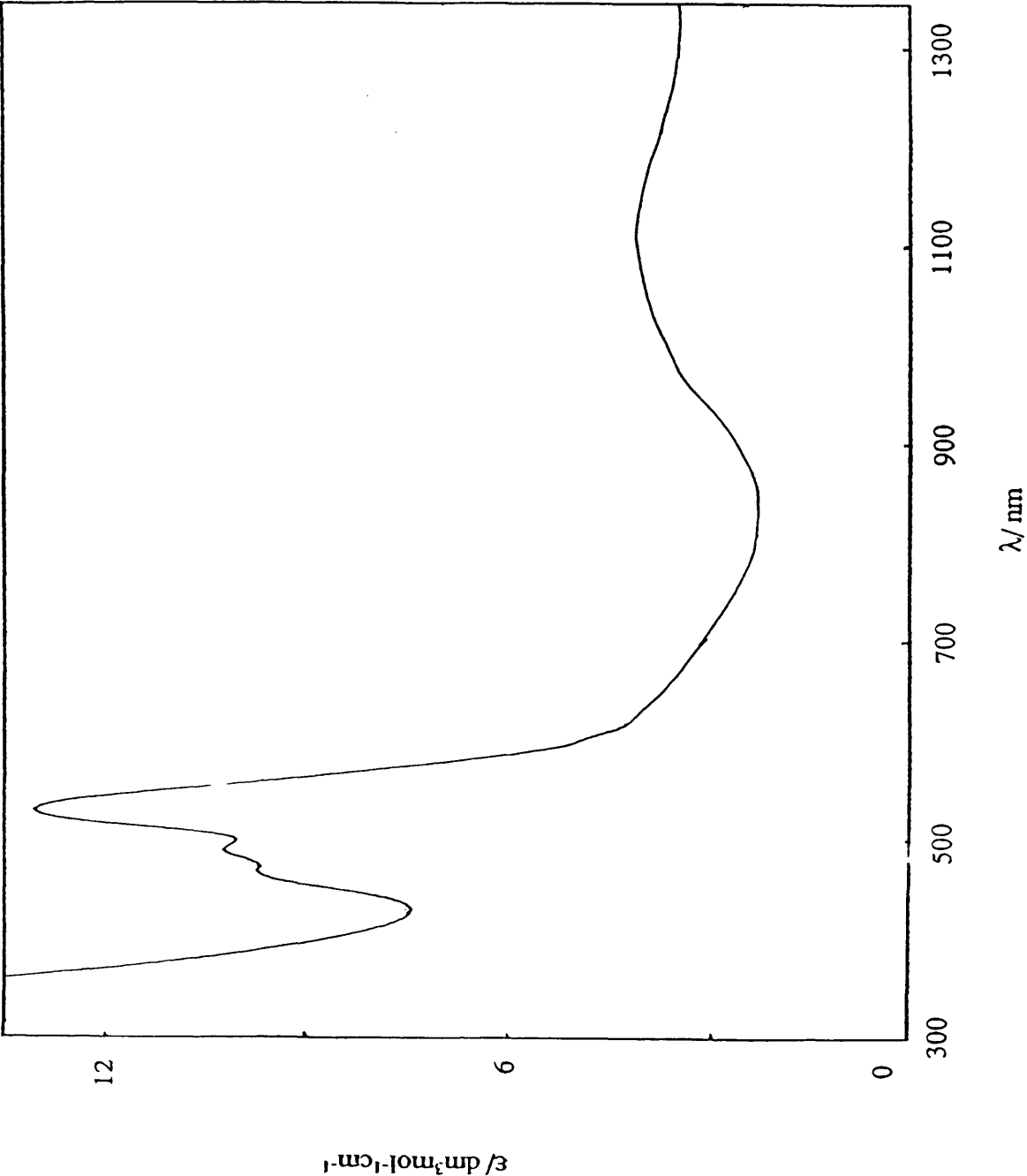
Fig.4.18(a). *Absorption Spectrum of* $[Co(II)L^5H_3][NO_3]_2$ *in water solution.*
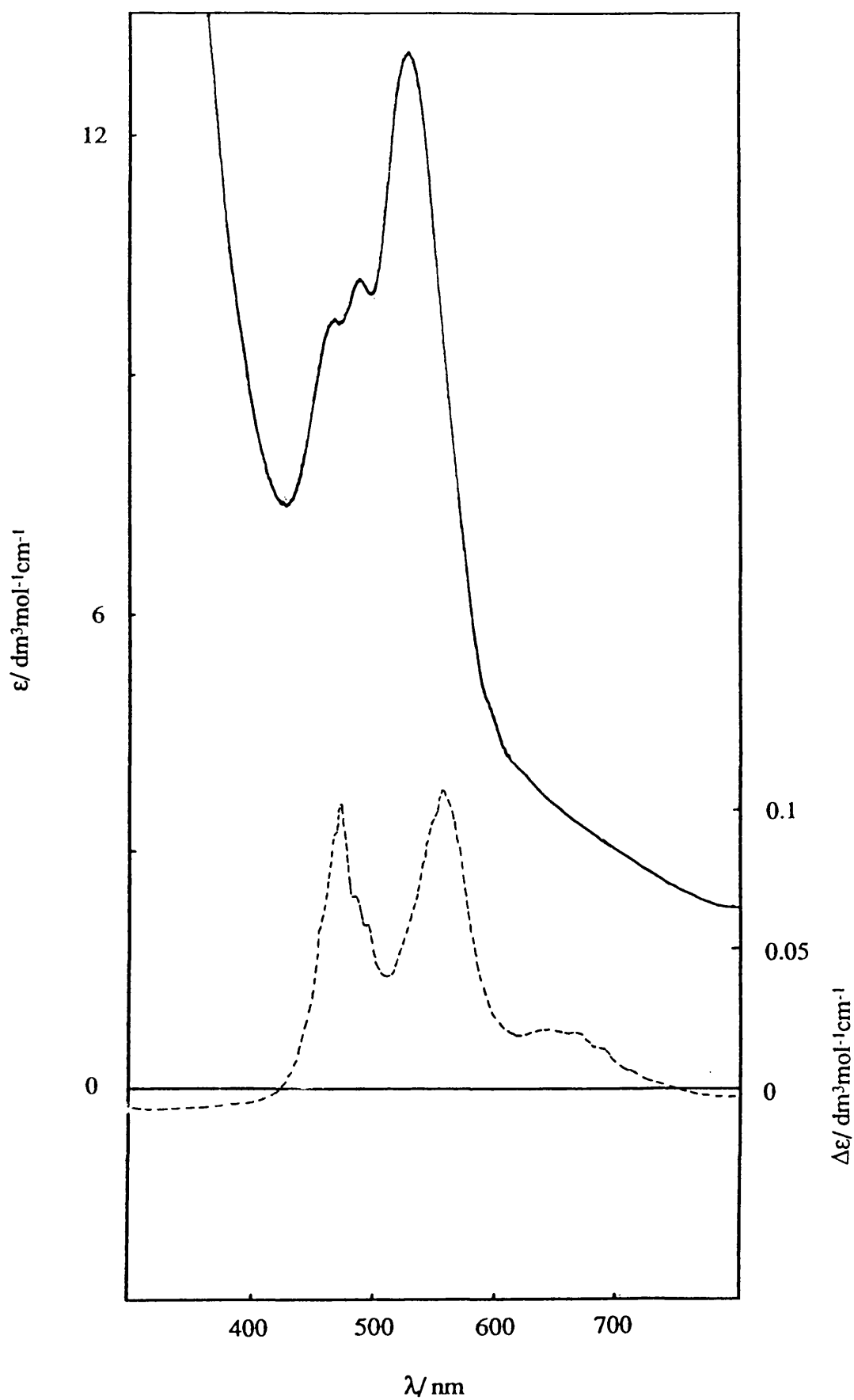
Fig.4.18(b). *Absorption and Circular Dichroism Spectra of* [Co(II)L⁵H₃][NO₃]₂ *in water*
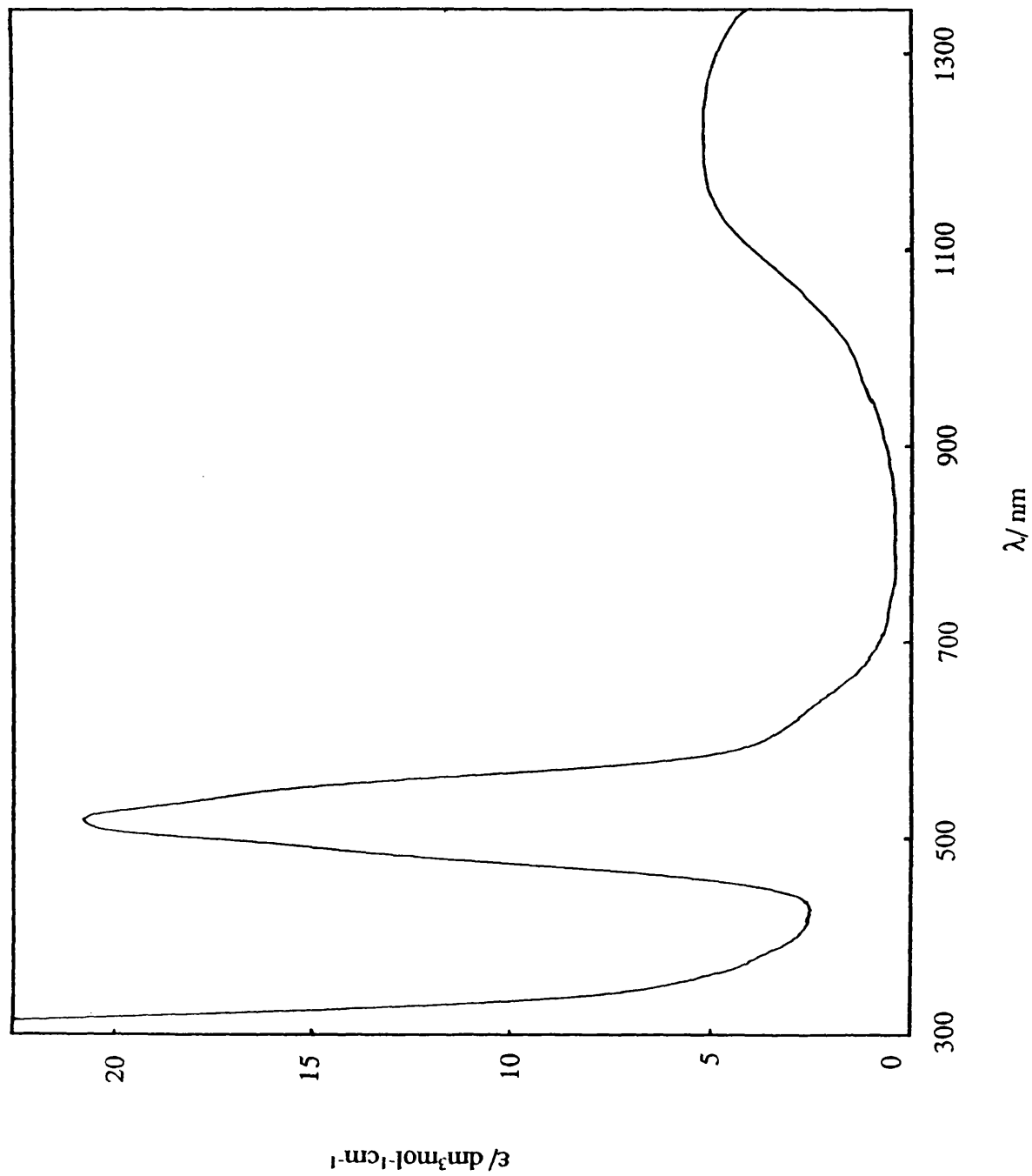
solution.

Fig.4.19(a). *Absorption Spectrum of* [Co(II)L7H₃][NO₃]₂ *in water solution.*
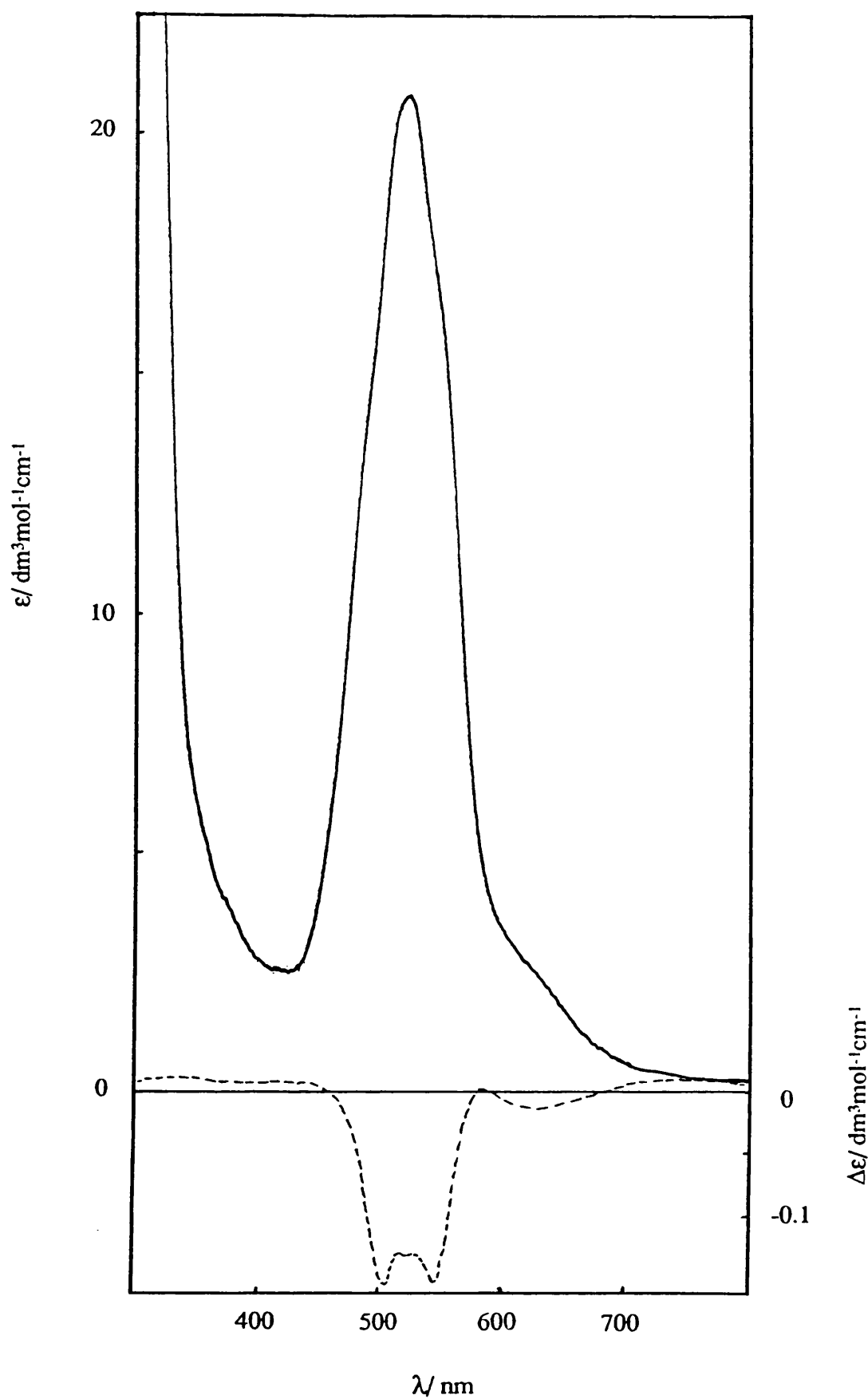
Fig.4.19(b). *Absorption and Circular Dichroism Spectra of* [Co(II)L⁷H₃][NO₃]₂ *in water*
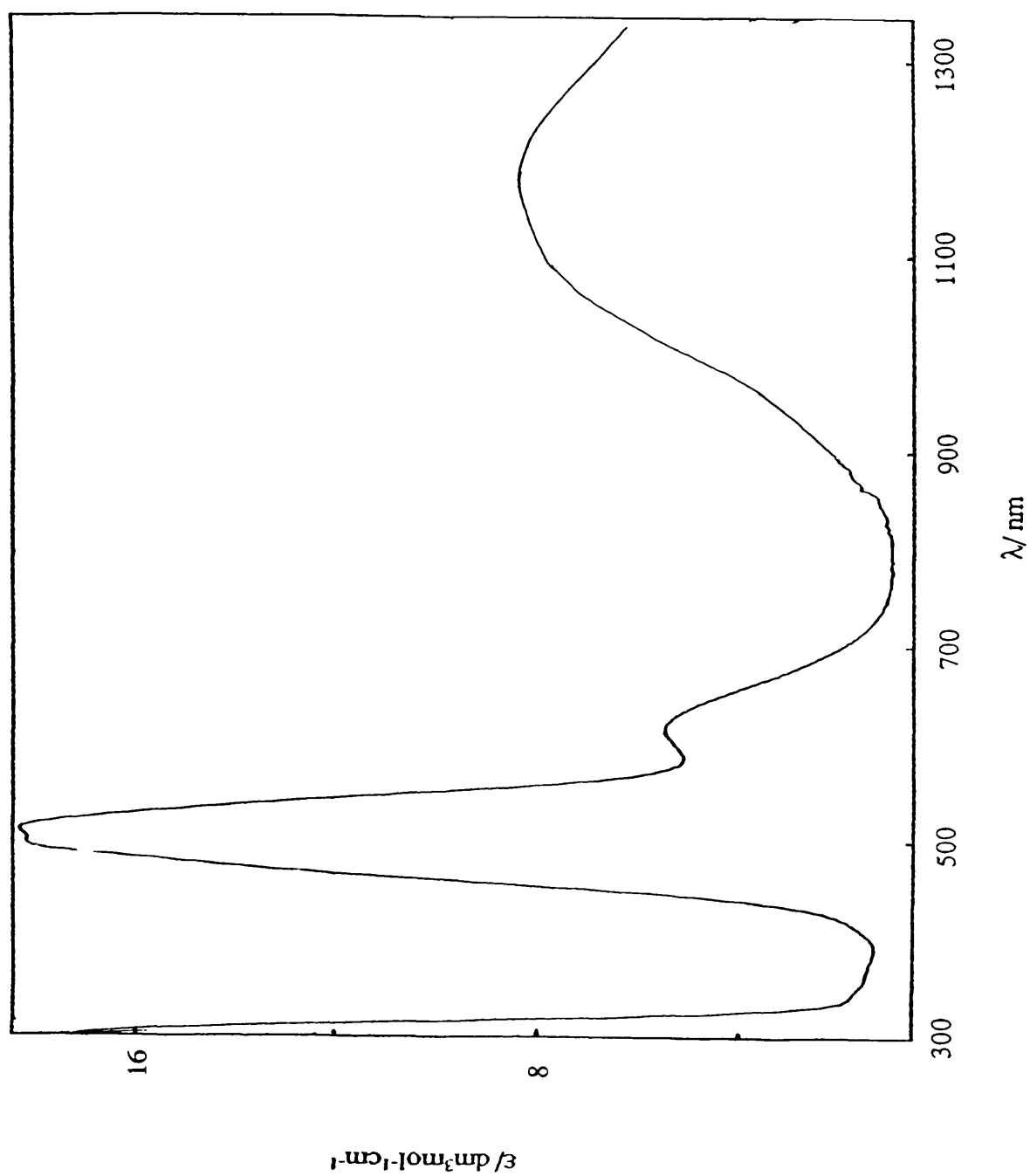
solution.

Fig.4.20(a). *Absorption Spectrum of* [Co(II)L⁸H₃][NO₃]₂ *in water solution.*
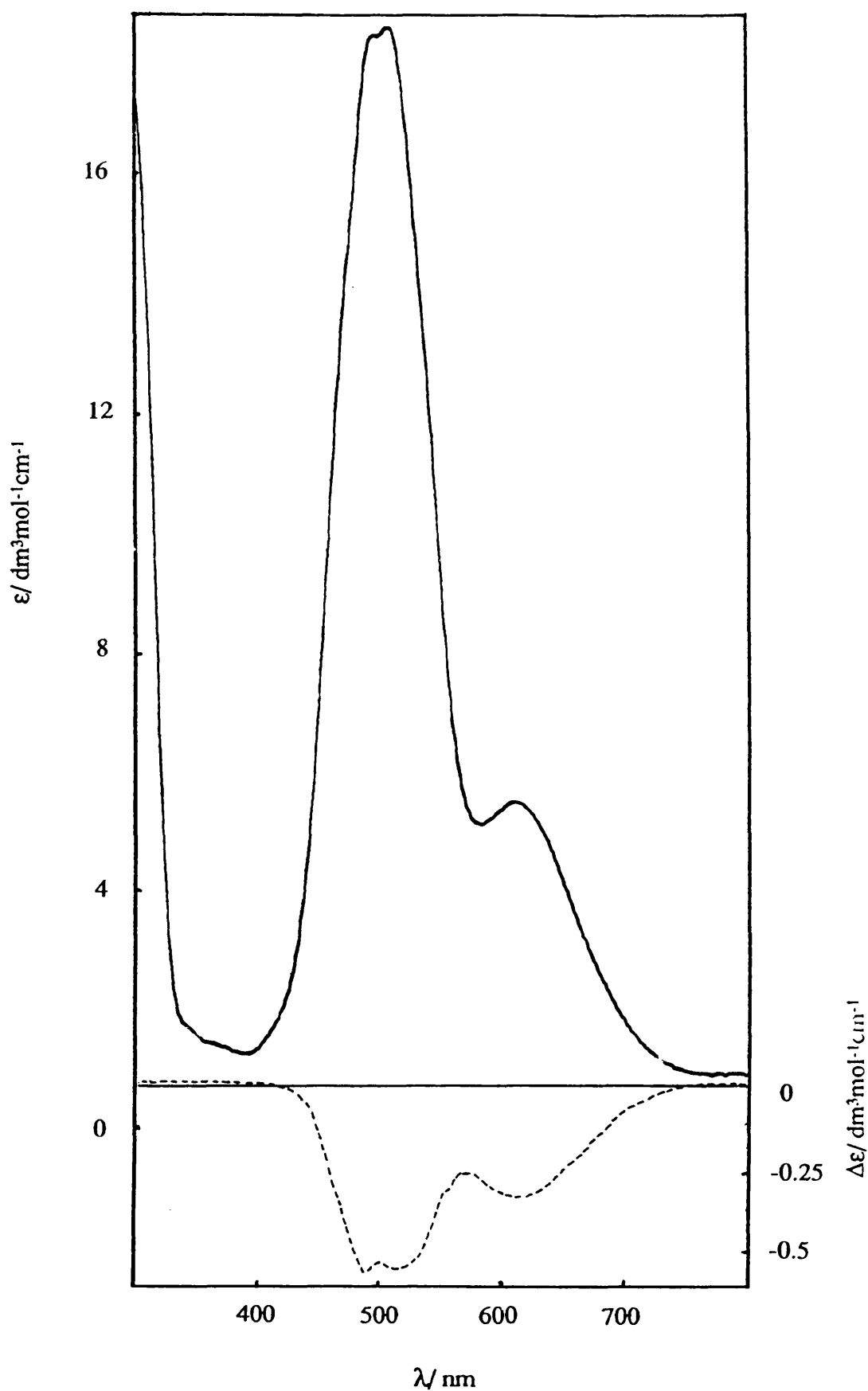
Fig.4.20(b). *Absorption and Circular Dichroism Spectra of* [Co(II)L⁸H₃][NO₃]₂ *in water*
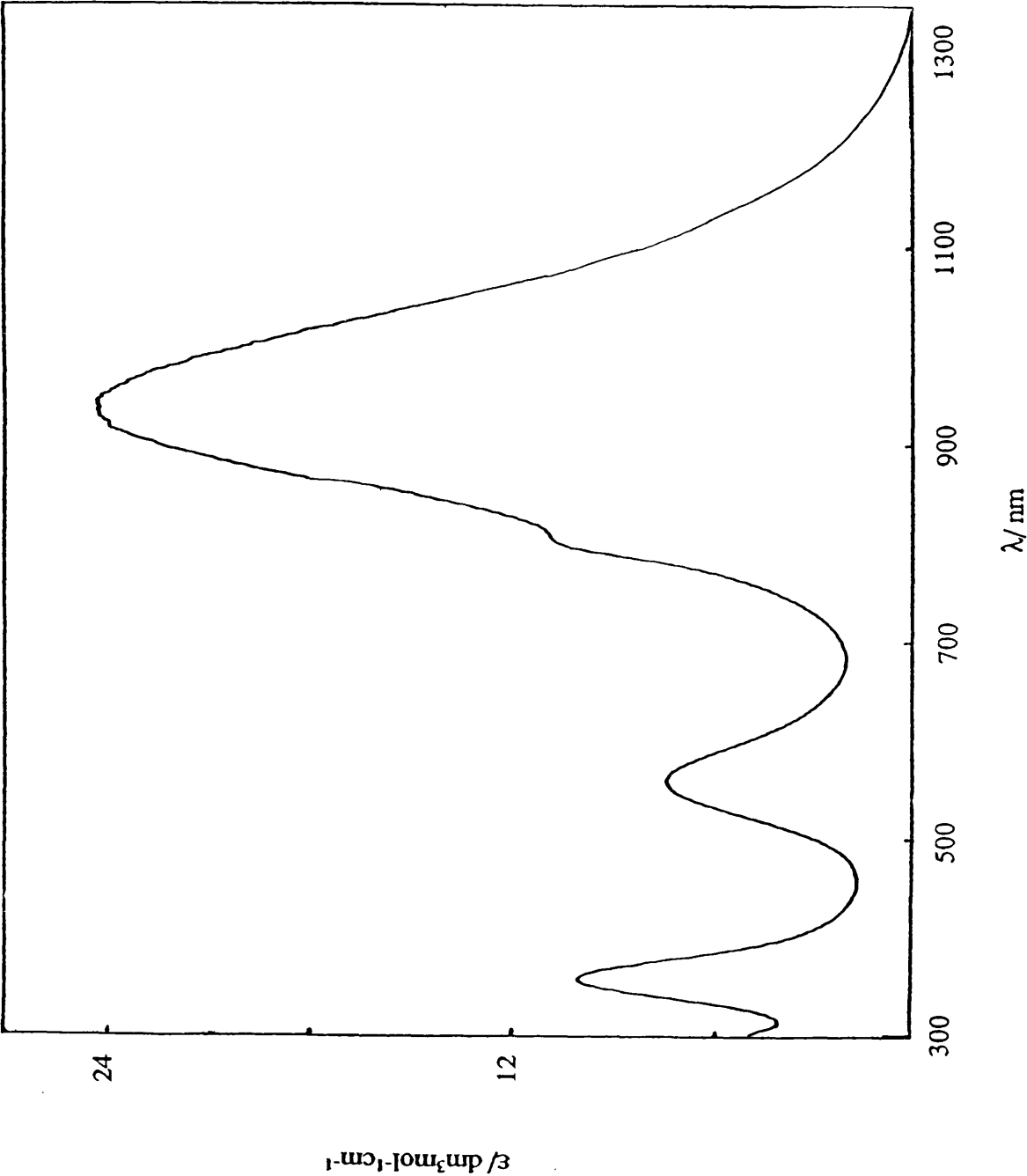
solution.

Fig.4.21. *Absorption Spectrum of* [Ni(II)L¹H₃][Cl]₂.H₂O *in water solution.*

λ/ nm

ε/ dm³mol⁻¹cm⁻¹
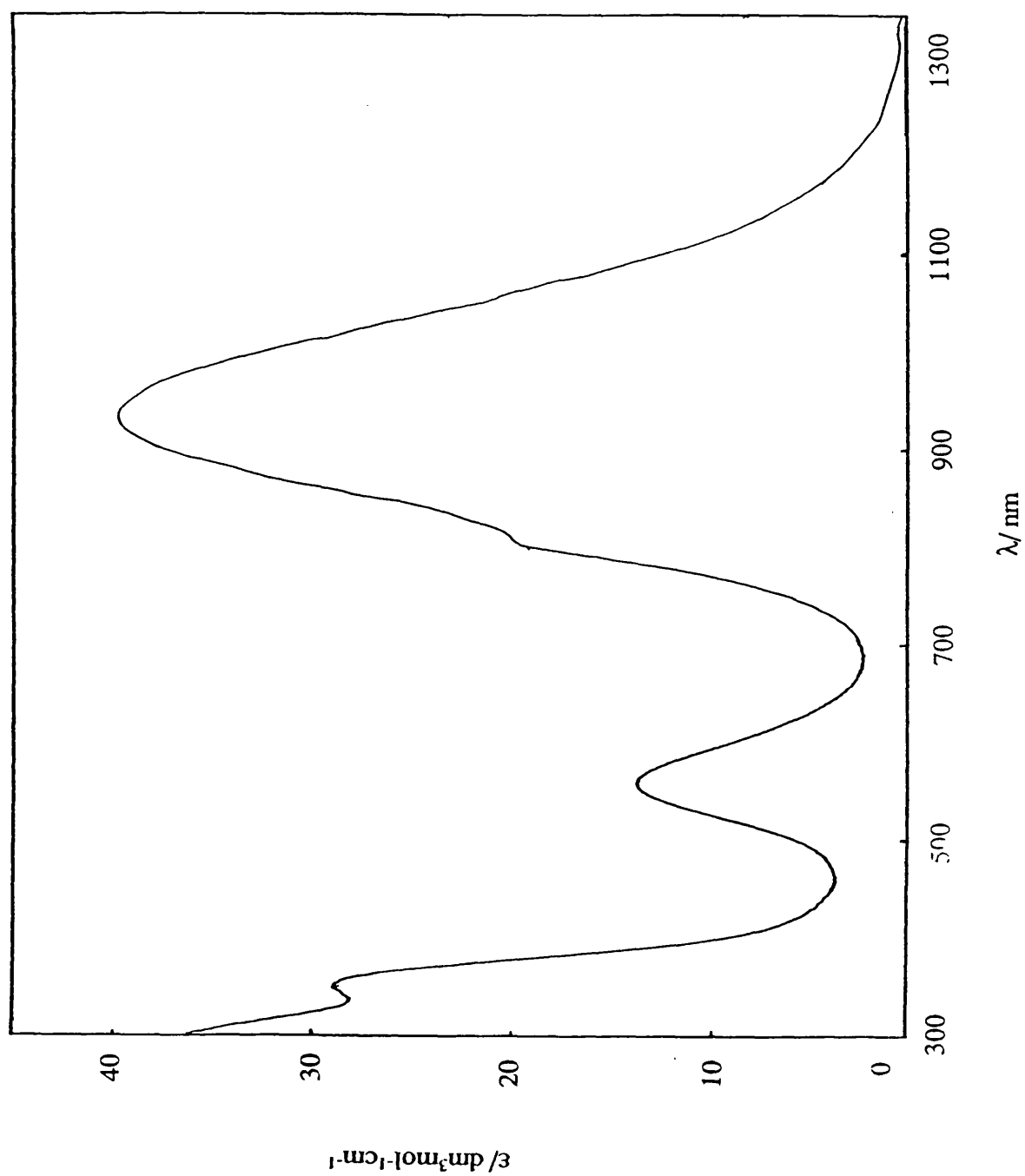
Fig.4.22(a). *Absorption Spectrum of* [Ni(II)L²H₃][NO₃][PF₆].H₂O *in water solution.*
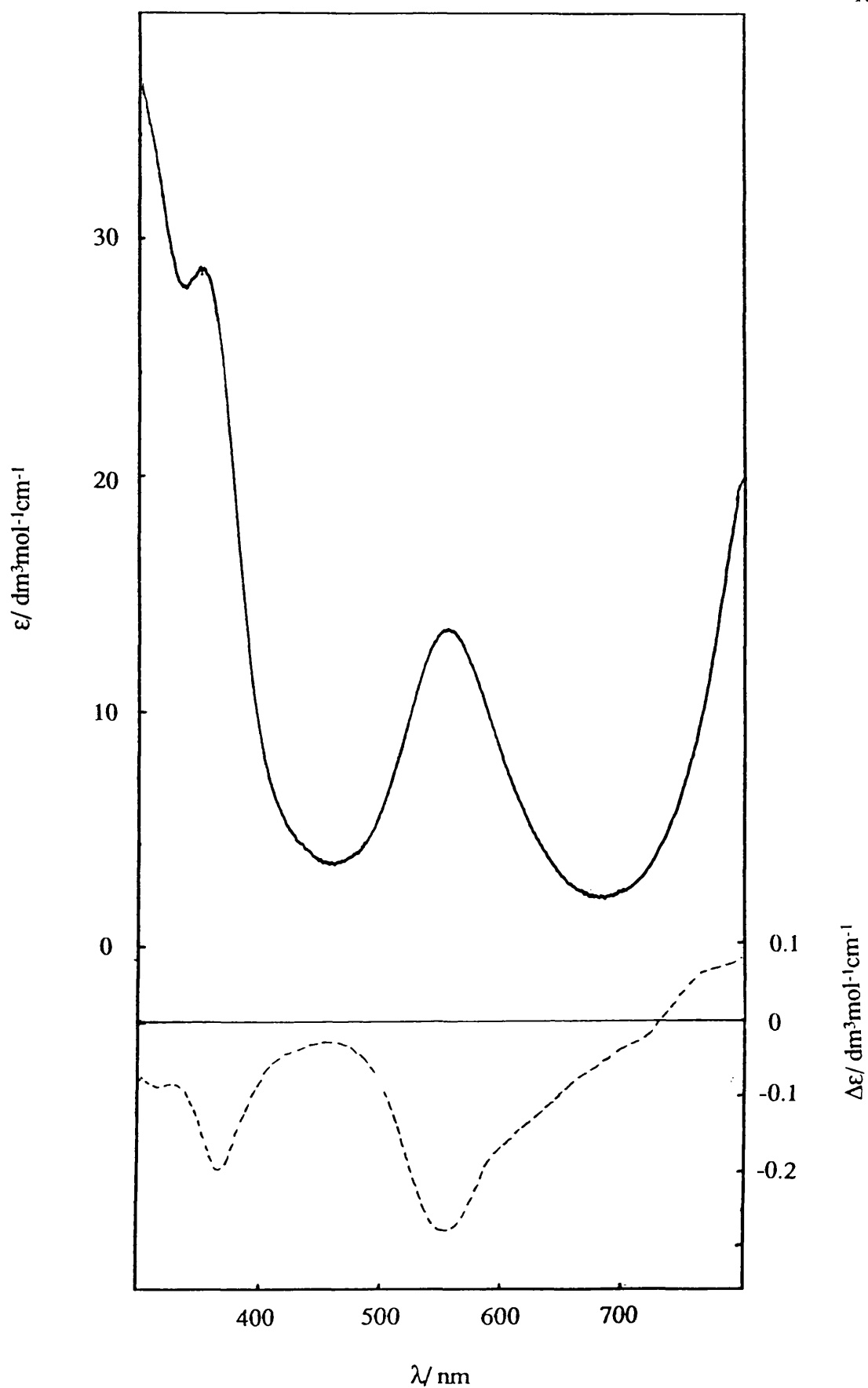
Fig.4.22(b). *Absorption and Circular Dichroism Spectra of* [Ni(II)L²H₃][NO₃][PF₆].H₂O
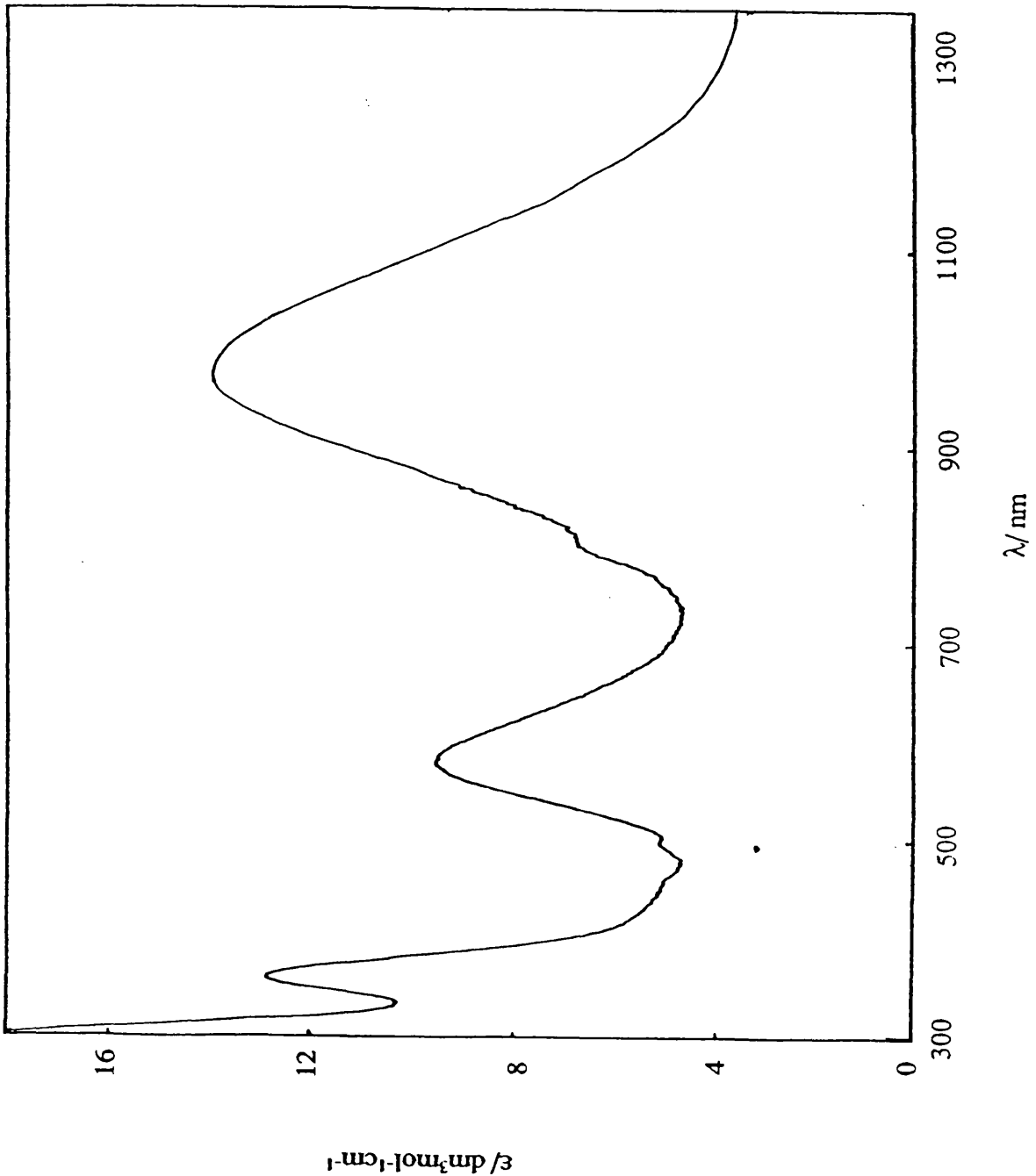
in water solution.

Fig.4.23(a). *Absorption Spectrum of* [Ni(II)L³H₃][PF₆]₂ *in water solution.*
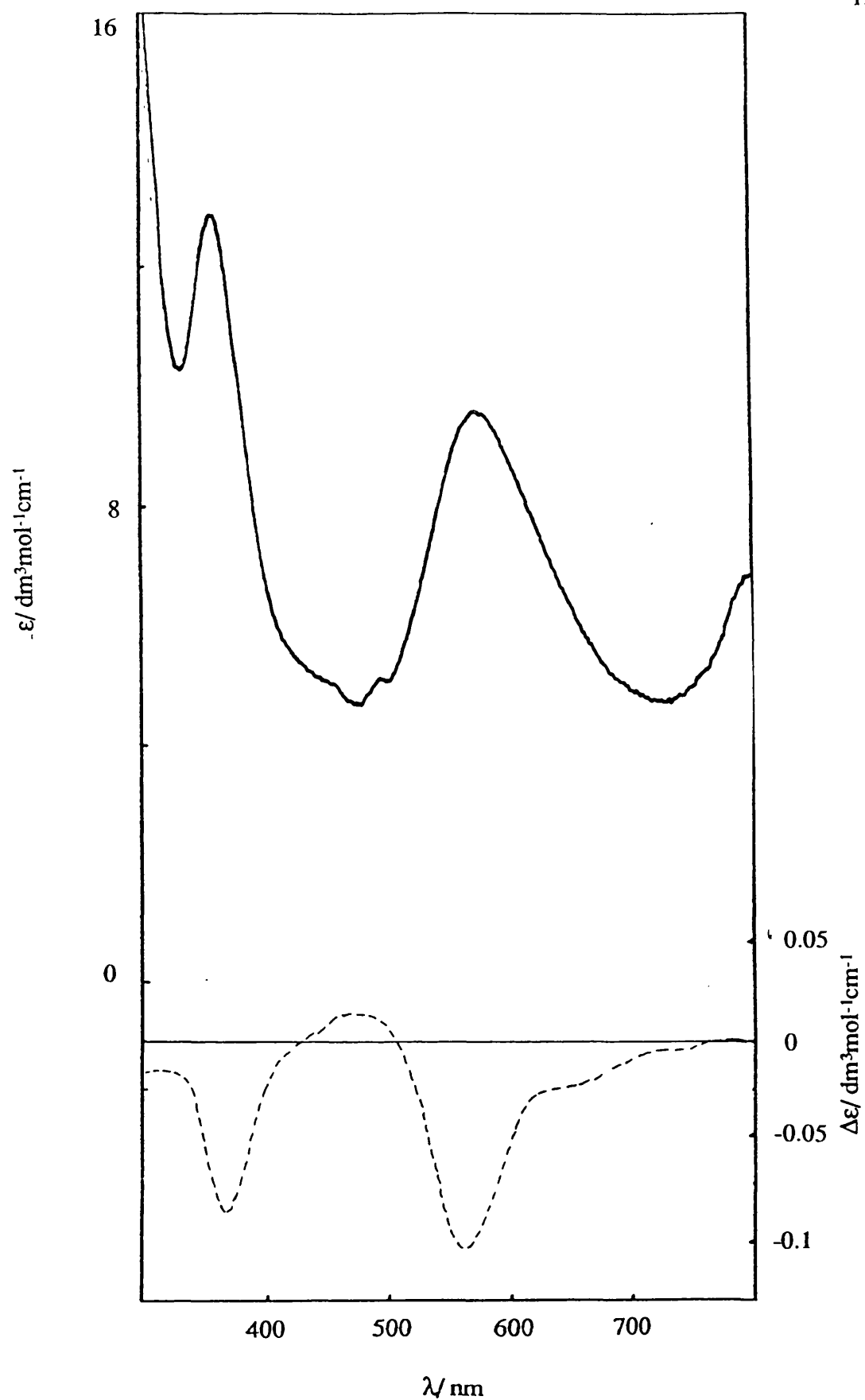
Fig.4.23(b). *Absorption and Circular Dichroism Spectra of* [Ni(II)L³H₃][PF₆]₂ *in*

acetonitrile solution.
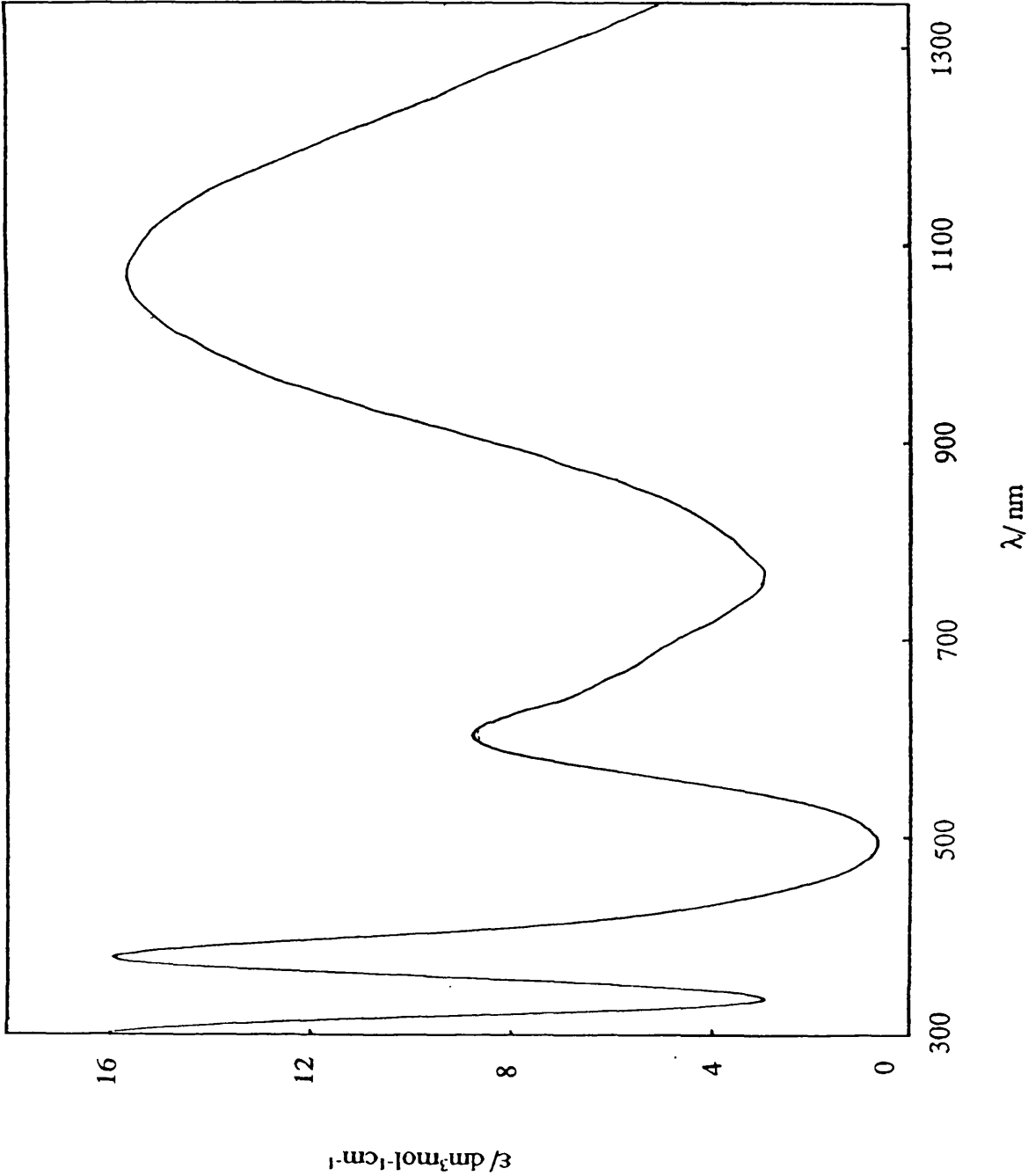
Fig.4.24(a). *Absorption Spectrum of* [Ni(II)L⁴H₃][NO₃]₂ *in water solution.*

λ / nm

$\varepsilon / dm^3 mol^{-1} cm^{-1}$
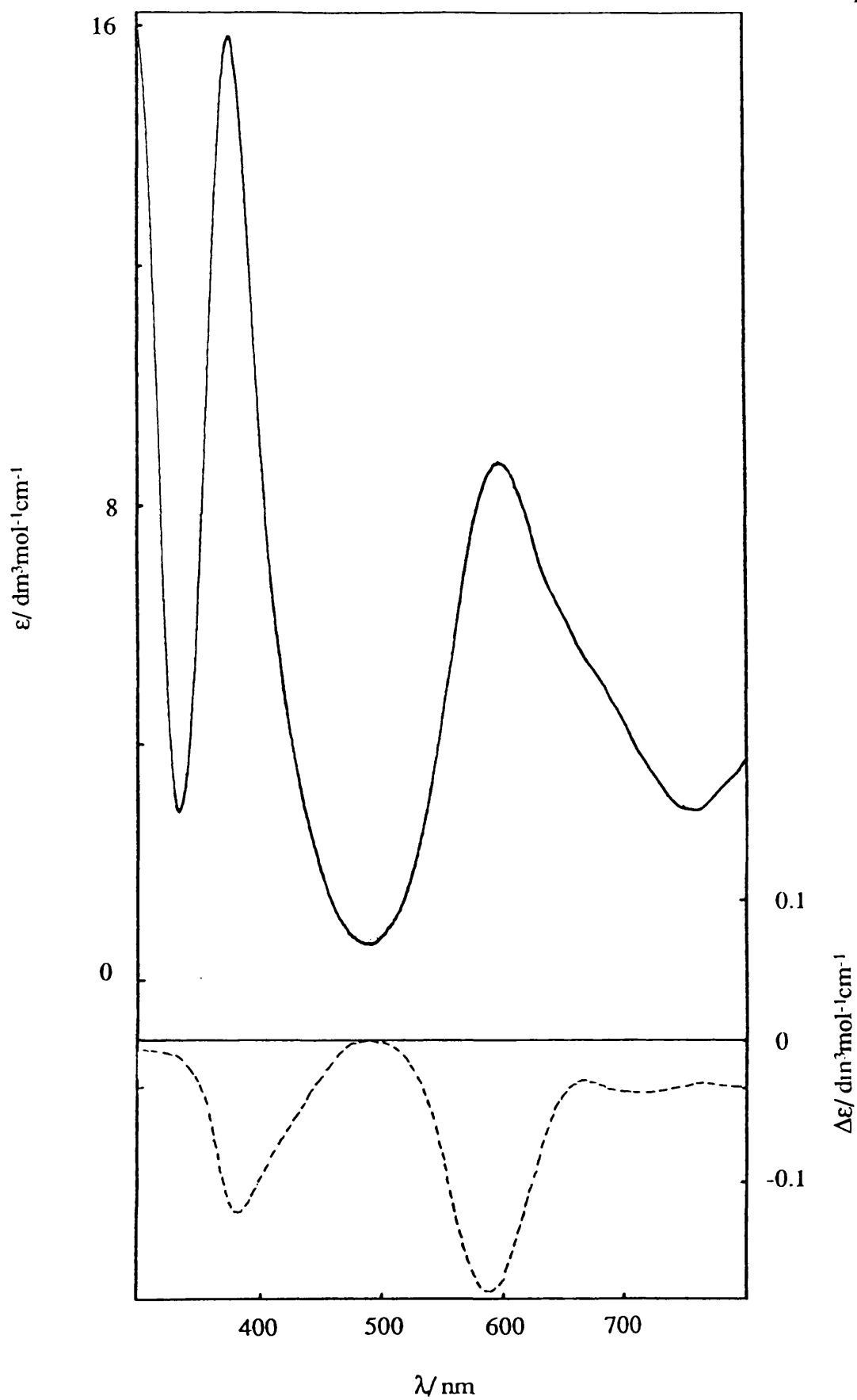
Fig.4.24(b). *Absorption and Circular Dichroism Spectra of* [Ni(II)L⁴H₃][NO₃]₂ *in water*
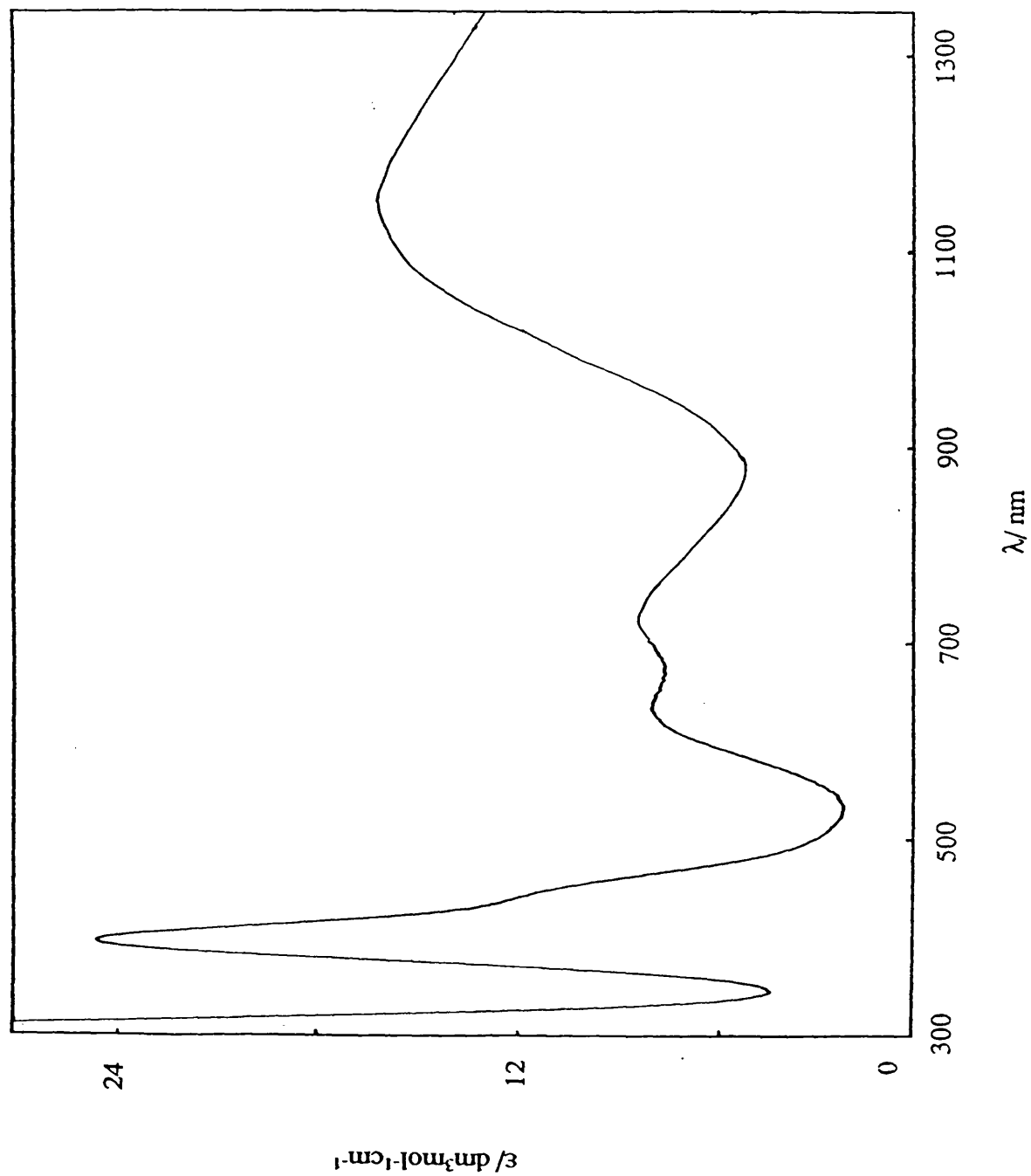
solution.

Fig.4.25(a). *Absorption Spectrum of* [Ni(II)L⁵H₃][NO₃]₂ *in water solution.*

λ/ nm

$\varepsilon/$ dm³mol⁻¹cm⁻¹

300 500 700 900 1100 1300

0 12 24
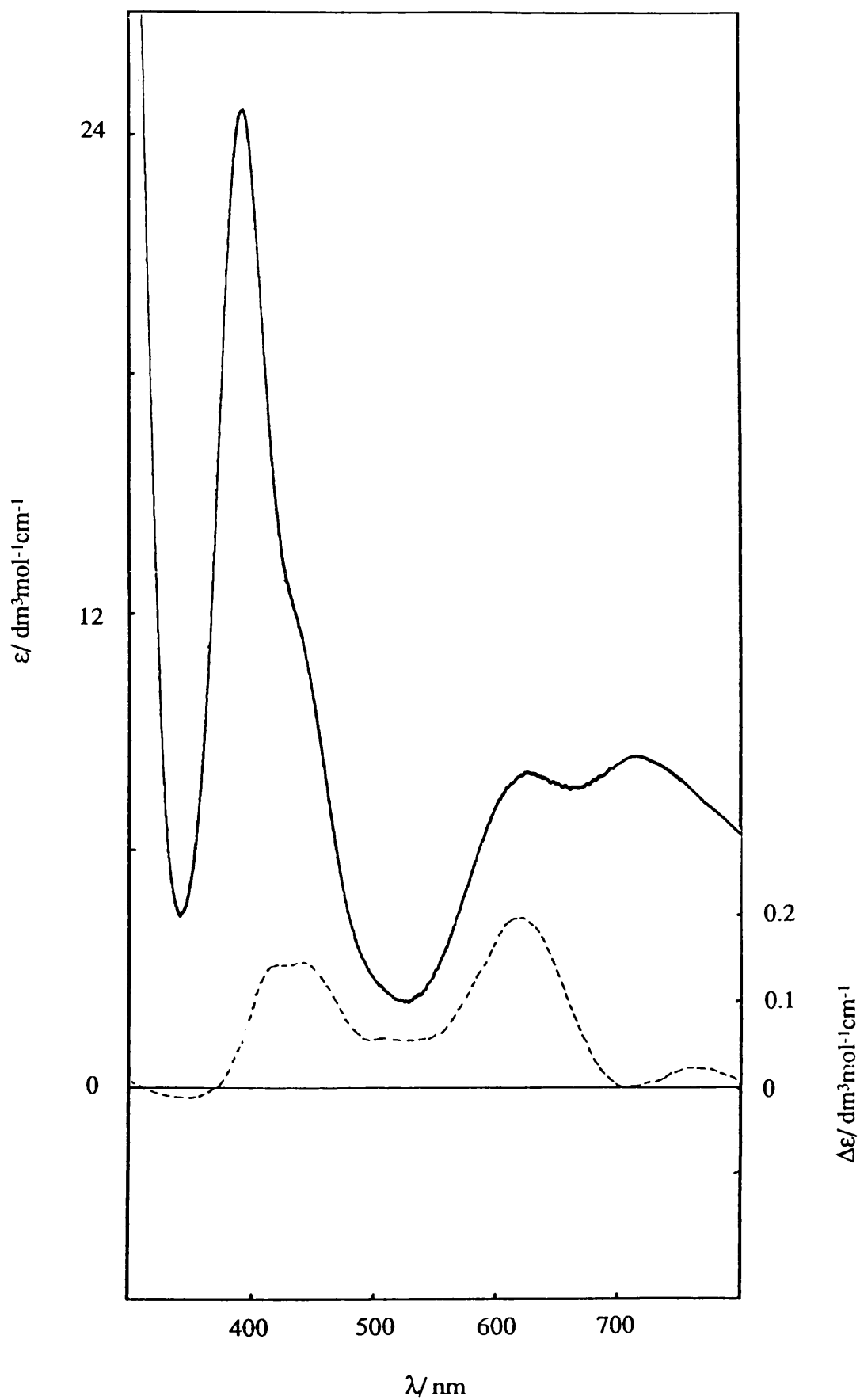
Fig.4.25(b). *Absorption and Circular Dichroism Spectra of* [Ni(II)L⁵H₃][NO₃]₂ *in water*
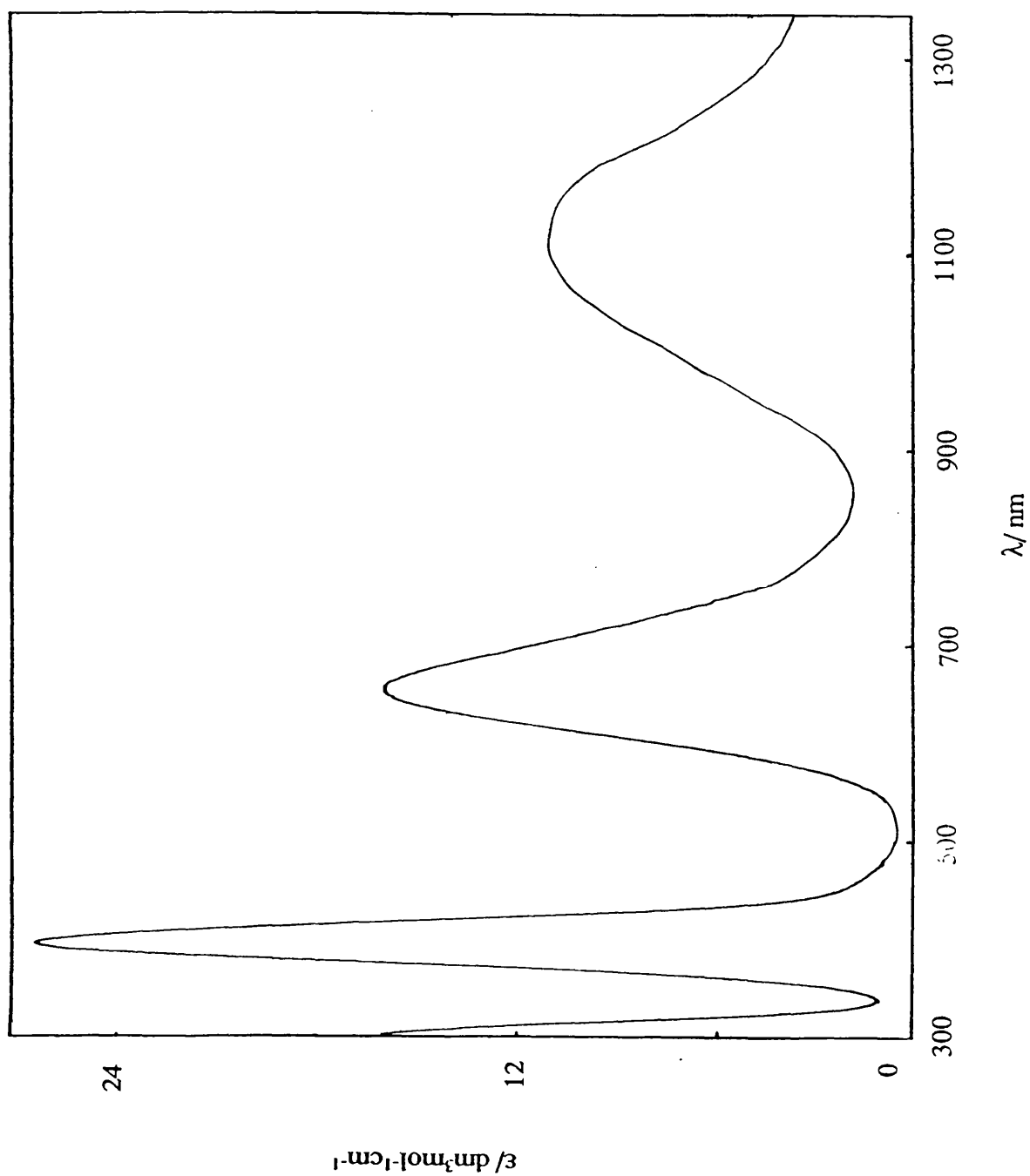
solution.

Fig.4.26(a). *Absorption Spectrum of* [Ni(II)L^{7}H$_3$][NO$_3$]$_2$ *in water solution.*
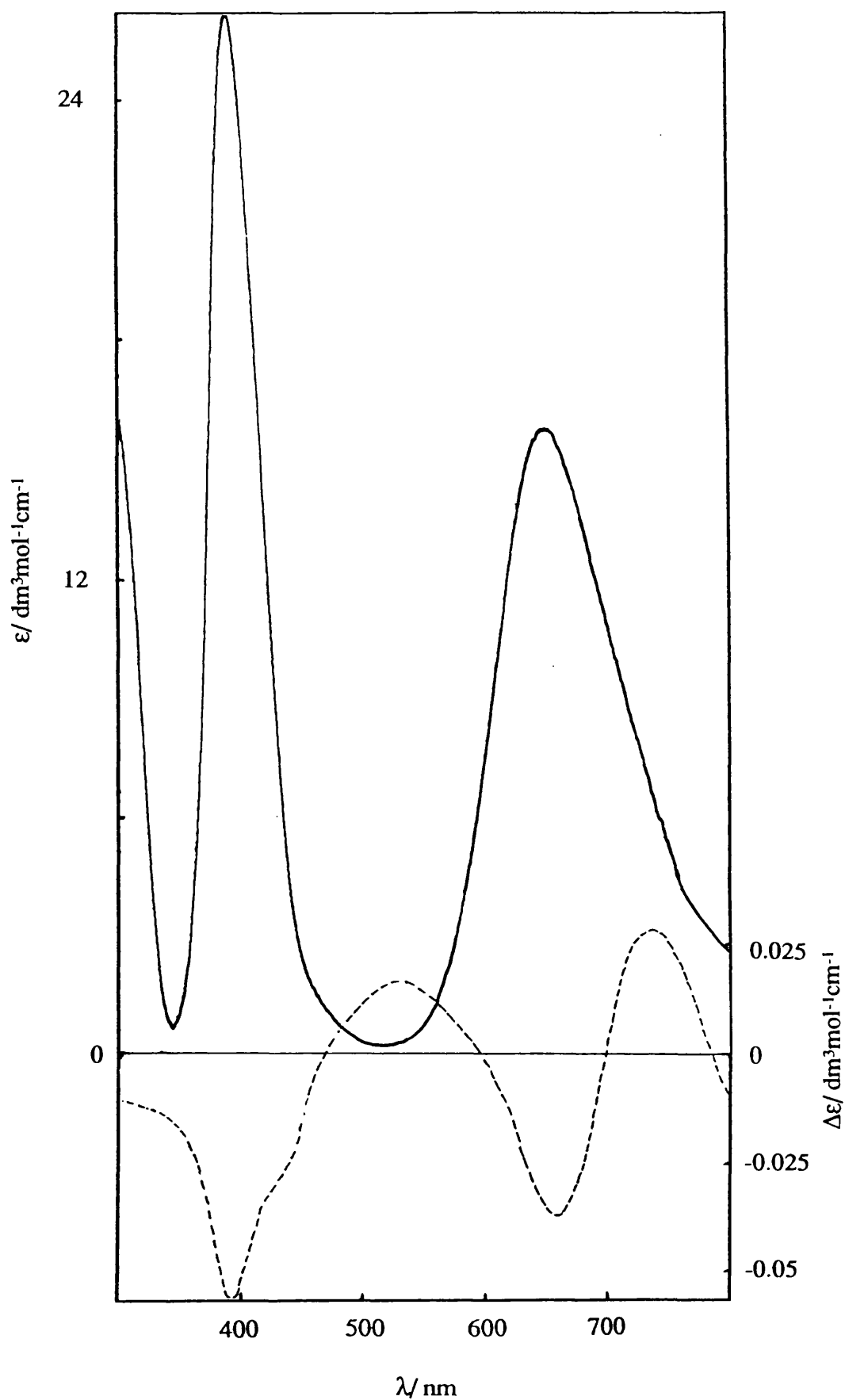
Fig.4.26(b). *Absorption and Circular Dichroism Spectra of* [Ni(II)L⁷H₃][NO₃]₂ *in water*
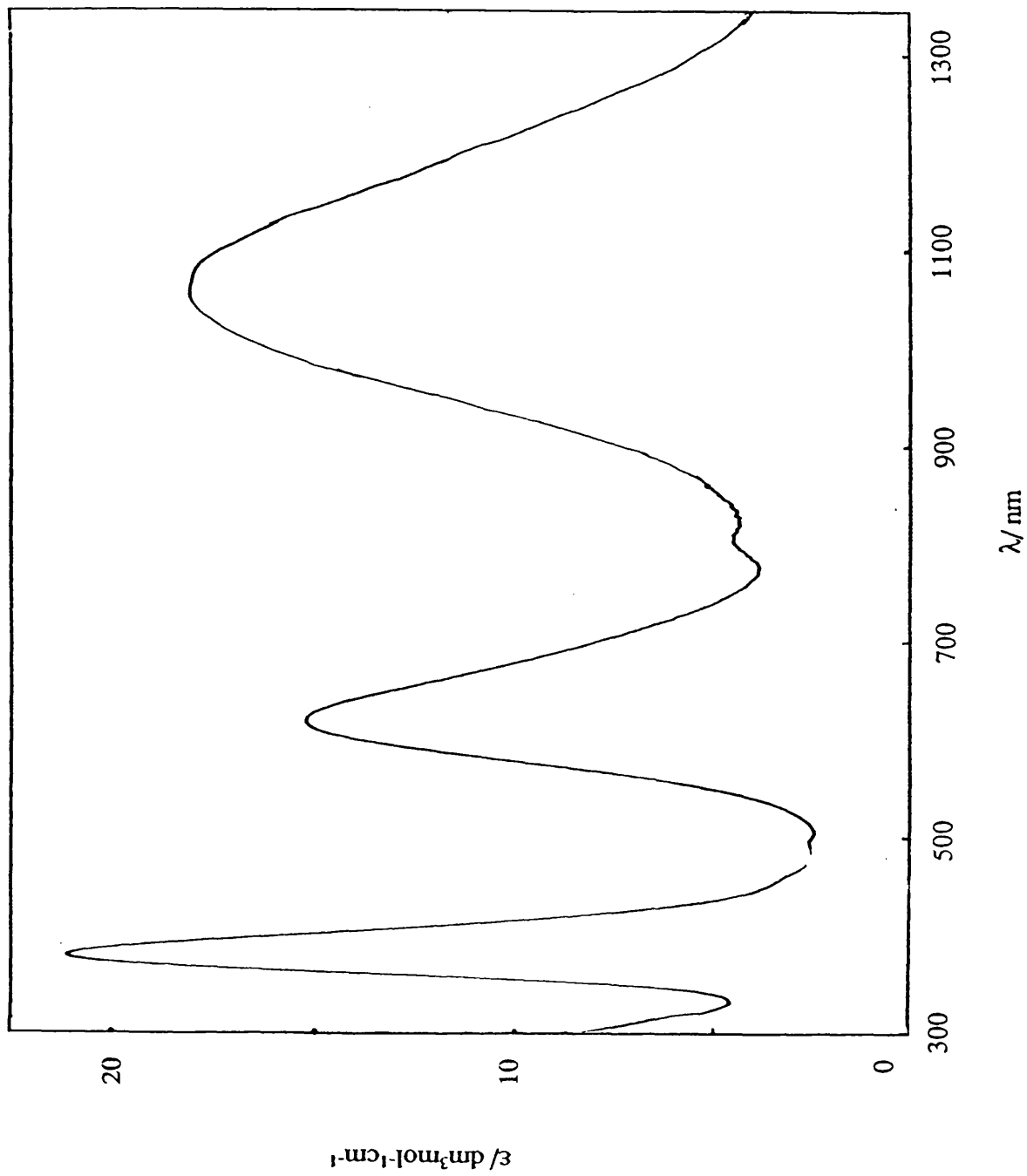
solution.

Fig.4.27(a). *Absorption Spectrum of [Ni(II)L⁸H₃][NO₃]₂ in water solution.*
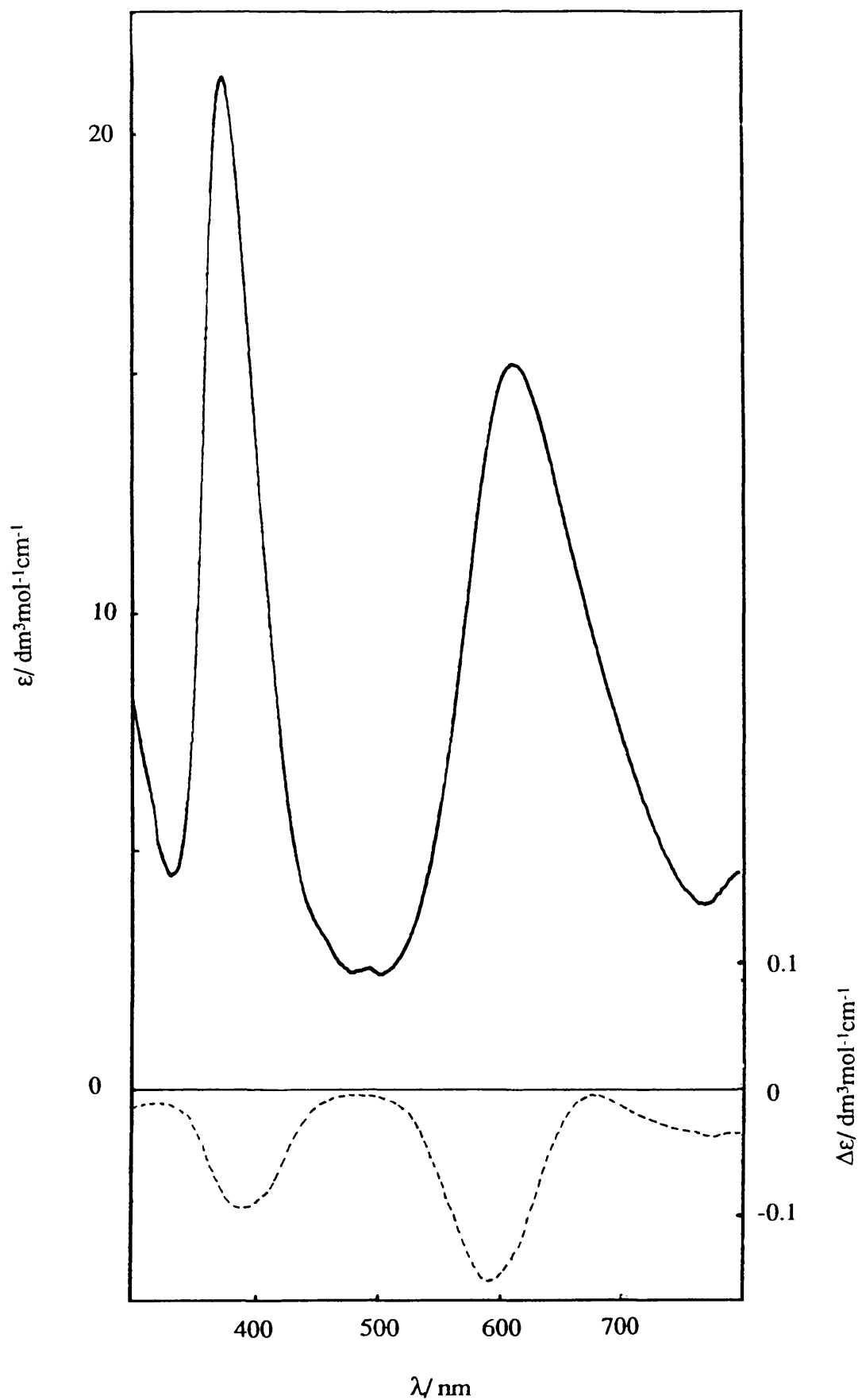
Fig.4.27(b). *Absorption and Circular Dichroism Spectra of* [Ni(II)L⁸H₃][NO₃]₂ *in water*

solution.

Fig.4.28(a). *Absorption Spectrum of [Ni(II)L⁹H₃][NO₃]₂ in water solution.*
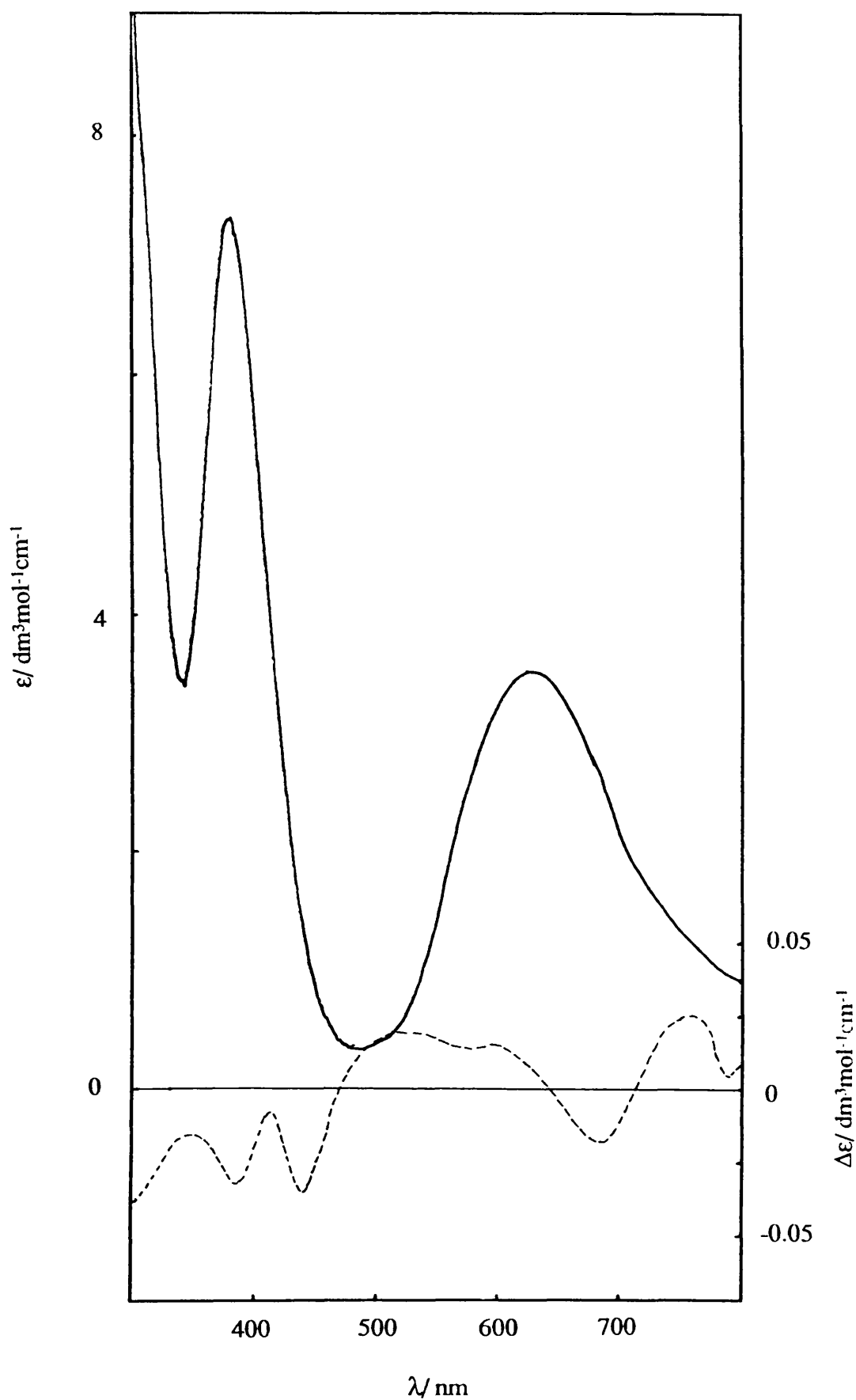
Fig.4.28(b). *Absorption and Circular Dichroism Spectra of* [Ni(II)L⁹H₃][NO₃]₂ *in water*
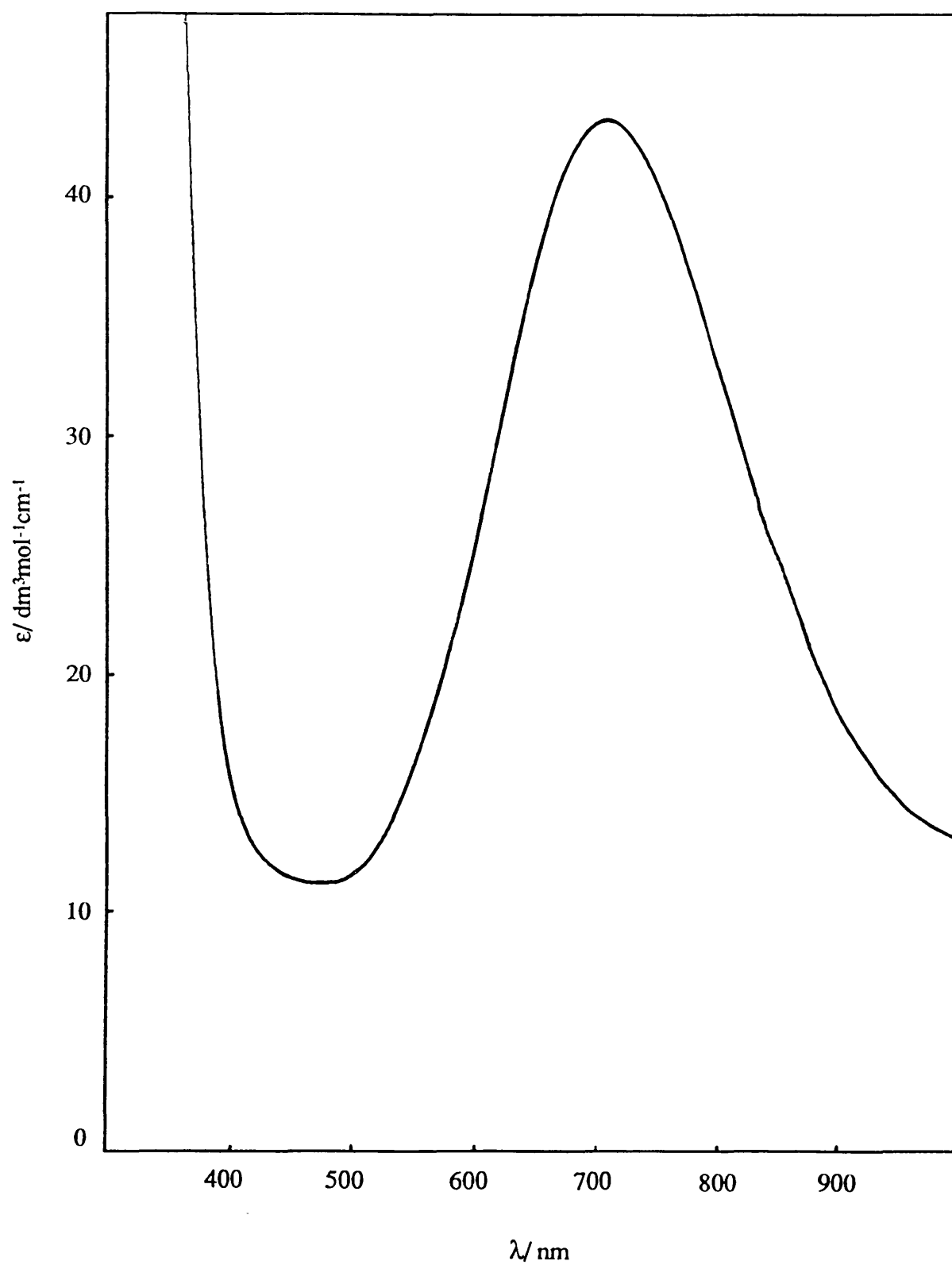
solution.

Fig.29. *Absorption Spectrum of* [Cu(II)L¹H₃][PF₆]₂ *in acetonitrile solution.*
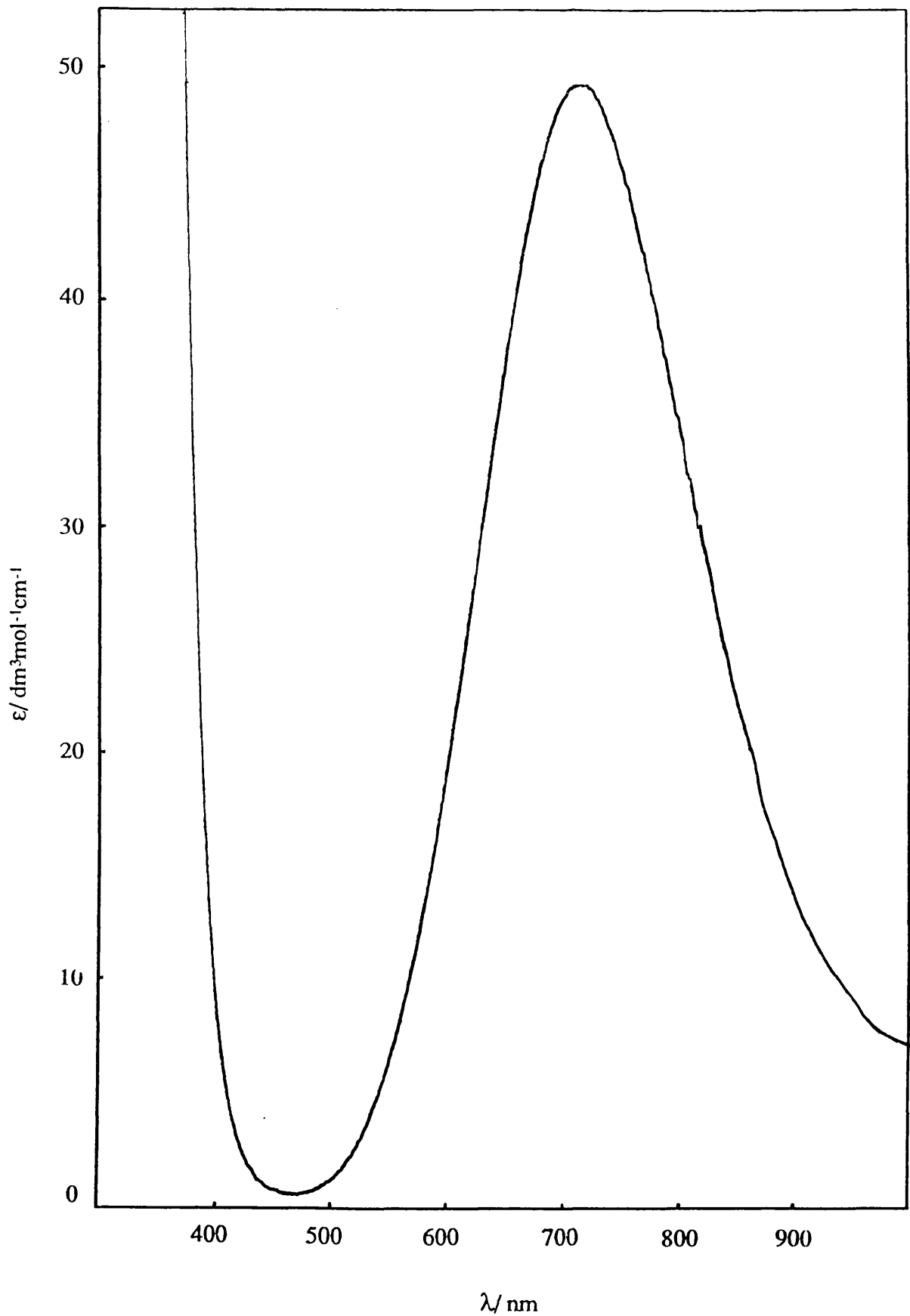
Fig.30(a). *Absorption Spectrum of* [Cu(II)L²H₃][PF₆]₂ *in acetonitrile solution.*
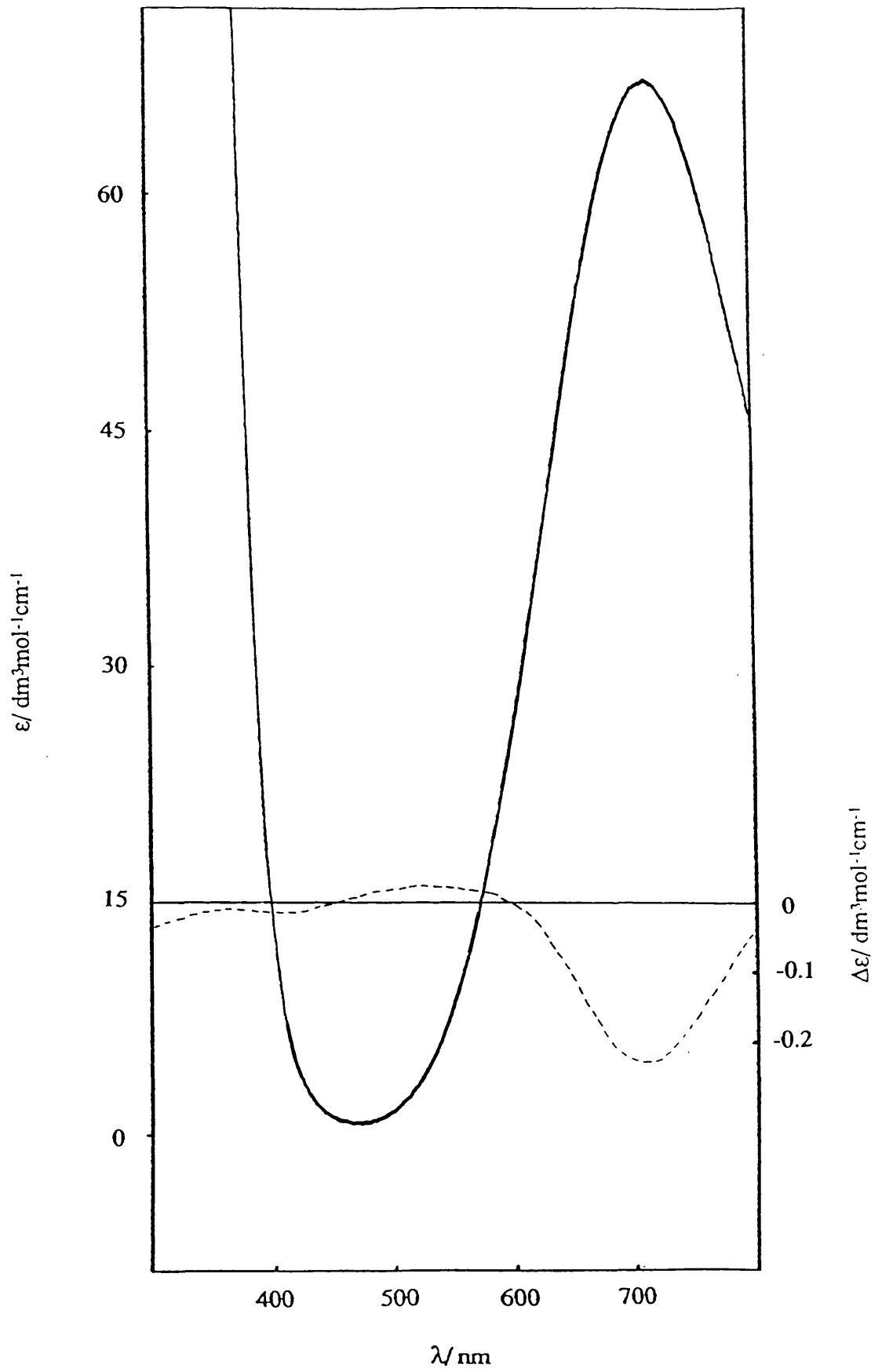
Fig.4.30(b). *Absorption and Circular Dichroism Spectra of* [Cu(II)L²H₃][PF₆]₂ *in*

acetonitrile solution.
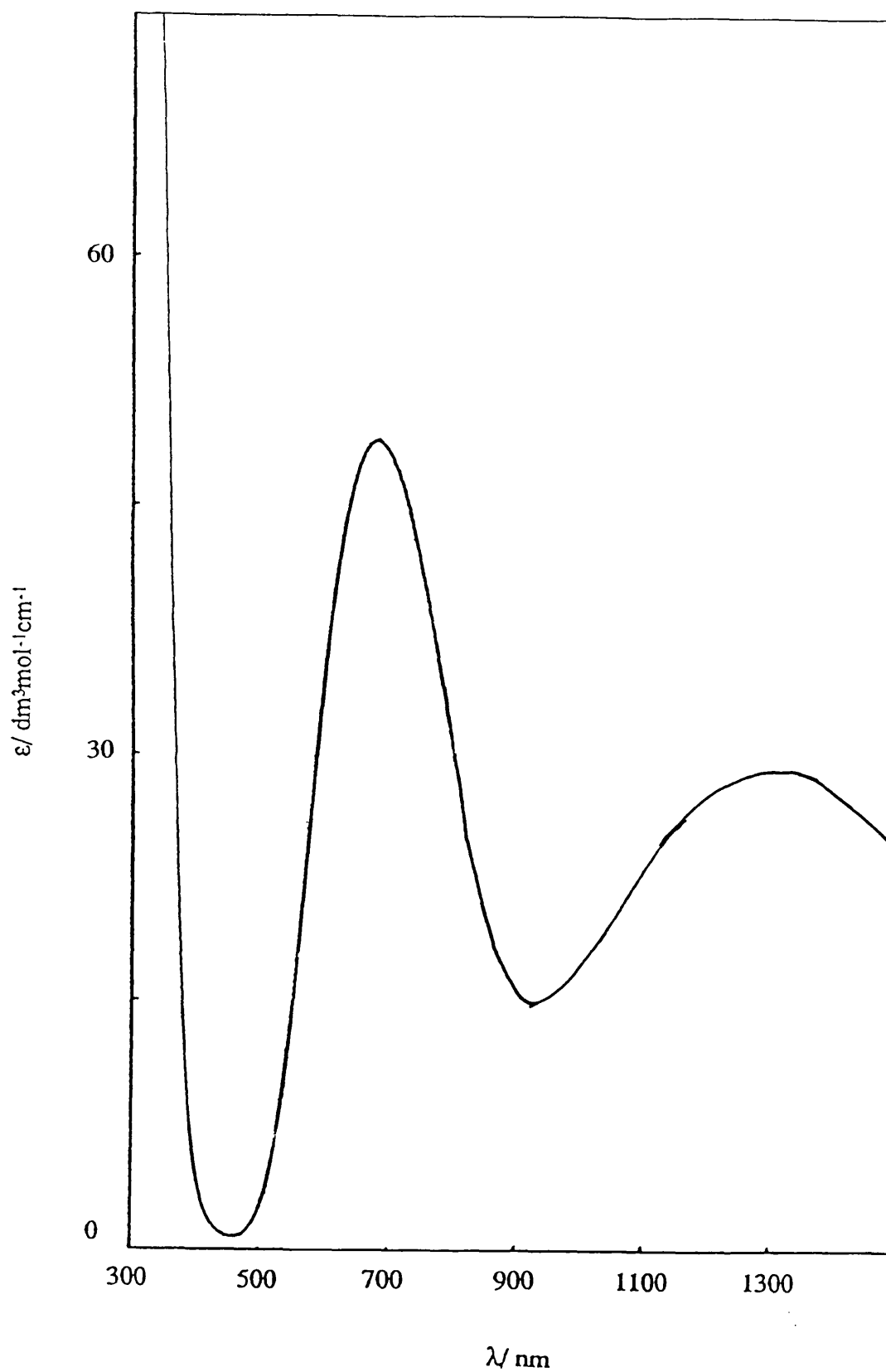
Fig.31(a). *Absorption Spectrum of* [Cu(II)L³H₃][PF₆]₂ *in acetonitrile solution.*
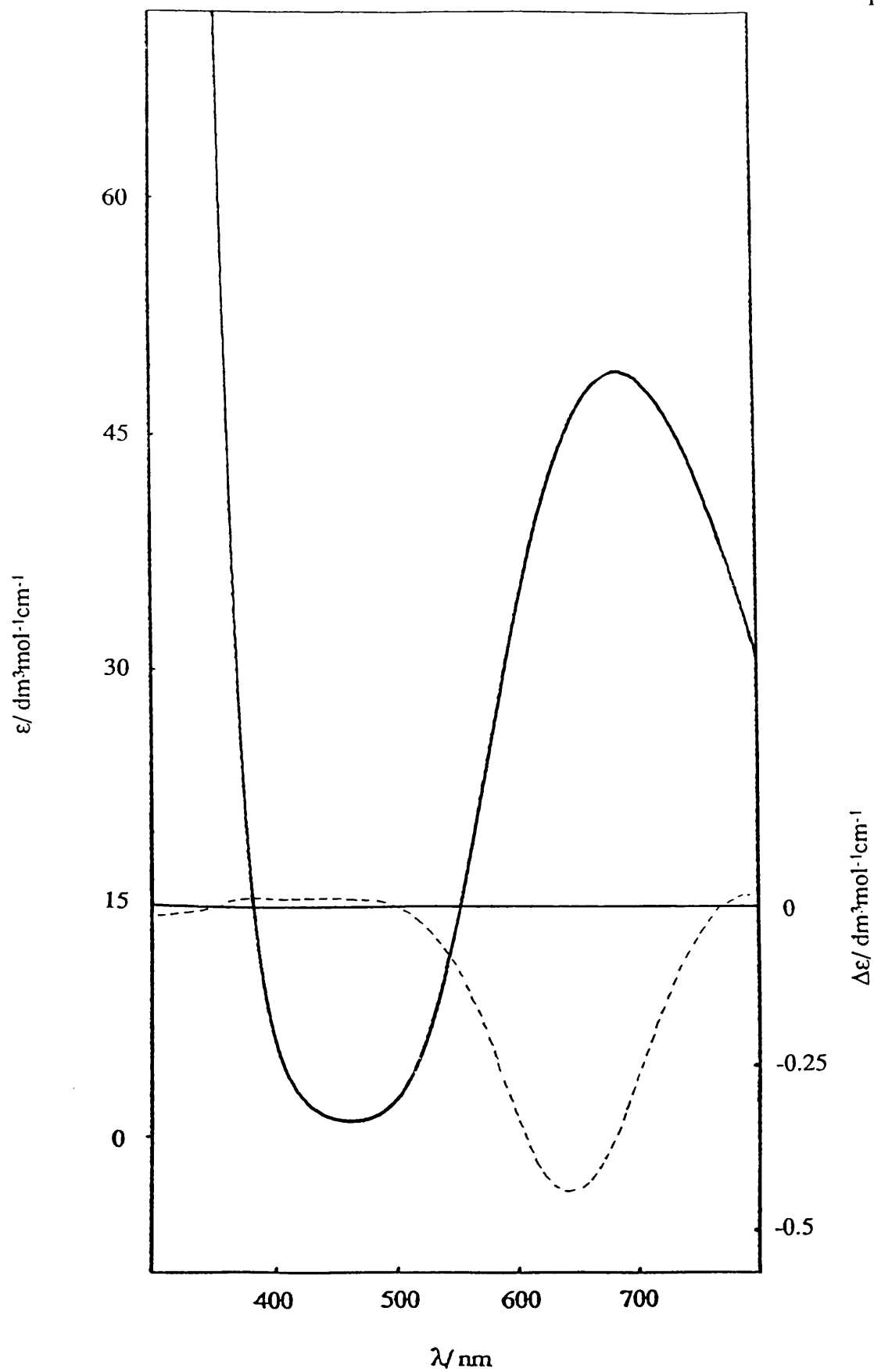
Fig.4.31(b). *Absorption and Circular Dichroism Spectra of* [Cu(II)L³H₃][PF₆]₂ *in*

acetonitrile solution.
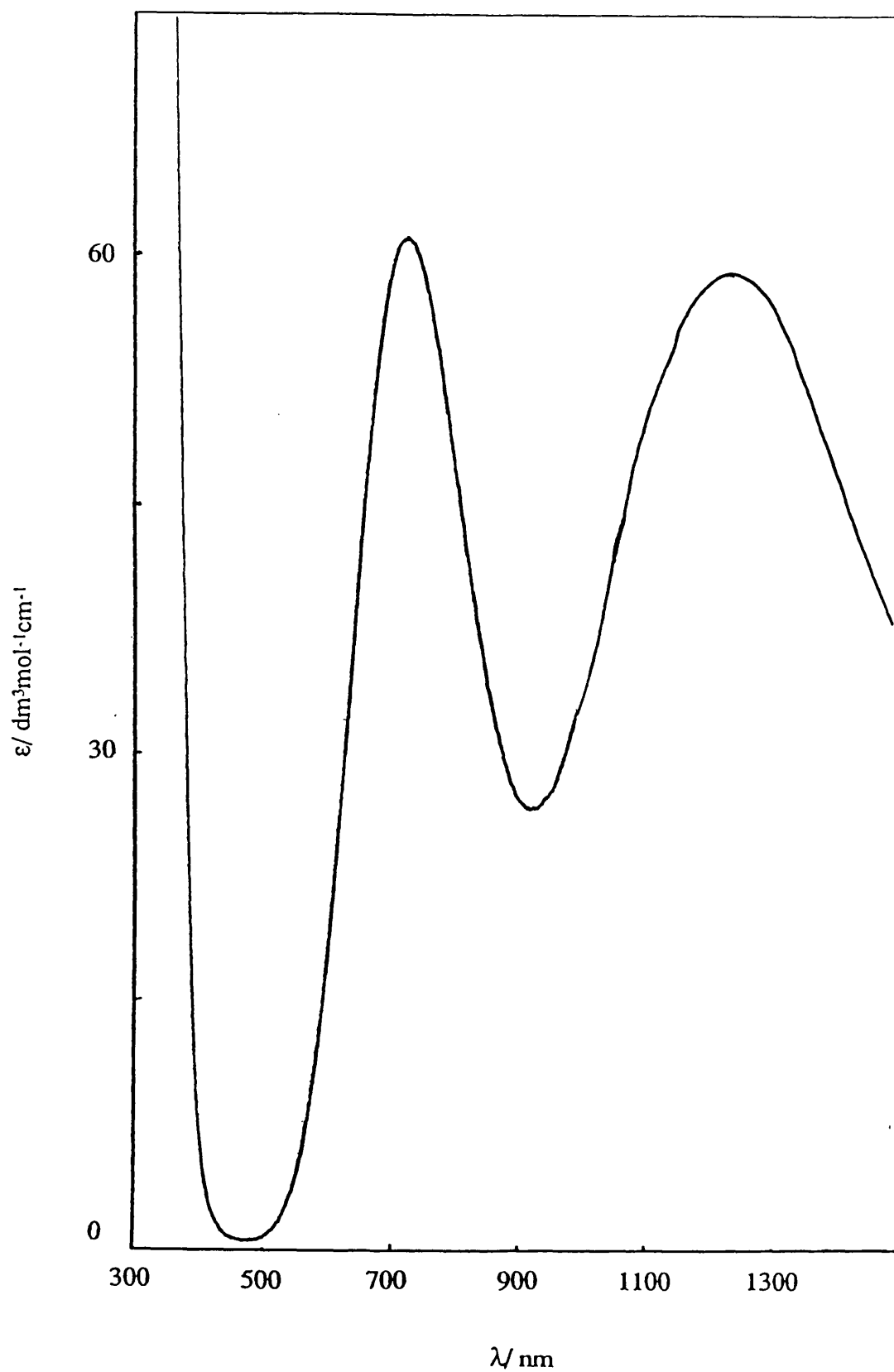
Fig.32(a). *Absorption Spectrum of* $[Cu(II)L^4H_3][PF_6]_2$ *in acetonitrile solution.*
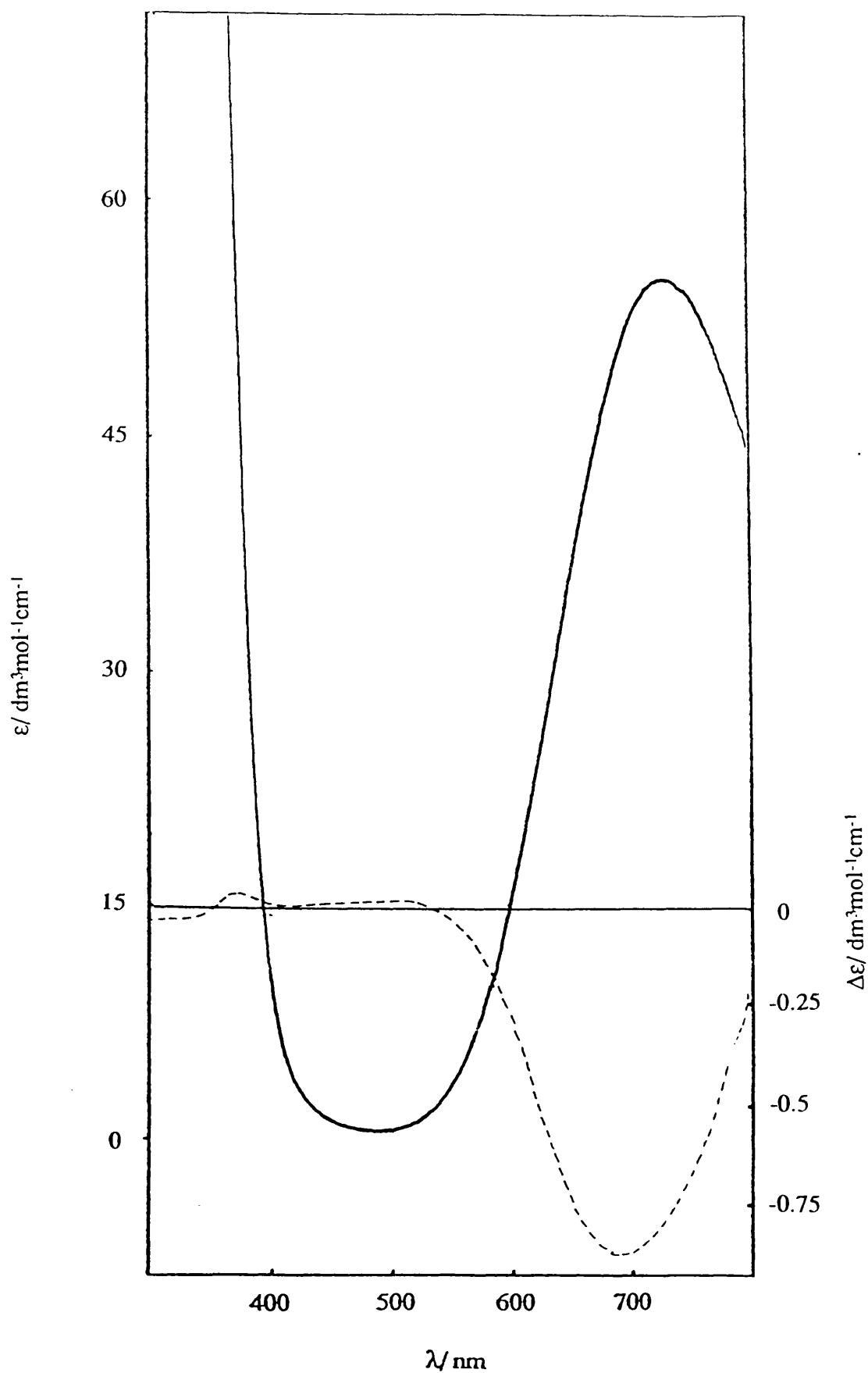
Fig.4.32(b). *Absorption and Circular Dichroism Spectra of* [Cu(II)L⁴H₃][PF₆]₂ *in*

acetonitrile solution.
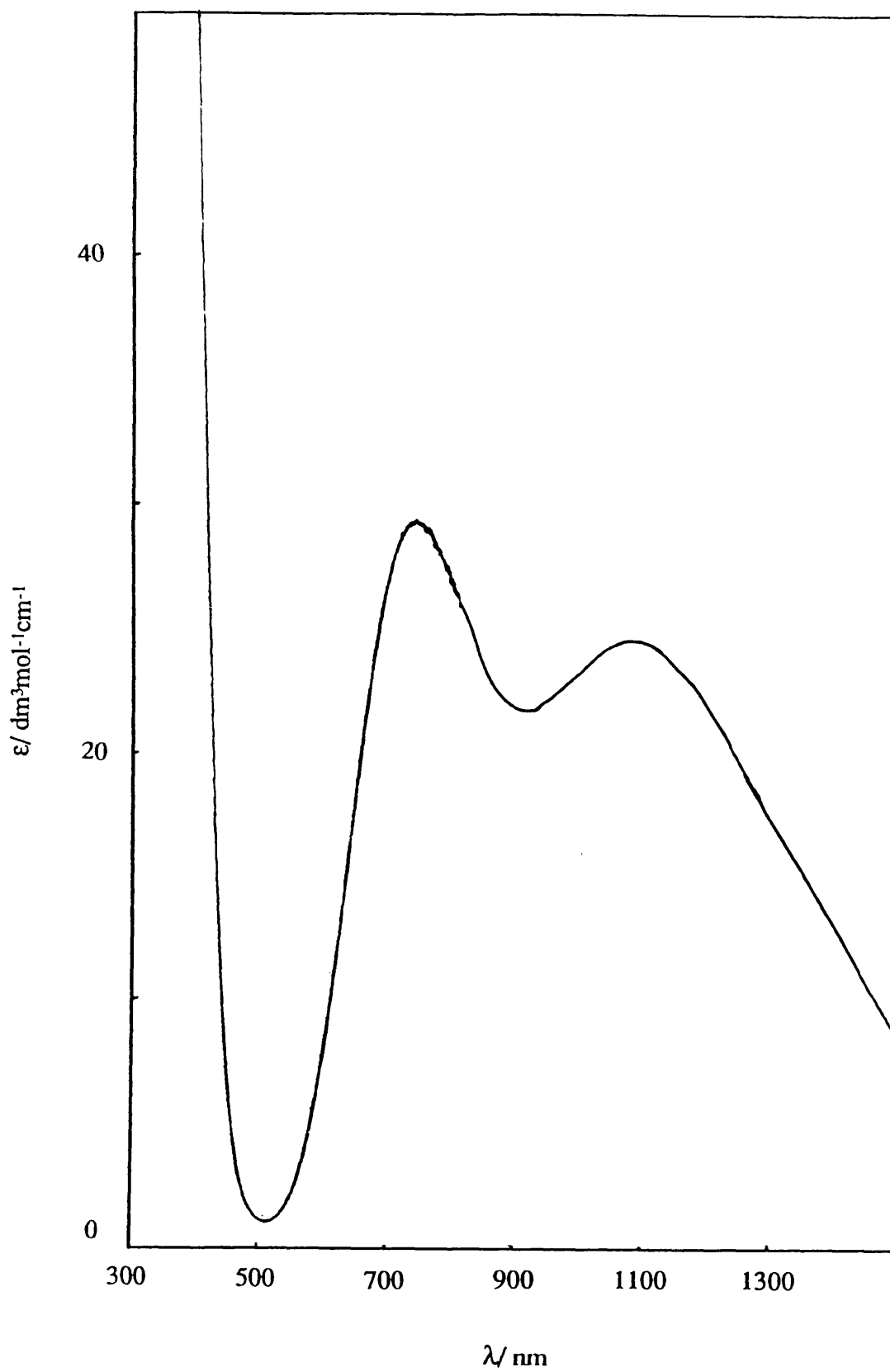
Fig.33(a). *Absorption Spectrum of* $[Cu(II)L^5H_3][PF_6]_2$ *in acetonitrile solution.*
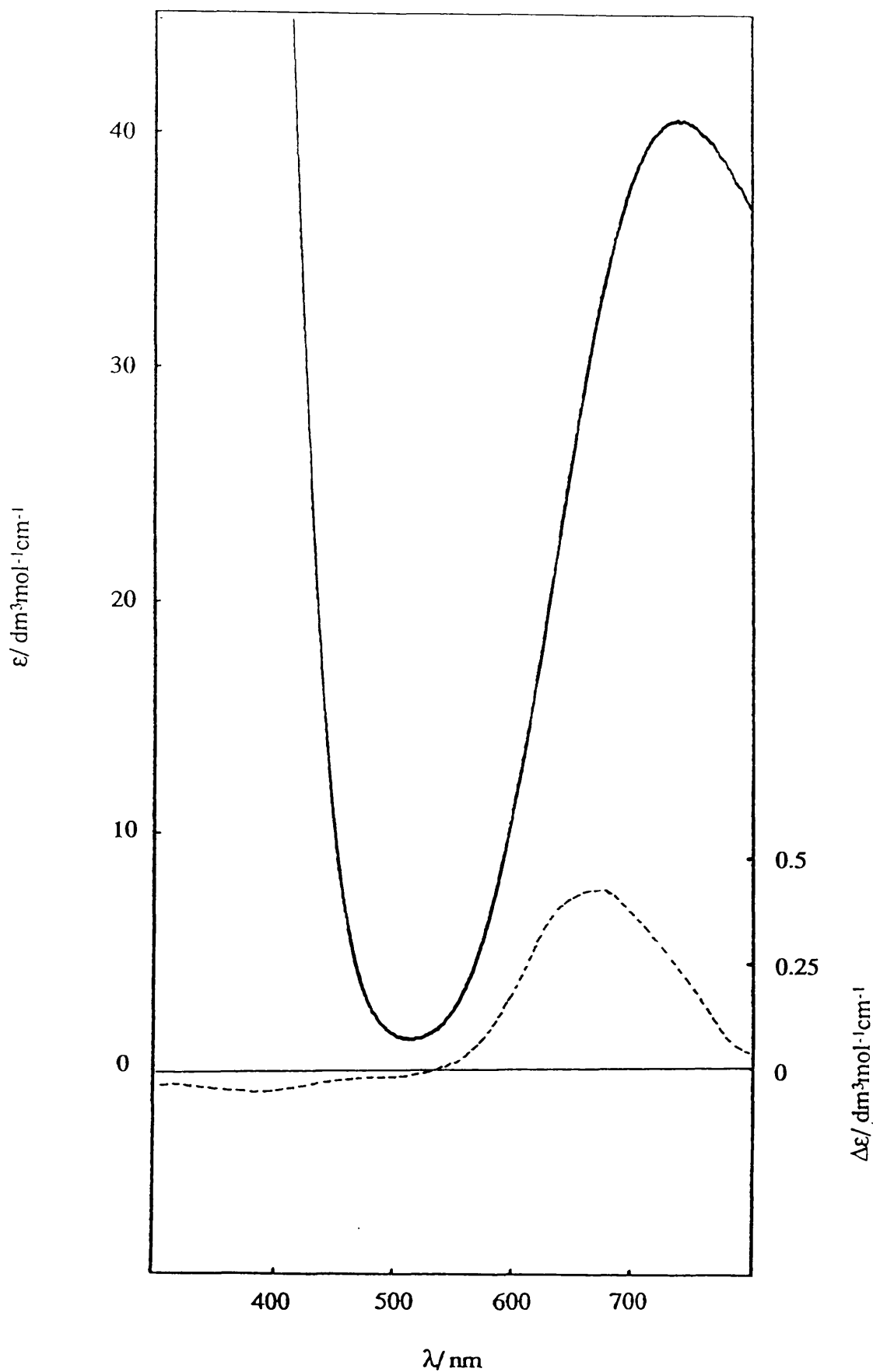
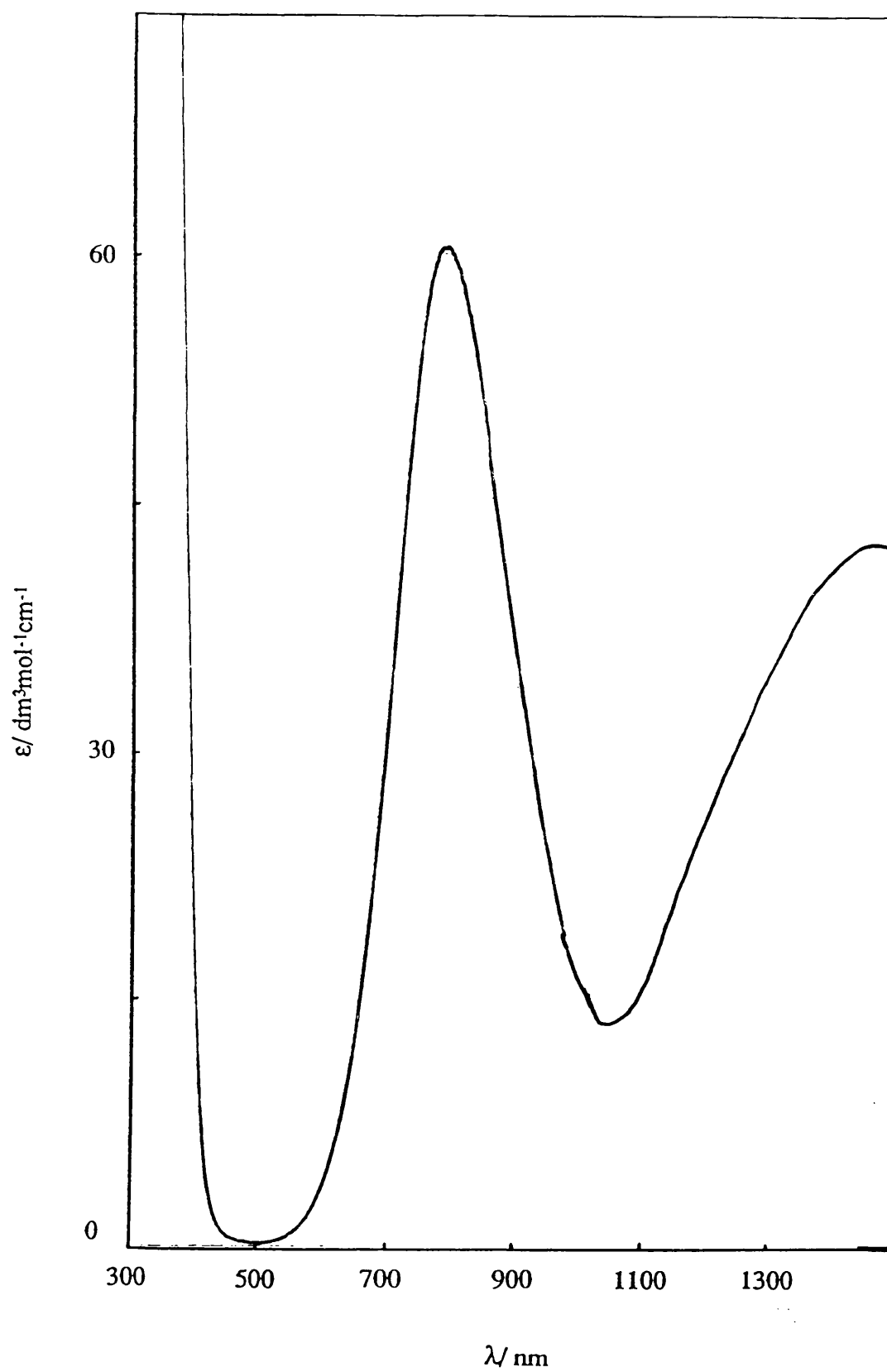**Fig.4.33(b).** *Absorption and Circular Dichroism Spectra of* [Cu(II)L⁵H₃][PF₆]₂ *in*

acetonitrile solution.

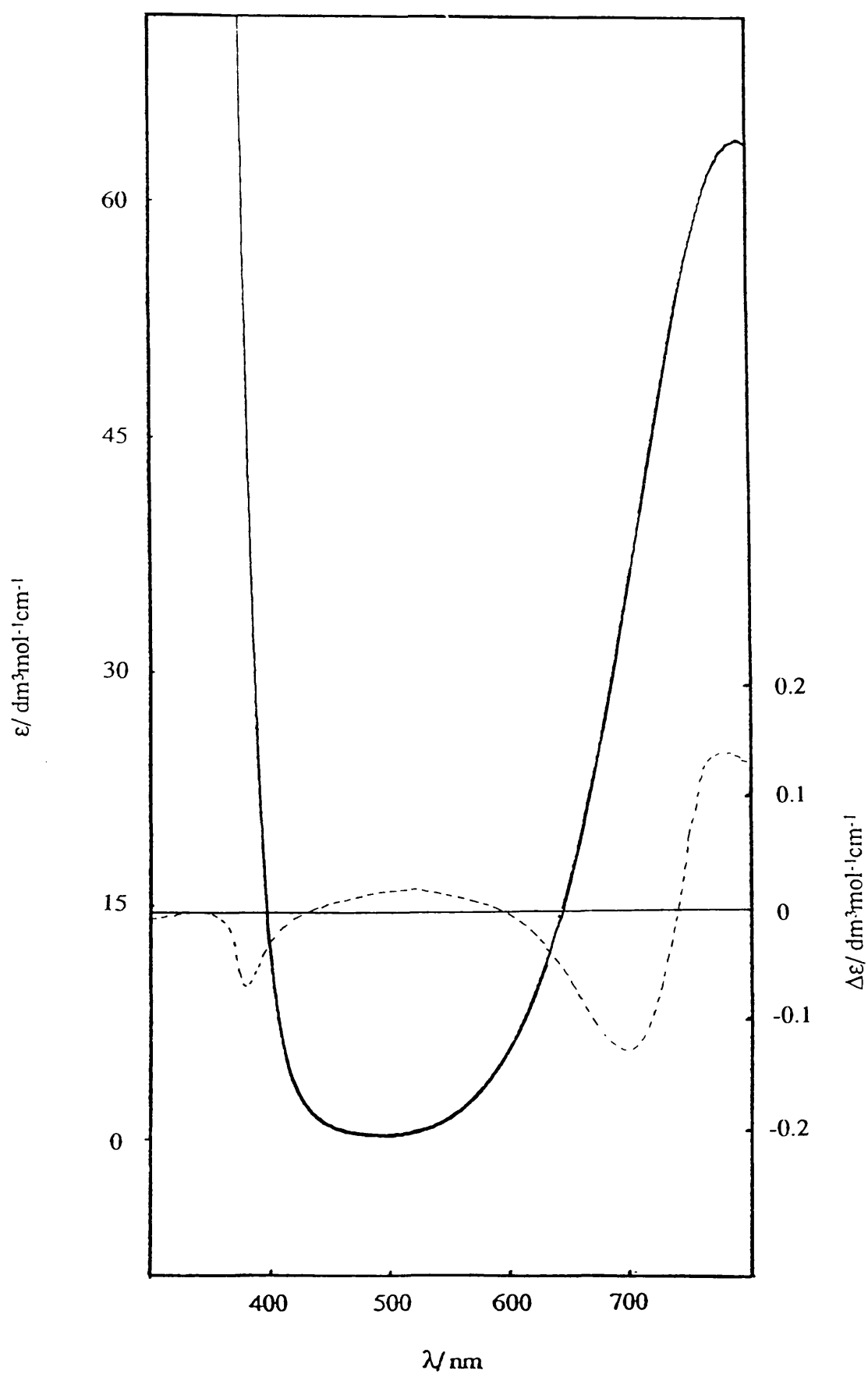**Fig.34(a).** *Absorption Spectrum of* [Cu(II)L⁷H₃][PF₆]₂ *in acetonitrile solution.*

Fig.4.34(b). *Absorption and Circular Dichroism Spectra of* $[Cu(II)L^7H_3][PF_6]_2$ *in acetonitrile solution.*

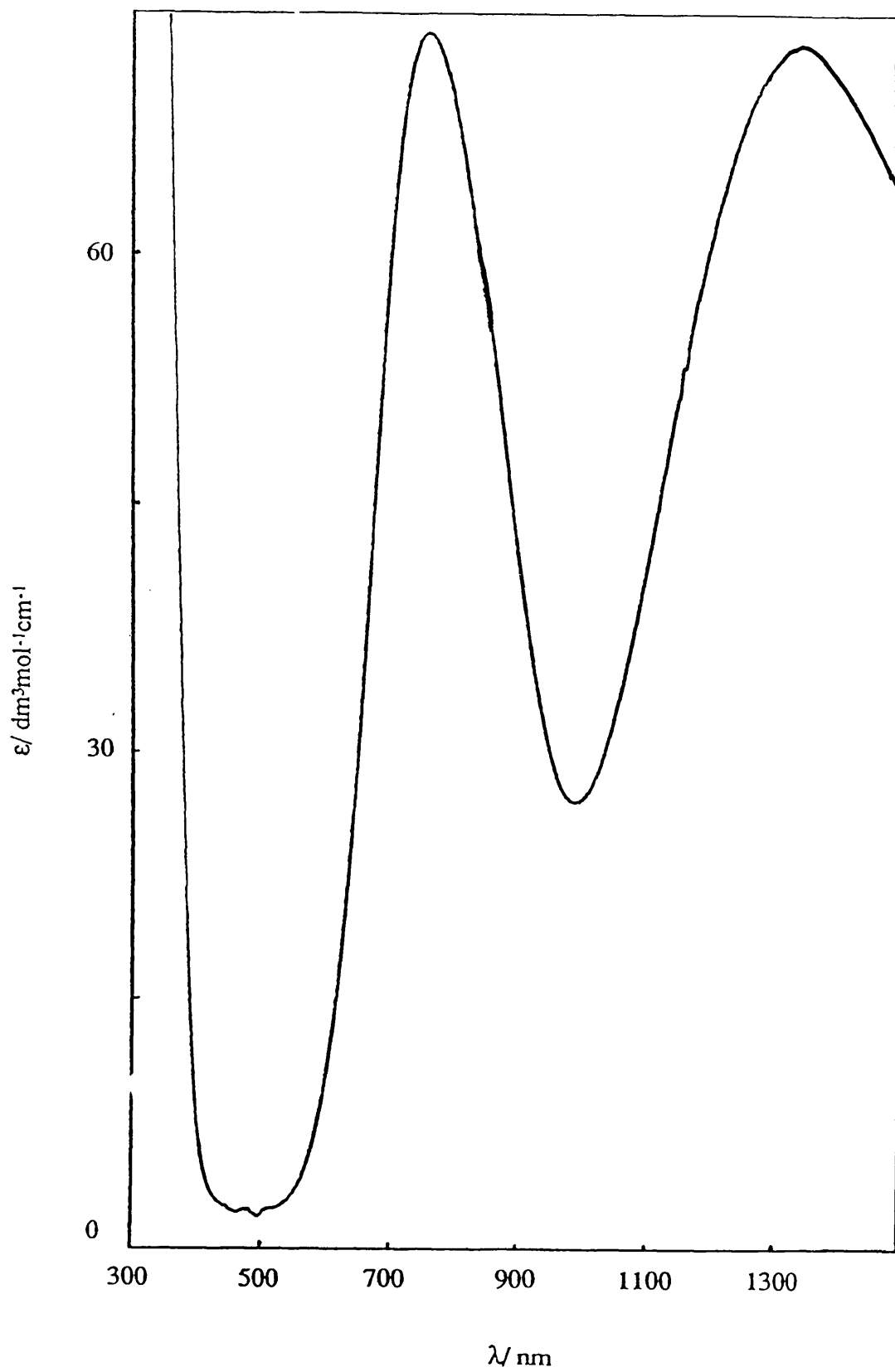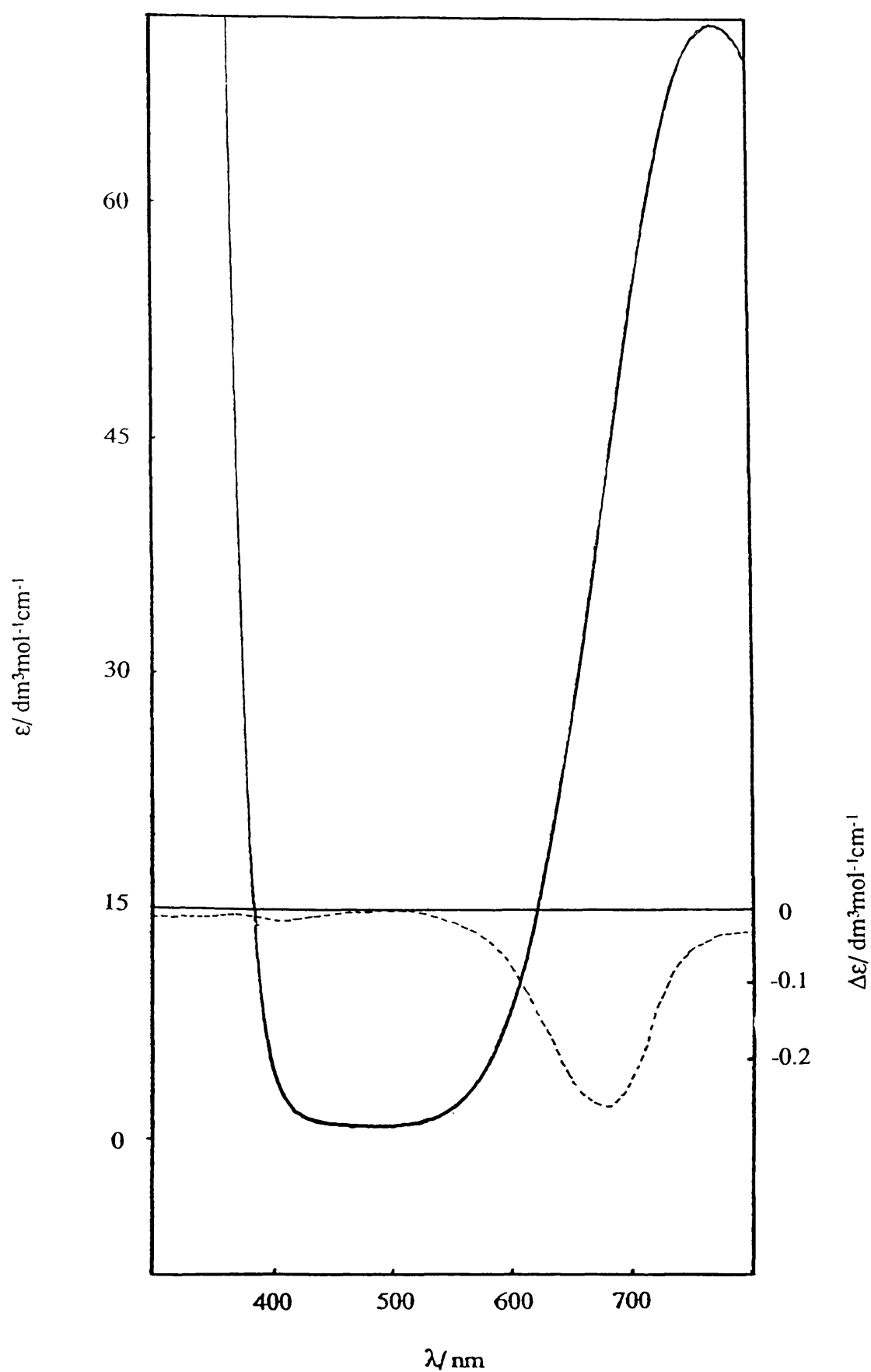**Fig.35(a).** *Absorption Spectrum of* $[Cu(II)L^8H_3][PF_6]_2$ *in acetonitrile solution.*

Fig.4.35(b). *Absorption and Circular Dichroism Spectra of* [Cu(II)L^{8}H$_3$][PF$_6$]$_2$ *in*

acetonitrile solution.

(4.3) CONCLUSIONS

Of the ligands prepared in this work, only L^1H_3 supports cobalt in the 3+ oxidation state. With 10 or more ring members Co(II) complexes are isolated. This is due to metal radius-to-ligand cavity fit, and the tendency for this type of ligand system to adopt trigonal prismatic geometry. The Co(II) complexes which have been crystallographically characterised display very distorted structures, and trigonal prismatic geometry is proving to be a common structural feature in N_3O_3 pendant-arm ligands, being observed in $[Co(II)L^3H_3]^{2+}$ and $[Co(II)L^5H_3]^{2+}$. With larger ring sizes, longer metal-to-ligand bond lengths are observed, which is reflected in the absorption spectra, with a shift towards lower energies. A persistent structural feature is hydrogen bonding to nitrate counter ions. In the case of L^3H_3 this results in the formation of a dimeric structure.

The Ni(II) and Cu(II) complexes prepared reflect the trends observed in the Co(II) complexes. For Ni(II), smaller ligand field splitting values are obtained for larger ring sizes, indicative of long metal-ligand bond lengths. Ni(II) has a larger LFSE value than Co(II) and Cu(II) in octahedral environments, and it is believed that the Ni (II) complexes will have geometries between that of octahedral and trigonal prismatic. This reflects the juxtaposition of the tendency for the ligands to present a trigonal array of donor atoms, and Ni(II) to prefer octahedral environments.

The absorption spectra of the Cu(II) complexes indicate severe trigonal distortion. By analogy to the Co(II) species discussed, it is probable that highly distorted six coordinate complexes exist in solution, whilst in the solid state different structures are possible. Given that L^3H_3 supports a Jahn-Teller distorted ion in $[Mn(II)L^3H_3L^3Mn(III)]^{2+}$, and that $[Co(II)L^3H_3]^{2+}$ has been shown to be trigonal prismatic, $[Cu(II)L^3H_3]^{2+}$ is most likely to be distorted trigonal prismatic in geometry. For Cu(II) metal-to-ligand size match is optimised in $[Cu(II)L^3H_3]^{2+}$.

References

1. Belal, A.A.; Farrugia, L.J.; Peacock, R.D.; Robb, J. *J. Chem. Soc. Dalton Trans.* **1989**, 931.

2. Larsen, E.; La Mar, G.N.; Wagner, B.E.; Holm, R.H. *Inorg. Chem*, **1972**, *11*, 2052.

3. Hancock, R.D. *Progress in Inorganic Chemistry*, Lippard S.J., Ed.; Wiley: New York, 1989, Vol. 37, p.187.

4. *Chemistry of the Elements*; N. N. Greenwood and A. Earnshaw; Pergammon; Oxford, 1984.

5. Farrugia, L.J.; Peacock, R.D. *Acta Crystallogr. Sect. C* **1991**, *C47*, 1312

6. Nonoyama, M.; Nonoyama, K. *Inorg. Chim. Acta.* **1979**, *35*, 231

7. *Inorganic Electronic Spectroscopy* (2nd Ed.), Studies in theoretical and Physical Chemistry, Lever, A.B.P.; Elsevier; Amsterdam; 1984.

8. Gillum, W.O.; Wentworth, R.A.D.; Childers, R.F.; *Inorg. Chem.* **1970**, *9*, 1825

9. Hathaway, B.J.; Billing, D.E.; *Coord. Chem. Rev.* **1970**, 5, 143.

10. Auerbeck,U.; Eckert, U.; Weighardt, K.; Nuber, B.; Weiss, J. *Inorg. Chem.* **1990**, *29*, 938.

11. Macdonald, N.M.; Peacock, R.D. Private communication.

CHAPTER 5

TITANIUM AND ZINC COMPLEXES OF N,N',N''-TRIS-2-HYDROXYETHYL-TRIAZAMACROCYCLES

"Year (n.). A period of 365 disappointments."

Ambrose Bierce, The Enlarged Devil's Dictionary.

CONTENTS

(5.1) INTRODUCTION

Titanium

The macrocyclic chemistry of titanium is very sparse, and for pendant-arm functionalised macrocycles, nonexistent. Titanium nitrogen bonds are very labile, which renders most complexes susceptible to hydrolysis. Reaction of titanium(IV) *bis*-(acetylacetonate) with 9aneN$_3$ in acetone solution results in the formation of an adamantane type [Ti$_4$(μ-O)$_6$(9aneN$_3$)$_4$]$^{4+}$ cluster (1). This compound is noteworthy in that the Ti-O bond lengths are short (1.824 Å), indicating some double bond character. The Ti-N bond lengths are long (2.230 Å), possibly indicative of a *trans* effect from the strongly bound μ-oxo ligands. To date no oxygen donor pendant-arm complexes have been reported.

Zinc

The chemistry of zinc is currently undergoing something of a renaissance. The presence of zinc in a many vital biological processes has been long recognised, but with the advent of macrocyclic chemistry there is much interest in modelling the bioinorganic chemistry of zinc.

To a large extent the function of zinc in biological systems is to act a polarizing group. This effect is very notable in enzymes such as carboxypeptidease A and carbonic anhydrase. In the former a zinc ion coordinates to the carbonyl oxygen atom of a peptide bond, resulting in the polarisation of the carbonyl group and renders the carbonyl carbon atom more susceptible to nucleophilic attack, namely hydrolysis. In carbonic anhydrase the zinc ion present actives a water molecule by increasing it's Bronsted acidity. This results in a zinc stabilised and highly nucleophilic hydroxide function, which reacts with a hydrogen-bonded carbon dioxide molecule to yield a bicarbonate ion.

It is important to note that the zinc triad differs markedly in it's coordination chemistry from other members of the transition series. With a d^{10} configuration the divalent cations show no electronic stereochemical preference (i.e. no LFSE). The range of possible geometries is larger than with metals with partially filled d shells. Given the large ionic radii of group IIB elements there is also the possibility of coordination numbers greater than six.

Recent studies by Adams *et al.* (2) of large ring size oxa-azamacrocycles with group IIB metals has shown that there is marked difference in affinity for Cd(II) over Zn(II). This is a reversal of the normal Zn(II) > Cd(II) affinity sequence, and has been labelled as a "structural dislocation" where there is juxtaposition of ligand flexibility and metal coordination requirements. In this case the cavity-to-metal fit is the cause of the dislocation with larger ring sizes favouring Cd(II) over Zn(II). In the current work this effect can be seen in the cobalt complexes detailed in the previous chapter where the

dislocation present is a tendency towards trigonal prismatic coordination. This effect cannot be attributed to metal to ligand size-match since L^3H_3 and L^5H_3 form trigonal prismatic complexes and L^4H_3 does not. Here it is possible ligand flexibility is the dominating factor.

Zn(II) has been shown elsewhere to adopt perfect trigonal prismatic geometry in the mixed metal dimeric complex $[Zn(II)L^1H_3L^1V(IV)][PF_6]_3$. Trigonal prismatic geometry is not unique in zinc coordination chemistry, but this is the only reported with a fully saturated ligand system.

(5.2) RESULTS AND DISCUSSION

(5.2.1) Titanium Complexes

In an initial experiment a sample of L^2H_3 dissolved in ethanol was added to an aqueous solution of $TiCl_3$ stabilised with $ZnCl_2$. The solution became a darker purple hue. Upon standing overnight the solution became colourless, and upon addition of $[NH_4][PF_6]$ a white precipitate was produced. This material did not analyse for any single complex, but appeared to be a mixture. The ^1H NMR. of the sample indicated a number of methyl resonances and was well resolved, indicating a complete oxidation of Ti(III) (d^1) to Ti(IV) (d^0). It is possible that this solution contained $[Zn(II)L^2H_3]^{2+}$ and free ligand.

Treatment of oxygen free solutions of $TiCl_3$ in water with L^1H_3 resulted in intense inky blue solutions. Addition of $[NH_4][PF_6]$ promoted the formation of a grey-blue microcrystalline precipitate. The absorption spectrum (of the chloride salt in water) displayed a single unsymmetrical band at 665 nm which corresponds to an approximate $10Dq$ value of 15000 cm^{-1}. This value is very low and comparable with $[Ti(III)(ROH)_6]^{3+}$ (16,800 cm^{-1}) (3). Therefore it is possible that L^1H_3 is bonded via the pendant-arm alcohol groups only. The CD spectrum indicated that this complex was optically active.

This material is rapidly oxidised in air to a grey-white powder, which upon analysis was found to be titanium dioxide. In sealed glassware this material decomposed completely within 48 hours. It is therefore probable that any $[Ti(IV)L^1H_3]^+$ is extremely susceptible to hydrolysis.

(5.2.2) Zinc Complexes

In the absence of LFSE it is assumed that structure a zinc complex will be dominated by the steric requirements of the particular ligand involved. The structures of the cobalt complexes presented in chapter four displayed some unusual coordination modes. Given that Co(II) and Zn(II) have similar ionic radii (74.5 pm and 74 pm respectively) it is not unreasonable to assume that the Zn(II) complexes will have similar structures. It was also noted in chapter four that it was probable $[(Co(II)L^3H_3)_2(NO_3)_2]^{2+}$ dissociated upon dissolution. Thus it is assumed that nitrate counter ions do not significantly interact with solvated complexes in solution.

The NMR spectra of the zinc complexes prepared will be individually discussed briefly before a general comparison is made. These studies are by no measure comprehensive but the spectra presented are all well resolved and are believed to devoid of exchange processes. In the ^1H-^{13}C spectra presented peak heights need not be similar to one dimensional ^1H or ^{13}C spectra.

(5.2.2.1) $[Zn(II)L^2H_3][PF_6]_2$.

$Zn(II)L^2H_3$ will show no stereochemical preference for octahedral over trigonal prismatic geometry. Indeed as discussed in chapter one there are circumstances in which

D_{3h} (or C_{3v}) symmetry is preferred by d^0 and d^{10} ions. The ^{1}H NMR spectrum of [ZnL^{2}H$_3$][PF$_6$]$_2$ in D$_3$COH solution is presented in fig.5.1(a). The spectrum is poorly phased due to high sample concentration. Both methyl resonances of the isopropyl group can are observed (δ=1.03 and δ=0.95). The methine resonances (δ=1.66; pr^i and δ=3.76) are also well resolved. The remainder of the spectrum is very complex. Comparison to the spectrum of the free ligand (fig.5.1 (b)) shows the expected downfield shift. The shift is not clear for the CH$_2$ residues, but for the methine and methyl resonances the degree of shift is proportional to the distance from the zinc centre. This is attributed to simple inductive deshielding. There is a broad weak signal at δ=7.95 ppm which assigned to the hydroxyl group protons.

The ^{13}C NMR and DEPT sequence (fig.5.1(c)) presents a much more simple picture. There are 7 resonances, indicating that in solution [Zn(II)L^{2}H$_3$]$^{2+}$ has accurate C_3 symmetry. With the resonances so sharply defined it is highly improbable that any exchange process is occurring. The wide dispersion of the resonances is indicative of octahedral geometry, since a trigonal prismatic ligand conformation would result in ring carbon atoms becoming almost equivalent. Thus it is likely that the TP geometry observed in [Zn(II)L^{1}H$_3$L^{1}V(IV)][PF$_6$]$_3$ is a function of the trigonally disposed O,O',O" hydrogen-bond acceptor face of the [V(IV)L^1]$^+$ moiety. Fig. 5.1(d) presents the ^{1}H-^{13}C correlation spectrum for [ZnL^{2}H$_3$][PF$_6$]$_2$. Here all ten expected proton resonances can be clearly observed. This spectrum demonstrates the source of the complexity of the CH$_2$ resonances (δ=2.73-3.21) in the ^{1}H spectrum, with each ring and arm residue bearing a pair of diastereotopic protons.

(5.2.2.2) [Zn(II)L^{3}H$_3$][PF$_6$]$_2$.

Only with L^{1}H$_3$, L^{2}H$_3$ and L^{7}H$_3$ is it possible for complexes to have true C_3 symmetry. However with L^{3}H$_3$ the departure from C_3 symmetry may only be small. As seen with [(Co(II)L^{3}H$_3$)(NO$_3$)$_2$][PF$_6$]$_2$, L^{3}H$_3$ may adopt trigonal prismatic coordination

and it is likely that $[Zn(II)L^3H_3][PF_6]_2$ will adopt a similar geometry. The ^1H spectrum of $[Zn(II)L^3H_3][PF_6]_2$ is presented in fig.5.2(a). The spectrum is well resolved, showing similar shifting compared to the free ligand as $[Zn(II)L^2H_3]^{2+}$. All peak integrals are of the appropriate values. A quintet due to D_2HCOH at $\delta=3.3$ overlaps with part of the spectrum but does not affect analysis. The lowfield pendant-arm methine resonances ($\delta=4.18$) all overlap at a position upfield of the methine resonance in $[Zn(II)L^2H_3]^{2+}$, due to inductive effect of the isopropyl group in L^2. The $C\underline{H}_2$ resonances at $\delta=2.5$-3.3 are assigned to those residues adjacent to a nitrogen atom. The region is complex due to each carbon atom being in a unique environment and bearing a pair of diastereotopic protons. Geminal coupling will further complicate the spin systems involved. The three methyl signals overlap at $\delta=1.28$, indicating a pseudo C_3 axis. The signals for the methylene residue in the middle of the C_3 bridge is most interesting. These two resonances ($\delta=1.70$ and 2.25) are attributed to pseudo-axial and pseudo-equatorial protons in the six membered chelate ring (see inset of fig.5.2(a)). These resonances are extremely complex, with each proton being vicinally coupled to 4 unique protons and geminally coupled to each other. From the data currently available it is not possible to determine which proton is responsible for which resonance; J resolved or selective decoupling experiments would be required.

There are three very weak signals at $\delta=7.76$, 8.29, 8.72. These are assigned as the hydroxyl protons of the pendant arm groups. It has been suggested that these signals are due to contamination of ammonium, ions but the signals are not evenly spaced and hence cannot be due to ^1H-^{14}N coupling. Why these resonances are so widely separated is not understood. As demonstrated in previous chapters these systems are very potent hydrogen-bond donors and bonding to solvent molecules at the O_3 "face" of $[Zn(II)L^2H_3]^{2+}$ may be the cause of the wide dispersion of hydroxyl signals.

The ^{13}C spectrum is presented in fig.5.2(b). Most apparent is the presence of only 14 resonances whilst there are 16 unique carbon atom present. The peak at $\delta=58.79$ ($\underline{C}H_2$) is most likely two be coincidental resonances. The signal at $\delta=64.67$ is a coincidental of methine and methylene resonances. The DEPT sequence indicates that this signal is a

methine resonance (90° pulse) and that it is also contains elements of a methylene resonance (135° pulse). The three lowfield methylene resonances (δ=64.67, 65.24, 65.44) are tentatively assigned as pendant arm resonances since the pattern of peak positions reflects that of the methyl resonances (δ=19.83, 20.24, 20.41). The remainder of the methylene resonances are assigned as ring carbon atoms.

The ^1H-^{13}C correlation spectrum is presented in fig.5.2(c). The three methyl groups are clearly resolved as doublets of very similar coupling constant. The carbon signal at δ=64.67 ppm is confirmed as a coincidental two carbon signal, as indicated by the large number of associated proton resonances. The CH_2 group in the middle of the C_3 bridge, unfortunately, is not well resolved.

From the NMR data it not possible to categorically define a solution state structure, although trigonal prismatic geometry is likely. What is clear is that the structure is not stereochemically labile. The structure of the analogous cobalt complex indicated that the six membered chelate ring was in a twist-boat configuration. Normally in "organic" systems such confomers are intermediates in boat-chair interconversions and have only a transient existence. Given the confines of macrocyclic system and the large ionic radius of Zn(II) it appears that this conformation is stable in this complex.

(5.2.2.3) $[Zn(II)L^4H_3][NO_3]_2$.

It is worth remembering that with L^4H_3 Co(II) adopted a highly distorted geometry between bicapped tetrahedral and octahedral. Thus it would be expected if $[Zn(II)L^4H_3]^{2+}$ and $[Co(II)L^4H_3]^{2+}$ were isostructural the NMR spectra of $[Zn(II)L^4H_3]^{2+}$ would indicate considerable asymmetry. This is indeed the case. The ^1H spectrum of $[Zn(II)L^4H_3][NO_3]_2$ in methanol solution is presented in fig.5.3(a). The methyl resonances (δ=1.26-1.30) are second order and very complex, although the signals are not widely dispersed. A broad region at δ=1.74-1.98 is assigned to the complex spin system comprising the methylene residues in the centre of the C_4 bridge. Again there is situation

in which each proton has 4 vicinal couplings and 1 geminal coupling. The ring and pendant-arm methylene resonances are spread over two broad regions of the spectrum (δ=2.31-2.96 and 3.13-3.34). The second of these regions is obscured by the residual solvent peak. Finally the pendant-arm methine groups appear as a large highly complex signal centred at δ=4.18. This signal is not symmetrical but appears as two complex signals in an approximate ratio of 1:2. This is explained by assuming $[Zn(II)L^4H_3]^{2+}$ has a pseudo two-fold axis of symmetry, with the C_4 bridge and one of the pendant arms lying on this axis and the other two pendant-arms on either side. The point group of $[Zn(II)L^4H_3]^{2+}$ must be C_I and it emphasised that this is approximate symmetry only. No resonances due to hydroxyl protons could be detected.

The ^{13}C spectrum and DEPT sequence (fig.5.3(b)) are most satisfying, with all 17 carbon atoms being resolved. The methyl resonances are very close together (δ=20.24, 20.28, 20.34), which may indicate that in solution the C_4 bridge in $[Zn(II)L^4H_3]^{2+}$ is in an *exo* configuration, rendering the methyl groups in approximately similar environments. The two central methylene resonances of the C_4 bridge are well resolved (δ=25.02 and 26.59) as are the other methylene resonances due Aring, and pendant-arm methylene residues. There is no indication in the spectra to suggest which methylene signals are those of the ring and those which are of the pendant-arm. The three methine resonances (δ=62.61, 63.05, 64.62) are interesting as that they are in a 2:1 pattern. This confirms the pseudo symmetry postulated from the ^1H data.

(5.2.2.4) $[Zn(II)L^5H_3][NO_3]_2$.

$[Co(II)L^5H_3][NO_3]_2$ was shown (chapter 5) to adopt a trigonal prismatic geometry. If this structure were maintained in $[Zn(II)L^5H_3][NO_3]_2$, a similar pseudo mirror plane symmetry observed in $[Zn(II)L^4H_3][NO_3]_2$ would be present. From a cursory glance at the ^1H spectrum (fig.5.4(a)) no pseudo symmetry is apparent. The methyl resonances (δ=1.25-1.30) appear as a second order pseudo triplet. These show a similar range of

dispersion to those of $[Zn(II)L^4H_3]^{2+}$. The methine resonances ($\delta=4.20$) appear to be very well resolved in a symmetrical multiplet and bear more resemblance to those of $[Zn(II)L^3H_3]^{2+}$ than $[Zn(II)L^4H_3]^{2+}$. However this picture is deceptively simple as the ^{1}H-^{13}C correlation spectrum will show (*vide infra*). The three methylene resonances in the centre of the C_5 bridge form a very complex multiplet ($\delta=1.4$-2.1). This spin system comprises three pairs of diastereotopic protons mutually vicinally and geminally coupled. There will also be coupling to the adjacent methylene residues attached to nitrogen atoms. The remainder of the methylene residues fall into three very complex regions ($\delta=2.36$-2.58; $\delta=2.73$-2.86; $\delta=3.28$-3.36). The integrals of these regions are approximately in the ratio 5:8:5 (the residual solvent signal has been accounted for). This pattern cannot be simply accounted for. As with $[Zn(II)L^4H_3]^{2+}$ no hydroxyl proton resonances could be detected.

In contrast to the ^{1}H spectrum the ^{13}C spectrum (fig.5.4(b)) is very simple. The three methyl groups ($\delta=20.20$, 20.44, 20.67) are very close together but can be clearly distinguished from one another. The central methylene residues of the C_5 bridge can also be identified ($\delta=21.70$, 23.73, 25.40). Some evidence for a pseudo mirror plane is found in the pendant-arm methine resonances ($\delta=62.26$, 66.77, 64.11). Here the 2:1 pattern of signals found in $[Zn(II)L^4H_3]^{2+}$ is repeated. The remainder of the signals are unambiguously assigned as ring and pendant-arm methylene resonances. There is no indication from this spectrum as to which signals are attributed to ring or arm carbon atoms.

The question of the complexity of ^{1}H spectrum and the integral ratio has not yet been addressed. The ^{1}H-^{13}C correlation spectrum is presented in fig.5.4(c). It is immediately apparent that the extreme complexity of the methylene resonances in the ^{1}H spectrum is due to each member of a diastereotopic pair of protons resonating at significantly different parts of the spectrum. The methine resonances on the carbon axis are well separated, but are very close together in ^{1}H direction. Again the 2:1 pattern is clearly seen. The complexity of the C_5 bridge spin system can not be appreciated from this spectrum due to low resolution.

Without more information it not possible to state whether $[Zn(II)L^5H_3]^{2+}$ in solution has a trigonal prismatic geometry or not. The presence of a pseudo plane of mirror symmetry tends to suggest that trigonal prismatic geometry is a strong possibility. The likelihood of a five coordinate species has not been dealt with. Given the low spread of methyl and methine resonances it is probable that all pendant-arms remain coordinated in solution. A five coordinate solution structure would results in much greater asymmetry and a greater range of peak dispersion.

(5.2.2.5) ^1H NMR Titration of L^1H_3.

The Cu(II) complexes detailed in the previous chapter indicated that the kinetics of complex formation are not simple. An NMR titration of L^1H_3 was undertaken to elucidate the complex formation process. A sample of L^1H_3 was dissolved in D_2O and aliquots of standardised zinc nitrate dissolved in D_2O were added. An equilibration period of one day was allowed between the addition of successive aliquots. The effect of addition of metal salt on the methyl region of the ligand is displayed in fig. 5.5.; the addition of 0.5 ml $Zn(NO_3)_2$ (aq.) represents 1:1 stoichiometry of metal salt to ligand. The internal reference was 1,4-dioxane.

The most obvious feature of the titration is the rapid diminution of the resonance due to the free ligand. At 0.1 ml (ligand/Zn(II) = 5/1) the methyl region consists of two main resonances and a weak doublet at 1.07 ppm. It can be speculated on this limited data that a 4:1 ligand to metal complex is initially formed, with one pendant-arm hydroxyl function of each ligand coordinated to the zinc centre. As successive aliquots are added the ligand and the initial complex resonances collapse giving rise to a new doublet which is unambiguously assigned to the methyl resonance of $[Zn(II)L^1H_3]^{2+}$. This description is highly speculative with more data being required for a more definitive assessment. However, this titration does indicate that an involved sequence of events is occurring in the formation of these complexes.
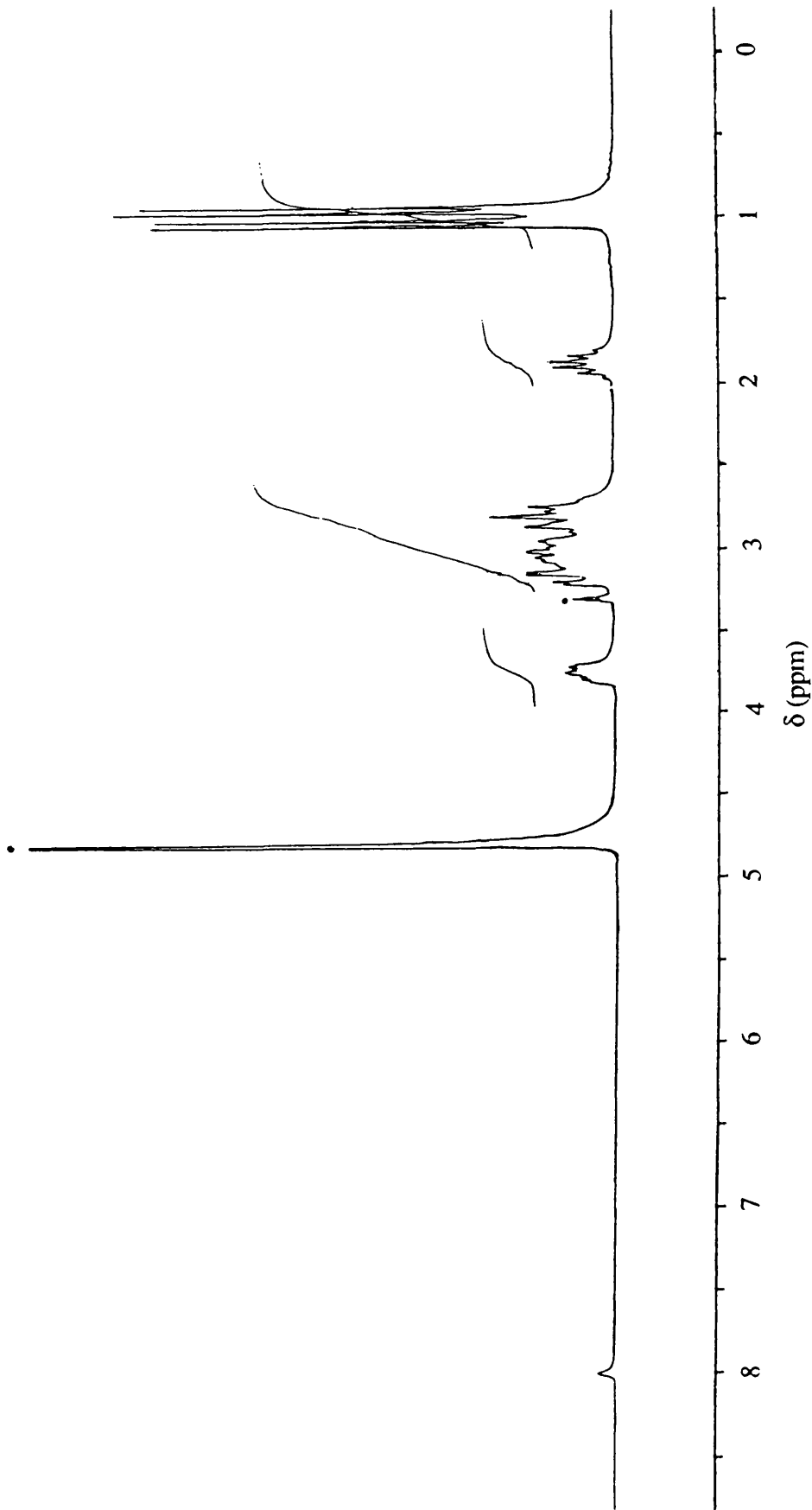
(5.2.3) **Spectra**.

Fig. 5.1(a). *^1H NMR of [Zn(II)L^{2}H$_3$][PF$_6$]$_2$ in D$_3$COH (".” indicates solvent).*
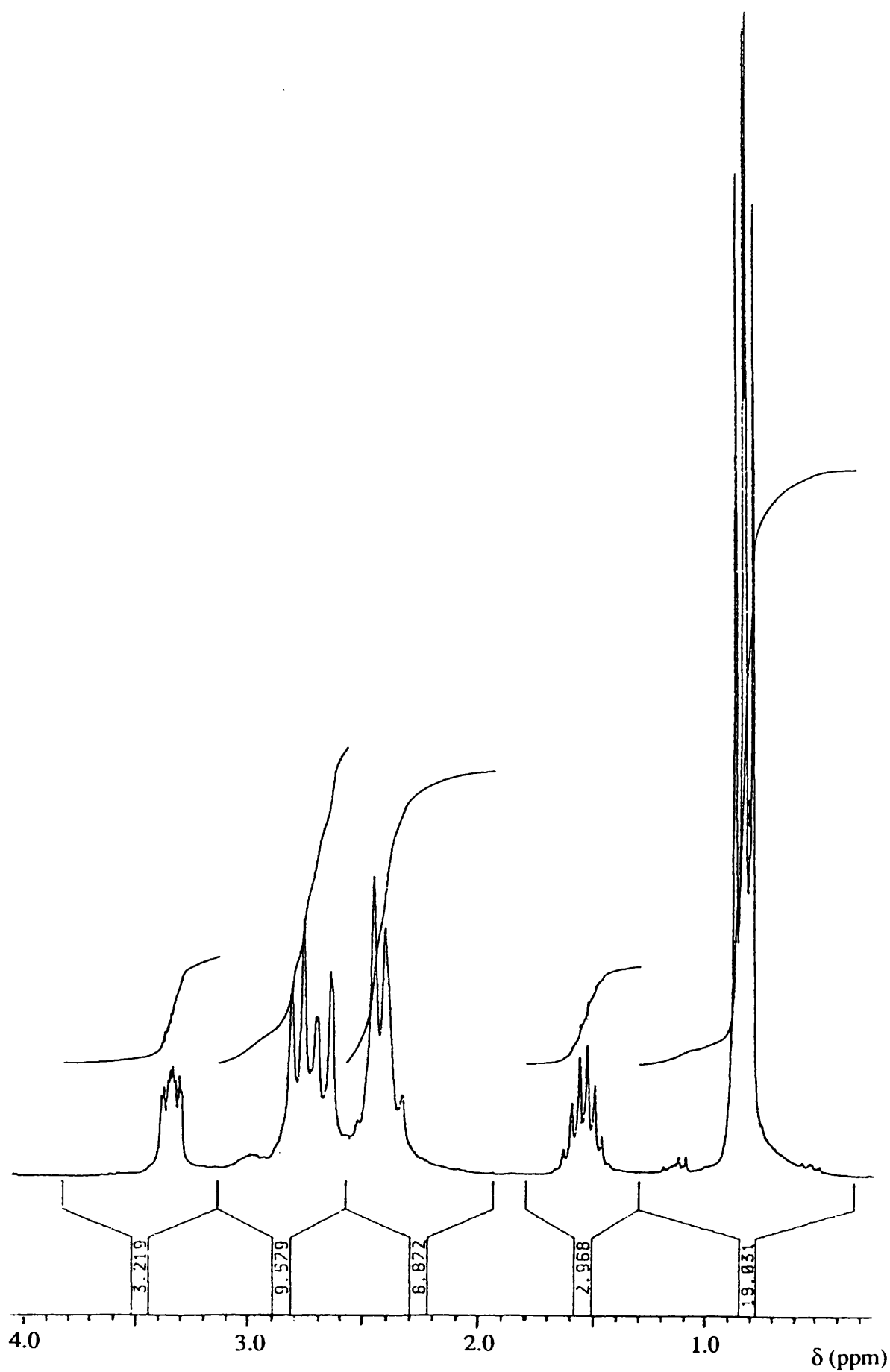
Fig. 5.1(b). *^{1}H NMR of N,N,',N''*-tris-[2(*R*)-hydroxy-3-methyl-butyl]-1,4,7-
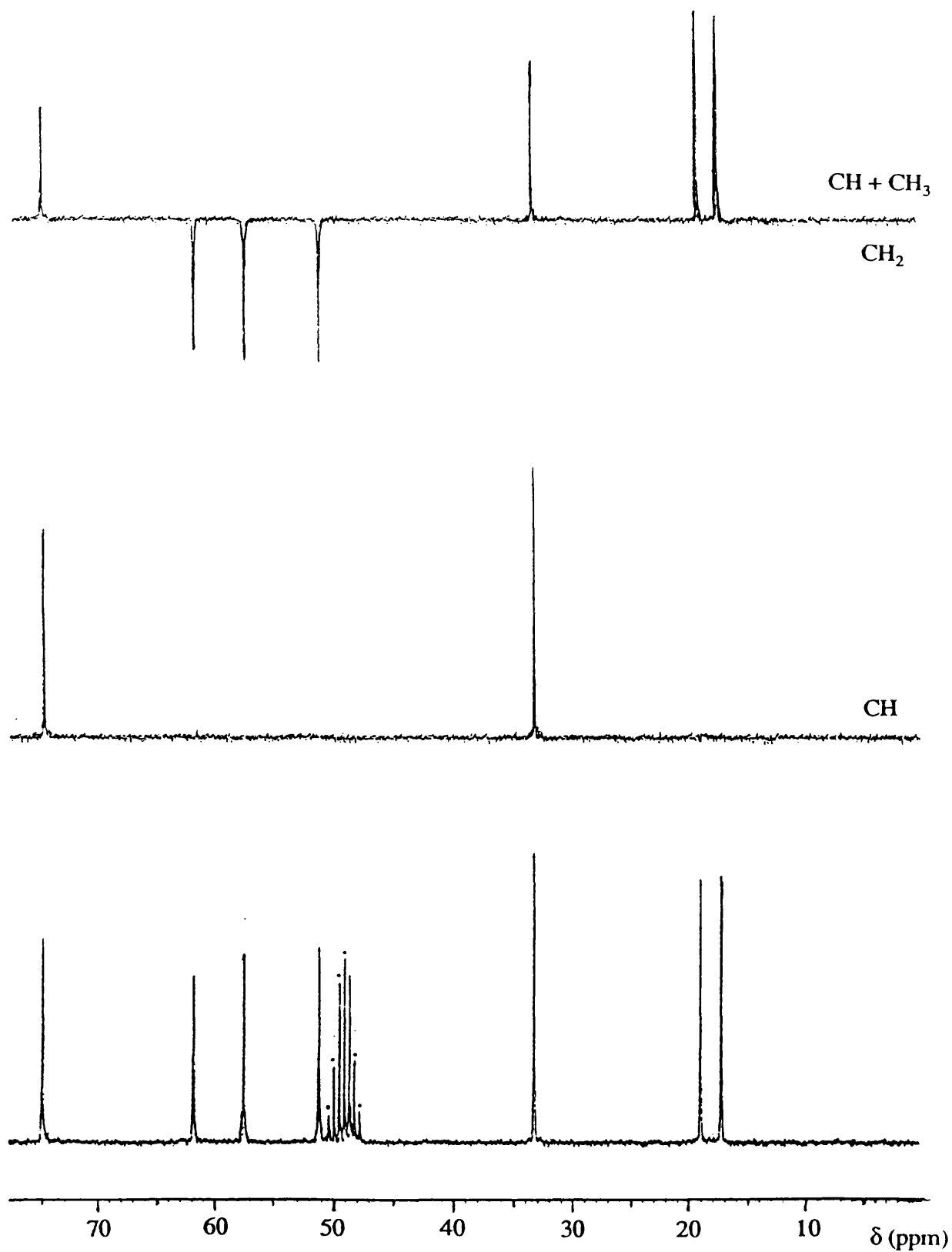
triazacyclononane (L^2).

Fig. 5.1(c). *^{13}C NMR and DEPT sequence of* [Zn(II)L^{2}H$_3$][PF$_6$]$_2$ *in* D$_3$COH.
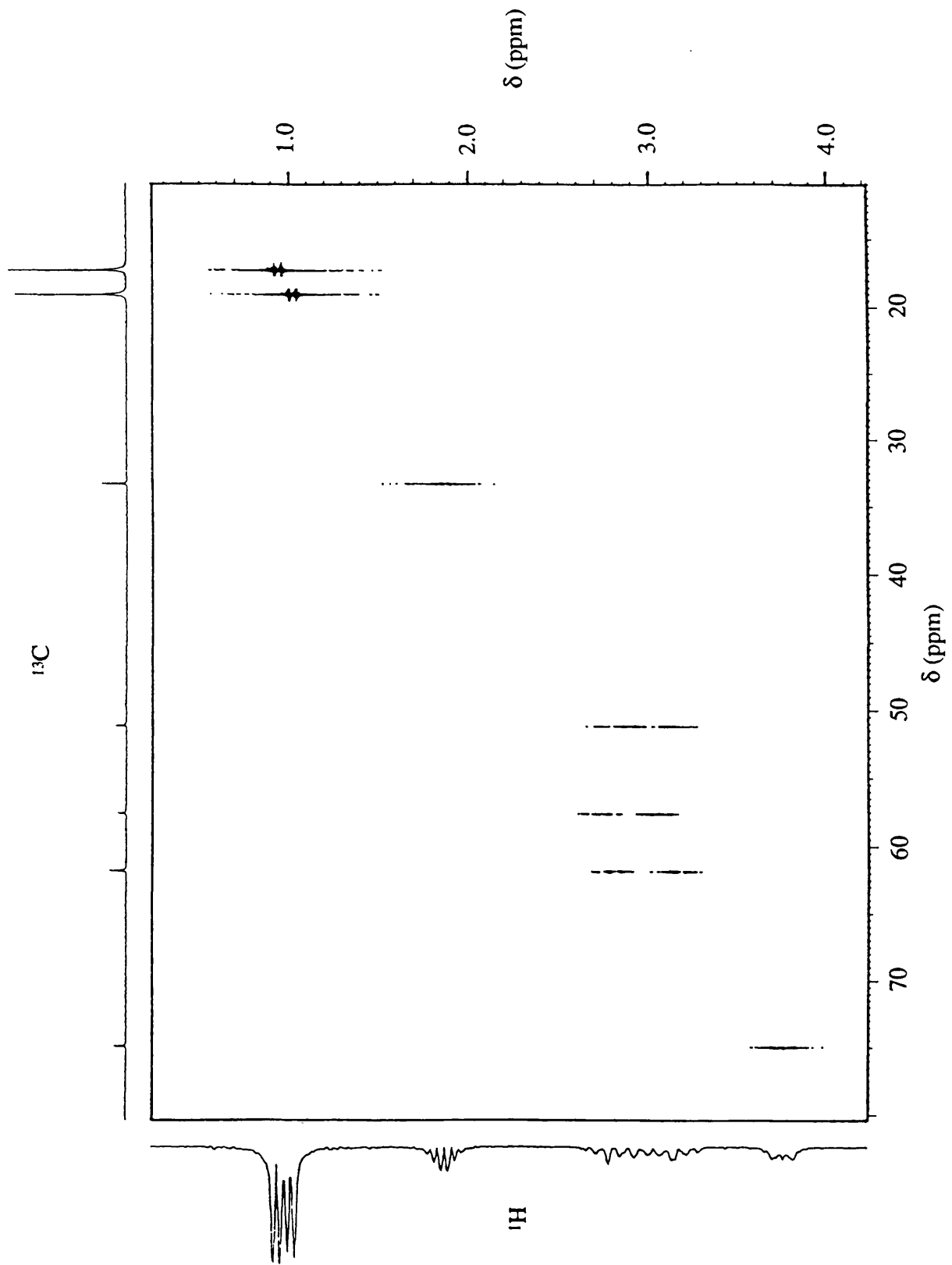
Fig. 5.1(d). *¹H-¹³C correlation spectrum of [Zn(II)L²H₃][PF₆]₂ in D₃COH.*
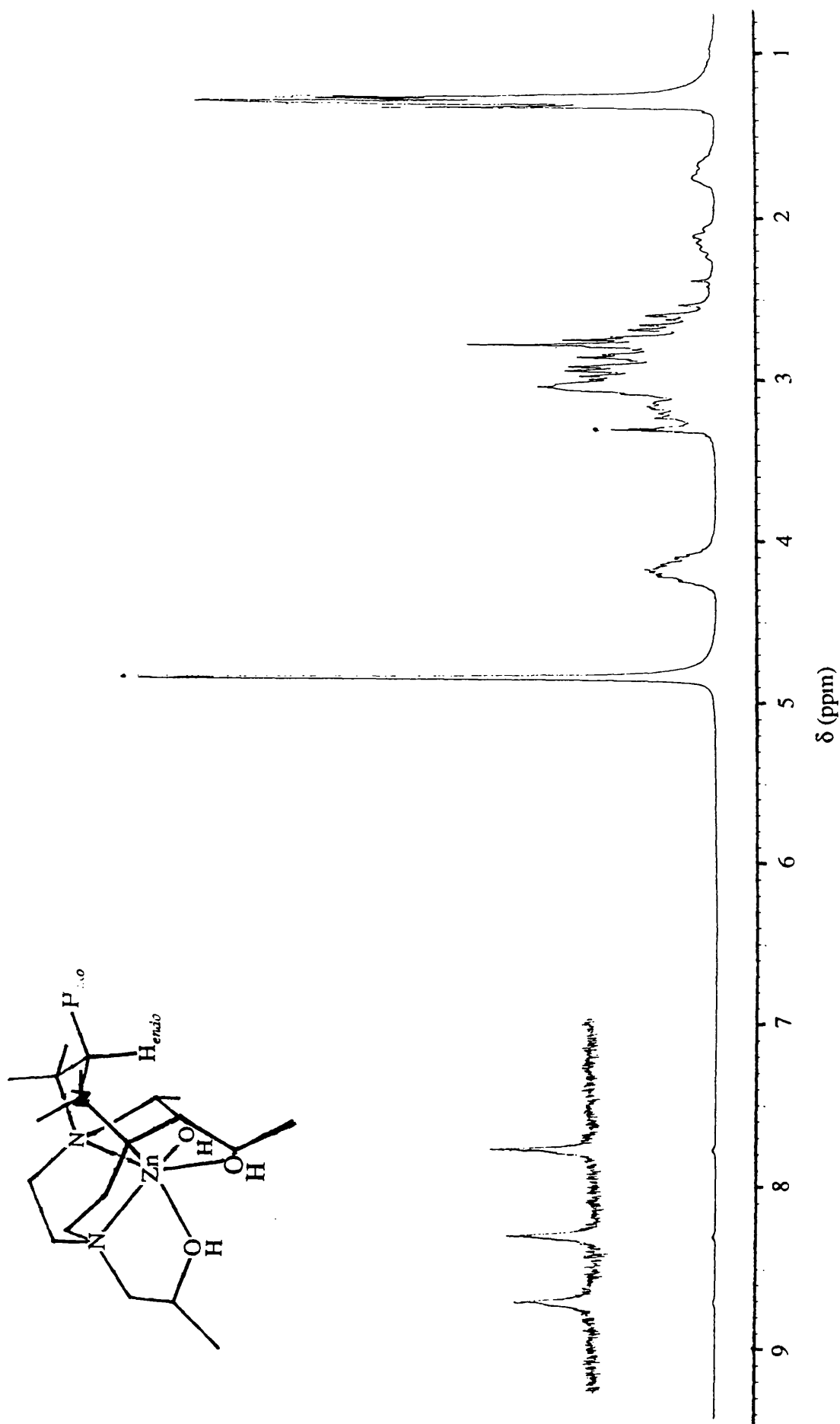
Fig. 5.2(a). *¹H NMR of [Zn(II)L³H₃][PF₆]₂ in D₃COH and configuration of the larger chelate ring.*
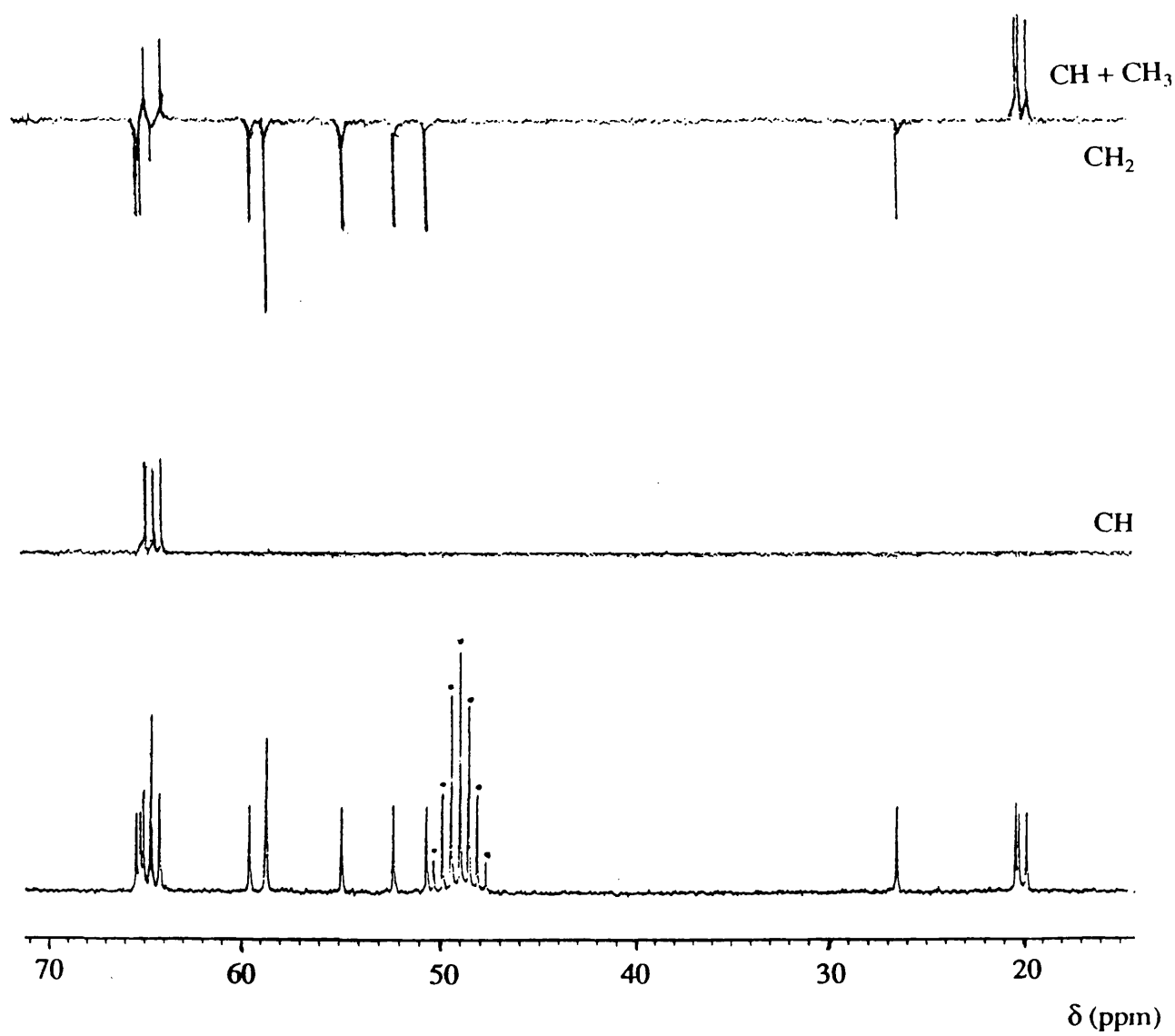
Fig. 5.2(b). *^{13}C NMR and DEPT sequence of* [Zn(II)L^{3}H$_3$][PF$_6$]$_2$ *in* D$_3$COH.
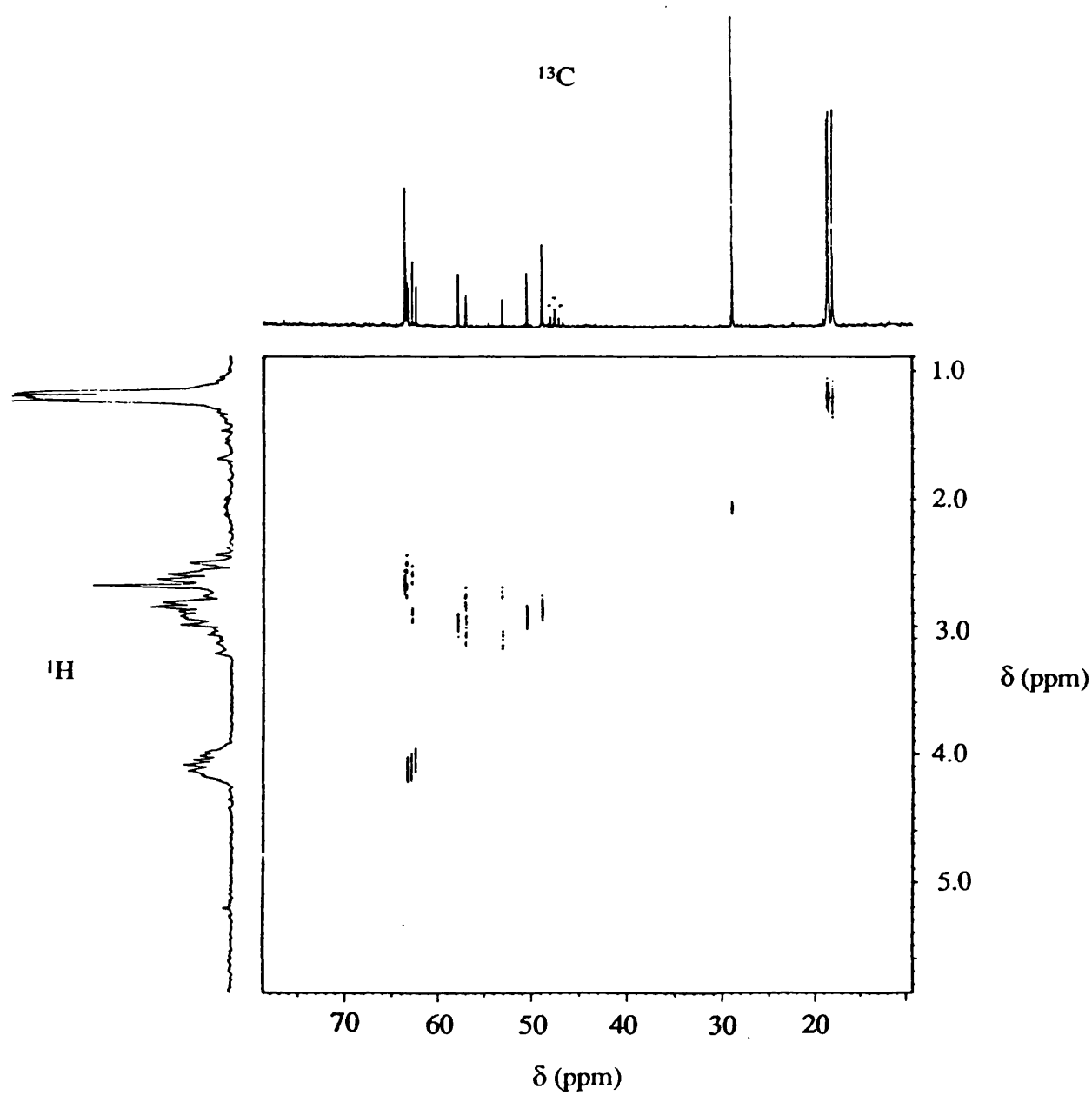
Fig. 5.2(c). *¹H–¹³C correlation spectrum of* [Zn(II)L³H₃][PF₆]₂ *in* D₃COH.

202

Fig. 5.3(a). *¹H NMR of* [Zn(II)L⁴H₃][NO₃]₂ *in* D₃COH. *Indication of pseudo two-fold axis of symmetry.*
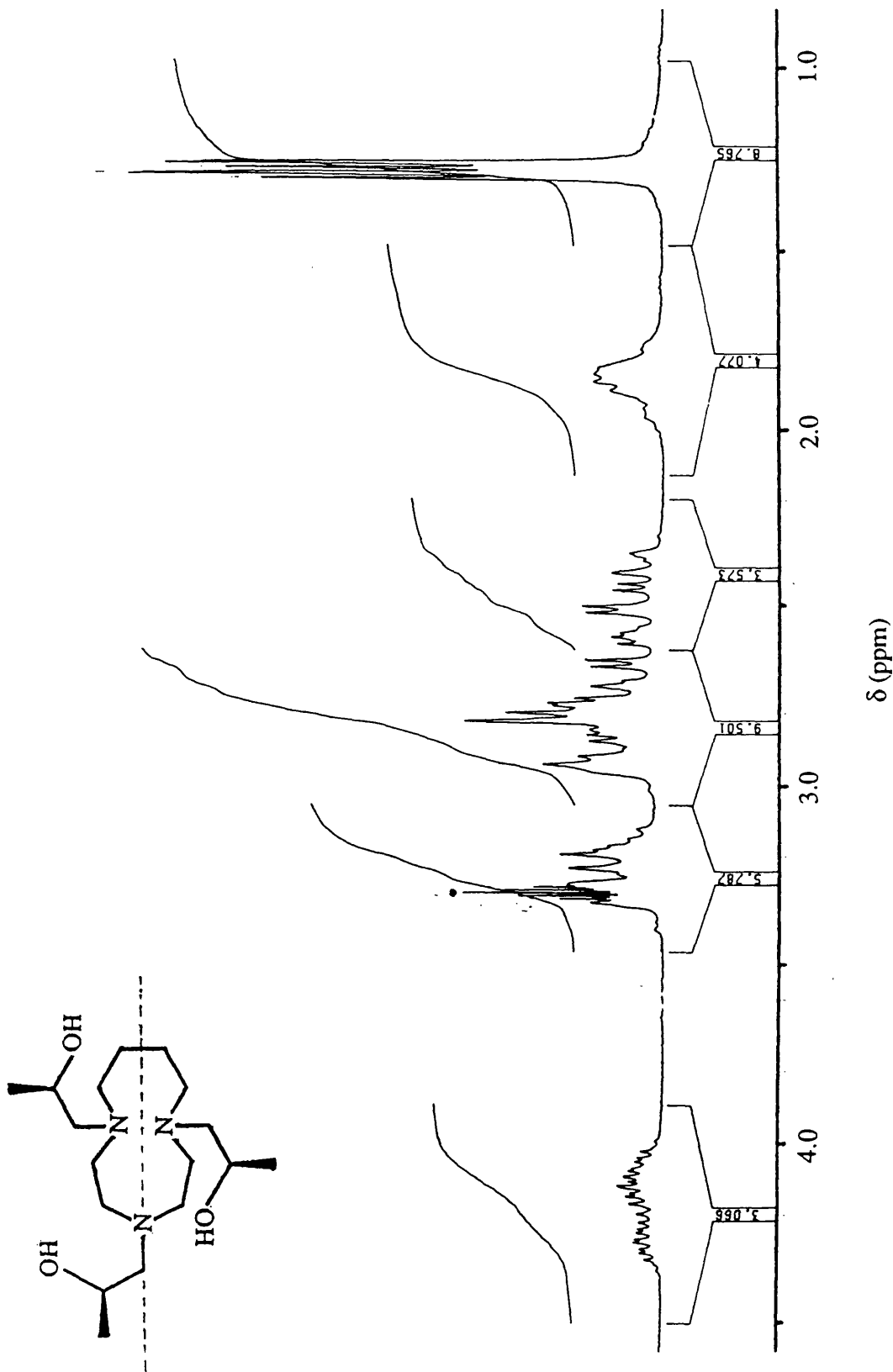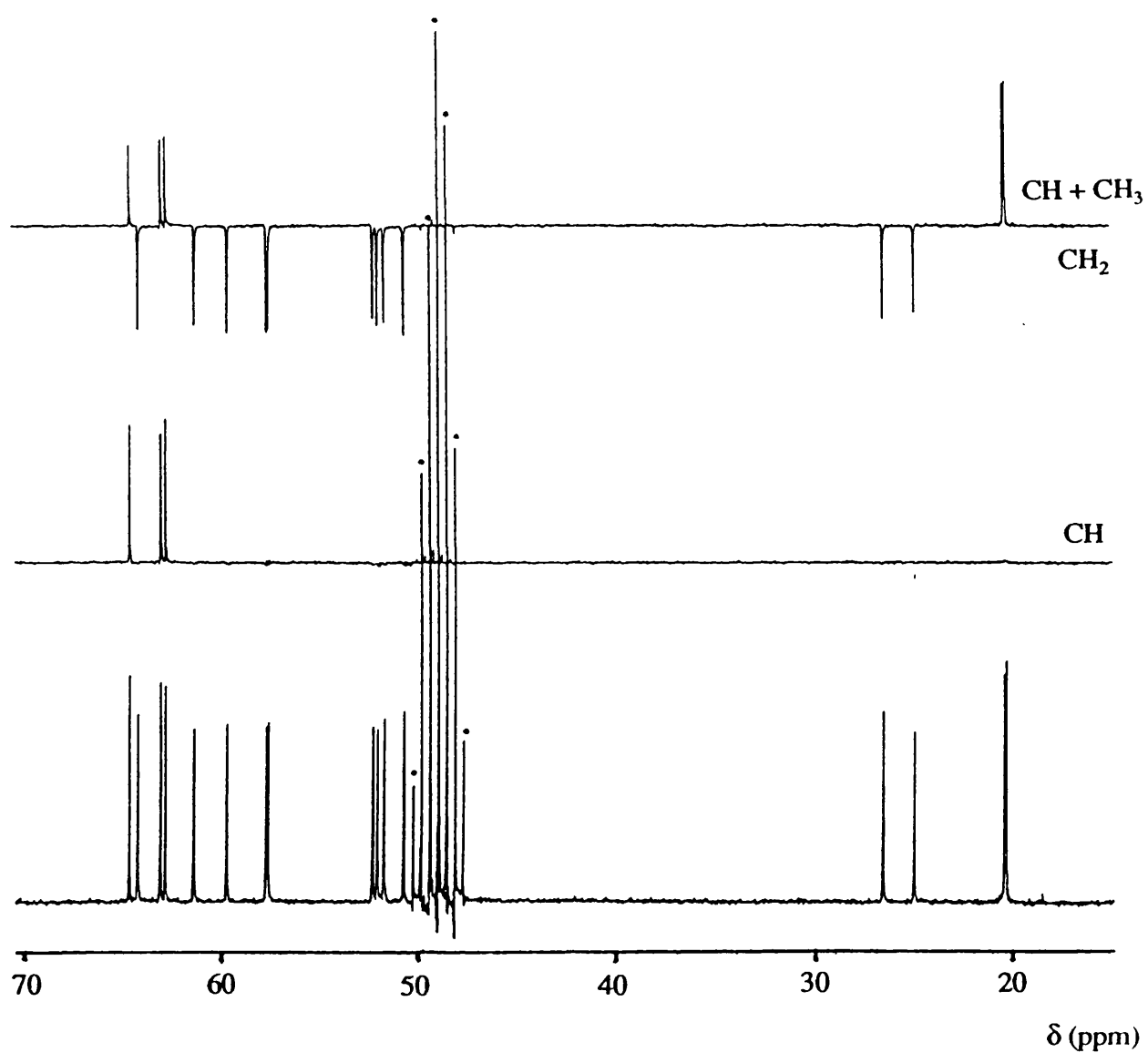
Fig. 5.3(b). *^{13}C NMR and DEPT sequence of* [Zn(II)L^{4}H$_3$][NO$_3$]$_2$ *in* D$_3$COH.

Fig. 5.4(a). *¹H NMR of* [Zn(II)L⁵H₃][NO₃]₂ *in* D₃COH. *Indication of pseudo two-fold axis*

of symmetry.

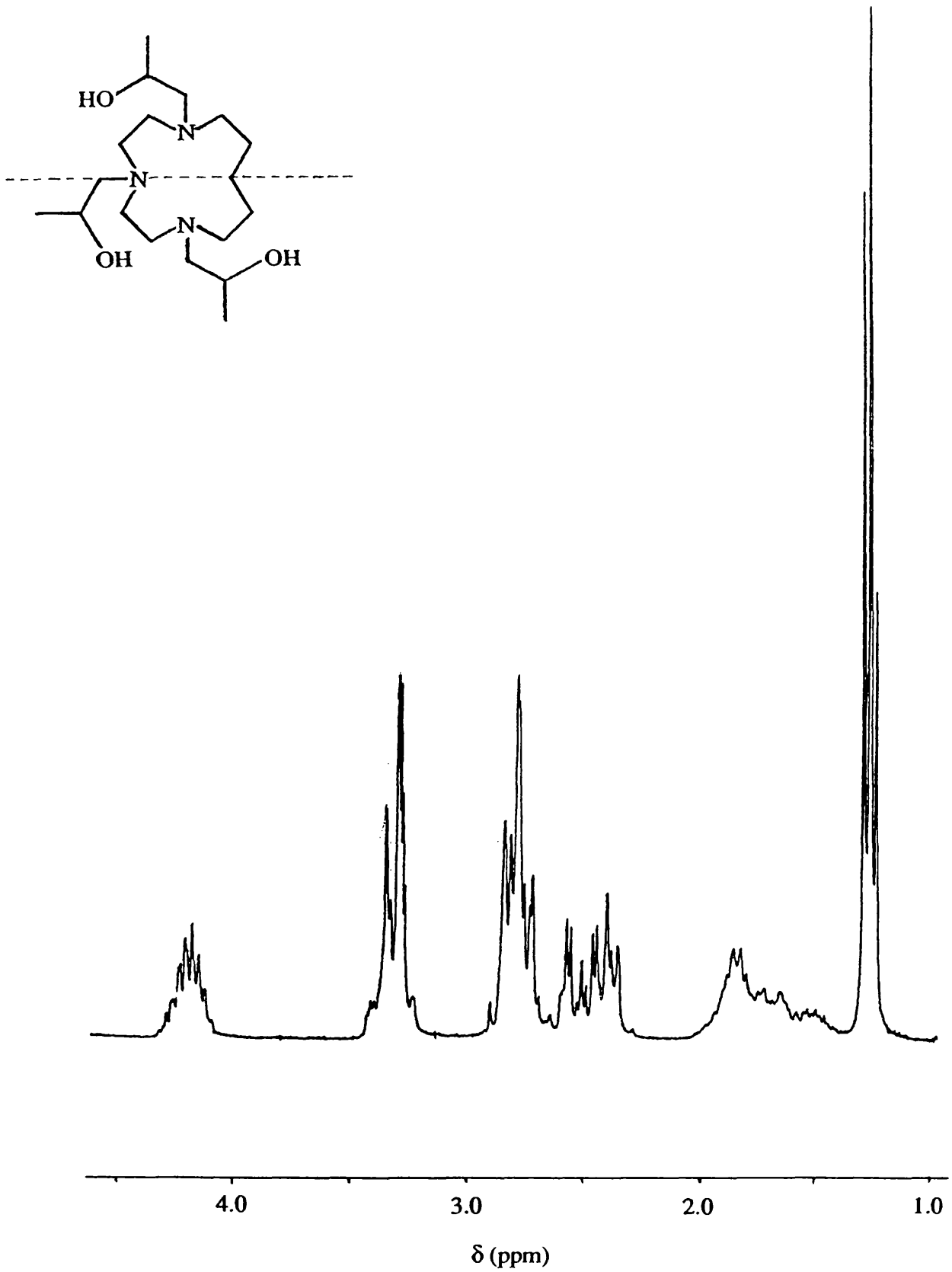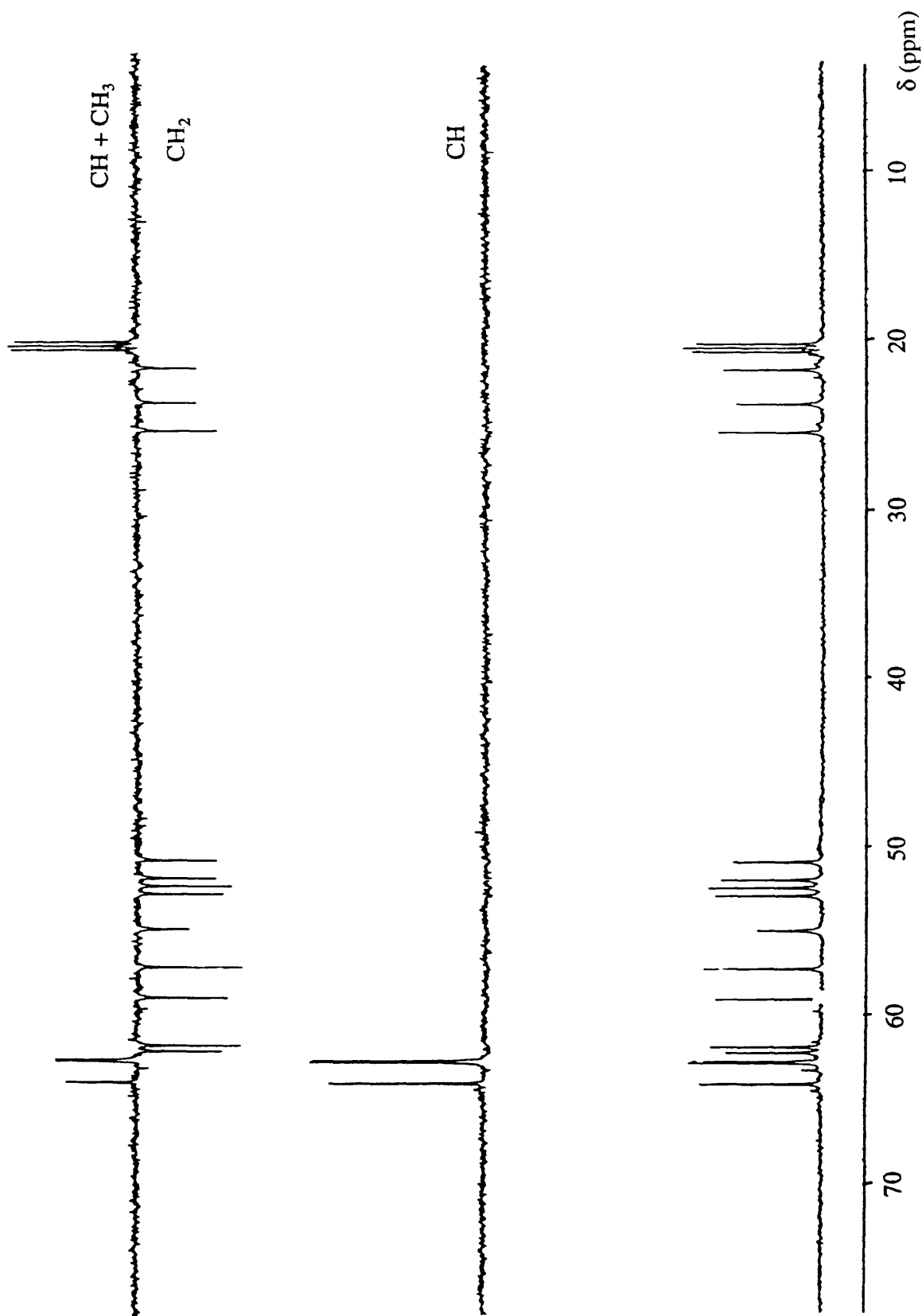Fig. 5.4(b). *^{13}C NMR and DEPT sequence of [Zn(II)L^{5}H$_3$][NO$_3$]$_2$ in D$_3$COH.*
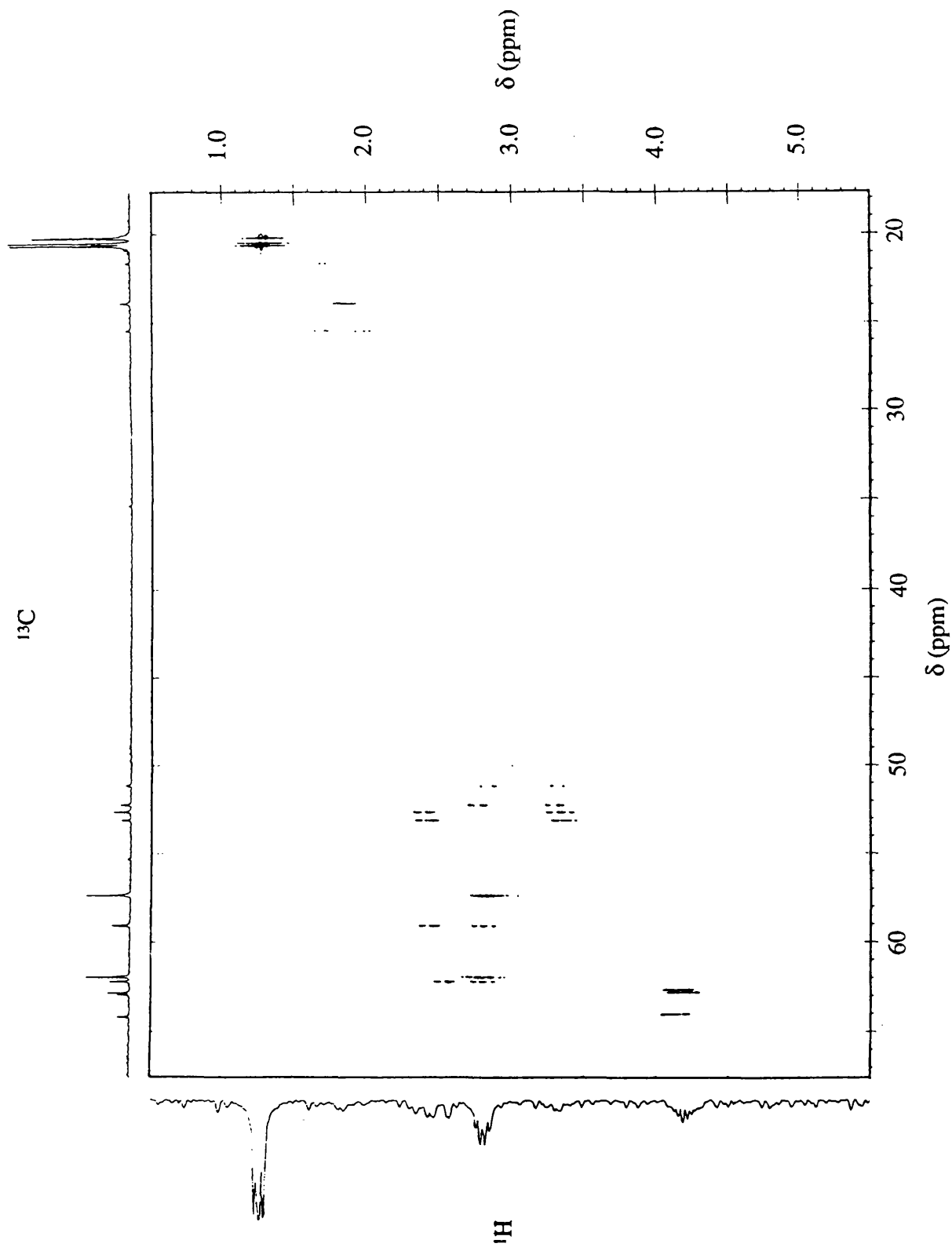
Fig. 5.4(c). $^1H-^{13}C$ correlation spectrum of $[Zn(II)L^5H_3][NO_3]_2$ in D_3COH.

Volume (ml) of Zn(NO₃)₂

stock solution added

0.50

0.40

0.30

0.20

0.10

0

1.3   1.2   1.1

δ (ppm)
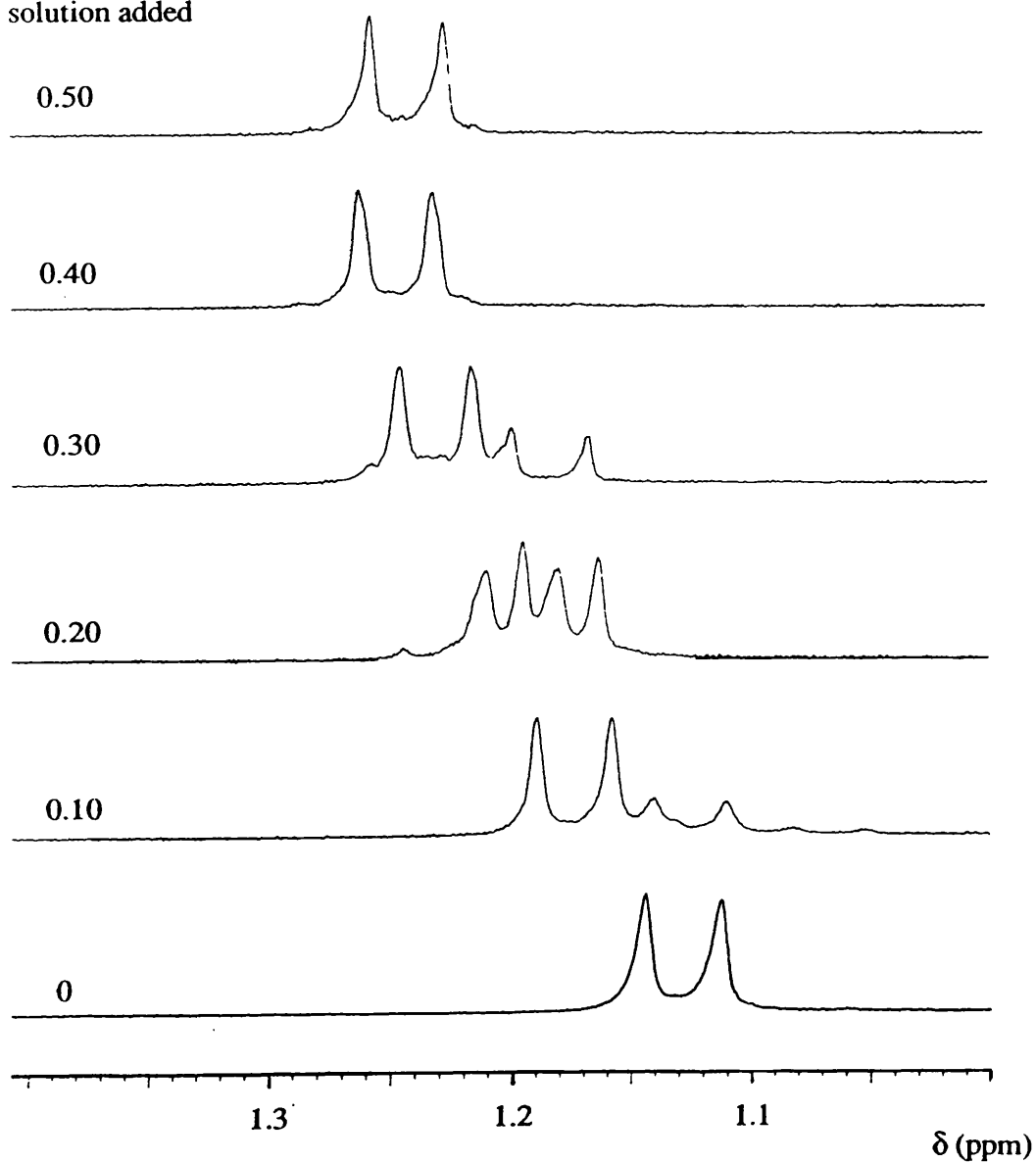
Fig. 5.5. *¹H NMR Titration of* L¹H₃ *with* Zn(NO₃)₂ *in* D₂O.

(5.3) CONCLUSIONS

The chemistry of L^1H_3 and L^2H_3 with titanium is complicated by the extreme oxygen sensitivity of the Ti(III) state and the susceptibility if the Ti(IV) to hydrolysis. The very low $10Dq$ value of the complex of L^1H_3 indicates that it is likely that L^1H_3 bonds *via* only oxygen donors.

NMR studies of the zinc complexes prepared indicate that the complexes remain six coordinate in solution. $[Zn(II)L^2H_3]^{2+}$ has C_3 symmetry in solution, and despite Zn(II) showing no stereochemical preference for octahedral or trigonal prismatic environments displays no fluxtionality. The wide dispersion of resonances in the ^{13}C spectrum is indicative of octahedral geometry.

The spectra of the other zinc complexes prepared are highly complex, but do not display any fluxtionality. The NMR titration of zinc nitrate and L^1H_3 indicates a complicated mechanism of complex formation, although more detailed analysis is required.

References

1. Weighardt, K.; Ventur, D.; Tsay, Y.H.; Kruger, C. *Inorg. Chim. Acta.*
   1985, *99*, L25

2. Adams, H.; Bailey, N.A.; Fenton, D.E.; Ford, I.G.; Kitchen, S.J.; Williams, M.G.;
   Tasker, P.A.; Leong, A.J.; Lindoy, L.F. *J. Chem. Soc. Dalton Trans.* **1991**, 1665.

3. Lever, A.B.P. Inorganic Electronic Spectroscopy. Studies in Physical and Theoretical
   Chemistry; Elsevier, Amsterdam, 1984; Vol. 33, p.419.

4. Macdonald, N.M.; Peacock, R.D. Private communication.

CHAPTER 6

GENERAL CONCLUSIONS

"The dark religions have departed, and sweet science reigns."

William Blake, Vala.

With the ligands prepared in this work a range of steric properties is spanned. As a consequence of this, the 9 and 10 membered rings support ions in a range of oxidation states (II, III and IV). The larger ring sizes support only divalent ions, on a size match selectivity.

With L^1H_3 and L^2H_3 V(IV), Co(III), Cr(III), Mn(II), Mn(IV), Ni(II), Cu(II) and Zn(II) complexes can be prepared and display a range of geometries from pseudo-octahedral to trigonal prismatic. Therefore, these two ligands show considerable stereochemical flexibility. Octahedral geometry is displayed by those ions with a significant LFSE. For those ions with a even d-orbital occupation, geometry is determined by *intermolecular* forces. The trigonal prismatic geometry observed in $[Mn(II)L^1H_3L^1Mn(IV)][PF_6]_3$ is believed to be a result of hydrogen bonding of the Mn(II) component to the Mn(IV). In this case the [Mn(II), Mn(IV)] structure is stabilised by each half of the dimer mutually presenting a preorganised trigonal array of hydrogen bond donor/acceptors. The intramolecular properties of L^1H_3 and L^2H_3 are very similar, but the intermolecular properties are very different, with the pendant-arm isopropyl groups preventing any hydrogen bonding to the trigonal alcohol/alkoxide face. Thus complexes of L^2H_3 are monomeric.

The steric properties of L^3H_3 are intermediate between those of the ligands with nine membered rings and those with 11 membered or larger rings. In contrast to L^1H_3, L^3H_3 supports only those ions with radii of an intermediate range (64.5 ppm [Mn(III)] - 74.5 ppm [Co(II)]). The addition of the extra methylene residue in L^3H_3 renders the ligand too large for effective coordination to hypersmall ions (Cr(III), Mn(IV) and Co(III)). The structure of $[Mn(II)L^3H_3L^3Mn(III)][PF_6]_2.H_2O$ is analogous to that of $[Mn(II)L^1H_3L^1Mn(IV)][PF_6]_3$, with the former having the lower average oxidation state due to the larger ring size. The structure of $[Cu(II)L^3H_3]^{2+}$ is believed to be pseudo-trigonal prismatic with a large d-orbital splitting achieved *via* a good cavity-to-metal radius match. This explains the resistance of $[Co(II)L^3H_3]^{2+}$ to aerobic oxidation since the

ionic radii of Cu(II) and Co(II) are quite similar. Simple models indicate that the presence of the C_3 bridge in L^3H_3 distorts the ligand in favour of trigonal prismatic geometry. This structure is seen in $[(Co(II)L^3H_3)_2(NO_3)_2][PF_6]_2$. With methyl substituents on the pendant-arms, a $[Co(II)L^3H_3]^{2+}$ moiety is sufficiently non-hindered for dimer formation *via* bridging nitrate ions. The dimer is close packed, with little free space between the subunits.

Ligands containing 11 membered or larger rings coordinate to divalent ions only, with coordination geometry determined by the stereochemical preferences of the metal ion and by the ring size and symmetry of the ligand. The structure of $[Co(II)L^4H_3]^{2+}$ is very distorted, lying between octahedral and bicapped tetrahedral, and that of $[Co(II)L^5H_3]^{2+}$ is of a truncated trigonal prism. Such a varied range of geometries in the Co(II) complexes of L^3H_3, L^4H_3 and L^5H_3 reflects the low preference for Co(II) for octahedral geometry. The structure of $[Co(II)L^5H_3]^{2+}$ is very unusual and reflects a tendency for N_3O_3 ligands to present a trigonal array of donor atoms. It was also observed that no complexes of L^6H_3 could be prepared. The C_6 bridge is too large to permit chelation of the nitrogen atoms at the 1 and 7 positions, and it is likely that the pendant-arm alcohol groups are too poorly σ-donating to form complexes, without ring nitrogen chelation, in the presence of water.

The weakest ligand field splitting was observed for complexes of L^7H_3. This implies that the three C_3 bridges of the macrocycle are a more severe dislocating factor than that presented by the other unsymmetrical ligands prepared. Models suggest that the structures of complexes should be approximately octahedral, but severely trigonally compressed, with the six membered chelate rings in twist-boat conformation.

Publications

Belal, A.; Fallis, I.; Farrugia, L.J.; Macdonald, N.M.; Peacock, R.D. *J. Chem. Soc., Chem Commun.* **1991**, 402.

Belal, A.; Chaudhuri, P.; Fallis, I.; Farrugia, L.J.; Hartung, R.; Macdonald, N.M.; Nuber, B.; Peacock, R.D.; Weiss, J.; Weighardt, K. *Inorg. Chem.* **1991**, *30*, 4397.